

Copyright is owned by the Author of the thesis. Permission is given for a copy to be downloaded by an individual for the purpose of research and private study only. The thesis may not be reproduced elsewhere without the permission of the Author.

**TREATMENT OF MEAT PROCESSING
WASTEWATER FOR CARBON,
NITROGEN AND PHOSPHORUS
REMOVAL IN A
SEQUENCING BATCH REACTOR**

A thesis presented in partial fulfilment of the requirements
for the degree of
Doctor of Philosophy
in Process & Environmental Technology
at Massey University

Nagalingam Thayalakumaran

2002

ABSTRACT

The typical New Zealand meat processing industry wastewater was treated by a laboratory scale Sequencing Batch Reactor (SBR) to determine an effective operating cycle for biological carbon, nitrogen and phosphorus removal. The Activated Sludge Model No. 1 and Model No. 2 with modifications were used to simulate the treatment of meat processing wastewater using the SBR.

The average values of main pollution parameters of the wastewater were characterised as 1390 mg total COD L⁻¹, 755 mg soluble COD L⁻¹, 75 mg L⁻¹ NH₃ – N, 145 mg L⁻¹ TKN and 34 mg L⁻¹ TP. The readily biodegradable COD (RBCOD) accounts for 15 – 18 % of the total COD, while the inert soluble and particulate portion were 4 % each.

In order to establish an effective operating cycle for the simultaneous removal of nutrients and organic carbon, different dissolved oxygen (DO) concentrations in the mixed liquor, duration of operating phases and hydraulic retention time (HRT) of a 6 h cycle were tested. The most effective cycle consisted of seven phases. The first two hours of the anaerobic period was followed by the aerobic and anoxic periods. The first aerobic period was maintained at a DO concentration of 0.5 ± 0.25 mg L⁻¹ for 1 h, the second aerobic period for 1 h at a DO concentration of 3.75 ± 0.25 mg L⁻¹ and the third aerobic period for half an hour at 0.5 ± 0.25 mg L⁻¹ DO concentration. A half an hour anoxic period followed the first aerobic period. A settling period of 0.75 h followed the third aerobic period. The last quarter of an hour was for decanting and idling. The solids retention time (SRT) was 15 d, while the HRT was 2.5 d. Greater than 99 % removal of biodegradable soluble COD, NH₃ – N and PO₄ – P was achieved in the effective operating cycle where the TN and TP in the wastewater were reduced to 10 mg L⁻¹ and 1.0 mg L⁻¹, respectively. In addition the soluble COD was reduced to 98 mg L⁻¹.

The key kinetic and stoichiometric parameters for ASM 1 and ASM 2 models were determined using batch tests. The heterotrophic maximum specific growth rate, yield coefficient and the half saturation constant were 2.0 d⁻¹, 0.63 mg cell COD (mg COD)⁻¹ and 8 mg L⁻¹ respectively. The maximum specific growth rate of autotrophs was 0.65 – 0.80 d⁻¹. The anaerobic phosphorus removal stoichiometric coefficients were also

determined in batch tests. During the anaerobic period, when 1 g of acetate COD was initially present, 1.48 g of PHA COD was stored while 0.48 g of P was released. The batch trials conducted using acetate to assess the influence of Mg^{2+} in P uptake showed that the Mg^{2+} could limit the P uptake and the uptake rate could be represented by Monod type kinetics. In the Monod kinetic expression the Mg^{2+} half saturation constant was found to be 4.7 mg L^{-1} . The molar ratio of Mg^{2+} with P was 0.21 during the anaerobic period, and 0.33 during the aerobic period.

The SBR performance was modelled using ASM 1 and ASM 2 models after the addition of more processes in these models. Ammonification of the soluble organic N process rate was modified in the ASM 1 model. Similarly it was necessary to add anoxic P uptake and anoxic growth processes involving PHA of Bio-P bacteria in the ASM 2 model. Glycogen storage and glycogen lysis processes of Bio-P bacteria were added in the ASM 2 model to understand the involvement of glycogen in P removal. Also a modification was performed to the storage process of poly-P in the ASM 2 model to account for potential Mg^{2+} limitation in meat processing wastewater treatment for P removal. During the settling period anoxic hydrolysis was assumed to be negligible. The calibrated ASM 1 and ASM 2 models in general well simulated the effluent $NH_3 - N$, $NO_3 - N$ and $PO_4 - P$ of SBR cycles carried out in distinctly different periods of time and in different batch tests.

As the calibrated modified ASM 2 model was able to predict the performance of an SBR cycle conducted over a time period of three months, it was used to identify the most promising treatment strategies of the SBR performance. Variation in duration of feed cycle during the first non-aerated mixed period did not affect the effluent $NO_3 - N$, $NH_3 - N$ and $PO_4 - P$ concentrations significantly. DO concentration of 3.75 mg L^{-1} during the third aerobic period instead of 0.5 mg L^{-1} increased the effluent $NO_3 - N$ and $PO_4 - P$ concentrations. The simulations confirmed that the operating conditions identified in a 6-h cycle period for the simultaneous organic carbon and nutrient removal are effective.

Acknowledgements

I wish to thank Professor Rao Bhamidimarri for his guidance and supervision over the past three years. I also thank Mr. Paul Bickers for his helpful discussions and suggestions.

Many thanks to Professor Bob Chong, Dr. Magnus Christensson and Mr. Ken Butler for their valuable suggestions.

Thanks to Dr. Manderson and Dr. John Brounland who gave me the fundamentals of microorganisms and MATLAB programming.

I am very grateful to Mr. Bruce, Mr. John Syke, and Mr. Andrew for their help in the reactor set up. Thanks to my fellow postgraduates in the lab. for their friendship.

Thanks to the Massey University for providing me with financial assistance for presenting papers at the IWA conference held in Melbourne and the Biotechnology conference held in Palmerston North.

Thanks to the Environmental Management Team of Manawatu Beef Packers in Fielding for allowing me to collect their wastewater.

I also wish to thank Dr. David Scotter and Dr. Tessa Mills for their help in proof-reading and editing my thesis.

Thanks to my wife, Thabo, and daughter, Varshi, for their patience and encouragement throughout the study.

Table of Contents

ABSTRACT.....	II
ACKNOWLEDGEMENTS.....	IV
TABLE OF CONTENTS.....	V
LIST OF FIGURES.....	VIII
LIST OF TABLES.....	XI
ABBREVIATIONS.....	XIII
CHAPTER I INTRODUCTION.....	1
1.1 BACKGROUND.....	1
1.2 APPROACH TAKEN IN THIS STUDY.....	3
CHAPTER II LITERATURE REVIEW	5
2.1 INTRODUCTION.....	5
2.2 SOURCES, TYPES AND CHARACTERISTICS OF MEAT PROCESSING WASTEWATER.....	5
2.2.1 Sources and types of meat-works waste	5
2.2.2 Characteristics of meat processing wastewater.....	6
2.3 ENVIRONMENTAL SIGNIFICANCE OF MEAT PROCESSING WASTEWATER DISCHARGE.....	8
2.4 TREATMENT TECHNOLOGIES FOR MEAT PROCESSING WASTEWATER.....	9
2.4.1 Primary treatment.....	9
2.4.2 Secondary treatment	11
2.4.2.1 Physicochemical treatment.....	12
2.4.2.2 Biological treatment	13
2.4.2.2.1 Anaerobic biological wastewater treatment.....	14
2.4.2.2.2 Aerobic biological treatment.....	18
2.4.2.2.3 Biological processes of nitrogen removal.....	20
2.4.2.2.4 Biological phosphorus removal.....	27
2.5 SEQUENCING BATCH REACTOR (SBR).....	31
2.5.1 SBR Operation	31
2.5.2 SBR vs. Conventional continuous flow activated sludge systems.....	33
2.5.3 Simultaneous nitrification and denitrification (SND)	34
2.5.4 Sludge settling in sequencing batch reactors.....	34
2.5.5 Modelling of Sequencing Batch Reactors treatment	35
2.6 SUMMARY.....	37
CHAPTER III METHODOLOGY.....	39
3.1 SOURCE AND TYPE OF WASTEWATER.....	39
3.2 START UP OF THE EXPERIMENT.....	39
3.3 SBR PERFORMANCE AND CHARACTERISATION OF WASTEWATER.....	41
3.3.1 Determination of chemical oxygen demand.....	42
3.3.2 Determination of total and volatile suspended solids (TSS and VSS).....	42
3.3.3 Determination of ammonia concentration	42
3.3.4 Total Kjeldahl nitrogen (TKN).....	43

3.3.5 Total phosphorus (TP) concentration	43
3.3.6 Oxidised nitrogen ($NO_x - N$) and soluble phosphate phosphorus ($PO_4 - P$) concentration.....	44
3.3.7 DO, pH, alkalinity and SVI measurements	44
3.4 INFLUENT SOLUBLE AND PARTICULATE INERT COD FRACTION.....	44
3.5 OXYGEN UPTAKE RATE (OUR) MEASUREMENT.....	45
3.6 ASSESSMENT OF READILY BIODEGRADABLE COD.....	46
3.6.1 Aerobic batch test	46
3.6.2 Anoxic batch test.....	46
3.7 MAXIMUM SPECIFIC GROWTH RATE OF HETEROTROPHS.....	47
3.8 HETEROTROPHIC DECAY COEFFICIENT.....	48
3.9 MAXIMUM SPECIFIC GROWTH RATE OF AUTOTROPHS.....	48
3.10 HETEROTROPHIC YIELD COEFFICIENT.....	48
3.11 SHORT CHAIN FATTY ACIDS (SCFA) MEASUREMENT.....	49
3.12 POLY- β -HYDROXYBUTYRATE AND POLY- β -HYDROXYVALERATE IN MICROBIAL BIOMASS.....	49
3.13 CARBOHYDRATE IN THE WASTEWATER.....	50
3.14 GLYCOGEN IN THE SLUDGE.....	51
3.14.1 Measurement conditions for acid hydrolysis method	51
3.14.2 Methodology for glycogen measurement in the sludge.....	52
3.15 SOLUBLE MAGNESIUM, POTASSIUM, CALCIUM AND IRON MEASUREMENT.....	53
3.16 MICROSCOPICAL OBSERVATION OF SLUDGE MORPHOLOGY (GRAM STAINING).....	53
CHAPTER IV CHARACTERISTICS OF WASTEWATER	54
4.1 INTRODUCTION.....	54
4.2 CONVENTIONAL POLLUTION PARAMETERS OF WASTEWATER.....	54
4.3 SHORT CHAIN FATTY ACID FRACTION OF THE WASTEWATER.....	57
4.4 ASSESSMENT OF INITIAL SOLUBLE AND PARTICULATE INERT COD IN THE WASTEWATER.....	58
4.5 READILY BIODEGRADABLE COD.....	62
4.5.1 Conceptual basis.....	63
4.5.2 Readily biodegradable COD measurement by batch OUR method	64
4.5.3 Readily biodegradable COD measurement by batch NUR method.....	66
4.6 SUMMARY.....	69
CHAPTER V PERFORMANCE OF SEQUENCING BATCH REACTOR.....	70
5.1 INTRODUCTION.....	70
5.2 PERFORMANCE OF THE SBR DURING RUN I.....	70
5.3 PERFORMANCE OF THE SBR DURING RUN II.....	77
5.4 PERFORMANCE OF THE SBR DURING RUN III (CENTRIFUGED WASTEWATER).....	82
5.5 PERFORMANCE OF THE SBR DURING RUN IV.....	85
5.6 SUMMARY.....	92
CHAPTER VI KINETIC CHARACTERISATION OF WASTEWATER.....	94
6.1 INTRODUCTION.....	94
6.2 KINETIC AND STOICHIOMETRIC CONSTANTS IN BIOLOGICAL ORGANIC CARBON AND NITROGEN REMOVAL.....	95
6.2.1 Heterotrophic yield coefficient.....	95
6.2.2 Maximum specific growth rate and half saturation constant of heterotrophs	97

6.2.3	<i>Maximum specific growth rate of autotrophs</i>	100
6.2.4	<i>Heterotrophic decay coefficient</i>	101
6.3	STOICHIOMETRIC AND KINETIC CONSTANTS IN BIOLOGICAL PHOSPHORUS REMOVAL	103
6.3.1	<i>Kinetic and stoichiometric coefficients for meat processing wastewater</i>	103
6.3.1.1	SBR cycle study	103
6.3.1.2	Stoichiometric coefficients using batch test	110
6.3.1.3	Stoichiometric coefficients with acetate batch tests	112
6.4	INFLUENCE OF CATIONS ON PHOSPHORUS REMOVAL	116
6.4.1	<i>Magnesium, potassium and calcium ions in phosphorus removal</i>	116
6.4.2	<i>Magnesium ion influence in phosphorus uptake</i>	120
6.5	ANOXIC PHOSPHORUS UPTAKE AND RELEASE	124
6.6	PHOSPHORUS RELEASE DURING THE PH ADJUSTMENT	127
6.7	SUMMARY	128
CHAPTER VII APPLICATION OF ACTIVATED SLUDGE MODELS		131
7.1	INTRODUCTION	131
7.2	ACTIVATED SLUDGE MODEL NO. 1 (ASM 1)	132
7.2.1	<i>Model description</i>	132
7.2.2	<i>Calibration of the modified ASM 1 model</i>	140
7.2.3	<i>Simulation of the SBR cycle described in Section 5.5</i>	143
7.2.4	<i>Sensitivity of the model parameters in ASM 1</i>	144
7.3	ACTIVATED SLUDGE MODEL NO. 2 (ASM2)	146
7.3.1	<i>ASM 2 model description</i>	146
7.3.2	<i>ASM 2 model modification</i>	148
7.3.3	<i>Calibration of the modified ASM 2</i>	155
7.3.4	<i>Simulation of batch test results with wastewater</i>	162
7.3.5	<i>Simulation of the batch test results with acetate (Trial II)</i>	165
7.3.6	<i>Simulation of the batch test results with acetate (Trial I)</i>	166
7.3.7	<i>Simulation of SBR cycle results described in Section 5.5</i>	168
7.3.8	<i>Sensitivity of parameters in the modified ASM 2 model</i>	169
7.4	APPLICATION OF THE MODIFIED ASM 2 MODEL	170
7.5	SUMMARY	173
CHAPTER VIII SUMMARY AND CONCLUSIONS		176
REFERENCES		181
APPENDIX A		194
APPENDIX B		197
APPENDIX C		198
APPENDIX D		203

List of Figures

Figure 2.1 Schematic diagram of a meat processing wastewater treatment system (Mikkelson & Lowery, 1992).....	10
Figure 2.2 Biological breakdown of organic matters (Henze, 2002)	14
Figure 2.3 An outline of the anaerobic process (Manderson, 2000).....	15
Figure 2.4 Possible microbial nitrogen conversions (Van Loosdrecht & Jetten, 1998).....	22
Figure 2.5 SBR operation for each tank for one cycle for the five discrete time periods (Irvine and Ketchum, 1989)	32
Figure 3.1 Laboratory scale sequencing batch reactor set-up.....	41
Figure 3.2 Schematic diagram of reactors set-up during wastewater inert COD measurement.....	45
Figure 3.3 Schematic diagram of the OUR measurement set-up.....	46
Figure 3.4 Schematic diagram of the respirometer and the chart recorder.....	47
Figure 4.1 Short chain fatty acid fractions of the wastewater.....	58
Figure 4.2 SCOD profiles of the filtered wastewater and glucose reactor.....	59
Figure 4.3 COD profiles of the filtered wastewater reactor.....	60
Figure 4.4 COD profiles of the raw wastewater reactor.....	60
Figure 4.5 Oxygen uptake rate profiles for meat processing wastewater.....	64
Figure 4.6 Nitrate uptake rate profile for meat processing wastewater.....	66
Figure 4.7 Influent COD fraction (average TCOD = 1390 mg L ⁻¹).....	66
Figure 4.8 OUR profile of a parallel OUR and NUR test in meat processing wastewater	68
Figure 4.9 NUR profile of a parallel OUR and NUR tests in meat processing wastewater.....	68
Figure 5.1 Influent and effluent COD during Run I.....	72
Figure 5.2 Influent N and P during Run I.....	73
Figure 5.3 Effluent N and P during Run I.....	74
Figure 5.4 Influent, effluent and sludge solids during Run I.....	75
Figure 5.5 SCOD, N and P profiles in a cycle study during Run I.....	76
Figure 5.6 DO and pH profiles in a cycle study during Run I.....	77
Figure 5.7 SCOD, N and P profiles in a cycle study during Run II.....	78
Figure 5.8 pH and DO profiles during a cycle study during Run II.....	79
Figure 5.9 Influent COD, N and P profiles during Run II.....	81
Figure 5.10 Effluent soluble COD, N and P profiles during Run II.....	81
Figure 5.11 Influent centrifuged COD, N and P profiles during Run III.....	82
Figure 5.12 Effluent SCOD, N and P profiles during Run III.....	83
Figure 5.13 Soluble COD, N and P profiles in a cycle study during Run III.....	84
Figure 5.14 DO and pH profiles in a cycle study during Run III.....	85
Figure 5.15 Influent COD, N and P profiles during Run IV.....	87
Figure 5.16 Effluent SCOD, N and P profiles during Run IV.....	87
Figure 5.17 VSS to TSS ratio at the end of the anaerobic and aerobic phases during Run IV.....	88
Figure 5.18 Soluble COD, N and P profiles in a cycle study during Run IV.....	89
Figure 5.19 N balance in a cycle study during Run IV.....	90
Figure 5.20 Alkalinity and pH profiles in a cycle during Run IV.....	91
Figure 5.21 Typical oxygen uptake rate profile during Run IV.....	92

Figure 6.1 Substrate removal with different S_0/X_0	96
Figure 6.2 Yield coefficient with $S_0/X_0 = 2$	96
Figure 6.3 A typical respirogram	97
Figure 6.4 Relationship between specific substrate removal rate and substrate in soluble meat processing wastewater	98
Figure 6.5 Linear profile of r_x with r_x/S	99
Figure 6.6 Maximum specific growth rate of autotrophs	101
Figure 6.7 Heterotrophic decay coefficient.....	102
Figure 6.8 Soluble phosphate phosphorus, nitrate nitrogen, SCFA COD, PHA COD and glycogen COD profiles during an SBR cycle	104
Figure 6.9 Soluble phosphate phosphorus, nitrate nitrogen, SCFA COD, PHA COD and glycogen COD profiles during a batch test with wastewater	111
Figure 6.10 Soluble phosphate phosphorus, nitrate nitrogen, SCFA COD, PHA COD and glycogen COD profiles during a batch test with acetate (Trial I)	114
Figure 6.11 Soluble phosphate phosphorus, nitrate nitrogen, SCFA COD, PHA COD and glycogen COD profiles during a batch test with acetate (Trial II)	115
Figure 6.12 Mg^{2+} , K^+ and Ca^{2+} profiles during the SBR cycle and batch tests	117
Figure 6.13 Relationships between the molar concentrations of Mg^{2+} , K^+ and Ca^{2+} with $PO_4 - P$	119
Figure 6.14 Mg^{2+} influence on phosphate uptake.....	121
Figure 6.15 Soluble Mg^{2+} , K^+ and Ca^{2+} in mixed liquor in a batch test with $10 \text{ mg L}^{-1} Mg^{2+}$ addition...	122
Figure 6.16 Relationship between Mg^{2+} concentration at the beginning of the anaerobic period and the P storage rate.	124
Figure 6.17 Anoxic – anoxic and anaerobic – aerobic batch tests	126
Figure 6.18 N and P profiles in an anoxic batch test.....	128
Figure 7.1 Flow diagram for model used by Cliff and Andrews (1981).....	133
Figure 7.2 Flow diagram for the ASM 1 model (Grady, 1989)	133
Figure 7.3 Distribution of COD fractions in wastewater	136
Figure 7.4 Illustration of death - regeneration and endogenous decay models (Orhon & Artan, 1994)...	138
Figure 7.5 Wastewater characterisation for nitrogenous components (Orhon and Artan, 1994)	139
Figure 7.6 Simulated and experimental $NH_3 - N$ and $NO_3 - N$ during the SBR cycle described in Section 6.3.1.1	143
Figure 7.7 Simulated and experimental $NH_3 - N$ and $NO_3 - N$ of the SBR cycle described in Section 5.5.	144
Figure 7.8 Metabolism of polyphosphate accumulating organisms (Mino <i>et al.</i> , 1995).....	148
Figure 7.9 Simulated and experimental $NH_3 - N$, $NO_3 - N$ and $PO_4 - P$ during the SBR cycle described in Section 6.3.1.1.	159
Figure 7.10 Simulated and experimental PHA COD and glycogen COD during the SBR cycle described in Section 6.3.1.1.	161
Figure 7.11 Simulated and experimental $PO_4 - P$, Mg^{2+} and SCFA COD during the SBR cycle described in Section 6.3.1.1.	162
Figure 7.12 Simulated and experimental $NH_3 - N$, $NO_3 - N$ and $PO_4 - P$ of batch test with wastewater.....	163
Figure 7.13 Simulated and experimental $PO_4 - P$, Mg^{2+} and SCFA COD batch test with wastewater	164
Figure 7.14 Simulated and experiment PHA COD and glycogen COD of batch test with wastewater.....	164
Figure 7.15 Simulated and experimental $PO_4 - P$ and HAc COD of acetate batch test (Trial II).	165
Figure 7.16 Simulated and experimental PHA COD and glycogen COD of acetate batch test (Trial II).....	166

Figure 7.17 Simulated and experimental $\text{PO}_4\text{-P}$ and HAc COD of acetate batch test (Trial I).....	167
Figure 7.18 Simulated and experimental PHA COD and glycogen COD of acetate batch test (Trial I)..	167
Figure 7.19 Simulated and experimental $\text{NH}_3\text{-N}$, $\text{NO}_3\text{-N}$ and $\text{PO}_4\text{-P}$ during the SBR cycle described in Section 5.5.	169
Figure 7.20 Simulated $\text{NH}_3\text{-N}$, $\text{NO}_3\text{-N}$ and $\text{PO}_4\text{-P}$ with varying filling times.....	171
Figure 7.21 Simulated $\text{NO}_3\text{-N}$, $\text{NH}_3\text{-N}$ and $\text{PO}_4\text{-P}$ with third aeration at 3.75 mg L^{-1} of DO concentration.	172
Figure 7.22 Simulated $\text{NO}_3\text{-N}$, $\text{NH}_3\text{-N}$ and $\text{PO}_4\text{-P}$ at TCOD concentrations of (a) 2050 and (b) 490 mg L^{-1}	173

List of Tables

Table 2.1 Constituents and sources of meat wastes (Bhamidimarri, 1991)	6
Table 2.2 Representative characteristics of meat processing plant effluents (Cooper & Russell, 1991).....	7
Table 2.3 Performance of an anaerobic lagoon receiving meat processing wastewater (Russell & Cooper, 1992).....	17
Table 3.1 Operating cycle of laboratory scale sequencing batch reactor (6-h cycle).....	41
Table 3.2 Percentage of glucose recovery at different digestion conditions.....	52
Table 3.3 The set wavelength and slit width (GBC 933 manual).....	53
Table 4.1 Characteristics of the wastewater.....	55
Table 4.2 Relationships between major pollution parameters.....	56
Table 4.3 Wastewater SCFA COD fraction changes in a $22 \pm 2^\circ\text{C}$ controlled room.....	58
Table 4.4 COD fractions of meat processing wastewater.....	60
Table 4.5 Fraction of biodegradable COD converted into inert microbial products.....	61
Table 4.6 Wastewater COD fractions.....	65
Table 5.1 Operating cycle of Run I (6-h cycle).....	71
Table 5.2 Operating cycle of Run II (6-h cycle).....	77
Table 5.3 Operating cycle of Run IV (6-h cycle).....	86
Table 6.1 Heterotrophic growth kinetic and stoichiometric constants.....	99
Table 6.2 Stoichiometric relationships among HAc, P, PHA and glycogen during anaerobic P metabolism.....	103
Table 6.3 TSS, VSS and sludge phosphorus content during the SBR and batch studies.....	105
Table 6.4 Carbon balance in anaerobic phosphorus metabolism.....	108
Table 6.5 COD conversion factors for some components in the P metabolism (Smolder <i>et al.</i> , 1995).....	109
Table 6.6 Stoichiometric relationships among HAc, P, PHA and glycogen during anaerobic P metabolism.....	109
Table 6.7 Sludge P and stored P content.....	113
Table 6.8 Carbon balance in aerobic P metabolism.....	116
Table 6.9 Molar ratios of cations with phosphate.....	118
Table 6.10 Magnesium influence in P uptake and release.....	121
Table 6.11 Relationship between Mg^{2+} concentration at the beginning of the anaerobic period and the P storage rate.....	123
Table 7.1 Activated sludge model No. 1 (Henze <i>et al.</i> , 1987a, b).....	135
Table 7.2 Kinetic and stoichiometric parameter values used after the calibration of ASM 1 model.....	142

Table 7.3 Sensitive kinetic and stoichiometric parameters of the ASM 1 model.....	145
Table 7.4 Composition of the biomass and the relation with MLSS and VSS.....	147
Table 7.5 Conversion factors i_{c_i} to be applied in the continuity equations of the modified ASM 2 model (Henze <i>et al.</i> , 1999).....	150
Table 7.6 Process rate equations (Henze <i>et al.</i> , 1995; Mino <i>et al.</i> , 1995).....	152
Table 7.7 Stoichiometry of hydrolysis processes.....	153
Table 7.8 Stoichiometry of the facultative heterotrophic organisms X_H	153
Table 7.9 Stoichiometry of the phosphorus accumulating organisms, PAO.....	154
Table 7.10 Stoichiometry of the growth and decay processes of nitrifying organisms X_{AUT}	154
Table 7.11 Stoichiometry of the processes describing simultaneous precipitation of phosphorus.....	154
Table 7.12 Parameters definition and values used in the modified ASM 2 model for meat processing wastewater.....	156
Table 7.13 Sensitive parameters in the modified ASM 2 model.....	170
Table A1 Meat processing wastewater and glucose reactor COD with time.....	194
Table B1 COD conversion table (Smolders <i>et al.</i> , 1995 b).....	197

Abbreviations

3H2MB	3-hydroxy-2-methylbutyrate
3H2MV	3-hydroxy-2-methylvalerate
3HB	3-hydroxybutyrate
3HV	3-hydroxyvalerate
AA	Anoxic-anoxic
AO	Anaerobic-aerobic
AS	Activated Sludge
ASM 1	Activated Sludge Model No. 1
ASM 2	Activated Sludge Model No. 2
Bio-P	Biological phosphorus removing bacteria
BNR	Biological nutrient removal
BOD	Biochemical Oxygen Demand (mg L^{-1})
BOD ₅	5 d biochemical oxygen demand (mg L^{-1})
BPR	Biological phosphorus Removal
b_A	Autotrophic decay coefficient (d^{-1})
b_H	Heterotrophic Task Group model decay coefficient (d^{-1})
b'_H	Heterotrophic biomass endogenous decay rate (d^{-1})
C	Carbon
Ca^{2+}	Calcium
COD	Chemical Oxygen Demand (mg L^{-1})
C_{T1}	Initial total COD in the reactor 1 (mg COD L^{-1})
$(C_T)_1, (C_T)_2$	Final total COD in the reactors 1 and 2 (mg COD L^{-1})
DAF	Dissolved air floatation
DO	Dissolved Oxygen (mg L^{-1})
EBPR	Enhanced Biological Phosphate Removal
f_{ES}, f_{EX}	Fraction of soluble and particulate inert COD generated in biomass decay
f_P	Fraction of biomass yielding to particulate products
F/M ratio	Food (substrate) to Mass (Biomass) ratio
H_2	Hydrogen
HAc	Acetic acid
HRT	Hydraulic Retention Time (d)
HMP	Hexametaphosphate
IAWPRC	International Association on Water Pollution Research and Control
IAWQ	International Association on Water Quality
IWA	International Water Association
i_{XB}	Mass of nitrogen per mass of COD in biomass
i_{XP}	Mass of nitrogen per mass of COD in products from biomass
K^+	Potassium
K_{Mg}	Magnesium half saturation constant (mg L^{-1})
K_{NH}	Ammonia half saturation coefficient for autotrophic biomass (mg L^{-1})
$K_{N,O}$	Nitrate half saturation coefficient for denitrifying heterotrophic biomass (mg L^{-1})
$K_{O,A}$	Oxygen half saturation constant for autotrophs (mg L^{-1})
$K_{O,H}$	Oxygen half saturation constant for heterotrophs (mg L^{-1})
K_S	Substrate half saturation coefficient (mg L^{-1})
K_X	Half saturation coefficient for hydrolysis of slowly biodegradable substrate ($\text{g slowly biodegradable COD (g cell COD)}^{-1}$)
k_a	Ammonification rate ($\text{m}^3 (\text{g COD d})^{-1}$)
Mg^{2+}	Magnesium
MLVSS	Mixed liquor volatile suspended solid
N	Nitrogen
N_2	Nitrogen gas
$\text{NH}_3 - \text{N}$	Ammonia nitrogen + Ammonium nitrogen
$\text{NO}_2 - \text{N}$	Nitrite nitrogen
$\text{NO}_3 - \text{N}$	Nitrate nitrogen, 0.6 Nitrite nitrogen plus nitrate nitrogen

$\text{NO}_x - \text{N}$	Nitrite nitrogen plus nitrate nitrogen
NUR	Nitrate Utilisation Rate ($\text{g NO}_3 - \text{N m}^{-3} \text{ h}^{-1}$)
OUR	Oxygen Uptake Rate ($\text{mg O}_2 \text{ L}^{-1} \text{ h}^{-1}$)
PAO	Phosphorus Accumulating Organisms
P	Phosphorus
PHA	Poly- β -hydroxyalkanoate
PHB	Poly- β -hydroxybutyrate
PHV	Poly- β -hydroxyvalerate
poly-P	Polyphosphate
$\text{PO}_4 - \text{P}$	Soluble phosphate phosphorus
ppm	Particles per million
Q	Influent flow rate ($\text{m}^3 \text{ s}^{-1}$)
q	Phosphorus uptake rate ($\text{mg P (g VSS d)}^{-1}$)
q_{max}	Maximum phosphorus uptake rate ($\text{mg P (g VSS d)}^{-1}$)
RBCOD	Readily biodegradable COD
R_{EQ}	Oxygen reduction equivalent
rpm	revolution per minute
r_x	Specific substrate removal rate (d^{-1})
r'_s	Substrate utilisation rate, $\text{g (m}^3\text{s)}^{-1}$
r'_x	Rate of biomass growth, $\text{g (m}^3\text{s)}^{-1}$
S	Substrate concentration in the reactor (mg L^{-1})
SBCOD	Slowly Biodegradable COD
SBR	Sequencing Batch Reactor
SCFA	Short Chain Fatty Acids
SCOD	Soluble COD (mg L^{-1}), defined as GFC filterable COD for this study
S_{G1}	Initial soluble COD in the glucose reactor (mg COD L^{-1})
S_H	Rapidly hydrolysable substrate (mg L^{-1})
S_I	Soluble inert substrate concentration (mg L^{-1})
SMP	Soluble Microbial Products
S_{Mg}	Soluble magnesium concentration (mg L^{-1})
SND	Simultaneous Nitrification and Denitrification
S_{ND}	Soluble biodegradable organic nitrogen (mg N L^{-1})
S_{NH}	Ammonia nitrogen + Ammonium nitrogen (g N m^{-3})
S_{NO}	Concentration of oxidised nitrogen (mg L^{-1})
S_O	Substrate concentration of the influent/ initial (mg L^{-1})
SOUR	Specific Oxygen Uptake Rate ($\text{mg O}_2 \text{ (g VSS h)}^{-1}$)
SRT	Solids Retention Time (d)
S_s	Readily biodegradable substrate concentration (mg COD L^{-1})
S_{T1}	Initial soluble COD in the reactors 1 and 2 (mg COD L^{-1})
$(S_T)_1, (S_T)_2$	Final soluble COD in the reactors 1 and 2 (mg COD L^{-1})
SVI	Sludge Volume Index (ml g^{-1})
TCA	Tricarboxylic acid
TCOD	Total COD
TKN	Total Kjeldahl Nitrogen (mg N L^{-1})
TN	Total Nitrogen (mg N L^{-1})
TP	Total Phosphorus (mg L^{-1})
TS	Total Solids (mg L^{-1})
TSS	Total Suspended Solids (mg L^{-1})
V_{ml}	Volume of mixed liquor
V_O	Initial reactor volume before feeding, m^3
VSS	Volatile Suspended Solids (mg L^{-1})
V_{WW}	Volume of wastewater
X	Biomass concentration in the reactor (mg L^{-1})
$X_{\text{B,A}}$	Active autotrophic biomass (mg COD L^{-1})
$X_{\text{B,H}}$	Active heterotrophic biomass (mg COD L^{-1})
X_I	Particulate inert substrate concentration (mg COD L^{-1})
X_{ND}	Particulate biodegradable organic nitrogen (mg N L^{-1})
X_O	Biomass concentration of the influent/initial (mg L^{-1})

X_S	Slowly biodegradable substrate (mg COD L ⁻¹)
$(X_T)_1$	Final particulate COD of raw wastewater reactor (mg COD L ⁻¹)
Y_A	Autotrophic yield coefficient (g Cell COD g N oxidised ⁻¹)
Y_H	Heterotrophic yield coefficient (g Cell COD g substrate COD ⁻¹)
Y_{obs}	Coefficient of observed biomass yield (g Cell COD g substrate COD ⁻¹)
Y_{SP}	Fraction of biodegradable COD converted into soluble inert microbial products
Y_{XP}	Fraction of biodegradable COD converted into particulate inert microbial products
$\hat{\mu}_H, \mu_{max}$	Maximum specific growth rate of heterotrophs (d ⁻¹)
$\hat{\mu}_A, \mu_{max,A}$	Maximum specific growth rate of autotrophs (d ⁻¹)
η_g	Correction factor for anoxic growth of heterotrophs
η_h	Correction factor for anoxic hydrolysis

Components in the ASM 2 model

S_A	Fermentation products (mg COD L ⁻¹)
S_{ALK}	Alkalinity of the wastewater (mol HCO ₃ L ⁻¹)
S_F	Fermentable, readily biodegradable organic substrates (mg COD L ⁻¹)
S_I	Inert soluble organic material (mg COD L ⁻¹)
S_{N2}	Dinitrogen (mg N L ⁻¹)
S_{NH4}	Ammonium plus ammonia nitrogen (mg N L ⁻¹)
S_{NO3}	Nitrate + 0.6times the Nitrite nitrogen (mg N L ⁻¹)
S_{O2}	Dissolved oxygen (mg O ₂ L ⁻¹)
S_{PO4}	Inorganic soluble phosphorus (mg P L ⁻¹)
X_{AUT}	Nitrifying organisms (mg COD L ⁻¹)
X_H	Heterotrophic organisms (mg COD L ⁻¹)
X_I	Inert particulate organic material (mg COD L ⁻¹)
X_{PAO}	Phosphate accumulating organisms (mg COD L ⁻¹)
X_{PHA}	A cell internal storage product of Bio-P (mg COD L ⁻¹)
X_{PP}	Polyphosphate (mg P L ⁻¹)
X_S	Slowly biodegradable substrates (mg COD L ⁻¹)
X_{TSS}	Total suspended solids (mg TSS L ⁻¹)

Conversion factors in the ASM 2 model:

i_{NSF}	N content of fermentable substrate S_F , g N(g COD) ⁻¹
i_{NSI}	N content of inert soluble COD S_I , g N(g COD) ⁻¹
i_{NXI}	N content of inert particulate COD X_I , g N(g COD) ⁻¹
i_{NXS}	N content of slowly biodegradable substrate X_S , g N(g COD) ⁻¹
i_{NBM}	N content of biomass X_H, X_{PAO}, X_{AUT} , g N(g COD) ⁻¹
i_{PSF}	P content of fermentable substrate S_F , g P(g COD) ⁻¹
i_{PSI}	P content of inert soluble COD S_I , g P(g COD) ⁻¹
i_{PXI}	P content of inert particulate COD X_I , g P(g COD) ⁻¹
i_{PXS}	P content of slowly biodegradable substrate X_S , g P(g COD) ⁻¹
i_{PBM}	P content of biomass X_H, X_{PAO}, X_{AUT} , g P(g COD) ⁻¹
i_{TSSXI}	TSS to X_I ratio, g TSS(g COD) ⁻¹
i_{TSSXS}	TSS to X_S ratio, g TSS(g COD) ⁻¹
i_{TSSBM}	TSS to biomass ratio for X_H, X_{PAO}, X_{AUT} , g TSS(g COD) ⁻¹
f_{SI}	Fraction of inert COD in particulate substrate, g COD(g COD) ⁻¹
f_{XI}	Fraction of inert COD generated in biomass lysis, g COD(g COD) ⁻¹

Stoichiometric parameters in the ASM 2 model:

Hydrolysis

f_{SI}	Production of S_I in hydrolysis
----------	-----------------------------------

Heterotrophic biomass: X_H

Y_H	Yield coefficient, g COD (g COD) ⁻¹
f_{XI}	Fraction of inert COD generated in biomass lysis

Phosphorus accumulating organisms: X_{PAO}

Y_{PAO}	Yield coefficient (biomass/PHA), g COD (g COD) ⁻¹
Y_{PO4}	PO ₄ release per X_{PHA} stored, g P (g COD) ⁻¹
Y_{PHA}	X_{PHA} requirement for X_{PP} storage, g COD (g P) ⁻¹
f_{XI}	Fraction of inert COD generated in biomass lysis
Y_{SA}	S_A requirement for X_{PHA} storage, g COD (g COD) ⁻¹
Y_{MgPHA}	Yield of magnesium during X_{PHA} storage g Mg (g COD) ⁻¹
Y_{MgXPP}	Yield of magnesium during X_{PP} storage g Mg (g P) ⁻¹

Nitrifying organisms: X_{AUT}

Y_A	Yield of autotrophic biomass per NO ₃ – N, g COD (g N) ⁻¹
f_{XI}	Fraction of inert COD generated in biomass lysis

Kinetic model parameters in the ASM 2 model

Hydrolysis of particulate substrate: X_S

K_h	Hydrolysis rate constant, d ⁻¹
η_{NO3}	Anoxic hydrolysis reduction factor
η_{fe}	Anaerobic hydrolysis reduction factor
K_{O2}	Saturation/inhibition coefficient for oxygen, g O ₂ m ⁻³
K_{NO3}	Saturation/ inhibition coefficient for nitrate, g N m ⁻³
K_X	Saturation coefficient for particulate COD, g X_S (g X_H) ⁻¹

Heterotrophic organisms: X_H

μ_H	Maximum growth rate on substrate, g X_S (g X_H d) ⁻¹
q_{fe}	Maximum rate for fermentation, g S_F (g X_H d) ⁻¹
η_{NO3}	Reduction factor for denitrification
b_H	Rate constant for lysis and decay, d ⁻¹
K_{O2}	Saturation/inhibition coefficient for oxygen, g O ₂ m ⁻³
K_F	Saturation coefficient for growth on S_F , g COD m ⁻³
K_{fe}	Saturation coefficient for fermentation, g COD m ⁻³
K_A	Saturation coefficient for growth on acetate, S_A , g COD m ⁻³
K_{NO3}	Saturation/ inhibition coefficient for nitrate, g N m ⁻³
K_{NH4}	Saturation coefficient for ammonium, g N m ⁻³
K_P	Saturation coefficient for phosphate (nutrient), g P m ⁻³
K_{ALK}	Saturation coefficient for alkalinity (HCO ₃), mol HCO ₃ m ⁻³

Phosphorus accumulating organisms: X_{PAO}

q_{PHA}	Rate constant for storage of X_{PHA} (base X_{PP}), g X_{PHA} (g X_{PAO} d) ⁻¹
q_{PP}	Rate constant for storage of X_{PP} , g X_{PP} (g X_{PAO} d) ⁻¹
μ_{PAO}	Maximum growth rate of X_{PAO} , d ⁻¹
η_{NO3}	Reduction factor for anoxic activity
b_{PAO}	Rate for lysis of X_{PAO} , d ⁻¹
b_{PP}	Rate for lysis of X_{PP} , d ⁻¹
b_{PHA}	Rate for lysis of X_{PHA} , d ⁻¹
K_{O2}	Saturation/inhibition coefficient for oxygen, g O ₂ m ⁻³
K_{NO3}	Saturation/inhibition coefficient for nitrate, g N m ⁻³

K_A	Saturation coefficient for acetate, S_A , g COD m^{-3}
K_{NH4}	Saturation coefficient for ammonium, g N m^{-3}
K_{PS}	Saturation coefficient for phosphorus in storage of X_{PP} , g P m^{-3}
K_P	Saturation coefficient for phosphate, g P m^{-3}
K_{ALK}	Saturation coefficient for alkalinity (HCO_3), mol HCO_3 m^{-3}
K_{PP}	Saturation coefficient for polyphosphate, g X_{PP} (g X_{PAO}) $^{-1}$
K_{MAX}	Maximum ratio of X_{PP}/X_{PAO} , g X_{PP} (g X_{PAO}) $^{-1}$
K_{IPP}	Inhibition coefficient for polyphosphate storage, g X_{PP} (g X_{PAO}) $^{-1}$
K_{PHA}	Saturation coefficient for PHA, g X_{PHA} (g X_{PAO}) $^{-1}$
q_{Gly}	Rate constant for glycogen storage, g X_{GLY} COD (g X_{PAO} COD d) $^{-1}$
K_{GLY}	Saturation coefficient for X_{GLY} , g X_{GLY} COD (g X_{PAO} COD) $^{-1}$
K_{PHAGLY}	Saturation coefficient for X_{PHA} for X_{GLY} storage, g COD (g X_{PAO} COD) $^{-1}$
b_{GLY}	Rate of lysis of X_{GLY} , d $^{-1}$
K_{Mg}	Mg^{2+} saturation constant, g Mg m^{-3}

Nitrifying organisms : X_{AUT}

μ_{AUT}	Maximum growth rate of X_{AUT} , d $^{-1}$
b_{AUT}	Decay rate of X_{AUT} , d $^{-1}$
K_{O2}	Saturation coefficient for oxygen, g O_2 m^{-3}
K_{NH4}	Saturation coefficient for ammonium (substrate), g N m^{-3}
K_{ALK}	Saturation coefficient for alkalinity (HCO_3), mol HCO_3 m^{-3}
K_P	Saturation coefficient for phosphorus, g P m^{-3}

CHAPTER I

INTRODUCTION

1.1 Background

The meat processing industry is one of the major export industries in New Zealand. Total inspected livestock slaughtering was over 30 million in 2000 and 2001 (Meat New Zealand statistical information, 2000 – 2001). The processing of meat requires large quantities of potable water and much of this becomes high strength COD and nutrient contaminated wastewater. A typical New Zealand meat processing industry produces up to $10,000 \text{ m}^3\text{d}^{-1}$ of wastewater with a pollution load equivalent to a city of 60,000 - 100,000 inhabitants (Bhamidimarri, 1991). Currently in New Zealand meat processing wastewater is treated primarily by screens, sedimentation tank or dissolved air floatation and secondarily by pond systems or land irrigation. Even though pond systems remove a substantial amount of organic carbon, nutrient removal is limited (Russell & Cooper, 1992). The biologically treated wastewater which is rich in ammonia nitrogen and nitrate nitrogen causes adverse impacts when discharged into the environment (Slaney & Van Oostrom, 1997).

The nutrient components of meat processing effluents can result in excessive biological growths in receiving waters (eutrophication), reduction of chlorine disinfecting efficiency and adverse public health effects (methemoglobinemia) in the water supply area. The presence of nitrogenous chemicals in water also results in a reduction in the sustainability of that water for industrial reuse due to corrosion and bio-growth in cooling tower and distribution structures (EPA, 1973). Unionized ammonia and hydrogen sulfide are extremely toxic to fish and other aquatic organisms. High concentration of biodegradable organic matter can result in oxygen depletion in rivers. Fat, oil, and grease may cause nuisance slicks on rivers, and the suspended solids and soluble organics contribute to the colour and turbidity of receiving waters. Therefore, treatment of meat processing wastewater has been directed towards the removal of both organic carbon and nutrients, which is a sequential process comprising a number of integrated stages.

Land irrigation of meat processing wastewater is an option as it contains nutrients for plant growth. But the nitrate infiltration rate through soil is high and overloading by

irrigation may cause groundwater pollution, especially in the winter season (Russell *et al.*, 1993). Continuous flow, suspended growth biological treatment processes have amply demonstrated their utility as secondary treatment units. Recently however, more stringent effluent quality requirements have forced industries to find better treatment alternatives such as the Sequencing Batch Reactor (SBR) (Orhon *et al.*, 1986) either as an additional step in the treatment system, or as an operational modification to an existing pond system (Subramaniam *et al.*, 1994; Slaney & Van Oostrom, 1997). The SBR activated sludge process is known to have several advantages over conventional continuous flow reactor systems such as no need for return activated sludge pipes and less land required and less process equipment to maintain, since only one vessel is used for all process operations (Irvine & Ketchum, 1989; Wilderer *et al.*, 2001).

Mathematical models are powerful tools by which the designers of biological wastewater treatment systems can investigate the performance of a number of potential systems under a variety of conditions. There are a number of models that can describe the biological treatment of wastewater. One of these is the Activated Sludge Model No. 1 (ASM 1) which allows prediction of organic matter degradation, nitrification and denitrification in suspended sludge systems (Henze *et al.*, 1987a). The ASM 1 model was a major step forward in modelling activated sludge systems. The phosphorus removal was included in the subsequent Activated Sludge Model No. 2 (ASM 2) by IAWQ Task Group (Henze *et al.*, 1995). Later on, Mino *et al.* (1995) proposed sub models for denitrification and glycogen storing capability of biological phosphorus removing bacteria (Bio-P). Default kinetic and stoichiometric parameters in the ASM 1 and ASM 2 models are based on domestic wastewater. To simulate the SBR performances in the treatment of meat processing wastewater using these models, kinetic and stoichiometric parameters for the wastewater have to be found.

This study aims to develop an effective operating cycle of SBR treatment of simultaneous biological removal of organic carbon and nutrients from meat processing wastewater and to simulate the SBR performance by using the ASM 2 model (Henze *et al.*, 1995) incorporating the sub models proposed by Mino *et al.* (1995) for the denitrifying and glycogen storing capability of Bio-P bacteria. In order to achieve these objectives, the wastewater selected was characterised and a number of key kinetic and stoichiometric parameters were determined.

1.2 Approach taken in this study

The meat processing wastewater for this study was collected from the meat processing plant of Manawatu Beef Packers, Fielding, New Zealand. In order to develop an effective operating cycle of SBR treatment of simultaneous removal of biological organic carbon and nutrients from meat processing wastewater, an SBR was set up in a controlled temperature room.

Chapter II reviews literature relevant to meat processing wastewater and its treatment. The background of biological organic carbon, nitrogen, phosphorus removal, SBR treatment technology, sludge bulking in SBR treatment and modelling of SBR performances are also reviewed.

The methodology utilised for the various experiments conducted and parameters determined in this study are outlined in Chapter III. Also in this chapter, suitable acid extraction conditions for glycogen measurement in the sludge are discussed.

Chapter IV discusses the conventional pollution parameters and the COD fractions of meat processing wastewater.

Chapter V discusses the different SBR operating cycle performances for treating meat processing wastewater for biological organic carbon and nutrients removal. An effective operating cycle for simultaneous removal of organic carbon and nutrients is described in this chapter.

Chapter VI discusses the key kinetic and stoichiometric parameters in Activated Sludge Model No. 1 (ASM 1) and ASM 2 for simulating the biological organic carbon, nitrogen and phosphorus removal from meat processing wastewater. Various processes involved in biological phosphorus removal are also discussed in this chapter. The results are used to modify the ASM 1 and ASM 2 models to suit the SBR treatment of meat processing wastewater and to calibrate and validate the models.

Chapter VII describes the ASM 1 and ASM 2 models. The modification required in the ASM 1 and ASM 2 models for processes involved in meat processing wastewater treatment by SBR are discussed. The calibration and validation of the models are described. Also described in this chapter is the prediction of SBR performance using the calibrated modified ASM 2 model.

A summary and the conclusions of this study together with recommendations for areas of further research are outlined in Chapter VIII.

CHAPTER II

LITERATURE REVIEW

2.1 Introduction

This chapter describes the current treatment technologies for meat processing wastewater, processes involved in these treatment technologies, basics of the SBR and modelling of SBR treatment processes, and summarises the reviews on these aspects.

Characterisation of wastewater is not only important to determine whether or not biological treatment of the wastewater is possible with or without pre treatment but is also necessary for design and operation of treatment processes. Therefore, the sources/types of the meat-works waste and meat wastewater characterisation are described first. In addition, the environmental significance of the discharge of the wastewater and the pollutant discharge limits are discussed, together with current treatment technologies for meat wastewater and the processes involved in these technologies. An in-depth review of the SBR has been included with regard to nitrogen, phosphorous and carbon removal. Finally, mathematical modelling of biological processes used in wastewater treatment especially using SBR is reviewed.

2.2 Sources, types and characteristics of meat processing wastewater

2.2.1 Sources and types of meat-works waste

Different processes in meat-works generate various types of wastes. Also, the contributions of these processes to the content and form of organics and nutrients in these wastes differ. The major portion of wastewater comes from the rendering, paunch processing and stockyard areas of the slaughterhouse. The components of wastes generated and their sources at a typical meat-works are summarised in Table 2.1 (Bhamidimarri, 1991). One of the major phosphorous sources in the wastewater is phosphate-based detergent cleaner (Macfarlane, 1995) as the slaughterhouse floors are washed by detergents, and sprayed by disinfectants and pesticides after the removal of separable solids.

Table 2.1 Constituents and sources of meat wastes (Bhamidimarri, 1991)

Constituent	Source
Proteinaceous matter	Blood washing, meat scraps from slaughterhouse and packaging area.
	Mucoid material from casings section
	Fleshing from fellmongery
	Rendering process drainage
Fat	Floor sweepings from slaughterhouse
	Rendering process
Paunch grass and faecal material	Stockyards
	Gut house
Inorganic chemicals	Fellmongery
	Hide and pelt house

2.2.2 Characteristics of meat processing wastewater

The characteristics of meat processing wastewater primarily depend on the processes at the meat-works and number and type of animals killed (Johns, 1995; Manjunath *et al.*, 2000). The characteristics also depend on the type of management practice related to water use and waste minimisation, particularly improved blood recovery and dry paunch dumping (Johns, 1995). The world-wide typical minimum amount of water usage is 1.3 - 2.5 m³ per beast (Johns, 1995) and about 1/3 of this is needed for lambs and sheep.

Meat processing effluents are highly organic in nature. They are characterised by high levels of organic nitrogen (protein) and fat, and typically contain large amounts of separable material. The characteristics of meat processing wastewater after primary treatment in New Zealand are summarised in Table 2.2 (Cooper & Russell, 1991).

**Table 2.2 Representative characteristics of meat processing plant effluents
(Cooper & Russell, 1991)**

Parameter	Range (mg L ⁻¹)	Representative value (mg L ⁻¹)
5 d biochemical oxygen demand (BOD ₅)	700-1,800	1,000
Chemical oxygen demand (COD)	1,000-3,000	2,000
Total Kjeldahl nitrogen (TKN)	70-180	110
Ammonia nitrogen (NH ₃ - N)	5-50	20
Total suspended solids (TSS)	200-1,200	500
Fat	100-900	400
Total phosphorus	5-20	12

The COD and organic nitrogen of primary treated meat processing effluent can be estimated using the following relationship (Russell, 1980).

$$\text{COD (mg L}^{-1}\text{)} = \text{organic nitrogen (mg L}^{-1}\text{)} \times 9 + \text{fat (mg L}^{-1}\text{)} \times 3 \quad (2.1)$$

$$\text{Organic nitrogen} = \text{TKN} - \text{NH}_3 - \text{N} \quad (2.2)$$

Most of the organic emanates are from blood and offal (Manjunath *et al.*, 2000). The physical nature of the screened (1-mm mesh) effluent COD is reported as 40 - 50 % of coarse suspended matter, which is insoluble and only slowly biodegradable, and the remainder as colloidal and soluble matter (Sayed *et al.*, 1987). This is different from domestic wastewater, in which the COD is present mainly in colloidal form. Wastewater COD is subdivided into readily biodegradable, slowly biodegradable and inert COD in activated sludge models (Henze *et al.*, 1987a; Henze *et al.*, 1995). Readily biodegradable COD (RBCOD) is the only substrate component considered to be directly related to microbial growth in the models. The RBCOD fraction in wastewater varies with the type of primary treatment, sampling time and storage period before it is analysed. The RBCOD content of meat processing plant effluent after primary treatment by sedimentation varies from 15 - 17 % of the total COD of the wastewater (Chang, 1999). However it is only 13 % of the total COD of an integrated meat processing wastewater after primary treatment by air floatation (Gorgun *et al.*, 1995). The slowly biodegradable COD is over 70 % of the total COD, in which roughly 1/3 is in the soluble/fine colloidal form and the remaining 2/3 is in the particulate form (Chang,

1999). The same author also reported that 10 % of the total COD was inert. Bickers and Van Oostrom (2000) found that the RBCOD in the paunch liquor (generated from gut house) and stick water (generated from rendering plant) was 315 mg L^{-1} and 2145 mg L^{-1} respectively, and that slaughterhouse wastewater and dilute blood contained little or no significant amount of RBCOD.

Independent rendering plant wastewater characteristics are quite different from those from an integrated slaughterhouse (Cooper & Russell, 1988; Metzner & Temper, 1990). Rendering plant wastewater is high in BOD and nitrogen concentrations (largely as ammonia), but low in phosphorus, in contrast to slaughterhouse wastewater (Frose & Kayser, 1985).

The temperature of slaughterhouse effluent varies significantly. In New Zealand it varies seasonally between $25 - 28^{\circ}\text{C}$ in summer and $15 - 18^{\circ}\text{C}$ in winter. In Europe it is frequently cool (20°C) in contrast to Australian effluent, which is routinely $30 - 35^{\circ}\text{C}$, but it can be even hotter in sub-tropical areas (Johns, 1995). The ammonia nitrogen concentrations may vary significantly between winter and summer, due to the more extensive degradation of raw material in summer, which boosts the levels of ammonia nitrogen (Johns, 1995).

2.3 Environmental significance of meat processing wastewater discharge

The nutrient components of meat processing effluents can result in excessive biological growth in receiving waters (eutrophication). Eutrophication has caused serious deterioration of many lakes and rivers around the world. Ammonia nitrogen acts as a primary nutrient that may stimulate phytoplankton and plant growth (Orhon & Artan, 1994). Nitrate is also a major nutrient, which-in excessive amounts-may induce prolific growth. Algae blooms occur if the concentration of inorganic nitrogen and phosphorus exceed respective values of 0.3 mg L^{-1} and 0.01 mg L^{-1} (Metcalf & Eddy, 1991). The decay and the decomposition of these plants and phytoplanktons result in odour, sediment and depletion of dissolved oxygen (DO). Depletion of DO affects the respiration of fish, benthic aquatic animals, and attached plant growth. This suffocation of aquatic aerobiosis results in both economic losses to the fishery industry and losses of bio-diversity in aquatic ecosystems.

In addition to the nutrients, the decaying of sediments of suspended solids from meat processing wastewater produces toxic products in anaerobic conditions. The degradation and decay of these sediments in anaerobic conditions produce hydrogen sulphide and unionised ammonia, which affect fish and shellfish. Free ammonia has shown acute toxicity to fish at TL_{50} (tolerance limit) values ranging from 0.083 to 4.6 $mg L^{-1}$ (EPA, 1985). Nitrification products in drinking water are related to methemoglobinemia (blue baby syndrome) and carcinogenesis (EPA, 1993). The EPA has set a maximum contamination level of 10 ppm for nitrate nitrogen in public water supplies. The presence of nitrogenous chemicals in water also results in a reduction in the sustainability of that water for industrial reuse due to corrosion and bio-growth in cooling tower and distribution structures (Barnes & Bliss, 1983). Fat, oil, and grease may cause nuisance slicks on rivers, and the suspended solids and soluble organics contribute to the colour and turbidity of receiving waters

There are regulations for the discharge of wastewater to water bodies in order to control pollution. In New Zealand, there is no fixed discharge effluent quality limit for industrial wastewater. The wastewater discharge quality limit depends on the local conditions of the industry site. Scandinavian countries have stringent effluent quality criteria (Henze, 1991). The limits enforced by the Danish wastewater action plan are: chemical oxygen demand (COD) $< 75 mg L^{-1}$, biochemical oxygen demand (BOD) $< 15 mg L^{-1}$, total nitrogen (TN) $< 8 mg L^{-1}$ and total phosphorus (TP) $< 1.5 mg L^{-1}$. These regulation limits set by EU are: TN $< 15 mg N L^{-1}$ and TP $< 2 mg P L^{-1}$ (Orhon & Artan, 1994).

2.4 Treatment technologies for meat processing wastewater

Treatment methods for meat processing wastewater can be categorized into primary, secondary and tertiary treatments. An example of a meat processing wastewater treatment system is shown in Figure 2.1 (Mikkelson & Lowery, 1992).

2.4.1 Primary treatment

The effectiveness of the meat processing wastewater treatment depends largely on the primary treatment system. The purpose of primary treatment is the removal of suspended solids and fats, oil and greases from slaughterhouse wastewater. Screening, settling (saveall) and dissolved air flotation (DAF) are widely used for these purposes.

Screening is simply entrapping the gross solid particles typically by a 0.5 – 2 mm sieve. A variety of screen types are used by the meat industry such as stationary, shaker and rotating screens. The screen material may be a woven wire or a wedge wire depending on the application. Manure is best removed by a shaker screen, and a revolving wedge-wire trommel screen removes the remaining wastes. Gross solids recovered from the screening process are transferred to the rendering department for processing without delay (Husband, 1995a).

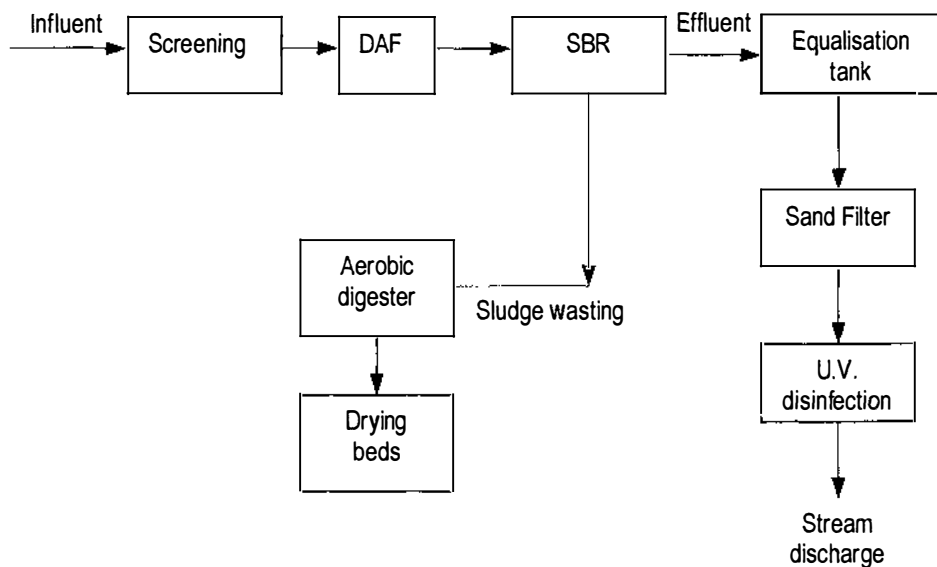


Figure 2.1 Schematic diagram of a meat processing wastewater treatment system (Mikkelsen & Lowery, 1992)

Following the effective removal of gross solids by screen, the effluent is passed through a settling tank. Settling is used on the principle that natural forces can float the fat and settle out the solids. During settling, the bulk of the remaining fat and settleable solids is removed. The recovered fats can be used to produce tallow. The settling tank can be a simple catch pit for the removal of fats and solids either manually or by a complex designed unit with top and bottom scrapers to remove fats and solids continuously. The performance of a settling tank depends on the effluent velocity, elimination of short-circuiting, a sufficient settling path, minimised turbulence induced by scrapers and the overflow rate (optimum - approximately $0.8 \text{ m}^3 (\text{m}^2\text{d})^{-1}$). A well-designed and managed settling tank can remove 85 % of the effluent fats. However, higher detention time and higher temperature effluent can reduce the efficiency of a settling tank (Husband, 1995a).

DAF operates on the same principle of a settling tank. However, it has improved performance by the use of fine air bubbles to assist the floatation of the floatable material. The fine air bubbles are formed when dissolved air in the solution under pressure is released with the incoming effluent at normal pressure in the floatation tank. Saturated air solution is formed with fresh water or recycled effluent from the DAF. Air to solids ratio has a significant influence in the performance of a DAF unit. Generally, an air to solids ratio of 0.03 is necessary to achieve good separation and recovery of fat and solids. A DAF unit can perform well at a loading rate between $9 - 12 \text{ m}^3 (\text{m}^2 \text{ h})^{-1}$. From a properly designed and well-managed DAF, more than 90 % fat and 70 % solid removal can be expected (Husband, 1995a). In the late 1970s large DAF units fitted with chemical precipitation were introduced into New Zealand, Europe and US for protein recovery from wastewater. This unit gave 75 – 80 % BOD₅ reduction (Hopwood, 1977) and had the additional advantage of removing large quantities of nitrogen and phosphorus. Most systems, however, had considerable operating problems including long retention times and low surface-overflow rate, which led to solids settling, large volumes of putrefactive and bulky sludge (0.8 - 1.2 kg dry sludge per kg BOD₅ removed), sensitivity of the system to flocculation and difficulties in sludge dewatering (Stebor *et al.*, 1990). Therefore, to overcome the problems in operating the DAF units, different modifications were done such as H₂O₂ was used with air instead of air only (Bremmell *et al.*, 1994; Green *et al.*, 1981; Steiner & Gec, 1992; Travers & Lovett, 1985).

Primary effluent treatment is far cheaper than the subsequent secondary or tertiary treatment and the recovered primary treatment solids and fat have saleable value (Johns, 1995).

2.4.2 Secondary treatment

Primary treated effluent is passed into the secondary treatment system. The main purpose of secondary treatment is to remove organic carbon and nutrient in the effluent after the removal of fats and solids in the primary treatment process. The secondary treatment system can be based on either a physicochemical process or a biological process.

2.4.2.1 Physicochemical treatment (PCT)

After the primary treatment the remaining colloidal dispersed protein and fat particles are suspended in the water and will not settle out of their own accord due to surface charge. The charge, which is normally negative around the particles, is removed by adding acid (sulphuric acid or hydrochloric acid) which lowers pH and/or by adding polyvalent cations such as iron (Fe^{3+}) or aluminium (Al^{3+}). This is known as *coagulation*. The neutralised particles can come together, form flocs and settle. Flocculation can be assisted by the addition of polyelectrolytes. Among several approaches considered for chemical treatment, the polyelectrolyte process, hexametaphosphate (HMP) process and lignansulphonate process are the main approaches. The optimum pH for the polyelectrolyte process, HMP process and lignansulphonate process are 5.0 - 5.5, 3.5 and 3.0 respectively. The cost of the HMP process is less than that of the polyelectrolyte process, and this process does not need extensive preliminary treatment to keep the cost down. In both processes, coagulated effluent is passed to a DAF unit for solid separation. Lignansulphonate is a better flocculating agent in terms of effectiveness in removing the BOD and the resistance of floc to shear. It can remove 90 % BOD of meat-work effluents. Its sludge can be processed directly into an ingredient for animal feed. But it is more costly than other flocculating agents. Sometimes, a two-stage pH adjustment can produce superior effluent compared to a single stage. To raise the pH, calcium hydroxide is used as an alkali (Husband, 1995b).

Physicochemical methods for nitrogen removal from wastewater include ammonia stripping and breakpoint chlorination. Ammonia stripping has been adopted to remove ammonia from rendering-plant wastewater using an aerated pond with lime addition (Kaszas *et al.*, 1992). However, in general it is not economical because of the large wastewater volumes of slaughterhouses, the high buffering capacity of the wastewater and the possibility of stripping offensive odours (Johns, 1995). Break point chlorination has also been used to remove ammonia - nitrogen (Witmayer *et al.*, 1985). However the formation of trihalomethane and other chlorinated organics during this process is of concern to the regulatory bodies (Kaszas *et al.*, 1992).

Chemical precipitation coupled with biological phosphorous removal is required to achieve very low phosphorus limits (Farrimond & Upton, 1993; Van Starckenburg *et al.*,

1993). Chemical precipitation plants are often added as a precautionary measure to biological nutrient removal (BNR) plants. The achievable limit of phosphorus by precipitation is about 0.3 mg L^{-1} which can be further reduced to $0.1 - 0.2 \text{ mg L}^{-1}$ if the effluent is subsequently treated by slow sand filters (Anon, 1987).

Plant can be located within a building to avoid any adverse effects on the environment. Together with an efficient primary treatment system, a final effluent can be produced such that it can be discharged to most of the municipal sewerage systems. Physicochemical treatment has some disadvantages, too. Its running cost is very high. A relatively large volume of sludge has to be handled. The sludge handling could be a significant cost either in terms of equipment to de-water and dispose of the material, or in removing the water during the rendering process (Husband, 1995b).

2.4.2.2 Biological treatment

Biological wastewater treatment is a process in which the microorganisms, in the presence of nutrients, convert the colloidal and soluble organic matters into gaseous products and cell tissue. Biologically, with proper analysis and environmental control, almost all wastewater can be treated (Metcalf & Eddy, 1991). Meat processing wastewater contains organic carbon and nutrients required for biological growth. Therefore, biological treatment has been commonly used in the meat processing industry (Cooper & Russell, 1991). In biological treatment, bacteria are the most important microorganisms and the protozoa, fungi, metazoan and algae are of secondary importance. A number of biologically dependent conversions such as biological growth, hydrolysis, decay and adsorption are of vital importance in biological treatment processes. Simplified bisubstrate and trisubstrate models describing the biological breakdown of organic matter by microorganism are shown in Figure 2.2 (Henze, 2002). A bisubstrate model can be used in the process description of conventional activated sludge plants, nitrifying and denitrifying plants and anaerobic plants. A trisubstrate model is particularly applicable for the description of biological phosphorus removal, but it could also be used for describing nitrogen removal. Biological treatment processes can be subdivided into anaerobic and aerobic processes.

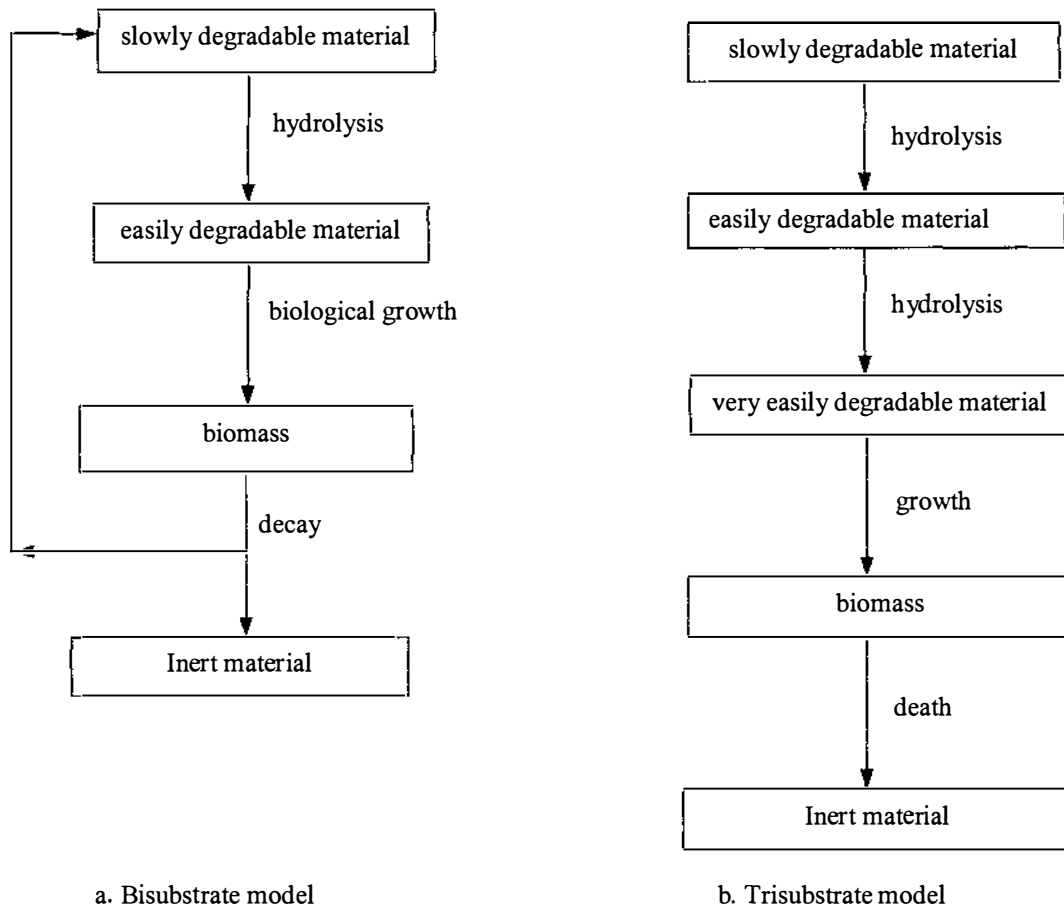


Figure 2.2 Biological breakdown of organic matters (Henze, 2002)

2.4.2.2.1 Anaerobic biological wastewater treatment

Anaerobic processes are carried out by a large and varied group of microorganisms which normally live in a symbiotic relationship. Most of the anaerobic bacteria like methane-forming bacteria are strictly anaerobic and thus cannot tolerate oxygen (Henze, 2002). In anaerobic biodegradation, complex organic matter is converted, in a series of steps, to end products—mostly methane (CH_4), carbon dioxide (CO_2), small quantities of hydrogen sulphide (H_2S) and hydrogen (H_2) (Figure 2.3). In the first step, carbohydrates, proteins and lipids are hydrolysed by extracellular enzymes into smaller units such as amino acids, sugars, triglycerides and fatty acids. In the second step, acidogenesis, these smaller units are further subjected to fermentation, β -oxidations, and other metabolic processes that lead to the formation of simple organic compounds, mainly short chain acids (e.g., acetic, propionic, butyric) and alcohols. In the third step, acetogenesis, intermediate products other than acetate and H_2 gas are transformed into acetate and H_2 gas by acetogenic bacteria. In the fourth step, methanogenesis, the end

product methane is produced either from decarboxylation of acetate by acetoclastic methanogens or through H_2 oxidation by H_2 utilising methanogens.

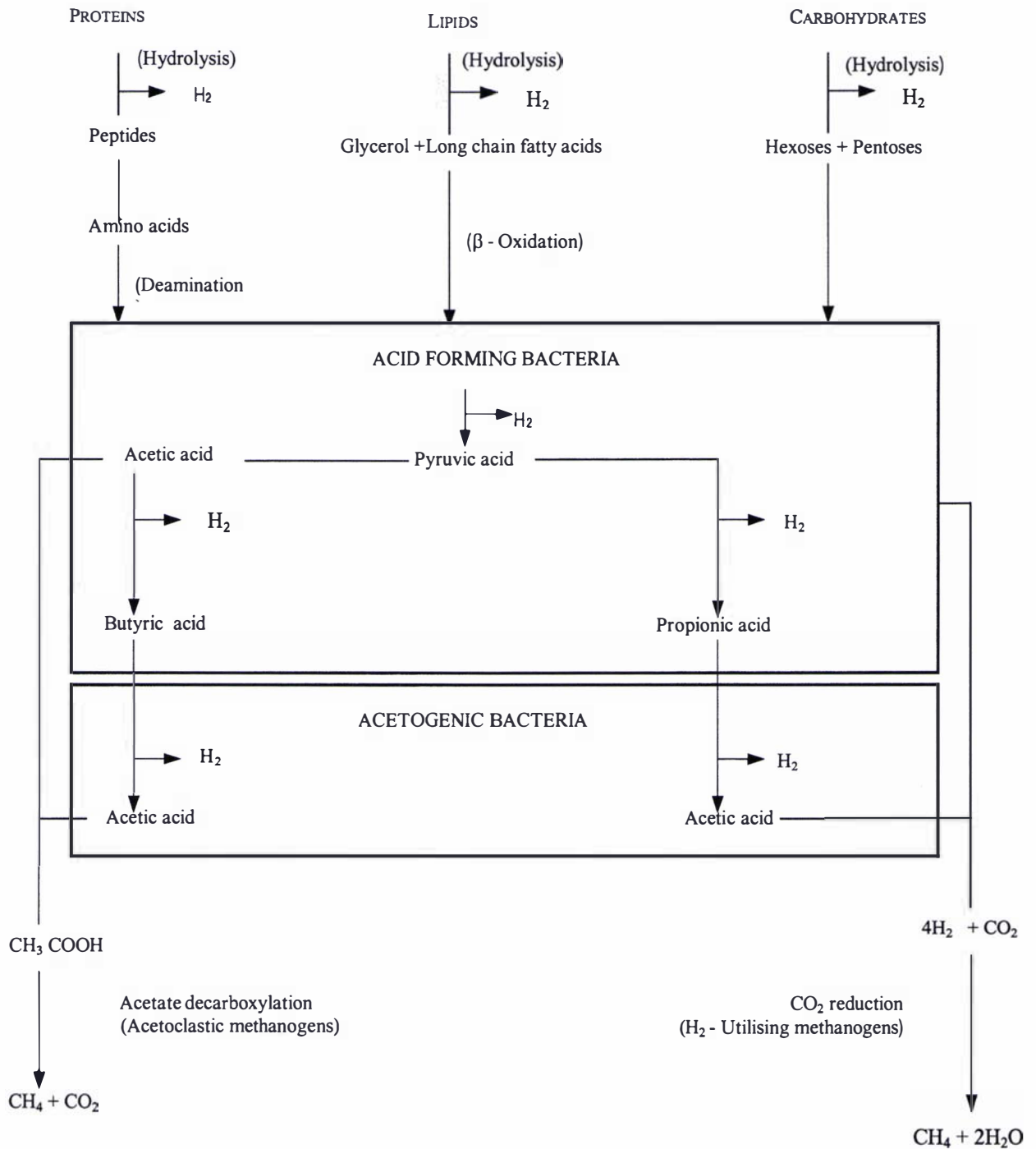


Figure 2.3 An outline of the anaerobic process (Manderson, 2000)

The anaerobic treatment processes are very sensitive to environmental conditions such as pH, temperature and dissolved oxygen (DO). The pH range of the aqueous environment in anaerobic reactors is optimum between 6.6 – 7.6. Below pH 6.2 the methane bacteria do not function (Metcalf & Eddy, 1991). In anaerobic wastewater treatment, methanogenesis from acetate has been shown to be the rate-limiting step.

Anaerobic wastewater treatment has some advantages and disadvantages compared with aerobic treatment (Bhamidimarri, 1991; Cooper & Russell, 1991; EPA, 1993; Metcalf & Eddy, 1991).

The advantages of the anaerobic treatment system are:

1. Capital costs and power consumption are lower since aeration is not required.
2. Methane gas, the end product of anaerobic processes, is economically valuable.
3. The biomass yield for anaerobic processes is much lower than that for aerobic systems; thus, less biomass is produced per unit of organic material used. This reduced biomass means savings in excess sludge handling and disposal and lower nitrogen and phosphorus requirements. The sludge produced is highly stabilised and more easily dewatered.
4. Higher influent organic loading is possible for anaerobic systems than for aerobic systems because the anaerobic process is not limited by the oxygen transfer capability at the high-oxygen utilisation rates in aerobic processes.
5. The acclimated sludge can be stored for long periods without deterioration.

The disadvantages of the treatment system are:

1. It requires a relatively larger reactor for long retention time due to the slow growth rate of anaerobic bacteria.
2. Energy is required by way of elevated reactor temperatures to maintain microbial activity at a practical rate.
3. Undesirable odours may be produced in anaerobic processes due to the production of H₂S gas and mercaptans.
4. Complete removal of nitrogen cannot be achieved.

5. Toxic gases such as ammonia and hydrogen sulfide are also produced during the treatment, which are harmful to methane-forming bacteria. Failure of anaerobic treatment has been observed during high concentration of sulphur in the wastewater.
6. Anaerobic bacteria are very sensitive to pH, DO, temperature, excessive oil and grease, finely dispersed colloidal material, heavy metals, anionic detergents and high cation concentration such as Na and Ca and shock loads.

Anaerobic lagoons have been widely used as anaerobic systems to treat meat processing wastewater. They have low construction and operating costs. The designed organic loading of anaerobic lagoons, treating meat processing wastewater is between $0.042 \text{ kg BOD}_5 (\text{m}^3\text{d})^{-1}$ and $0.382 \text{ kg BOD}_5 (\text{m}^3\text{d})^{-1}$. At these loading rates BOD_5 removal range is between 58 and 95 %. The depth of lagoons is typically between 4 to 7 m. Table 2.3 shows the performance of an anaerobic lagoon receiving meat processing wastewater at an average hydraulic retention time (HRT) of 11 d and lagoon temperatures of $20^\circ - 25^\circ\text{C}$ (Russell & Cooper, 1992). Synthetic floating covers have been installed in anaerobic lagoons to trap the odour and biogas (Dague *et al.*, 1990; Safley & Westerman, 1992).

Table 2.3 Performance of an anaerobic lagoon receiving meat processing wastewater (Russell & Cooper, 1992)

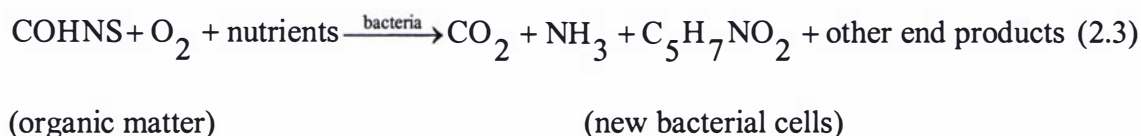
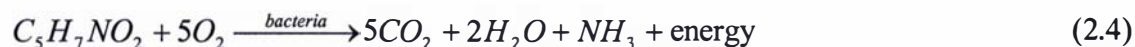
Product	Influent (mg L^{-1})	Effluent (mg L^{-1})	Removal (%)
COD	1385	355	74
Soluble COD	595	190	68
TSS	450	155	66
TKN	80	85	-
$\text{NH}_3 - \text{N}$	24	58	-
Organic N	56	27	52
Fat	210	45	79

High rate systems such as anaerobic filters (AF), anaerobic contact reactors (AC) and up flow anaerobic sludge blanket reactors (UASB) have also been used to treat meat processing wastewater. The advantages of these high rate systems are that they take up little land area and they are totally enclosed. Because they are enclosed, odours cannot escape, so the systems can be used in urban areas, and the methane gas generated by the microorganisms can be easily collected and utilised (Johns, 1995). But most of them have been experiencing failure mostly when the sulphur content is high (Bhamidimarri, 1991).

2.4.2.2.2 Aerobic biological treatment

The aerobic biological process requires DO in the wastewater. The aerobic processes in treatment plants are carried out by very large and diversified groups of microorganisms such as *Pseudomonas*, *Flavobacterium*, *Micrococcus*, and *Aeromonas* (Henze, 2002). Aerobic biological treatment involves removal of organic carbon, nitrogen and phosphorus from the wastewater. In this section only the carbon removal is described and the nitrogen and phosphorous removal are explained in Section 2.4.2.2.3 and 2.4.2.2.4 respectively. Aerobic treatment processes are classified into suspended growth or attached growth processes. In activated sludge processes, the microorganisms involved in the processes are maintained in suspension. Activated sludge process, aerated lagoons and Sequencing Batch Reactor (SBR) use the principle of the suspended growth biological wastewater treatment process for the removal of carbonaceous organic matter. The SBR treatment system is discussed later, in Section 2.5.

The activated sludge process is an established aerobic biological process in which bacteria and other microorganisms break down complex organic material into more simple and stable substances, thereby removing soluble and suspended organic polluting matter from wastewater. The principal elements are the aeration tank where effluent is thoroughly mixed with activated sludge and air and a final settling tank where the settled sludge is removed from the purified water to be recycled by the return-activated sludge pumps. When sludge is recycled, a portion of the settled biomass returns to the aerobic reactor to maintain the desired concentration of biomass in the aerobic biological reactor. Another portion is wasted to control the design solids retention time (SRT) (Metcalf & Eddy, 1991). During the breakdown of the organic substrate, a portion of the energy obtained from the reaction is used for biological synthesis and the remainder satisfies the energy required for growth. A small portion of the energy is used for cellular maintenance. The organisms also undergo progressive autooxidation in their cellular mass (Metcalf & Eddy, 1991). In the reactor, the bacterial culture carries out the conversion in general accordance with the stoichiometry shown in Equation 2.3 and Equation 2.4 (Metcalf & Eddy, 1991).

Oxidation and synthesis:**Endogenous respiration:**

For treating the meat processing wastewater by an activated sludge system the DO concentration in the aerobic reactor should be high enough to biodegrade the slowly biodegradable substrates such as fat and to avoid poorly settling sludge. Hopwood (1977) reported poor settling floc in activated sludge systems while treating slaughterhouse wastewater. This was found to be due to a combination of the high fat content of the influent and a low DO concentration in the activated sludge reactor. Travers and Lovett (1984) found that at low DO ($< 0.5 \text{ mg L}^{-1}$), fat degradation was inhibited (56 % removal). This led to poorly settling sludges (SVI $> 250 \text{ ml g}^{-1}$) with a high fat concentration and excessive numbers of filamentous microorganisms. In contrast, high DO concentrations (up to 4 mg L^{-1}) correlated with rapid fat degradation (90 % removal), better settling sludge and fewer filamentous microorganisms (Travers & Lovett, 1984). More than 95 % ammonia removal (Green *et al.*, 1981; Witmayer *et al.*, 1985) was achieved in biological carbon removal activated sludge plants of slaughterhouse and rendering plant wastewater treatment when the DO concentration was above 2.0 mg L^{-1} and the temperature was above 10°C .

Design criteria for activated sludge treatment of slaughterhouse wastewater are widely published (Heddle, 1979; Hopwood, 1977; Lovett *et al.*, 1984; Travers & Lovett, 1984). Most systems are of the extended aeration type to minimise sludge production. French design criteria for activated sludge systems treating slaughterhouse wastewater recommend the organic loading rate of $0.3 - 0.35 \text{ kg BOD}_5 (\text{m}^3 \cdot \text{d})^{-1}$ in the design of an activated sludge treatment system (Johns, 1995).

An aerated lagoon is a basin in which the wastewater is treated either on a flow through basis or with solids recycling. The solids recycling system is similar to a modified activated sludge system. The solids in the effluent of the aerated lagoon are composed of a portion of the incoming suspended solids, the biological solids produced

from waste conversion, and occasionally small amounts of algae (Metcalf & Eddy, 1991).

Advantages of aerobic treatment compared to anaerobic treatment are (Metcalf & Eddy, 1991; Greenfield & Johns, 1995):

1. Aerobic processes provide the oxygen required for microbial nitrification by which ammonia is converted first to nitrite and then to nitrate.
2. Provides a high quality effluent in terms of carbonaceous and nitrogenous BOD.
3. Simple and low capital cost.

Disadvantages of aerobic treatment compared to anaerobic treatment are:

1. Energy intensive treatment process as energy is required for maintenance of adequate concentration of dissolved oxygen and for mechanical mixing.
2. Aerobic processes involve high sludge yields and high nutrient requirement.
3. System performance is likely to be impaired by flow and load transients.
4. When dealing with strong wastes, system tends to be ineffective.

Aerobic biological carbon removal kinetic and stoichiometric parameters are important in design aspects such as solids residence time and sludge production rates. Kinetic parameters are also of interest due to the variations that have been attributed to the dominant microorganism type present and reactor configuration imposed. Also, current mathematical models require kinetic and stoichiometric parameters related to that wastewater. The key kinetic and stoichiometric parameters are variously reported in the literature. The half saturation constant, maximum specific growth rate, aerobic yield and endogenous decay rate of heterotrophs were 10 - 176 mg COD L⁻¹, 1.14 - 4.2 d⁻¹, 0.4 - 0.45 mg VSS (mg COD)⁻¹ and 0.043 - 0.49 d⁻¹ respectively determined for the meat processing wastewater (Annachatre and Bhamidimarri, 1993; Chang, 1999; Gorgun *et al.*, 1995). These parameters depend on the wastewater, reactor configuration and the loading pattern (Ekama *et al.*, 1986).

2.4.2.2.3 Biological processes of nitrogen removal

The microbial oxidation of ammonium and reduction of nitrate or nitrite was first reported at the end of the 19th century (Van Loosdrecht & Jetten, 1998).

The relevant transformations that are likely to occur in the biological nitrogen removal mechanism of wastewater are summarised below (Orhon & Artan, 1994).

1. The microbial degradation of nitrogen-containing compounds and the release of nitrogen as ammonia, mainly through deamination reactions.
2. The incorporation of nitrogen into cells by synthesis and its removal by excess sludge (8 – 12 % of VSS).
3. The microbially mediated redox transformations, including nitrification and denitrification.

Microbial nitrogen removal can take place with alternating periods of aerobic and anoxic conditions. Organic nitrogen is firstly deaminated to ammonia nitrogen by enzymatic reactions and the process is defined as *ammonification*. The ammonification process is the rate limiting step in the reaction pathway and has been determined to be a first order reaction (Wong-Chong & Loehr, 1975) with an average rate constant at 20°C and pH 6.5 to 9.0 of 0.111h^{-1} , reaching a maximum of 0.240h^{-1} at pH 8.0. The rate of ammonification is dependent on both the concentration and form of organic nitrogen supplied. Ammonification of soluble organic nitrogen compounds, except urea, is assumed to be dependent on the availability of terminal electron acceptors (Oles & Wilderer, 1991). There should be a difference in the rate of ammonification during aerobic and anoxic conditions. When sufficient oxygen is supplied, most of the ammonia nitrogen is then oxidised by nitrifying microorganisms (mainly *Nitrosomonas* and *Nitrobacters*) to nitrite and nitrate, with a small portion of it being assimilated into microbial cells. When conditions are anoxic, denitrifiers (facultative heterotrophs) convert oxidised nitrogen to nitrogen gas (Orhon & Artan, 1994). Figure 2.4 shows the possible microbial nitrogen conversions (Van Loosdrecht & Jetten, 1998).

A range of microbial processes has been reported to occur in wastewater treatment plants, for example aerobic denitrification, heterotrophic nitrification, anaerobic ammonium oxidation (ANAMMOX) (Van Loosdrecht & Jetten, 1998) and denitrification by autotrophic nitrifying bacteria (Bock *et al.*, 1995; Schmidt and Bock, 1997).

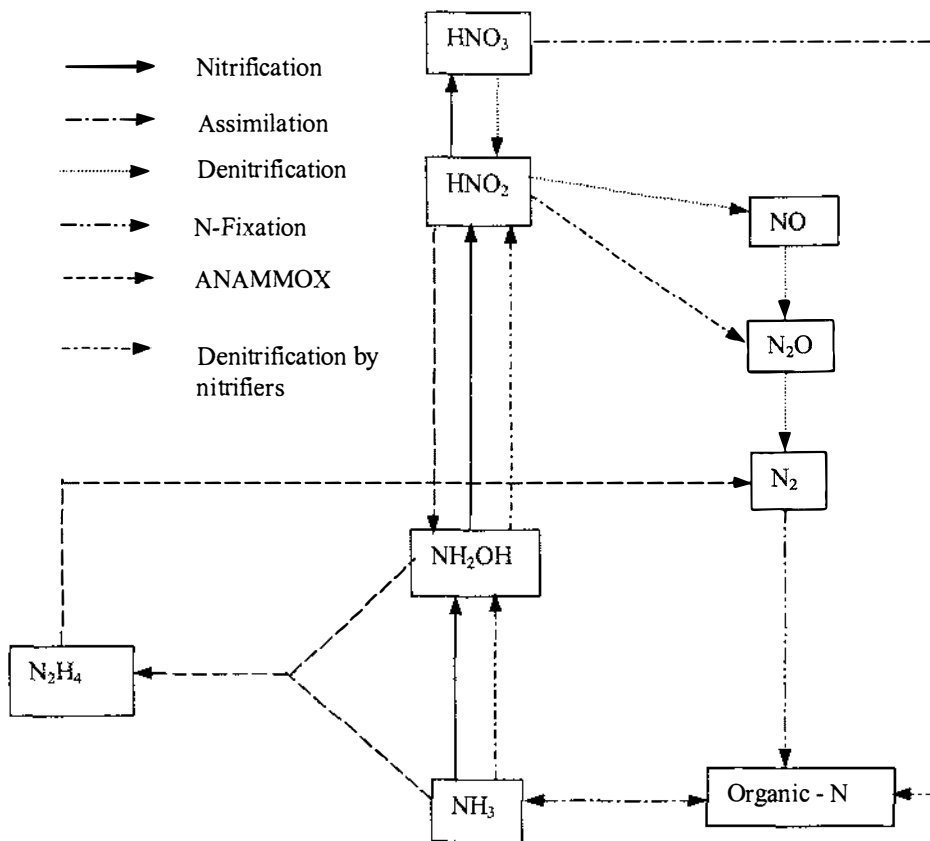
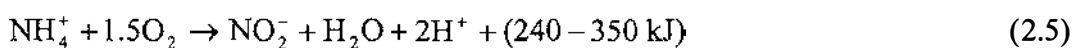


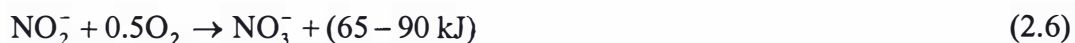
Figure 2.4 Possible microbial nitrogen conversions (Van Loosdrecht & Jetten, 1998)

Rates described for aerobic denitrification or denitrification by autotrophic nitrifiers are so low that these conversions probably do not play a significant role under practical conditions. Heterotrophic nitrification may be of relevance only when the wastewater contains a high COD/N ratio (> 10). Anaerobic ammonium oxidation can occur in fully autotrophic systems with very long sludge retention times or in biofilms systems. This conversion offers great opportunity since it allows denitrification using ammonium as an electron donor, that is no organic substrate is added in the nitrogen removal process (Van Loosdrecht & Jetten, 1998).

Nitrification:

The principal microbes of nitrification in a natural system are *Nitrosomanas* and *Nitrobacter*, which oxidise ammonia sequentially to nitrite (nitrification), given by the Equation 2.5 and nitrate (nitrification), by the Equation 2.6 (Barnes & Bliss, 1983).





These are classified as *chemo-autotrophic* bacteria as the energy released in these reactions is used by the organisms to synthesise their organic requirements from inorganic carbon sources such as carbon dioxide, bicarbonate and carbonate. Therefore the alkalinity is consumed during nitrification, with values of 7.14 to 8.64 g alkalinity g $\text{NH}_3 - \text{N}^{-1}$. There are other autotrophic bacteria genera capable of obtaining energy from the oxidation of ammonia (Barnes & Bliss, 1983). Focht and Chang (1975) indicated the possibility of heterotrophic nitrification by diverse genera of bacteria, fungi, and actinomycetes. However the autotrophic nitrification rate is about ten times greater than heterotrophic nitrification (Barnes & Bliss, 1983).

Nitrifiers are very sensitive to environmental factors and inhibitors. For example, in kinetic experiments, reaction from ammonium to hydroxylamine can be inhibited by thiourea and the reaction from hydroxylamine to nitrite can be inhibited by hydrazine (Sharma & Ahlert, 1977). Apart from the energy substrate nitrogen, nitrifier growth can also be limited by the availability of the growth substrate, inorganic carbon, or the terminal electron acceptor, DO. In wastewater treatment systems CO_2 is present in excess as a result of carbonaceous oxidation. Dissolved oxygen, however, is frequently present at a level at which nitrifier growth is less than the maximum value. Normally nitrification systems are operated at high DO concentrations because bulk liquid DO concentrations below 0.5 to 2 mg L^{-1} inhibit nitrification (EPA, 1993).

The optimum pH for nitrification has been variously reported to be between 7.5 and 8.6 (Metcalf & Eddy, 1991) and 7.0 to 8.2, with a maximum at 7.9 (Antoniou *et al.*, 1990). Temperature also exerts a tremendous influence on the growth of nitrifying bacteria. For temperature correction on nitrification rate, an Arrhenius temperature dependency coefficient, 1.083 was found by Bickers (1996a) for meat processing wastewater.

Both reactions of ammonia and nitrite oxidation were determined to be zero order when the ammonia concentration was above 2 mg L^{-1} (Argaman & Brenner, 1986; Harremoes & Sinkjaer, 1995; Wong-Chong & Loehr, 1975). The ammonia oxidation rate constant was maximum at pH 7.5 to 7.8 (Antoniou *et al.*, 1990; Wong-Chong and Loehr, 1975), while the nitrite oxidation rate constant increased up to a pH of 9. As the ammonium oxidation reaction is generally considered the rate limiting step, significant

nitrite concentrations are not normally observed; however at high pH and ammonium concentration (Azimi & Horan, 1991; Münch *et al.*, 1996; Wong-Chong & Loehr, 1975) or in the transient conditions, the increase in the ammonia oxidation rate (Stenstrom & Song, 1991) was suggested as being responsible for nitrite accumulation in reactors.

A range of nitrification rates has been measured in practice with Argaman and Brenner (1986) having recorded a specific nitrification rate of $95.8 \text{ mg N (g MLVSS)}^{-1} \text{ h}^{-1}$; and Metcalf and Eddy (1991) of between 2.08 and $25.0 \text{ mg N (g MLVSS)}^{-1} \text{ h}^{-1}$. Specific nitrification rates of between 1.3 and $7.8 \text{ mg N (g MLVSS)}^{-1} \text{ h}^{-1}$ were measured by McClintock *et al.* (1993), with the rate generally found to decrease as the SRT was increased. Bickers (1996a) found the nitrification rate on meat balance pond effluent as $1.97 \text{ mg N (g MLVSS)}^{-1} \text{ h}^{-1}$.

The net energy produced in nitrite oxidation is much less than that produced in ammonium oxidation. Therefore the cell yield for *Nitrobacter* is less than that of *Nitrosomanas* for each amount of nitrogen oxidised (Sharma & Ahlert, 1977). The maximum specific growth rate of autotrophs was $0.56 - 0.78 \text{ d}^{-1}$ in meat processing wastewater at 20°C (Chang, 1999; Sözen *et al.*, 1996).

Nitrifying bacteria grow much more slowly than the rate required for organic carbon removal. Thus a much higher aerobic SRT is required to allow the necessary nitrifying bacteria to grow in activated sludge processes. The results, if no other adjustments are made on SRT, are a much larger suspended solids inventory, requiring construction of much larger biological reactors having a high HRT (Daiger & Parker, 2000).

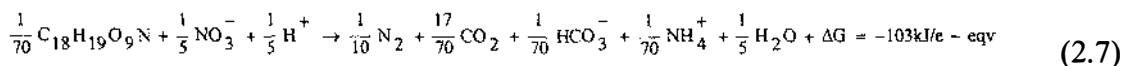
For the nitrogen removal process it is beneficial if ammonium is oxidised only to nitrite and thereafter denitrified. Many experiments have been performed to do this. Most often a change in pH has been reported to inhibit the nitrite oxidisers (Abeling & Seyfried, 1992; Anthonisen *et al.*, 1976; Turk & Mavinic, 1989). A small change in pH can have a rather strong effect on the concentration of ammonia and nitric acid which are toxic to the *Nitrobacter* bacteria (Hellinga *et al.*, 1998). A second option is the washout of nitrite oxidisers based on growth rate. At elevated temperatures ($> 15^\circ\text{C}$) the ammonium oxidising bacteria have a higher growth rate than the nitrite oxidisers. Controlling the sludge age is a good operating procedure for a stable partial nitrification (Beccari *et al.*, 1979; Hellinga *et al.*, 1998; Randall & Buth, 1984). Also substrate competition can be used to out-compete nitrite oxidisers. The lower affinity of oxygen

for nitrite oxidisers compared to ammonium oxidisers can be used to selectively restrict the growth of nitrite oxidisers (Hanaki *et al.*, 1990; Laanbroek & Gerards, 1993; Turk & Mavinic, 1989). Denitrification of nitrite will also decrease the growth of nitrite oxidisers. This can be achieved by creating anoxic conditions inside the flocs or by rapid circulation between aerobic and anoxic conditions. Operating the treatment plant at low DO concentration can lead to a stable situation where nitrite oxidisers are out-competed (Van Loosdrecht *et al.*, 1998).

Denitrification:

Denitrification is the reduction of nitrate to nitrogen gas. The process is anaerobic, as nitrate is the oxidising agent (Henze, 2002). Denitrification occurs where nitrate and no or low oxygen concentrations are present at the same time. The conversion of nitrate to nitrogen gas has many intermediates including HNO₂, NO, and N₂O. Denitrification requires an electron donor (COD), which can be an organic material or reduced compounds such as sulphide or hydrogen. Under electron donor limitation these intermediates can be readily formed. Moreover, when cells are subject to transitions between aerobic and anoxic conditions, formation of these intermediates is enhanced (Otte *et al.*, 1996; Van Bentum *et al.*, 1998).

The energy yielding process for denitrifying bacteria which uses organic matter in wastewater as an energy and carbon source can be written as (Henze, 2002),



If all the energy is used for growth, the maximum yield constant of denitrifiers can be around 0.40 kg biomass (kg organic matter)⁻¹ which is 15 % lower than that of aerobic heterotrophic conversion. If nitrate is assimilated instead of ammonium the maximum yield constant is changed to 0.36 kg biomass (kg organic matter)⁻¹. If ammonium is present, the bacteria will always use it as the nitrogen source. This will be the case in (almost) all types of ordinary wastewater (Henze, 2002). The energy source used has an effect on the denitrification rate. The maximum denitrification rate obtainable from the easily biodegradable part of raw wastewater and methanol is 7 - 20 mg NO₃ - N (g VSS h)⁻¹, ethanol and raw wastewater is 1 - 5 mg NO₃ - N (g VSS h)⁻¹ and endogenous biomass and methane is 0.2 - 0.5 mg NO₃ - N (g VSS h)⁻¹ (Henze, 1991).

The temperature dependency of the denitrification processes resembles that of the aerobic heterotrophic processes (Henze, 2002). The Arrhenius temperature coefficients on different carbon sources such as the primary treated meat processing wastewater, balance pond meat effluent, acetate and endogenous biomass were found to be 1.078, 1.091, 1.086 and 1.07 respectively by Bickers (1996b).

The denitrification process increases the alkalinity of the water. For every mole of nitrate converted, one mole equivalent of alkalinity is produced. If ammonium is used as a nitrogen source, this will reduce the alkalinity production by one equivalent per mole of ammonium assimilated. Therefore the net alkalinity production is 0.85 equivalent per mole $\text{NO}_3 - \text{N}$ (Henze, 2002).

The pH dependency of the denitrification process resembles that of other biological processes (Henze, 2002). The optimum pH is around 7 to 9, but with variations depending on local conditions. Big differences can be observed between short-term and long-term pH dependency as the microbial system can slowly be adapted to the given pH. The pH of the mixed liquor profoundly affects the rates of denitrification relative to the presence of DO. A pH value in the acid range will permit active denitrification in the presence of DO; whereas strict anaerobic conditions are mandatory at pH levels above 7.0. Since most of the activated sludge plants operate at-or near-neutral pH, anaerobic conditions should be maintained to promote denitrification (Eckenfelder, 1980). A low pH (< 7) plays an important role for the end product resulting from the denitrification since an increasing amount of nitric oxides, especially N_2O , will be produced when the pH value declines (Henze, 2002).

Bickers and Van Oostrom (2000) reported that paunch liquor and stick water had high RBCOD so that they could be used as external carbon sources for denitrification. Further, they found that the specific denitrification rates for stick water and paunch liquor of 5.3 to $10.5 \text{ mg NO}_x - \text{N} (\text{g VSS h})^{-1}$ were greater than those for slaughter floor wastewater and dilute blood of 2.0 to $2.85 \text{ mg NO}_x - \text{N} (\text{g VSS h})^{-1}$. The endogenous denitrification rate was $0.51 \text{ mg NO}_x - \text{N} (\text{g VSS h})^{-1}$.

A continuous, two-stage, anoxic aerobic pilot plant activated sludge biological nutrient removal system was tested on slaughterhouse effluent in Italy. Denitrification rates of $2.08 - 8.8 \text{ mg NO}_3 - \text{N} (\text{g VSS h})^{-1}$ were achieved at temperatures of $20 - 23^\circ\text{C}$ (Beccari *et al.*, 1979).

Although denitrification is said to require the absence of oxygen, while nitrification requires the presence of oxygen, simultaneous nitrification and denitrification in the same reactor has been suggested for nitrogen removal by Suwa *et al.* (1992). This is discussed further in Section 2.5.3.

2.4.2.2.4 Biological phosphorus removal

Biological phosphate removal from wastewater can be achieved in two ways: stoichiometric coupling to microbial growth and enhanced storage in the biomass as polyphosphate (poly-P). Minimum P removal by stoichiometric coupling in activated sludge biomass is 1 – 1.5 % of VSS (Bickers *et al.*, 2001; Henze, 2002). The enhanced storage of phosphate in the biomass was formerly called “luxury uptake” (Levin & Shapiro, 1965) and is the key mechanism in the enhanced biological phosphate removal (EBPR) process.

The EBPR is achieved by circulation of activated sludge through anaerobic and aerobic phases, coupled with the introduction of influent wastewater into the anaerobic phase (Barnard, 1975). By these anaerobic and aerobic conditions the microorganisms, which accumulate poly-P and thus have a high phosphorus content, are selected and grow to dominate in the process. Excess sludge with high phosphorus content removed from the sludge waste increases the removal efficiency of phosphorous (Mino *et al.*, 1998).

In the early days it was thought that *Acinetobacter* was the organism solely responsible for the biological phosphorus accumulating process (Fuhs & Chen, 1975; Yeoman *et al.*, 1988). However, now it is well known that phosphorus-accumulating ability is widespread among heterotrophic microorganisms present in wastewater and biomass in biological treatment processes. All these organisms are termed as Bio-P bacteria, or Phosphorus Accumulating Organisms (PAOs) (Henze, 2002). In a treatment plant for biological phosphorus removal several groups of heterotrophs (Bio-Ps non-denitrifying, Bio-Ps denitrifying, Non-Bio-Ps non-denitrifying, Non-Bio-Ps denitrifying, Glycogen Accumulating Organisms (GAOs), *Microthrix*) are active and compete for the substrate, especially for short chain fatty acids (SCFA), that is needed for the phosphorus storage mechanism (Henze, 2002).

When an anaerobic phase is introduced in which activated sludge is mixed with the influent wastewater, microorganisms capable of anaerobically taking up carbon sources from the influent are favoured. Bio-Ps can do this because they are capable of

hydrolysing the stored poly-P to supply energy for the anaerobic uptake of the carbon sources. Therefore, in the anaerobic phase, Bio-Ps take up the carbon sources and store them in the form of poly- β -hydroxyalkanoate (PHA) accompanied by degradation of poly-P and consequent release of orthophosphate. In the following aerobic as well as anoxic phase, Bio-Ps grow and take up orthophosphate to recover the poly-P level by using the stored PHA as the carbon and energy source (Arvin, 1983; Comeau *et al.*, 1987; Henze *et al.*, 1999; Mino *et al.*, 1998). Since PHA is a reduced polymer, its synthesis requires reducing power (Mino *et al.*, 1998). Wentzel *et al.* (1991) pointed out two possible biochemical models to explain the source of the reducing power, the Mino model and the Comeau-Wentzel model. In the Mino model (Arun *et al.*, 1988), the reducing power is considered to be derived from degradation of intracellularly stored carbon. In the Comeau-Wentzel model (Comeau *et al.*, 1986; Wentzel *et al.*, 1986) partial oxidation of acetyl CoA through the TCA cycle is assumed to produce the required reducing power (Mino *et al.*, 1998).

The theoretical stoichiometry of the Mino model explained the experimentally observed stoichiometry of anaerobic acetate uptake, PHA formation, glycogen utilisation and CO₂ production by Bio-P-enriched sludges (Sato *et al.*, 1992, 1996; Smolders *et al.*, 1994a). Pereira *et al.* (1996) incubated ¹³C labelled acetate with a Bio-P-enriched sludge under anaerobic conditions (with no nitrite or nitrate) and found that a small fraction of the labelled carbon from acetate was released as CO₂. Also based on a redox balance considerations, they concluded that the reducing power generated in the observed degradation of glycogen was insufficient to account for the PHA production. These are strong indications that a small fraction of acetate is metabolised through the TCA cycle under anaerobic conditions supplying a minor part (30 %) of the reducing power for PHA formation. Pereira *et al.* (1996) and Hesselmann *et al.* (2000) proposed a partial TCA cycle model to explain the generation of extra reducing equivalents.

Both poly-P and glycogen are needed for the anaerobic uptake of organic substrates by Bio-Ps. The poly-P supplies energy and the glycogen supplies reducing power as well as energy. Both can be limiting substances for the anaerobic substrate uptake. Under normal conditions, neither poly-P nor glycogen, is totally depleted at the end of the anaerobic phase and they are stored to greater levels than needed for routine anaerobic metabolism (Mino *et al.*, 1998). However, Kuba *et al.* (1996) and Brdjanovic *et al.* (1998a) reported that, when acetate is fed in excess, the anaerobic uptake of

acetate by a Bio-P-enriched sludge stops. This is not because of poly-P limitation or PHA saturation, but because of exhaustion of glycogen. Brdjanovic *et al.* (1998a) further suggested that poly-P (energy source) would be limiting at high pH, since more energy is required for acetate transport through the membrane at high pH (Smolders *et al.*, 1994a, b). Brdjanovic *et al.* (1998b) studied the ability of the enriched Bio-P to utilise organic substrate (acetate) anaerobically under the condition of poly-P limitation and surplus glycogen content in the biomass. They showed that, under these conditions, almost no acetate was taken up and concluded that Bio-P could not use glycogen conversion to PHA as the sole energy source under anaerobic conditions. Hesselmann *et al.* (2000) suggested that the energy required for anaerobic uptake of organic substrates by Bio-P is supplied by glycolysis, hydrolysis of poly-P and probably also by the hydrolysis of pyrophosphate and the efflux of MgHPO_4 .

Poly- β -hydroxybutyrate (PHB) was first recognised as a storage polymer in the anaerobic phase of the EBPR process (Buchan, 1983). Later, Comeau (1987) verified the fact that the PHB-like polymer contains PHB and Poly- β -hydroxyvalerate (PHV) as a monomeric unit. Satoh *et al.* (1992) further revealed that the storage polymer consists of four monomeric units of PHB, PHV, 3-hydroxy-2-methylbutyrate (3H2MB) and 3-hydroxy-2-methylvalerate (3H2MV). Now, the polymer is called PHA (Mino *et al.*, 1998).

It has been reported that Bio-Ps are sustained on SCFA like acetate and propionate (Wentzel *et al.*, 1985). Many laboratory scale EBPR reactors have been successfully operated with acetate as the major carbon source (Smolders *et al.*, 1994a). In the EBPR process mathematical models (Henze *et al.*, 1995; Smolders *et al.*, 1995a) it is assumed that Bio-Ps utilise only SCFA. However, a wide range of organic matter including carboxylic acids, sugars and amino acids have been reported to be utilised anaerobically by Bio-P-enriched sludges (Satoh *et al.*, 1996). Hood and Randall (2001) reported that for the phosphorus removal process among SCFA, acetic and iso-valeric acids were the most efficient substrates, and propionic acid was the least efficient substrate.

Barker and Dold (1996), Kern-Jespersen and Henze (1993) and Sorm *et al.* (1996) reported that some Bio-Ps were able to utilise nitrate and oxygen as oxidants. This means that the occurrence of phosphorus accumulation could be accompanied by denitrification. Therefore, the effect of denitrifying Bio-P has also been included as a modification to the ASM 2 (Henze *et al.*, 1999; Isaacs *et al.*, 1995; Mino *et al.*, 1995) to

account for observations of decreasing phosphate concentrations under anoxic conditions.

Aeration promotes the uptake of excess phosphate by activated sludge bacteria. Lowering the pH value or anaerobiosis causes this phosphate to be released in the medium (Levin & Shapiro, 1965). However, Fuhs and Chen (1975) found that the anaerobic phase is not itself necessary to induce the release of phosphate from the bacteria into the supernatant. The same authors suggested that the CO₂ accumulation and the lowering of the pH, which are the results of anaerobiosis, might be important factors in inducing the release of phosphate from the bacteria (Fuhs & Chen, 1975).

The alkalinity of the system is slightly affected by the Bio-P process (Henze *et al.*, 1999). The alkalinity reduction by the release of negative ion phosphate is counter-balanced by the cations as they (magnesium, potassium and calcium) are co-transported during biological phosphorus release and uptake (Comeau *et al.*, 1987). Alkalinity increases during the storage of PHA under various electron donors (Henze *et al.*, 1999). In the anaerobic period CO₂ is released during fermentation, during part of the TCA cycle and during utilisation of glycogen as energy source (Henze, 2002; Hesselmann *et al.*, 2000; Pereira *et al.*, 1996). Increases in dissolved CO₂ concentration and alkalinity in the liquid decrease the pH (Dold & Marais, 1987). A sharp decrease of pH was observed at the beginning of the anaerobic stage due to phosphate release (Lee *et al.*, 2001).

Several modified 'single sludge' activated sludge configurations have been developed for enhanced simultaneous carbon, nitrogen and phosphorus removal. The most common of these include the five-stage 'Bardenpho' and 'UCT' processes (Bickers *et al.*, 2001; Metcalf and Eddy, 1991). All these systems feature alternating anaerobic and aerobic zones, often with internal recycling to minimise the concentration of nitrate in the anaerobic zone.

External disturbances, such as excessive rainfall, loading, aeration, and nitrate loading to the anaerobic zone, have been reported to be the causes of deterioration in biological phosphorus removal processes (Wang *et al.*, 2002).

2.5 Sequencing Batch Reactor (SBR)

The term “Sequencing Batch Reactor” refers to biological reactors which are repeatedly filled and drained (Oles & Wilderer, 1991). In terms of treatment an *SBR* is defined as *an activated sludge process designed to operate under non-steady state conditions* (Irvine & Ketchum, 1989). An SBR operates in a batch mode with aeration and sludge settlement both occurring in the same tank. This differs from conventional activated sludge treatment where the wastewater flows from one vessel to another, each vessel performing a specific treatment operation. An SBR tank carries out the functions of equalisation, aeration and sedimentation in a time sequence rather than in the conventional space sequence of continuous flow systems. In addition, the SBR system can be designed with the ability to treat a wide range of influent volumes-whereas the continuous system is based upon a fixed influent flow rate. In the SBR process, the influent is also fed continuously, but in batches to each SBR reactor (Mikkelsen & Lowery, 1992). An SBR operates under a series of periods, which constitute a cycle. The cycle generally consists of fill, react, settle, decant and idle periods. The use of these periods allows a single reactor to act as a series of reactors and a clarifier in conventional activated sludge treatment. By manipulating these periods within a single cycle, an SBR can accomplish most of what a continuous flow plant can accomplish with several reactors, each operating under a different condition. Different environments can be created in an SBR by controlling process equipment such as aerators, mixers, pumps and decanters during a cycle. The process can be controlled and co-ordinated by a programmable logic controller together with a personnel computer by plant personnel.

2.5.1 SBR Operation

Irvine and Ketchum (1989) described the SBR and the different phases of an SBR in detail (Figure 2.5). During the “fill” period, influent wastewater is added to the biomass that was left in the SBR from the previous cycle. The length of the “fill” period depends on the number of SBRs, the volume of the SBRs, and the nature of the flow of the wastewater source, which can be either intermittent or continuous. The wastewater may, or may not, be mixed during this period. Filling ends when the wastewater has reached the maximum water level, or at some fraction of that if multiple fill periods are used during a cycle. The “react” period occurs after a fill period. In most cases the SBR is mixed during this period. Aeration may, or may not, be used depending on the SBR’s objective and operation. After the react period, a ‘settle’ period takes place. During the

settle period, the SBR acts as a clarifier. The solids, including biomass and particulate substrate, settle and leave the relatively clear effluent on top. “Decant” occurs at the end of the settle period.

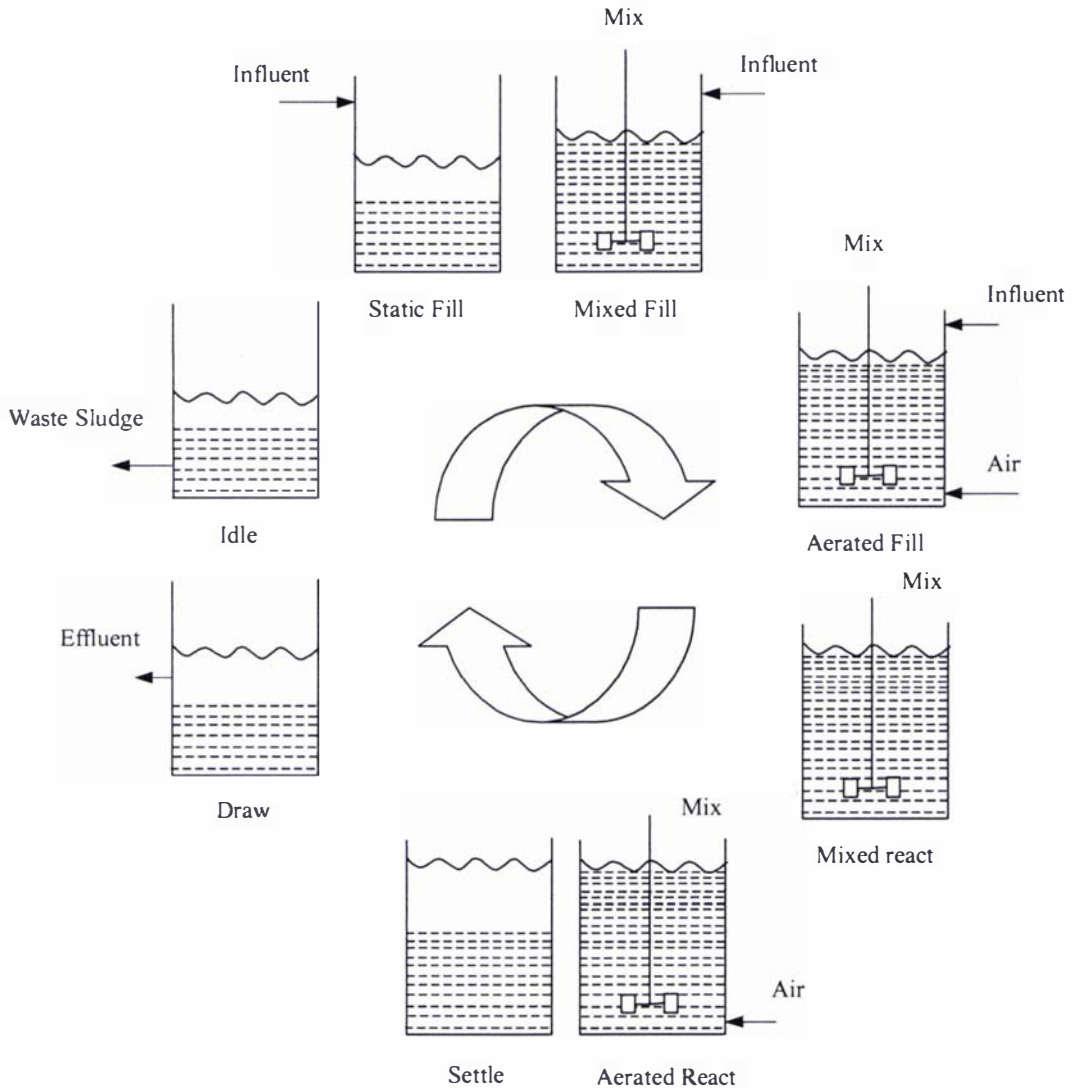


Figure 2.5 SBR operation for each tank for one cycle for the five discrete time periods (Irvine and Ketchum, 1989)

Nitrogen and/or phosphorus in addition to COD removal would be possible in an SBR if operating conditions were properly modified to introduce anaerobic, anoxic and aerobic conditions into a time cycle. However, the methodology for optimising the operation of this process has not yet been established, because of diversity of its operating conditions (Artan & Tasli, 1999). It is reported that substrate feeding under non-aerated conditions is a prerequisite for efficient nutrient removal and single instantaneous feeding is suggested for more effective phosphorus removal and good sludge settleability (Okada *et al.*, 1991).

SBR systems have also been reported to function well on slaughterhouse wastewater. Subramaniam *et al.* (1994) achieved very high removal of nitrogen and phosphorus manipulating the nature of the anaerobically treated feed to the SBR tank. The partial pre-treated (by anaerobic pond) slaughterhouse wastewater which contained 190 mg L^{-1} total nitrogen and 50 mg L^{-1} total phosphorus, was reduced to less than 20 mg L^{-1} TN and 5 mg L^{-1} TP (Keller *et al.*, 1997). The nitrogen and phosphorus removals of 92 and 85 % achieved respectively from a beef slaughterhouse effluent treatment using an SBR at a F/M ratio of 0.07 d^{-1} , HRT 10 - 12 d and a sludge age of 30 - 35 d (Johns, 1995). Willers *et al.* (1993) reported that slurries of animal manure (< 2 % dry solids) had been treated in SBR systems to achieve BOD₅, TKN, NH₃ - N and PO₄ - P removals of better than 95 %, the last by addition of lime.

Selection of SBR dimensions for biological carbon and nutrient removal is available in the literature (Artan *et al.*, 2001; Orhon & Artan, 1994).

2.5.2 SBR vs. Conventional continuous flow activated sludge systems

The SBR Activated Sludge process is known to have several advantages over conventional continuous flow activated sludge systems and is considered as an alternative to these systems (Wanner, 1992; Wilderer *et al.*, 2001). The following are the advantages of the SBR system.

- Lower capital and operating cost because there is no need for external clarifiers and associated return sludge pump and piping.
- Greater ability to meet effluent limitations since batch kinetic reactions occur without short circuiting.
- Better resistance to sludge bulking, since the biomass undergoes cyclic feast famine conditions.
- Greater system flexibility and control since the cyclic format can be easily modified at any time to offset changes in process conditions, influent characteristics or effluent objectives.
- Less land required and less process equipment to maintain, since only one vessel is used for all process operations.

It also has some disadvantages such as formation of floating clumps from denitrification, need for a flow equalisation tank during high flow rates, and there are

chances of solids escape during decanting. Generally, larger sized equipment is needed for effluent flow and air supply.

2.5.3 Simultaneous nitrification and denitrification (SND)

In simultaneous nitrification denitrification (SND), both nitrification and denitrification take place under the same macroscopic conditions, usually at an average DO concentration between 0.5 and 1.0 mg L⁻¹ (Münch *et al.*, 1996; Subramaniam *et al.*, 1994). Denitrification systems are usually operated in the absence of measurable DO because it can inhibit denitrification. The advantages of using SND rather than alternating nitrification and denitrification periods in SBRs are that SND could decrease the time necessary to remove the nitrogen, there is a reduction of COD required for denitrification, there are higher denitrification rates and a lower biomass yield (Turk and Mavinic, 1989; Munch *et al.*, 1996; Keller *et al.*, 1997).

2.5.4 Sludge settling in sequencing batch reactors

Sludge settling is a common problem in activated sludge systems including SBR treatment. Although SBRs have better resistance to sludge bulking, they can be susceptible to the proliferation of filamentous microorganism and subsequent interference with biomass settling.

The most commonly proposed factors influencing the growth of filamentous microorganisms are (Leonard, 1996):

1. Reactor configuration
2. Substrate type
3. Substrate concentration
4. Dissolved oxygen concentration
5. Availability of nutrients
6. Biomass age
7. Biomass concentration
8. pH
9. Temperature

The extent of filamentous growth and effect of sludge settleability is measured as the Sludge Volume Index (SVI) of the mixed liquor. The SVI is the volume that a unit mass of mixed liquor solids occupies after a defined settling period (0.5 h), a high SVI value (more than 150 ml g⁻¹) being indicative of filamentous bulking (Jenkins *et al.*, 1993; Leonard, 1996).

A treatment cycle structure which comprises repetitive phases of operation, regardless of the necessity for nutrient reduction, can be effective in avoiding or controlling the predominance of filamentous population in a reactor (Mikkelsen & Lowery, 1992).

Lakay *et al.* (1999) reported that induction of the selector effect, via intermittent feeding to the SBR does not control low F/M filaments in intermittent aeration systems for nutrient removal. They found that continuous aerobic and continuous anoxic conditions reduce low F/M filament bulking whereas alternating anoxic-aerobic conditions with 30 – 40 % aerobic and 60 – 70 % anoxic conditions result in maximum proliferation of low F/M filaments. Filamentous organisms proliferate in systems with sludges exposed to alternating anoxic-aerobic conditions in SBRs in which nitrate and/or nitrite exceeding 5 and/or 1 mg N L⁻¹ respectively are present throughout the anoxic period just prior to the aerobic period.

Ekama *et al.* (1996) reported that neither kinetic selection (aerobic or anoxic selectors) nor metabolic selection (anaerobic selectors) control low F/M filament proliferation. Since with kinetic and metabolic selection, RBCOD is taken up preferentially by floc-formers, the continued proliferation of low F/M filaments appears to indicate that they are able to compete for and utilise slowly biodegradable COD for growth.

Wanner *et al.* (1987) showed that no substrate gradient was needed for suppression of filamentous growth under anaerobic conditions. The introduction of anoxic conditions always resulted in very fast and effective improvement in sludge settling characteristics (Chiesa and Irvine, 1985; Wanner *et al.*, 1987).

2.5.5 Modelling of Sequencing Batch Reactors treatment

Mathematical models of activated sludge and other treatment processes have served as evaluation tools of system performance for a variety of process configurations, load conditions and operating strategies. Models also enable improved design of large-scale

plants based on limited experimental results, but supported by mathematical extrapolations.

The IAWPRC Task Group for Mathematical Modelling for Design and Operation of Biological Wastewater Treatment offered a new trend in activated sludge modelling. The most well known mathematical model proposed by the IAWQ Task Group for describing the performance of single sludge processes is the Activated Sludge Model No. 1 (ASM1) which incorporates carbon and nitrogen removal (Henze *et al.*, 1987). The ASM 1 was applied successfully for the SBR system (Oles & Wilderer, 1991). The ASM 3 (Gujer *et al.*, 1999) was developed after correcting for some defects in ASM 1. The ASM 1 has been updated to include biological phosphorus removal, which resulted in the ASM 2 (Henze *et al.*, 1995). Wentzel *et al.* (1989) proposed the first comprehensive structured EBPR model. This model was restructured as ASM 2 (Mino *et al.*, 1998). These models are based on the partial TCA cycle for deriving the reducing power required for PHA formation (Smolders *et al.*, 1995b). The ASM 2 also corrected some defects in the ASM 1 for biological carbon and nitrogen removal. The ASM 2d (Henze *et al.*, 1999) included denitrification capability of Bio-P bacteria. Mino *et al.* (1995) proposed sub models for ASM 2 for the capability of Bio-P bacteria to denitrify and store glycogen. Biological phosphorus removal is also described by the General model (Barker & Dold, 1997). These models are called *parametric models* (Ky *et al.*, 2001). The Technological University of Delft (TUD) developed a metabolic model (Murnleitner *et al.*, 1997; Smolders *et al.*, 1995a, b; van Veldhuizen *et al.*, 1999) for phosphorus removal. These models also differ in their way of dealing with the maintenance energy required by the biomass. The concept of death regeneration is used in the ASM 1, ASM 2, ASM 2d and the General models, whereas endogenous respiration is used in the ASM 3 and TUD models (Ky *et al.*, 2001).

The ASM 1 and ASM 2 models were first developed by referring to the continuous flow activated sludge systems. In order to apply these models to other versions of the activated sludge processes such as the SBR-which is time oriented in contrast to the space oriented continuous flow activated sludge reactors-the models required changes in the basic mass balance equations. The basic mass balance equations in SBR treatment can be written as in Equation 2.8 and Equation 2.9 (Oles & Wilderer, 1991).

$$\frac{dS}{dt} = \frac{Q(S_o - S)}{V_o + Qt} - r_s \quad (2.8)$$

$$\frac{dX}{dt} = \frac{-Q(X_0 - X)}{V_0 + Qt} + r'_x \quad (2.9)$$

Where, Q = The influent flow rate, $\text{m}^3 \text{s}^{-1}$

S_0 and X_0 = Substrate and biomass concentration of the influent, mg L^{-1}

V_0 = The initial reactor volume before feeding, m^3

S and X = Substrate and biomass concentration in the reactor, mg L^{-1}

r'_s = Substrate utilisation rate, $\text{g} (\text{m}^3 \text{s})^{-1}$

r'_x = Rate of biomass growth, $\text{g} (\text{m}^3 \text{s})^{-1}$

These models consist of a matrix of kinetic and stoichiometric equations describing the biological processes generally occurring in biological wastewater treatment. Basic concepts of the ASM 1 and ASM 2 models as well as the kinetics and stoichiometric relationships are discussed in detail in Chapter VII. The default parameter values given in the ASM 1 and ASM 2 are based on domestic wastewater.

To successfully use the model to describe and design wastewater treatment processes using an SBR, influent characteristics and many kinetic and stoichiometric parameters must be known. Influent wastewater characteristics are described in Chapter IV. While many parameters are constant for most wastewater and treatment processes, some of the important parameters must be determined through experimentation or calibrating to existing experimental data as discussed in Chapters VI and VII.

The modelling of activated sludge processes for COD and nitrogen removal has become a standard practice and valuable instrument for the design and operation of activated sludge processes. With respect to the modelling of biological phosphorus removal (BPR), practical use, however, is still limited. This is partly due to the complexity of the process, but also to limited experience (Meijer *et al.*, 2001).

2.6 Summary

Meat processing wastewater contains significant amounts of biodegradable organic carbon, nitrogen and phosphorus. The characteristics of the wastewater vary with the sources and types of meat-works waste. The existing treatment methods in New Zealand result in incomplete removal of nitrogen and phosphorus and they are having adverse effect on the environment. Screening, Save-all (settling) and DAF are widely used in the

primary treatment of meat processing wastewater. In secondary treatment PCT and biological treatment are employed. Several biological processes are involved in organic carbon and nutrients removal. The environment required for heterotrophic, autotrophic and Bio-P bacteria for simultaneous removal of organic carbon and nutrients is manipulated to achieve simultaneous removal of organic carbon and nutrients and to avoid the sludge settling problem. SBR treatment technology is currently used in the meat processing wastewater treatment after partial pre-treatment to remove a substantial amount of organic carbon in COD enriched wastewater. The SBR treatment has some advantages over the continuous flow activated sludge system. The methodology for optimising the anaerobic, aerobic and anoxic phases for simultaneous removal of organic carbon and nutrients has not been established. Substrate feeding under non-aerated conditions is a prerequisite for efficient nutrient removal, and single instantaneous feeding is suggested for more effective phosphorus removal and good sludge settleability.

There are different activated sludge models for predicting combined organic carbon and nutrient removal from wastewater. The ASM 2 is a parametric model developed based on domestic wastewater. The kinetic and stoichiometric parameters have to be found for meat processing wastewater to predict the removal of organic carbon and nutrients by SBR treatment.

Based on the conclusions from the literature review, the objectives of this study were set as:

1. To investigate the treatment of meat processing wastewater using a sequencing batch reactor for maximising simultaneous organic carbon, nitrogen and phosphorus removal.
2. To understand the anaerobic, anoxic and aerobic processes and the interaction between nitrogen and phosphorus during the simultaneous organic carbon, nitrogen and phosphorus removal.
3. To evaluate the suitability of ASM 1 and ASM 2 models of the treatment of meat processing wastewater by a sequencing batch reactor.

CHAPTER III

METHODOLOGY

3.1 Source and type of wastewater

The wastewater used for this study was collected from the meat processing plant of Manawatu Beef Packers Fielding, New Zealand. The collection point is located after the primary treatment (screening and sedimentation tank) and before the first anaerobic pond. The meat wastewater was collected fortnightly on Mondays between 2.30 and 3.30 p.m. as this period preceded the plant cleaning and floor washing operations and stored in a 4°C refrigerator until used in experiments. The wastewater consisted of faecal material and urine from stockyards, paunch contents, blood, fat, and residual tissue from slaughtering and boning processes. The big particles were removed by sieving through 1 mm steel mesh at the collection point. The plant processes included slaughtering and boning but there were no rendering or fellmongering processes.

3.2 Start up of the experiment

A sequencing batch reactor (SBR) with maximum operating volume of 15 L was set up as shown in Figure 3.1 in a temperature controlled room. The SBR was constructed from acrylic material with dimensions of 18.9 cm diameter and 75 cm height. It had sampling ports with taps at 10 cm intervals along the reactor length and there was an aeration port at the base. The bottom and the top of the reactor had a removable base and cover. A magnetic stirrer was used to mix the wastewater in the reactor. A programmable time controller was used to control different operating phases. Feeding, decanting and sludge wasting volumes were controlled by a level controller. Influent was added using a peristaltic pump through a bottom port at a constant pump speed. Decanting and sludge wasting were controlled using a solenoid valve and gravity flow. Air was supplied from a compressed air supply and a solenoid valve and a non-return valve controlled the flow. Oil and grease in the compressed air was trapped before supplying to the reactor. The rate of airflow was maintained at 6 L air (L volume. h)⁻¹. The dissolved oxygen (DO) level was controlled by a YSI model 57 DO meter with an YSI 57 probe and the recorder port was

connected to a DO switching box. The DO switching box was able to switch on at two different DO levels. The feed tank was filled on alternate days. The wastewater in the feed tank was mixed during the fill cycle. Decanting was done through a top port above the settled supernatant level. Sludge was wasted through a mid reactor port immediately at the end of aeration.

Initially 7.5 L wastewater was placed in the SBR and seeded with 7.5 L of mixed liquor from the aerobic pond. This aerobic pond is currently used at the site to treat the meat processing wastewater. The initial operating conditions are shown in Table 3.1. The solids retention time (SRT) was 15 d, while the hydraulic retention time (HRT) was 1.5 d.

Selection of an appropriate SRT for simultaneous removal of organic carbon, nitrogen and phosphorus removal is important. Solids retention time is the average number of days that the microorganisms are kept in the SBR. When the daily biodegradable COD load is small in comparison with the quantity of sludge in the SBR, the daily sludge production will be low in comparison to the quantity of sludge in the SBR. Therefore the sludge age will be high. High sludge ages are associated with low specific sludge production (Metcalf and Eddy, 1991).

The autotrophic bacteria are slow growers when compared to the heterotrophs, therefore the selection of SRT relies on the autotrophs being maintained in the SBR treatment system. The SRT is calculated by dividing the mass of solids under aeration by the mass of waste solids. Escape of sludge from the effluent will reduce the SRT. For example, assume that the solids concentration of the mixed liquor at the end of aerobic period is 2750 mg L^{-1} , and the concentration of the effluent is 100 mg L^{-1} , and that the sludge removal volume is 1 L d^{-1} , while the decanted volume is 5 L d^{-1} . Then the SRT is equal to $(2750 \times 15) / (2750 \times 1 + 100 \times 5)$ or 12.7 d. This is comparable to the design SRT of 12.5 d required for preventing washout of autotrophs from the reactor. It shows, if the cell concentration in the effluent increases above 100 mg L^{-1} , the treatment system may fail due to insufficient nitrification. The design SRT required in this study for preventing washout of autotrophs is explained in Section 5.2.

Given a constant organic load on the SBR reactor, with an increase in the SRT the PHB fraction reduces (Smolders *et al.*, 1995). The effect of the SRT on the PHB content

will directly affect the growth of bio-P. Therefore too long a SRT is not helpful for simultaneous removal of organic carbon, nitrogen and phosphorus.

Table 3.1 Operating cycle of laboratory scale sequencing batch reactor (6-h cycle)

Reactor Sequence	Time (h)
Fill and non-aerated mix	2.0
Aerated, mixed react 1	1.5
Non-aerated mixed react (anoxic)	0.5
Aerated mixed react 2	1.0
Settle	0.50
Decant and idle	0.50

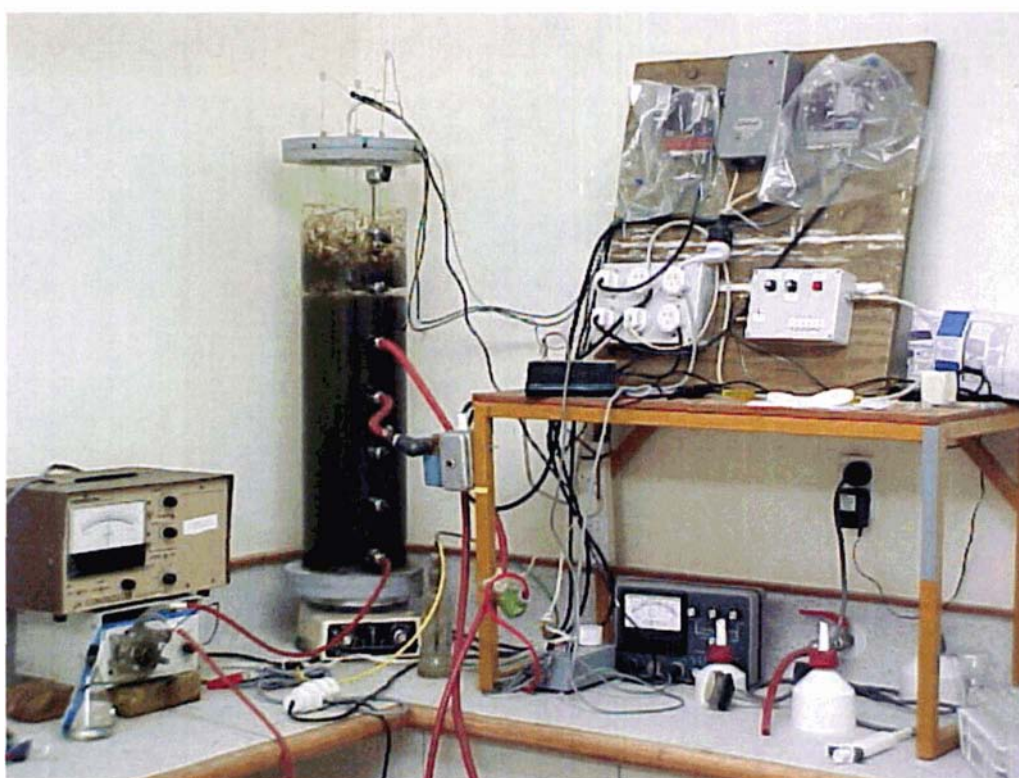


Figure 3.1 Laboratory scale sequencing batch reactor set-up

3.3 SBR performance and characterisation of wastewater

Typical characteristics of the wastewater and effluent from the reactor such as chemical oxygen demand (COD), total suspended solids (TSS), volatile suspended solids (VSS), total Kjeldahl nitrogen (TKN), ammonia nitrogen, oxidised nitrogen ($\text{NO}_x - \text{N}$), total phosphorus (TP), soluble phosphate phosphorus ($\text{PO}_4 - \text{P}$), pH, DO and alkalinity were measured according to *Standard Methods* (APHA, AWWA and WEF, 1995). Cyclic

performance of the reactor was analysed after at least three SRT periods.

3.3.1 Determination of chemical oxygen demand (COD)

Total COD (TCOD) and soluble COD (SCOD) were measured by the closed reflux colorimetric method as given in Section 5220 D of *Standard Methods* (APHA, AWWA and WEF, 1995). SCOD was defined as the COD of a filtrate that had passed through a glass fibre paper (GF/C grade filter) of 1.2 μ pore size in this study. All TCOD analyses were performed in triplicate whereas SCOD were in duplicate, and the average values were taken for the results. Absorbance of the cooled samples was read at 600 nm on a Shimadzu UV-1201, UV/VIS spectrophotometer, using a glass cuvette with a 1 cm path length.

A standard curve was prepared using potassium hydrogen phthalate standards in the range of 0 to 900 mg L⁻¹ COD. Samples were diluted before analysis as necessary to give a final COD in the required range. The TCOD of the wastewater samples was usually analysed using a 1:2.5 dilution, whereas the SCOD was usually undiluted. The interference of nitrite in the COD measurement was assumed as negligible as nitrite concentration was low during this study.

3.3.2 Determination of total and volatile suspended solids (TSS and VSS)

TSS and VSS were measured according to the procedure in Sections 2540D and 2540E of *Standard Methods* (APHA, AWWA and WEF, 1995). A Contherm Series Five oven was used to dry filtered solids samples at 104 \pm 1°C and a NEY M525 Series II muffle furnace was used to ignite the oven-dried samples. Filter papers were prepared by placing them into the muffle furnace at 550 \pm 25°C, for 20 minutes and then cooling and storing them in a desiccator containing silica gel (BDH, Poole, England) until needed. All analyses were performed in duplicate, and the average values were taken for the result. The solids were weighed on a Mettler AE200 balance.

3.3.3 Determination of ammonia nitrogen concentration

Ammonia was analysed by either preliminary distillation (Büchi 323 distillation unit) followed by titration (Mettler DC25 titrator) as outlined in Section 4500-NH₃ B and C or by the manual phenate method outlined in Section 4500-NH₃ F of *Standard Methods*

(APHA, AWWA and WEF, 1995). To analyse the ammonia in the wastewater and the reactor effluent, distillation followed by the titration method was used. The samples were distilled into 30 mL of 4 % borate buffer by a Büchi 323 distillation unit. The distillation unit was set at 30 and 70 mL of water and NaOH respectively. The distilled samples were back titrated in the auto titrator (Mettler DC25 titrator) with 0.1 N HCl in Mode 2. Samples with a volume of 25 mL and 200 mL were taken for the ammonia analysis in wastewater and the reactor effluent respectively. The manual phenate method was used in cycle studies. In the phenate method, absorbance was measured at 640 nm in the spectrophotometer. A standard curve was prepared for phenate method in the range of 0 to 3 $\mu\text{g NH}_3 - \text{N}$ and 0.1 mL of soluble samples were taken into analysis.

3.3.4 Total Kjeldahl nitrogen (TKN)

The TKN was measured by a micro Kjeldahl method as outlined in Section 4500-N_{org}B of *Standard Methods* (APHA, AWWA and WEF, 1995). Wastewater samples of 25 mL and effluent samples of 50 mL in duplicate were taken in Kjeldahl tubes in 6 tubes slot. Concentrated H₂SO₄ (13 mL) and one 5 g TKN digester tablet were added into each tube. The 5 g tablet contained 97.5 parts of Na₂SO₄, 1.5 parts of CuSO₄.5H₂O and 1 part of Se. A manifold and water extraction tube connected all 6 tubes. The samples were digested for one and a half hours in a Büchi 435 digester. Digestion was continued for few minutes following white flumes were produced. After the digestion had been completed the tubes were allowed to cool. At this stage the digested samples were clear in colour. Then the samples were distilled and back titrated as described in Section 3.3.3.

3.3.5 Total phosphorus (TP) concentration

The TP was measured by the ascorbic acid method as outlined in Section 4500-P E of *Standard Methods* (APHA, AWWA and WEF, 1995). To find out the influent and sludge total phosphorus contents, 0.5 ml samples were used. Absorbance was measured at 880 nm in the spectrophotometer.

3.3.6 Oxidised nitrogen ($\text{NO}_x - \text{N}$) and soluble phosphate phosphorus ($\text{PO}_4 - \text{P}$) concentration

$\text{NO}_x - \text{N}$ and $\text{PO}_4 - \text{P}$ were analysed by ion chromatography (Dionex-100, column type AS9-HC, elluent 9 mM Na_2CO_3 , flow rate = 60.0 mL h^{-1} and the injection volume = $25 \mu\text{L}$). The ion chromatography was calibrated to analyse $\text{NO}_x - \text{N}$ and $\text{PO}_4 - \text{P}$ in the range of $0 - 25 \text{ mg L}^{-1}$ and $0 - 45 \text{ mg L}^{-1}$ respectively. The wastewater and reactor samples were filtered by $0.45 \mu\text{m}$ membrane filter paper before the injection.

3.3.7 DO, pH, alkalinity and SVI measurements

An ORION model 230A pH meter measured wastewater and mixed liquor pH. The DO was measured by a YSI model 57 oxygen meter. Alkalinity was measured according to Section 2320B of *Standard Methods* (APHA, AWWA and WEF, 1995). The Sludge Volume Index was measured according to Section 2710D of *Standard Methods* (APHA, AWWA and WEF, 1995). The settled volume of the sludge after 0.5 h was measured in the reactor during the settling period.

3.4 Influent soluble and particulate inert COD fraction

The inert soluble and particulate COD in the wastewater were measured following the concept outlined by Orhon *et al.* (1999a). Three 2 L conical flasks were set. One was filled with 1.75 L of raw wastewater; another was filled with GF/C filtered wastewater and the last was filled with glucose solution. The glucose solution was prepared such that it had approximately the same COD as in the filtered wastewater. The key nutrients and salts; KH_2PO_4 (50.3 mg), NH_4Cl (219.3 mg), $\text{MgSO}_4 \cdot 7\text{H}_2\text{O}$ (117.6 mg), $\text{CaCl}_2 \cdot 2\text{H}_2\text{O}$ (28.98 mg) and $\text{FeCl}_2 \cdot 4\text{H}_2\text{O}$ (34.2 mg) were added to the glucose reactor. The three flasks were seeded with sludge (final VSS = 35 mg L^{-1}) obtained at the end of the aerobic phase of the SBR. The reactors were constantly aerated to maintain a DO concentration of more than 6 mg L^{-1} . The reactor set-up is shown in Figure 3.2. The experiment was conducted in a controlled room at 22°C . The pH was maintained between 6.8 and 7.5 during the experiment. The TCOD and SCOD were measured every two-four days for up to 24 d. The wastewater soluble and particulate inert COD were obtained by Equation 3.1 and Equation 3.2 (Orhon *et al.*, 1999a).

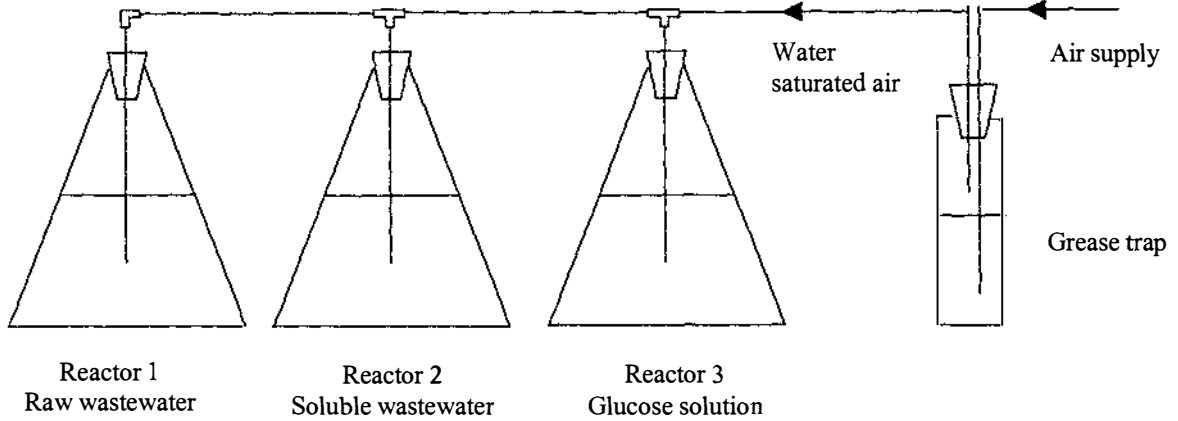


Figure 3.2 Schematic diagram of reactors set-up during wastewater inert COD measurement

$$S_{I1} = \frac{(S_T)_2 - f_{ES} Y_H S_{T1}}{(1 - f_{ES} Y_H)} \quad (3.1)$$

$$X_{I1} = \frac{(X_T)_1 - f_{EX} Y_H (C_{T1} - S_{I1})}{(1 - f_{EX} Y_H)} \quad (3.2)$$

- Where C_{T1} – Initial total COD in the reactor 1 (mg COD L⁻¹)
- S_{T1} – Initial soluble COD in the reactors 1 and 2 (mg COD L⁻¹)
- S_{G1} – Initial soluble COD in the glucose reactor (mg COD L⁻¹)
- $(C_T)_1, (C_T)_2$ – Final total COD in the reactors 1 and 2 (mg COD L⁻¹)
- $(S_T)_1, (S_T)_2$ – Final soluble COD in the reactors 1 and 2 (mg COD L⁻¹)
- f_{ES}, f_{EX} – Fraction of soluble and particulate inert COD generated in biomass decay
- $(X_T)_1$ – Final particulate COD of raw wastewater reactor (mg COD L⁻¹)
- Y_H – Heterotrophic yield coefficient (mg cell COD (mg COD)⁻¹)

3.5 Oxygen uptake rate (OUR) measurement

A sample was taken from the reactor and re-aerated to about 8.0 mg L⁻¹ DO concentration. The aerated sample was transferred to a 30 mL narrow mouth conical flask. The conical flask mouth and the YSI DO 57 probe fitted together tightly as shown in Figure

3.3. The escaped wastewater made a shield from re-aeration during the OUR measurement. The OUR was recorded by a Seckonic, SS-250F chart recorder at 1800 mm per h. The distance in the chart for 1 mg L⁻¹ DO uptake, which was also noted, was 31 mm.

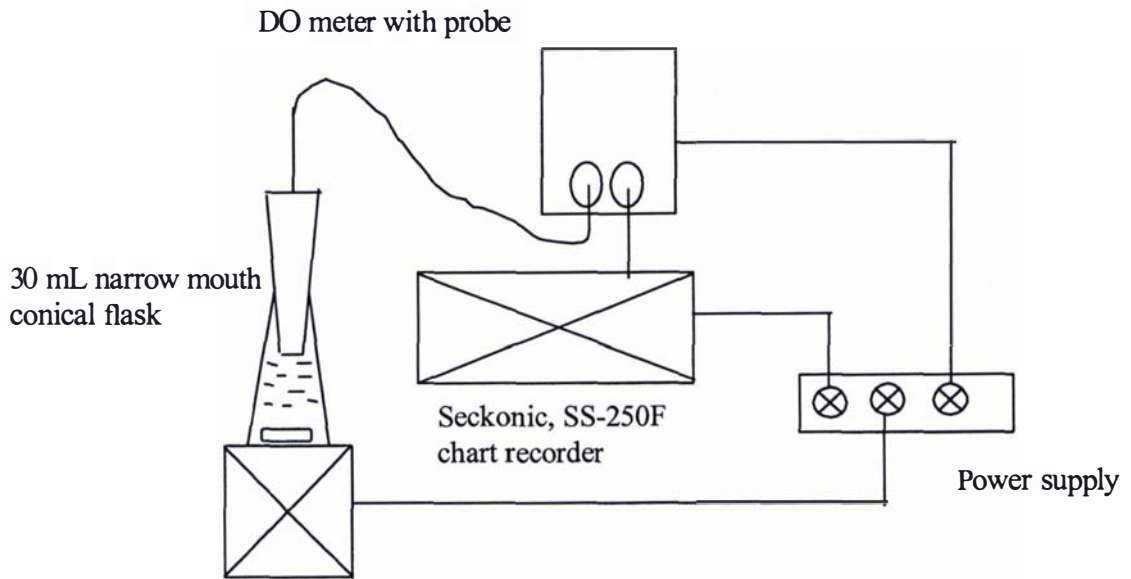


Figure 3.3 Schematic diagram of the OUR measurement set-up

3.6 Assessment of readily biodegradable COD

3.6.1 Aerobic batch test

The RBCOD was measured following the concept outlined by Ekama *et al.* (1986). Wastewater of 500 mL was taken in a 2 L conical flask. Mixed liquor was withdrawn from the SBR operated at a quasi steady state and aerated for 2 h (with 25 mg L⁻¹ allylthiourea) and then added to the wastewater such that the TCOD:VSS ratio was 1:1. The flask was aerated at 22°C in a controlled shaker. The shaker was operated at 200 rpm. Samples of 25 mL in size were withdrawn every 10 – 20 minutes and OURs were observed. Then the samples were returned to the flask. The OUR was observed for 4 to 5 h.

3.6.2 Anoxic batch test

Mixed liquor of 1 L was collected at the end of the aerobic phase from the SBR. It was aerated for 2 h continuously so that no residual biodegradable COD remained in the mixed liquor. It was then purged with nitrogen gas until the DO decreased to 0 mg L⁻¹. In a 2 L

fermenter, 750 ml wastewater and the mixed liquor were added so that the initial TCOD:VSS was 0.5 – 0.8. It was mixed using a magnetic stirrer while purging with nitrogen gas. The pH was maintained between 7 – 7.5 during the experiment. Forty mg L⁻¹ nitrogen (of final concentration) was added from the stock solution of 0.143 M potassium nitrate solution. NO_x – N concentrations were measured at 0.25-h intervals for the first hour and then measured every 0.5 h for another 3 - 4 h. Initial and final SCOD and VSS were also measured.

3.7 Maximum specific growth rate of heterotrophs

Sludge of 500 mL was withdrawn from the SBR at the end of the aerobic phase. The sludge was aerated for 2 h to ensure that there was no exogenous substrate. The aerated biomass was transferred to a respirometer (Leonard, 1996). Figure 3.4 shows the schematic diagram of the respirometer and the chart recorder.

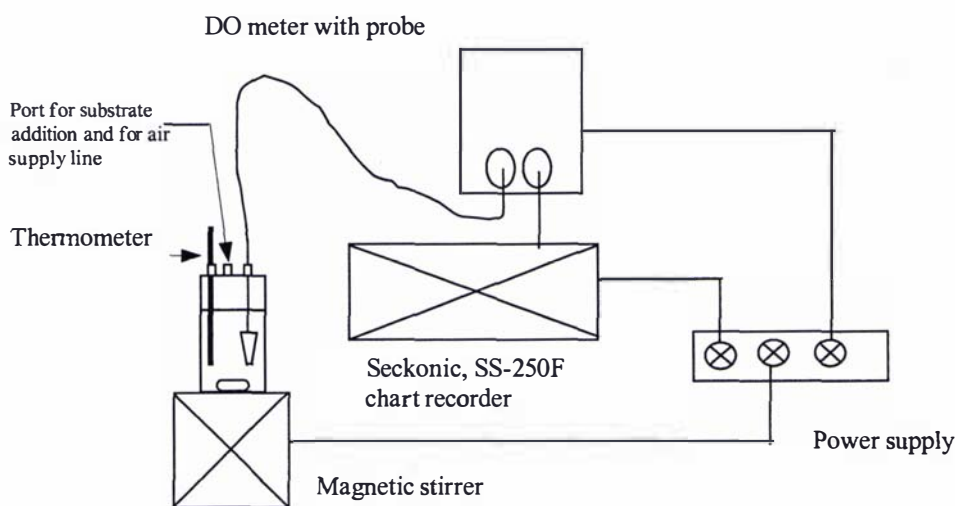


Figure 3.4 Schematic diagram of the respirometer and the chart recorder

The respirometer was sealed to prevent re-aeration during the OUR recording. The respirometer was re-aerated until DO concentration of wastewater reached 8 mg L⁻¹ and then the aeration was stopped and the OUR was recorded on the chart recorder. Once a measurable straight line was obtained, a known amount of soluble meat processing wastewater was added, and the new OUR recorded until the OUR was parallel to the initial

straight-line slope (endogenous OUR). At the end of the test, the respirometer was re-aerated and after the OUR had returned to a stable endogenous rate, the process was repeated for other initial substrate concentrations. Four runs with different substrate concentrations were performed. The experiment was conducted in a controlled room at 22° C. No nitrification inhibitor was added.

3.8 Heterotrophic decay coefficient

One L of mixed liquor was withdrawn in a 2 L conical flask from the SBR at the end of the aerobic period. Nitrification was inhibited by the addition of 20 mg L⁻¹ of allylthiourea. The flask was mixed at 200 rpm and aerated in a temperature controlled shaker at 22° C. The OUR was observed for 6 d. The flask pH was adjusted between 7.0 – 7.5 with 1 M Na₂CO₃ after each sample had been taken.

3.9 Maximum specific growth rate of autotrophs

One L of wastewater was added to a 2 L conical flask. Mixed liquor at the end of the aerobic period from the SBR was also added so that the initial TSS concentration was 50 mg L⁻¹ as suggested by Sözen *et al.* (1996). The contents in the flask were mixed and aerated in a controlled shaker at 22°C. The speed of the shaker was kept at 200 rpm. Samples were taken twice daily for 4 d and NO_x – N concentrations were analysed. The flask pH was adjusted between 7.0 – 7.5 with 1 M Na₂CO₃ after each sample had been taken.

3.10 Heterotrophic yield coefficient

Wastewater was centrifuged at room temperature at 5000 rpm for 0.25 h and filtered with 1.2 µm pore size GF/C filter. To a 2 L conical flask, 500 mL of filtered wastewater was added. Settled sludge was also added to the flask at different SCOD:VSS ratios. The flask was mixed and aerated in a temperature controlled shaker at 22°C. The speed of the shaker was kept at 200 rpm. Every 0.5 - 1 h samples were taken to analyse SCOD and TCOD for up to 8 h. VSS was also measured in alternate samples. CODs and VSSs were also measured after 24 h when the initial COD:VSS ratio was greater than 1. Yield coefficient was calculated using the Equation 3.3 and Equation 3.4 (Henze *et al.* 1987a).

$$\text{cell COD} = \text{total COD} - \text{soluble COD} \quad (3.3)$$

$$Y_H = \frac{\Delta \text{cell COD}}{\Delta \text{soluble COD}} \quad (3.4)$$

3.11 Short chain fatty acids (SCFA) measurement

A filtered sample (0.45 μm membrane filter) of 1 ml was taken in a 1.5 ml vial with a flat top cap (Eppendorf tube). The sample was acidified with 20 μl of 100 % formic acid. This sample was subsequently analysed in a VEGA SERIES gas chromatograph (GC 6000 VEGA SERIES 2 with a flame ionisation detector, carrier gas helium, SUPELCO Nukol column 15 m length \times 0.53 mm diameter and film thickness of 0.5 μm). Pressure gauge readings of helium, hydrogen and air were set at 30, 70 and 100 kPa respectively. The temperature of the injection port was set at 220°C. The flame ionisation detector port was set at 220°C. The GC was operated using a temperature programme (100°C for 1 minute, then increased at a rate of 10°C min^{-1} until 180°C and maintained at 180°C for 1 minute and then cooled to 100°C). A 1 μl of the sample was injected. After the injection the needle was washed with de-ionised water. Chromatograph output signal data were manipulated by DAPA 4.0 software installed on a personal computer. The SCFA standards were designed to measure acetate (C_2), propionate (C_3), isobutyrate (i- C_4), n-butyrate (n- C_4), iso-valeric (i- C_5), n-valeric (n- C_5) and n-caproic acid (n- C_6) concentrations of between 0 - 500 mg L^{-1} . The wastewater SCFA COD was determined from the sample taken from the feed tank. Since the feed tank was maintained in the controlled room (22°C), the SCFA COD and the RBCOD could increase in the feed tank.

3.12 Poly- β -hydroxybutyrate and poly- β -hydroxyvalerate in microbial biomass

Poly- β -hydroxybutyrate (PHB) and poly- β -hydroxyvalerate (PHV) were measured according to the concept of Comeau *et al.* (1988). Samples of 50 to 100 ml were collected and acidified with a few drops of concentrated H_2SO_4 . Then the samples were centrifuged and the sludge pellets were lyophilised. Lyophilised sludge of 20 mg was combined with 2 ml of acidified methanol (3 % H_2SO_4), containing benzoic acid as the internal standard and 2 ml of chloroform. The acidified methanol solution was prepared in a 500 ml volumetric

flask with 150 mg benzoic acid (Sigma Co. St Louis, USA), 15 ml concentrated H₂SO₄ and the remaining volume was made up with methanol. Samples and standards were heated for 3.5 h at 100°C in COD tubes (volume, 15 ml) with Teflon-lined caps. After cooling to room temperature, 1 ml de-ionised water was added to the samples and shaken vigorously for 10 minutes. The phases were allowed to separate. About 0.5 ml methyl ester was carefully withdrawn from the bottom phase with a pasteur pipette into 1.5 ml vials. In the vials 2 - 3 Na₂SO₄ granules were taken to absorb the water for a day. The samples were subsequently analysed in the gas chromatograph. The temperature of the injection port was set at 230°C. The flame ionisation detector port was set at 230°C. The GC was operated using a temperature programme (80°C for 1 min, then increased at a rate of 6°C min⁻¹ to 155°C and maintained at 155°C for 1 min). One µl of the sample was injected (split ratio: 1/5). The needle was wiped with a glass filter before injection. After the injection the needle was washed with hexane. Chromatograph output signal data were manipulated by DAPA 4.0 software installed on a personal computer. Stock PHB/PHV solution was prepared with about 25 mg of commercial PHB/PHV (Aldrich Chem. Co., Milw., USA) taken in a 25 ml volumetric flask and dissolved with 25 ml chloroform. Three standards were prepared as below,

Chloroform 1.71 ml, PHB/PHV stock solution 0.29 ml and methanol solution 2 ml.

Chloroform 1.15 ml, PHB/PHV stock solution 0.85 ml and methanol solution 2 ml.

Chloroform 0.6 ml, PHB/PHV stock solution 1.4 ml and methanol solution 2 ml.

3.13 Carbohydrate in the wastewater

Carbohydrate in the wastewater was measured by the anthrone method according to the procedure outlined by Jenkins *et al.* (1993). Seventy five percent volume to volume H₂SO₄ reagent was prepared adding 750 mL concentrated H₂SO₄ to 250 mL distilled water. It was allowed to cool to room temperature, then 200 mg anthrone was added to 5 mL pure ethanol and made up to 100 mL with 75 % H₂SO₄. The anthrone reagent was prepared fresh each time. Samples of 0.5 mL were taken in COD tubes (triplicates) and made up to 1 ml with distilled water. Using 100 µg mL⁻¹ glucose standard and distilled water, 0, 10, 25, 50 and 75 µg glucose standards were prepared each in water to a final volume of 1.0 mL.

All tubes were chilled in an ice water bath. About 5.0 mL of chilled anthrone reagent was added to each tube, mixed thoroughly and kept in the ice water bath. All tubes were transferred to the boiling water bath (100°C) for exactly 10 minutes. The tubes were then transferred immediately to the ice water bath again. The absorbance of all tubes was measured at 625 nm using the distilled water tube as a blank. A standard straight-line curve was prepared by plotting absorbance versus glucose concentration. Samples of carbohydrate concentration were calculated as glucose.

3.14 Glycogen in the sludge

Glycogen plays an important role in biological phosphorus removal from wastewaters. It has been measured indirectly using the anthrone method and the phenol method or HPLC analysis for glucose after acid hydrolysis (Mino *et al.*, 1998). These analytical methods possibly overestimate the glycogen as these methods are for total carbohydrate or for total glucose measurement. These methods were subject to errors, especially in activated sludge plants where a large fraction of non-Bio-P bacteria are present, adding to a non-glycogen-glucose (Brdjanovic *et al.*, 1998a). Brdjanovic *et al.* (1998a) developed a bioassay method with the assumption that glycogen is the limiting factor for anaerobic acetate uptake and it was tested in acetate fed reactors. In the presence of both Bio-P bacteria and significant amounts of Glycogen Accumulating Organisms (GAOs), the bioassay may not give an accurate result due to a different stoichiometric coupling between acetate uptake and glycogen consumption in the Bio-P and GAOs anaerobic metabolism (Mino *et al.*, 1998).

3.14.1 Measurement conditions for the acid hydrolysis method

Extraction of glycogen by acid hydrolysis depends on the heating temperature, acid concentration and the period of digestion (Ginsburg & Robbins, 1984). Glycogen hydrolysis is given by Equation 3.5.



To establish the measurement conditions, pure glucose and glycogen (Glycogen oyster, BDH bio chemicals Ltd. Poole, England) were used to test the recovery of glucose under different digestion conditions.

Table 3.2 shows the percentage of recovery obtained in glucose measurement by the acid hydrolysis method under different heating temperatures, duration and acid concentrations used. The 0.6 N HCl acid digestion at 100°C for 2 h gave the highest recovery of 99 % among the digestion conditions. When the duration was increased from 2 h to 2.75 h, the recovery was slightly decreased. A one-hour digestion showed a lower percentage of recovery of glycogen. Glucose appeared to be caramelised when digested at 150° C for 2 h. Degradation of glucose was reflected by the light brown colour of the digested samples. A lower percentage of recovery was obtained in the raw glycogen samples compared to oven dried and desiccated samples, which could be attributed to the water absorption by raw glycogen samples.

Table 3.2 Percentage of glucose recovery at different digestion conditions

Digestion condition	% recovery			
	Glucose	Oven dried glycogen	Desiccated glycogen	Raw glycogen
0.6 N HCl at 100°C for 1 h	98.4			71.0
0.6 N HCl at 100°C for 2 h	99.0	90.1	89.0	82.2
0.6 N HCl at 100°C for 2.25 h	97.8			81.8
0.6 N HCl at 100°C for 2.5 h	96.7			80.2
0.6 N HCl at 100°C for 2.75 h	96.6			80.6
0.6 N HCl at 120°C for 1 h	97.8			81.8
0.6 N HCl at 150°C for 2 h	49.1			
0.8 N HCl at 100°C for 2 h	96.7		89.0	
0.8 N H ₂ SO ₄ at 100°C for 2 h	98.1		80.9	

Therefore, in this study 0.6 N HCl hydrolysis at 100°C for 2 h was selected as the most suitable acid hydrolysis condition for glycogen measurement.

3.14.2 Methodology for glycogen measurement in the sludge

Freeze-dried samples of 20 mg and three glucose standards were taken in COD tubes. Four mL of 0.6 N HCl were added to each tube and digested at 100°C in a water bath for 2 h. The tubes were then allowed to cool to room temperature. The cooled tubes were shaken vigorously for 10 minutes, then allowed to settle overnight. Following this all tubes were measured for glucose using a YSI enzyme kit (Model 2700 SELECT Biochemistry analyser, membrane 2365, detection range 0 – 9 g L⁻¹ at 25 µL sample size, calibration

point 2.5 g L^{-1} , precision 2 %). A YSI buffer solution was used for sample pH adjustment. The glycogen content was expressed in mg per g dry mass.

3.15 Soluble magnesium, potassium, calcium and iron measurement

The metal concentrations were measured by flame atomic absorption spectrometry (GBC 933 AA, automatic wavelength and slit control and are controlled from an external computer). Table 3.3 shows the set wavelength and the slit width for the different metals. The AA was calibrated for each metal in the working range. The interferences in measuring potassium were removed by adding 1000 mg L^{-1} sodium. The interferences in magnesium and calcium measurements were removed by 2000 mg L^{-1} strontium.

Table 3.3 the set wavelength and slit width (GBC 933 manual)

Metal	Wave length (nm)	Slit width (nm)	Working range ($\mu\text{g (mL)}^{-1}$)	Sensitivity $\mu\text{g (mL)}^{-1}$	Lamp current/ Flame type
Magnesium	285.2	0.5	0.1 - 0.4	0.003	3 mA/ air-acetylene
Calcium	422.7	0.5	1 – 4	0.02	10 mA/ air-acetylene
Potassium	769.9	0.5	1.1 - 4.4	0.024	6 mA/ air-acetylene
Iron	248.3	0.2	2 – 9	0.05	7 mA/ air-acetylene

3.16 Microscopic observation of sludge morphology (Gram staining)

A thin smear of sludge waste sample was prepared on a microscope slide and was allowed to air dry. Then the air dried slide smear was stained for 0.02 h with crystal violet reagent and then rinsed with water. Again it was stained with iodine reagent for 0.02 h and rinsed well with water. The slide was held at an angle and decolourised with 95 % ethanol added drop by drop to the smear for 16 – 25 s. Then it was stained with safranin for 0.02 h and then rinsed with water. The slide was blotted dry. It was then examined under oil immersion at 1000X magnification with direct illumination (blue violet is positive; red is negative). The reagents were prepared according to Jenkin *et al.* (1993).

CHAPTER IV

CHARACTERISTICS OF WASTEWATER

4.1 Introduction

Wastewater characteristics are important for determining whether or not biological treatment of the wastewater is possible with or without pre-treatment. This is the only experimental data that provides the necessary information for the design of the appropriate treatment scheme and interpretation of most operational problems. Further, the quality of the wastewater characterisation is important when evaluating the performance and prediction of the biological wastewater treatment by the Activated Sludge Model No. 1 and Model No. 2.

This chapter describes the conventional pollution parameters and COD fractions of a meat processing wastewater.

4.2 Conventional pollution parameters of wastewater

Table 4.1 shows the conventional pollution parameters of the primary treated meat processing wastewater observed between the end of year 1999 and mid-year 2001. The wastewater was collected between 2.30 –3.30 p.m. to ensure that it gave representative samples from all types of wastewater sources (Annachatre & Bhamidimarri, 1993; Chang, 1999). This study was aimed to treat the mixture of the wastewater that originates from the slaughterhouse, boning process, stockyard and gut house process. The timing of sample collection was chosen to ensure that the sample was collected before the plant cleaning and floor washing operations began. In the morning, the wastewater originates mostly from the stockyard. The wastewater mixes with the previous day left wash off water. Around noon, the wastewater originates mostly from the slaughterhouse. Most of the plant processes continue during 2.30 – 3.30 p.m. As the wastewater was collected during 2.30- 3.30 p.m, it is expected to contain a mixture of effluents originated from slaughterhouse, boning process, stockyard and gut house process and represents the combined wastewater. The wastewater characteristics were measured on the day following the collection from the meat processing plant. Organic carbon in the wastewater was estimated by measuring the chemical oxygen demand (COD). COD, unlike 5d biochemical oxygen demand (BOD₅), may be used as a direct parameter to yield the stoichiometric equivalent of carbonaceous substrate, with the

provision that its biodegradable fraction is ascertained. This fraction reflects the appropriate electron balance among substrate, biomass and electron acceptors (Orhon *et al.*, 1999b).

The average total COD (TCOD), soluble COD (SCOD), total phosphorus (TP), ammonia nitrogen ($\text{NH}_3 - \text{N}$), total Kjeldahl nitrogen (TKN) and alkalinity as CaCO_3 were comparable to the values of 1352, 707, 31.2, 69.5, 127 and 325 mg L^{-1} , respectively reported by Chang (1999) for the same meat processing wastewater.

Table 4.1 Characteristics of the wastewater

Parameter	Concentrations mg L^{-1}			Number of samples (n)
	Range	Average	Standard deviation (σ)	
Total COD (TCOD)	490-2050	1390.0	402	23
Soluble COD (SCOD)	400-1010	755.0	145	23
Total Kjeldahl nitrogen (TKN)	105-177	145.0	28	22
Ammonia nitrogen ($\text{NH}_3 - \text{N}$)	26-116	75.0	27	22
Total phosphorus (TP)	25-47	34.2	7	7
Nitrite nitrogen ($\text{NO}_2 - \text{N}$)	0.0-2.14	0.6	0.6	22
Nitrate nitrogen ($\text{NO}_3 - \text{N}$)	0.0-4.32	1.0	1.2	22
Soluble phosphate phosphorus ($\text{PO}_4 - \text{P}$)	6.3-28.7	18.0	5.6	22
Total suspended solids (TSS)	230-655	446.3	150.4	17
Volatile suspended solids (VSS)	220-625	409.9	140.4	17
Alkalinity as CaCO_3	160-455	273.5	95.9	11
PH	6.15-7.03	6.58	0.26	15
Magnesium (Mg^{2+})	8.94-9.41	9.24	0.31	5
Calcium (Ca^{2+})	14.41-25.6	18.51	4.46	4
Potassium (K^+)	35.8-45.3	41.28	5.05	4
Iron	0.79-0.92	0.9	0.1	3

The conventional parameters observed in this study were in the range of, or close to, the characteristics reported for the New Zealand meat processing industries by Cooper and Russell (1991). The upper range of oxidised nitrogen concentration observed in this study may come from the component of the wastewater originating from the stockyards. The average wastewater pH is near neutral, which is good for biological nutrient removal. The average alkalinity of the wastewater is high enough to buffer the pH reduction due to nitrification. However, the lower range of the alkalinity values demonstrate that the inappropriate treatment procedure may lead to a reduction in the

pH level-which could be harmful for microorganisms, especially nitrifiers (Henze, 2002). Cations such as magnesium (Mg^{2+}) and potassium (K^+) required for biological P removal (Rickard & McClintock, 1992) were 9.21 and 41.2 $mg L^{-1}$ respectively. Lower concentrations of Mg^{2+} in the meat processing wastewater may be a limiting factor during the treatment of biological P removal. Lower concentrations of calcium (Ca^{2+}) and iron in the wastewater indicate that the P removal by precipitation will be low during the biological P removal. Table 4.2 shows the relationships between major pollution parameters.

Table 4.2 Relationships between major pollution parameters

SCOD/ TCOD	$PO_4 - P /$ TP	Particulate COD/VSS	VSS/TSS	$NH_3 - N /$ TKN	TCOD/ TKN	TCOD/ TP
0.54	0.53	1.55	0.92	0.52	9.6	40.6

The high VSS/TSS ratio indicates that most of the solids are biodegradable and only 8 % are influent fixed solids, mostly of inorganic matter. These are likely to pass through the reactor undegraded. The particulate COD/VSS ratio of 1.55 demonstrates that the wastewater has mostly organic matter. The ratio of particulate COD/VSS for domestic wastewater has a value of 1.35 (Orhon *et al.*, 1999b).

Soluble COD, $PO_4 - P$ and $NH_3 - N$ that are easily utilised by microorganisms were found to be more than 50 % of the TCOD, TP and TKN respectively. The ratio of TCOD to TKN was more than 8 and is thus suitable for N removal by nitrification and denitrification (Henze, 1991). The ratio of TCOD to TP was less than 50, which may not be enough to achieve the desired effluent P concentration by biological P removal alone (Pitman, 1991). It is therefore apparent that the conventional treatment strategies for biological nutrient removal of meat processing wastewater may not be appropriate to achieve the desired effluent quality. The TCOD:TKN:TP ratios of 100:10.4:2.5 indicates that N and P removal could not be achieved by biomass growth coupling alone. The required ratio of TCOD:TKN:TP for biomass growth is 100:5:1 (Eckenfelder & Musterman, 1995). Therefore enhanced nutrient removal technology is needed to treat meat processing wastewater.

The carbohydrate concentration of the wastewater was between 40 – 70 mg L⁻¹. The COD exerted by the carbohydrate was about 5 % of the TCOD. Fat and protein contribute to the remaining wastewater COD. From the empirical equation suggested by Russell (1980) for TCOD, the average fat concentration was determined as 237 mg L⁻¹ (51% of TCOD). Annachhatre and Bhamidimarri (1993) reported a higher fat COD contribution of 70 – 90 % in meat processing wastewater. In domestic wastewater fats contribute less COD than do the carbohydrates and the protein (Metcalf & Eddy, 1991).

4.3 Short chain fatty acid fraction of the wastewater

Short chain fatty acids (SCFA) are an important carbon source needed for biological N and P removal processes. Low molecular weight fatty acids contribute much to the readily biodegradable COD (RBCOD) fraction. Hood and Randall (2001) reported that in the 2-5 carbon SCFA, acetic and iso-valeric acids are the most efficient, and propionic acid is the least efficient, substrates for biological P accumulating bacteria (Bio-P). Internal storage products of Bio-P depend on the type of the fatty acids which it consumes (Hood & Randall, 2001; Sato *et al.*, 1992). The types of internal storage products are important in biological P removal (Hood & Randall, 2001).

Figure 4.1 shows the fractions of the SCFA COD to the total SCFA COD. Samples were taken from the feed tank to analyse the SCFA COD fractions. The figure illustrates that 50 % of the total SCFA COD was due to acetic and iso-valeric acid and other SCFAs contributed the remaining 50 %. Of the remaining SCFA, 28 % of the total SCFA COD was contributed by the propionic acid. The SCFA COD of the wastewater ranged from 11 to 23 % of the TCOD (average = 17.5 %). The SCFA COD fractions changed during the storage period as well as in the feed tank.

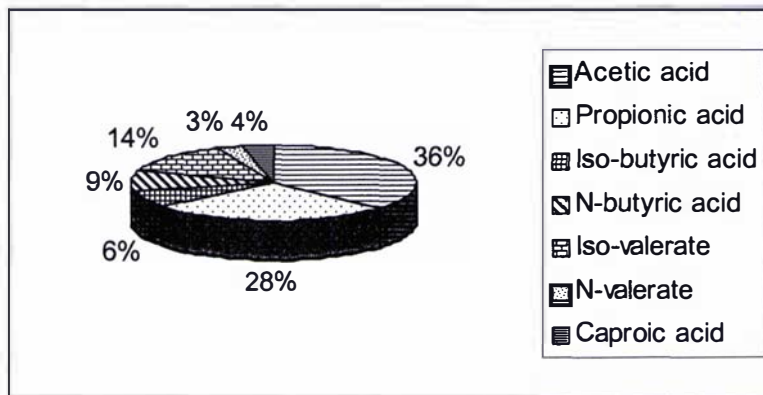


Figure 4.1 Short chain fatty acid fractions of the wastewater

A change in the wastewater SCFA COD fractions was observed during the retention time (maximum 2 d) in the feed tank. Freshly collected wastewater was transferred to the feed tank and samples were analysed for SCFA, TCOD and SCOD for two consecutive days. Table 4.3 shows the variation in SCFA COD fraction in the wastewater during the retention time in the feed tank. The SCFA COD fraction increased from 11.2 % in the fresh sample to 17.2 % in the second day sample. The increase in the SCFA COD fraction was probably from the fermentation of rapidly hydrolysable COD in the wastewater. The growth of the anaerobic biomass was reflected by the net increase in the particulate COD.

Table 4.3 Wastewater SCFA COD fraction changes in a $22 \pm 2^\circ\text{C}$ controlled room

Time (d)	TCOD (mg L^{-1})	Soluble COD (mg L^{-1})	Particulate COD(mg L^{-1})	SCFA COD(mg L^{-1})	SCFA COD/TCOD
0	1485	752	733	167	11.2
1	1629	692	937	240	14.7
2	1779	660	1119	306	17.2

4.4 Assessment of initial soluble and particulate inert COD in the wastewater

A major drawback in the use of COD as a design parameter for carbonaceous substrate is the fact that it includes, aside from a biodegradable fraction, all non-biodegradable compounds that are also oxidised and quantified in the test. This drawback is being overcome by new techniques that may be used separately to identify biodegradable and inert (residual) COD fractions (Orhon & Artan, 1994). The total

biodegradable COD is one of the key parameters in activated sludge design as it indicates the magnitude of organic carbon potentially removable by biological means from wastewater. A number of methods have so far been proposed for the estimation of inert COD fractions in wastewater (Orhon *et al.*, 1999a). They showed experimentally that the assumption of a constant f_{EX} coefficient defining the residual fraction of endogenous biomass (Henze *et al.*, 1987a) was not justified and they proposed a unified procedure for the experimental assessment of inert COD fractions of wastewater, as well as residual microbial products. A review of the soluble microbial products (SMP) in wastewater treatment systems was given by Barker and Stuckey (1999).

The experimental procedure, (Orhon *et al.*, 1999a) used to determine the influent soluble and particulate microbial products is explained in Chapter III. Figures 4.2 – 4.4 show the COD profiles for the three parallel batch tests conducted in this study. Figure 4.2 indicates that the immediate removal of soluble COD from the glucose reactor was slower than from the filtered wastewater reactor. This implies that the biomass from the SBR was not acclimatised immediately in the media to remove glucose as a substrate. All the reactors CODs stabilised after approximately 14 d. Table 4.4 shows the COD fractions of meat processing wastewater. Calculations of inert COD fractions are shown in Appendix A.

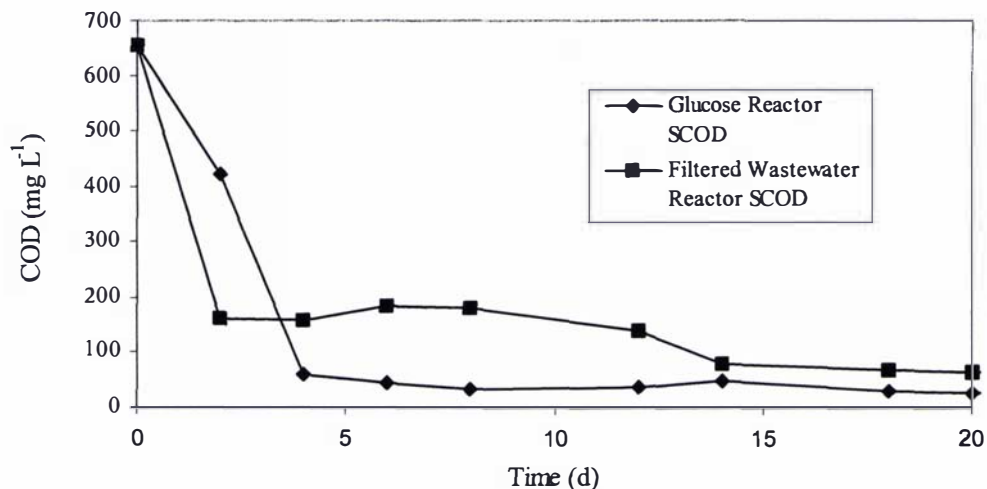


Figure 4.2 SCOD profiles of the filtered wastewater and glucose reactor

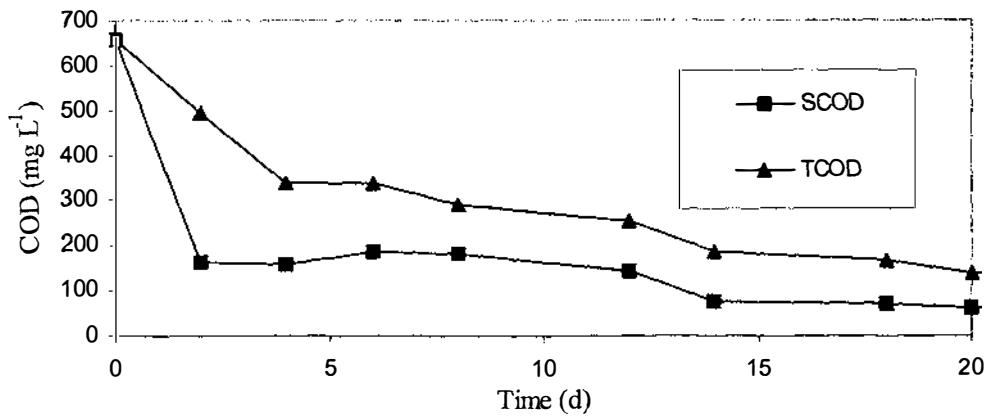


Figure 4.3 COD profiles of the filtered wastewater reactor

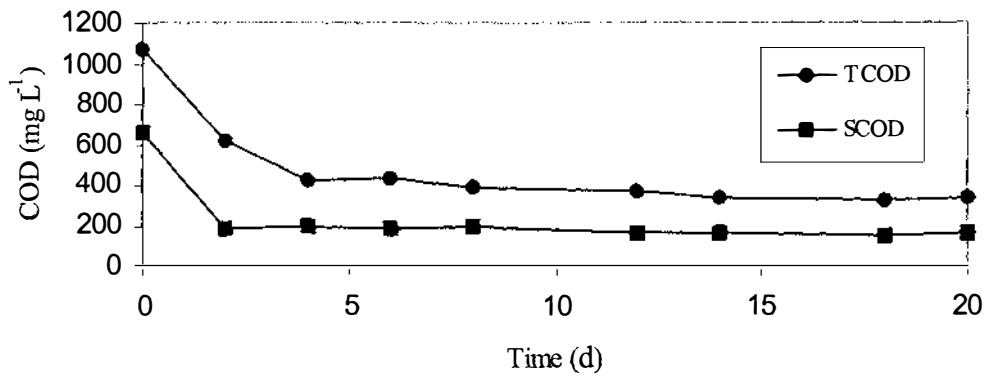


Figure 4.4 COD profiles of the raw wastewater reactor

Table 4.4 COD fractions of meat processing wastewater

Parameter												Reference
C_{T1} (mg L^{-1})	S_{T1} (mg L^{-1})	$(S_P)_2$ (mg L^{-1})	S_{I1} (mg L^{-1})	S_{S1} (mg L^{-1})	X_{P2} (mg L^{-1})	X_{I1} (mg L^{-1})	$S_{S1}/$ C_{T1}	$S_{I1}/$ C_{T1}	$(S_P)_2 /$ C_{T1}	$X_{P2}/$ C_{T1}	$X_{I1}/$ C_{T1}	
1072	656	23.3	38.8	612.2	68.2	46.9	0.57	0.04	0.02	0.06	0.04	This study
1941	674	86	63	611	157	120	0.31	0.03	0.01	0.09	0.06	Chang (1999)
2600	1140	-	30	1110	-	305	0.43	0.01	-	-	0.12	Gorgun <i>et al.</i> (1995)

C_{T1} - Total COD of the wastewater, mg L^{-1}

S_{T1} - Soluble COD of the wastewater, mg L^{-1}

$(S_P)_2$ - Soluble COD due to microbial products, mg L^{-1}

S_{I1} - Influent inert soluble COD, mg L^{-1}

S_{S1}	- Influent soluble biodegradable COD, mg L^{-1}
X_{P2}	- Particulate COD due to microbial products, mg L^{-1}
X_{I1}	- Influent inert particulate COD, mg L^{-1}

Influent soluble and particulate inert COD fractions were about 4 % each in the wastewater. The results found in this study are similar to those of Chang (1999) but are slightly different from those of Gorgun *et al.* (1995), however, their reported values were for integrated meat processing wastewater. Germirli *et al.* (1991) reported a soluble inert fraction of 0.055 in terms of SCOD for meat processing wastewater. The soluble biodegradable COD fraction was higher in this study compared to others. This could be due to the higher percentage (61 %) of SCOD fraction found in the wastewater used in this study compared to observed 35 % and 44 % in their wastewater respectively. However, the average wastewater SCOD fraction was higher than 50 % during this study similar to the values reported by Chang (1999). The higher fraction of soluble biodegradable COD indicates the presence of a higher fraction of easily biodegradable COD fraction in the wastewater.

Soluble and particulate microbial products of about 2 % and 6 % found in this study are comparable to 1 % and 9 % reported by Chang (1999). The production of soluble microbial products was less than the production of particulate microbial products. The total inert SCOD in the wastewater and the soluble microbial products was 6 % of the TCOD of the wastewater. Table 4.5 shows the fraction of biodegradable COD converted into inert microbial products.

Table 4.5 Fraction of biodegradable COD converted into inert microbial products

	Y_{SP}	f_{ES}	Y_{XP}	f_{EX}
This study	0.038	0.06	0.11	0.174
Chang (1999)	0.049	0.08	0.089	0.141
Gorgun <i>et al.</i> (1995)	0.04	0.06	-	-

Where,

Y_{SP} - fraction of biodegradable COD converted into soluble inert microbial products

Y_{XP} - fraction of biodegradable COD converted into particulate inert microbial products

- f_{ES} - the fraction of soluble inert COD generated in biomass decay
 f_{EX} - the fraction of particulate inert COD generated in biomass decay

The fraction of soluble and particulate inert microbial products generated in biomass decay was similar to values reported by Chang (1999) and Gorgun *et al.* (1995). The fraction of particulate inert COD fraction generated in the biomass decay was slightly less than the recommended value of 0.2 in the Activated Sludge Model No. 1 (ASM 1) (Henze *et al.*, 1987a) for domestic wastewater. The total value of particulate and soluble microbial inert COD fractions of 0.23 (0.06 + 0.17) was slightly higher than the recommended value of 0.2 in the ASM 1. This constant value of 0.2 could be assumed for meat processing wastewater in the activated sludge models where only constant particulate inert fractions are generated due to the biomass decay. However, the generation of particulate microbial products is wastewater specific (Orhon *et al.*, 1999a).

The production of soluble microbial products (SMP) and their identification will vary in a treatment plant according to the influent strength, hydraulic retention time (HRT), solids retention time (SRT), organic loading rate (OLR) and the physiology of the microorganisms. The presence of SMP in the effluents from a biological treatment processes is of particular interest in terms of achieving discharge consent levels for BOD and COD. SMP also exhibit several characteristics, such as toxicity and metal chelating properties, that affect the performance of the treatment system, and their presence has also been shown to adversely affect the kinetic activity and flocculating and settling property of the sludge (Barker & Stuckey, 1999). Therefore, the identification of the SMP from meat processing wastewater treatment and minimising their production is a fertile area for future research.

4.5 Readily biodegradable COD

Dold *et al.* (1980) recognised that the wide array of organic matter in wastewater may be evaluated in two broad groups represented by markedly different rates of biodegradation. This approach was further elaborated for the identification and the mechanistic description of readily biodegradable and slowly biodegradable COD components (Henze *et al.*, 1987a, b).

The correct assessment of the readily biodegradable COD (RBCOD) in wastewater is of great theoretical and practical significance. RBCOD is the only substrate component directly related to microbial growth in current models, also it allows the calculation of the other important COD fraction, namely the slowly biodegradable COD (SBCOD), representing the bulk of the influent COD content. SBCOD is often the critical model component for the modelling and design of an activated sludge system, especially for industrial wastewater (Cokgor *et al.*, 1998).

4.5.1 Conceptual basis

Almost all the methods proposed for the determination of readily biodegradable organic matter rely on respirometric analysis of activated sludge behaviour. They propose either oxygen uptake rate (OUR) measurements in dynamic systems (Ekama *et al.*, 1986) or OUR/nitrate utilisation rate (NUR) measurements in aerobic/anoxic batch reactors (Ekama *et al.*, 1986; Kappeler & Gujer, 1992; Kristensen *et al.*, 1992; Sollfrank & Gujer, 1991). Batch reactors are often preferred, because they are simpler to operate and problems and interference inherently associated with reactor hydraulics could be avoided (Cokgor *et al.*, 1998).

The aerobic batch test consists of obtaining and evaluating an oxygen uptake rate profile (OUR curve), with a pre-selected volume of wastewater (V_{ww}) of known TCOD strength being mixed with a pre-selected volume of mixed liquor (V_{ml}) of known MLVSS concentration in an aerated and stirred batch reactor. The aerobic batch experiments rely on the assumption that the high OUR level in the first phase of the test relates to the utilisation of the RBCOD initially present in the wastewater. The OUR is expected to drop to a lower plateau correlated only to the hydrolysis of the slowly biodegradable COD (Ekama *et al.*, 1986). The current mechanistic explanation of the activated sludge process, however, involves simultaneously occurring microbial processes, as described by the endogenous decay or the death regeneration models (Henze *et al.*, 1987a; Orhon & Artan, 1994). Equation 4.1 may be used to find readily biodegradable COD (S_s) from the OUR curve (Ekama *et al.*, 1986).

$$S_s = \frac{\Delta S}{1 - f_x Y_H} \cdot \frac{V_{ml} + V_{ww}}{V_{ww}} \quad (4.1)$$

Where, Y_H and f_X are the heterotrophic yield coefficient and the ratio of biomass COD to VSS. The term ΔS , is defined as the area above the second plateau of the OUR profile, as indicated in Figure 4.5.

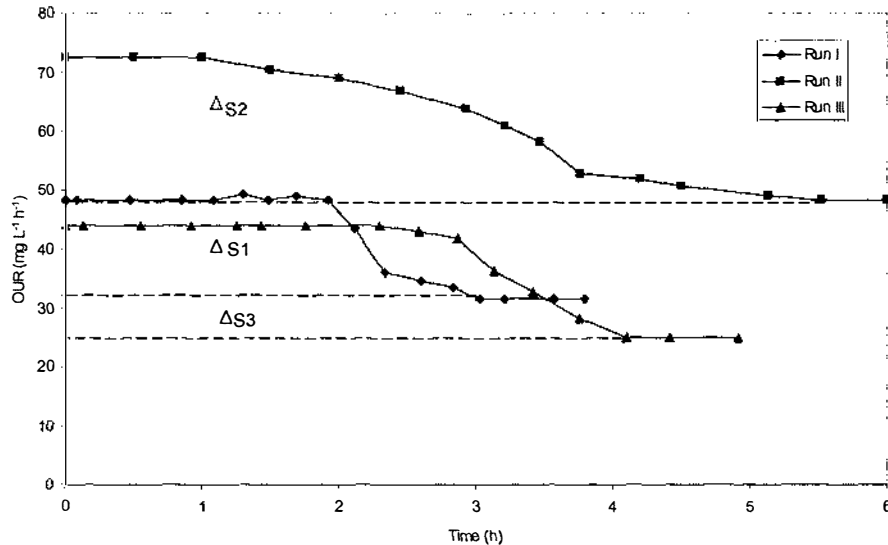


Figure 4.5 Oxygen uptake rate profiles for meat processing wastewater

The same parameter may also be calculated from the N profile in an anoxic batch reactor. In this test, the RBCOD (S_S) fraction of the wastewater sample is detected as associated with the initial N utilisation rate. The amount of N consumed (ΔN_1 as shown in Figure 4.6) due to the oxidation of S_S , corrected for the interference of the hydrolysed substrate could be used to calculate the S_S content of the sample, by means of the Equation 4.2 (Ekama *et al.*, 1986).

$$S_S = \frac{2.86}{1 - f_X Y_H} \cdot \Delta N_1 \cdot \frac{V_{mi} + V_{ww}}{V_{ww}} \quad (4.2)$$

4.5.2 Readily biodegradable COD measurement by batch OUR method

Henze (1992) describes the RBCOD fraction (S_S) as being limited to small molecules of volatile fatty acids, carbohydrates, alcohol and amino acids, with a molecular weight below about 1000. But in raw wastewater a fraction of the COD with molecular weight below 1000 is not readily biodegradable but belongs to organic matter that can be rapidly hydrolysed. The rapidly hydrolysable matter S_H , is described as that which would be hydrolysed under aerobic conditions within a few hours, and a general approximation for its estimation is given as:

$$S_H = \text{Total soluble COD} - S_I - S_S \quad (4.3)$$

Three batch tests were carried out with an initial ratio of mass of COD with respect to the mass of VSS approximately 1. The OUR profiles are shown in Figure 4.5. The $f_X Y_H$ value was taken as 0.63 which was determined in other experiments in this study (Chapter VI). Table 4.6 shows the percentage of the RBCOD together with rapidly hydrolysable COD in terms of the TCOD of the wastewater.

Table 4.6 Wastewater COD fractions

Trial	TCOD (mg L⁻¹)	SCOD (mg L⁻¹)	RBCOD (mg L⁻¹)	Soluble inert COD (mg L⁻¹)	Rapid hydrolysable COD (mg L⁻¹)
Run I	850	480 (56%)	146 (17.2%)	34 (4%)	300 (35%)
Run II	1663	918 (55%)	278 (16.7%)	67 (4%)	573 (34%)
Run III	1462	940 (64%)	238 (16.3%)	58 (4%)	644 (44%)
Average	1325	779 (59%)	221 (16.7%)	53 (4%)	506 (38%)

The RBCOD fraction was 15 - 18 % of the total COD, which was similar to the reported value by Chang (1999). The RBCOD fraction was slightly higher than the 13 % reported by Gorgun *et al.* (1995) for integrated meat processing wastewater. Rapidly hydrolysable COD was between 34 - 44 % which is slightly higher than the value of 28 % reported by Gorgun *et al.* (1995). Since the average SCOD of the wastewater was about 54 % and the readily biodegradable and the inert COD fraction was 21 % (17+4), the rapidly hydrolysable COD could be closer to 33 % of the TCOD. A summary of COD fractions is shown in Figure 4.7.

The slowly hydrolysable COD was 42 % (583 mg L⁻¹) of the TCOD (1390 mg L⁻¹). The average VSS was 410 mg L⁻¹ as shown in Table 4.1. Therefore the ratio of slowly hydrolysable COD to VSS was 1.42. This is exactly the same as the theoretical biomass conversion factor (Orhon & Artan, 1994) and it could be assumed that most of the slowly hydrolysable CODs were from organic origin. Since average SCFA COD was 17.5 % as previously reported in this study (Section 4.3), it could be assumed that RBCODs are in the form of SCFA COD in this study. However, the exact relationship between RBCOD and SCFA COD has to be determined in future studies. Typical values of 10 - 15 % for readily biodegradable and 15 - 25 % for rapidly hydrolysable

COD reported for domestic wastewater by Henze (1992) are slightly less than the corresponding values in the meat processing wastewater in this study.

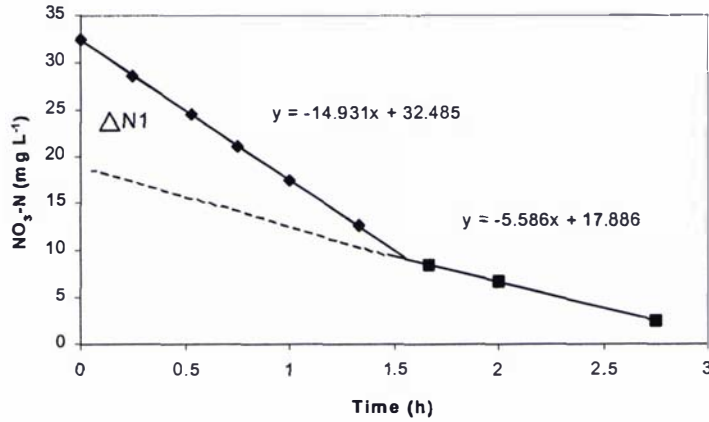


Figure 4.6 Nitrate uptake rate profile for meat processing wastewater

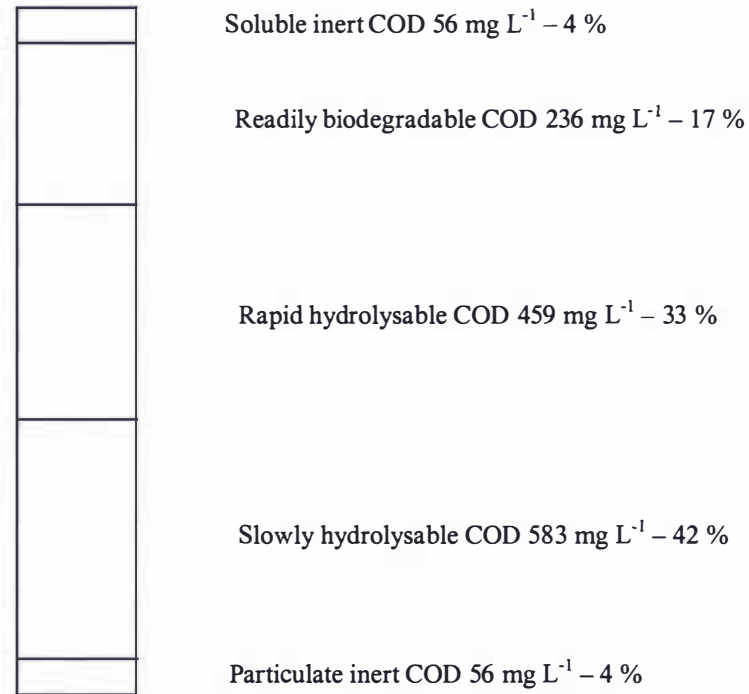


Figure 4.7 Influent COD fraction (average TCOD = 1390 mg L⁻¹)

4.5.3 Readily biodegradable COD measurement by batch NUR method

Average readily biodegradable COD determined by the NUR method was between 23 – 24 % of the TCOD in the three Trials. This higher fraction compared to the OUR method could be explained by the lower yield coefficient in the anoxic condition than in

the oxic condition (Cokgor *et al.*, 1998; McClintock *et al.*, 1988). The Anoxic yield coefficient was calculated using the Equation 4.4 (Cokgor *et al.*, 1998).

$$\frac{1 - f_X Y_{HD}}{1 - f_X Y_H} = \frac{1 - 1.42 * Y_{HD}}{1 - 1.42 * 0.45} = \frac{23.5}{16.5} \quad (4.4)$$

The anoxic yield coefficient (Y_{HD}) was $0.34 \text{ g VSS (g COD)}^{-1}$ that is closer to 0.37 found for domestic wastewater by Cokgor *et al.* (1998). Orhon *et al.* (1996) theoretically calculated the anoxic yield for domestic wastewater as $0.5 \text{ g-cell COD (g COD)}^{-1}$ on the basis of energetic considerations. The aerobic and anoxic yield coefficients were 0.50 and $0.27 \text{ g VSS (g COD)}^{-1}$ on synthetic wastewater (McClintock *et al.*, 1988).

Measurement of oxidised nitrogen ($\text{NO}_3 - \text{N} + \text{NO}_2 - \text{N}$) or $\text{NO}_3 - \text{N}$ did not yield acceptable results when coupled with appreciable $\text{NO}_2 - \text{N}$ accumulation in the course of the experiment. In such cases, the electron equivalence of the RBCOD consumption is best satisfied by the following equation (Henze, 1986; Sozen *et al.*, 1998).

$$\text{N} = \text{NO}_3^- - \text{N} + 0.6\text{NO}_2^- - \text{N} \quad (4.5)$$

The two different RBCOD fractions were confirmed by the parallel OUR and NUR tests. OUR and NUR profiles are shown in Figures 4.8 and 4.9 in a parallel OUR and NUR test. The RBCOD fractions were 15.7 % and 23.7 % by OUR and NUR methods respectively. The NUR profiles were sometimes observed to be non-linear possibly due to a sudden release of phosphorus when the pH was adjusted. This observed phenomenon will be discussed further in Chapter VI.

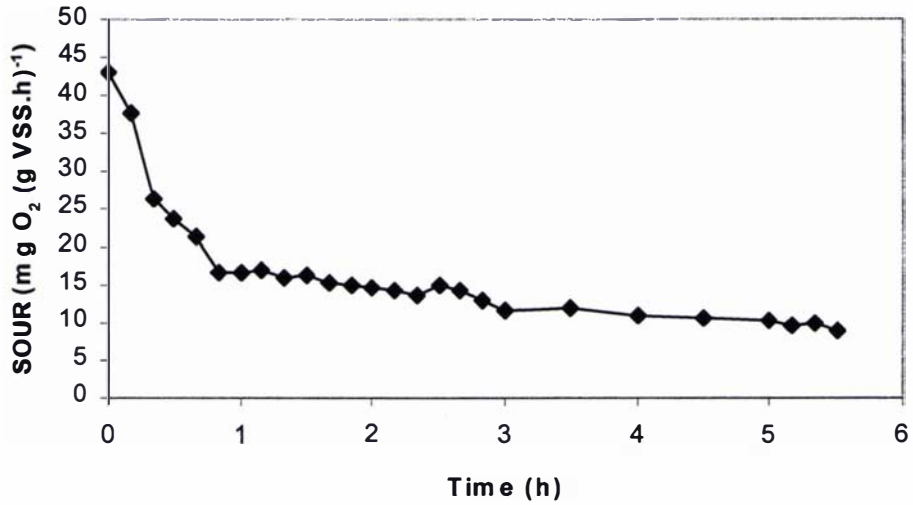


Figure 4.8 OUR profile of a parallel OUR and NUR test in meat processing wastewater

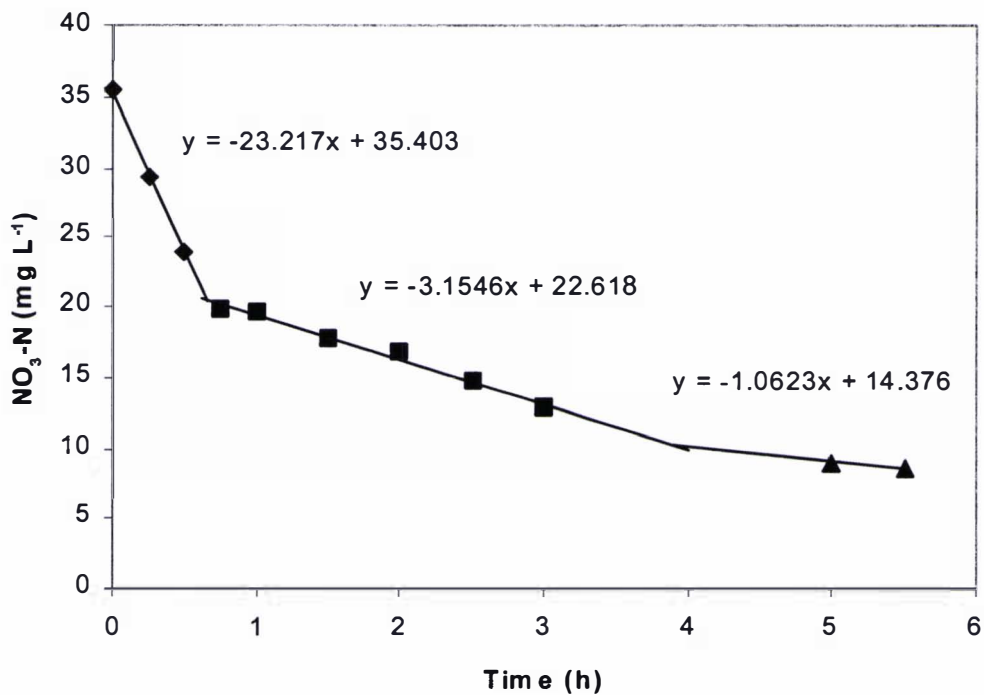


Figure 4.9 NUR profile of a parallel OUR and NUR tests in meat processing wastewater

Specific nitrogen uptake rates related to RBCOD, slowly biodegradable COD and endogenous respiration were 10 - 12 mg N (g VSS.h)⁻¹, 1.2 - 4.2 mg N (g VSS.h)⁻¹ and 0.5 - 0.7 mg N (g VSS.h)⁻¹ respectively at room temperature (22 ± 2°C). These

denitrification rates are within the maximum rates achievable with different carbon substrates such as wastewater and endogenous biomass at 20°C reported by Henze (1991). The denitrification rates of RBCOD and slowly biodegradable COD are comparable to the rates of 5.3 – 10.5 and 2 – 2.8 mg NO_x – N (g VSS.h)⁻¹ observed by Bickers and Van Oostrom (2000) for stick water, paunch liquor, slaughter floor wastewater, and dilute blood. A maximum denitrification rate of 10 - 12 mg N (g VSS. h)⁻¹ was obtained when acetate was used as the substrate instead of meat processing wastewater.

4.6 Summary

The conventional pollution parameters concentrations were in the range of, or close to, the concentrations reported for the New Zealand meat processing industries. SCOD, PO₄ – P and NH₃ – N were found to be more than 50 % of the TCOD, TP and TKN respectively. The ratios of TCOD:TKN and TCOD:TP were 9.6 and 40.6 respectively.

The average COD exerted by carbohydrate, protein and fat were 5, 44 and 51 % of the average TCOD respectively. The inert soluble and particulate COD fractions were 4 % each. The fraction of particulate inert COD generated by the biomass decay was 0.17. The wastewater contained 15 - 18 % of RBCOD. The rapidly hydrolysable COD of the wastewater was 33 % of the TCOD. The SCFA COD varied from 11 % to 23 % of the TCOD. Of the RBCOD of the meat processing wastewater more than 65 % was SCFA COD. Acetic and iso-valeric acids contributed 50 % of the total SCFA COD. The RBCOD found by the NUR method was higher than that found by the OUR method possibly due to a lower anoxic yield coefficient. The anoxic yield coefficient was 0.34 g VSS (g COD)⁻¹.

Specific nitrogen uptake rates related to RBCOD, slowly biodegradable COD and endogenous respiration were 10 – 12 mg N (g VSS.h)⁻¹, 1.2 – 4.2 mg N (g VSS.h)⁻¹ and 0.5 – 0.7 mg N (g VSS.h)⁻¹ respectively.

CHAPTER V

PERFORMANCE OF SEQUENCING BATCH REACTOR

5.1 Introduction

The characteristics of the primary treated meat processing wastewater for aerobic bio treatment were discussed in Chapter IV. The conventional pollution parameters such as COD, TKN, TP, and $\text{NH}_3 - \text{N}$ for the meat processing wastewater in this study were in the range of, or closer to, the characteristic values reported for the New Zealand meat processing industries by Cooper and Russell (1991). The TCOD:TKN:TP ratios of 100:10.4:2.5 determined for the meat wastewater indicate that N and P could not be removed only by biomass growth coupling. Hence enhanced nutrient removal technology is needed to treat the wastewater. As discussed previously in Chapter II, Sequencing Batch Reactor (SBR) technology has been developed and used in recent years for simultaneous organic carbon and nutrient removal (Keller *et al.*, 1997). Prior to treatment using an SBR, pre-treatment by anaerobic pond has been employed for organic carbon rich wastewaters to reduce the aeration requirement (Subramaniam *et al.*, 1994). As the meat processing wastewater used in this study has a COD of 1390 mg L^{-1} on an average, pre-treatment is probably not required. For effectively removing combined organic carbon and nutrient using an SBR the operating conditions should be properly manipulated to introduce anaerobic, anoxic and aerobic conditions into a time cycle.

In this chapter establishment of an effective operating cycle for the treatment of simultaneous removal of organic carbon and nutrient from primary treated meat processing wastewater is discussed. Hydraulic retention time (HRT), dissolved oxygen (DO) concentration in the mixed liquor and different periods of operating phases were investigated to establish the effective operating cycle.

5.2 Performance of the SBR during Run I

Start up of the SBR is explained previously in Chapter III. Selection of solids retention time (SRT) is important in a nutrient removal activated sludge plant. In the activated sludge plant autotrophic biomass is usually a small fraction of the total biomass and it is dominated by heterotrophic organisms. The selection of SRT, therefore, relies on the autotrophs being maintained in the treatment system. The

minimum required sludge age to prevent the washout of nitrifiers from the reactor is given by Equation 5.1 (Orhon & Artan, 1994). Values for the maximum specific growth rate of autotrophs in mixed cultures oxidising $\text{NH}_3 - \text{N}$ under optimal conditions in the laboratory have been reported in the literature to be in the range from 0.34 to 0.65 d^{-1} for domestic wastewater (Henze *et al.*, 1987a,b). However higher values between 0.65 – 0.8 d^{-1} were determined as the maximum specific growth rates of nitrifiers in meat processing wastewater in this study (Chapter VI).

$$SRT \geq \frac{1}{\mu_{\max,A} - b_A} \quad (5.1)$$

where $\mu_{\max,A}$ is maximum specific growth rate of autotrophs and b_A is decay rate of autotrophs. The SRT of 15 d was selected in this study with minimum safety factor of

1.2 ($\frac{1}{\text{fraction of aeration}} \times \frac{1}{(0.34 - 0.15)} \approx 12.5$). Where fraction of aeration period in

the cycle time, $\mu_{\max,A}$ and b_A were taken as 0.42, 0.34 d^{-1} and 0.15 d^{-1} respectively. A higher SRT value of 20 d was used by Subramaniam *et al.* (1994) to treat meat processing wastewater. The HRT was kept at 1.5 d during Run I. Dissolved oxygen was not controlled at a particular concentration and the air-flow rate was less than 4.8 L air (L volume.h) $^{-1}$ during this run. The influent feed time was 0.5 h. During this run the reactor was placed in a controlled temperature room at $22 \pm 2^\circ\text{C}$. The operating phases of the SBR are shown in Table 5.1.

Table 5.1 Operating cycle of Run I (6-h cycle)

Reactor Sequence	Time (h)
Fill and non-aerated mix	2.0
Aerated mixed react 1	1.5
Non-aerated mixed react (anoxic)	0.5
Aerated mixed react 2	1.0
Settle	0.50
Decant and Idle	0.50

During the initial period excess foam was observed in the reactor during aeration. Foam rose up to the lid of the SBR and created a short circuit in the level controllers.

Figure 5.1 shows the influent and effluent COD profiles during this run. The organic loading rate (OLR) on a volumetric basis was 1 kg COD ($\text{m}^3.\text{d}$) $^{-1}$. The OLR was above the recommended rate of 0.60 – 0.70 kg COD ($\text{m}^3.\text{d}$) $^{-1}$ for activated sludge systems

treating slaughterhouse wastewater (Johns, 1995). The effluent SCOD was between 5 – 12 % of the influent TCOD. The total effluent inert SCOD was expected to be about 6 % (originating both from wastewater and biomass). The occasional poor performance of the SBR might have been due to the loss of biomass with the effluent from previous cycles due to filamentous bulking. Microscopic observation after Gram staining of the sludge smear confirmed the abundant of Gram negative filaments. Filamentous bulking in activated sludge plants could be due to one of the five major causes (i) low F/M (or equivalently long sludge age) conditions (ii) low DO in the aeration tank (iii) septic or high sulphide influent (iv) low pH and (v) nutrient deficiencies (Jenkins *et al.*, 1993). Although the SBR received high organic loaded wastewater which favours the floc formers rather than the different types of filaments the prevalence of inadequate DO in the reactor might have been a reason for the filamentous bulking observed during this run (Chiesa & Irvine, 1985).

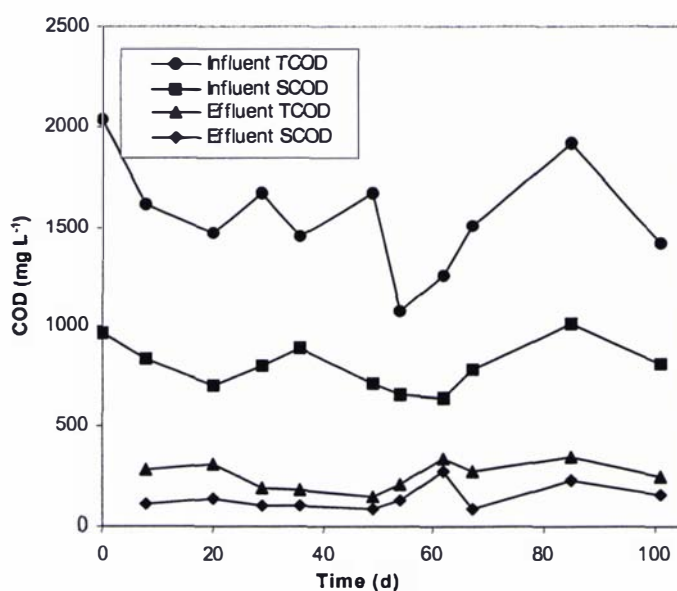


Figure 5.1 Influent and effluent COD during Run I

With sludge bulking, the reactor operation was disturbed occasionally by one of the following causes, 1. Problems in aeration control 2. Problems in flow controls due to failure of pumps 3. Clogging of feed tubes 4. Failure in solenoid valves for controlling decant and sludge waste 5. Short circuits in level controls. Later, most of the operational problems were identified and corrective actions were taken.

Figure 5.2 shows the N and P concentrations variation in the influent. Figure 5.3 shows the variation in N and P concentrations in the effluent. The effluent TKN and $\text{NH}_3 - \text{N}$ concentrations increased with time and showed incomplete nitrification. High values of $\text{NH}_3 - \text{N}$ might have been due to inadequate aeration coupled with higher OLR. Concentration of $\text{NO}_2 - \text{N}$ was greater than $\text{NO}_3 - \text{N}$ in the effluent much of the time. This could have been due to inhibition of $\text{NO}_2 - \text{N}$ oxidation by inadequate aeration and/or high OLR (Van Loosdrecht & Jetten, 1998). When effluent equivalent concentration of $\text{NO}_3 - \text{N}$ ($0.6\text{NO}_2 - \text{N}$ plus $\text{NO}_3 - \text{N}$) was above 7.41 mg L^{-1} , the effluent $\text{PO}_4 - \text{P}$ concentration was also above 10 mg L^{-1} and showed no enhanced biological phosphate removal (EBPR). This indicates that the wastewater RBCOD was not enough for combined N and P removal when the effluent $\text{NO}_3 - \text{N}$ was above 7.4 mg L^{-1} .

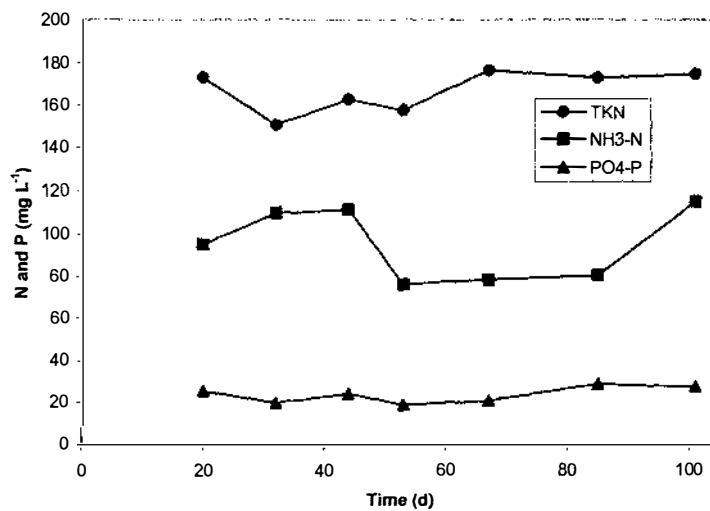


Figure 5.2 Influent N and P during Run I

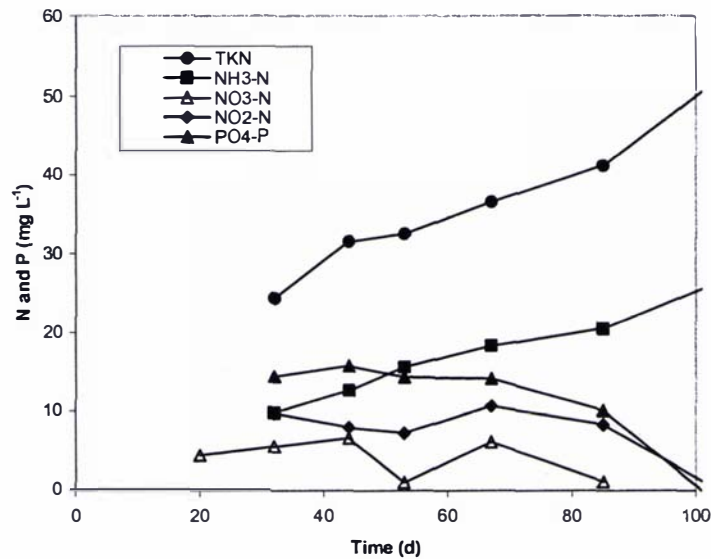


Figure 5.3 Effluent N and P during Run I

Steady state in a treatment system can be defined as the situation where, the effluent characteristics such as soluble COD, $\text{NH}_3 - \text{N}$, $\text{NO}_2 - \text{N}$, $\text{NO}_3 - \text{N}$ and $\text{PO}_4 - \text{P}$ concentrations remain constant with time. SBR systems necessarily are dynamic, and the concept of steady state is not relevant. However, if we operate an SBR system with a fixed influent loading, the SBR system will attain a quasi "steady state" (the input could be either a **Constant Input** or a **Variable Input**). That is, the mixed liquor VSS at the end of aeration, effluent soluble COD, $\text{NO}_3 - \text{N}$ and $\text{PO}_4 - \text{P}$ concentrations would be repeated identically from cycle to cycle, where the term "cycle" refers to the longest cycle in the dynamic system (not necessarily the cycle time of the SBR). For example, the cycle time of a Variable Input influent element typically would be 24 hours, and this would be the quasi steady state cycle time (provided of course that the SBR cycle time is less than 24 hours which usually is the case). A general guideline for the time a dynamic system takes to reach a quasi "steady state" is three to four times the longest time constant in the system (Ky *et al.*, 2001). In the case of SBR systems usually the longest time constant will be the SRT (or sludge age).

Figure 5.4 shows the TSS and VSS concentrations in the effluent. Occasionally the TSS and VSS concentrations reached above 100 mg L^{-1} . High effluent solids concentration may be due to the dispersed growth observed in the sludge smear by microscope. The mixed liquor VSS and TSS increased steadily for up to 50 d. Due to the occasional escape of high concentration of biomass with effluent, the SBR system did not reach a quasi steady state.

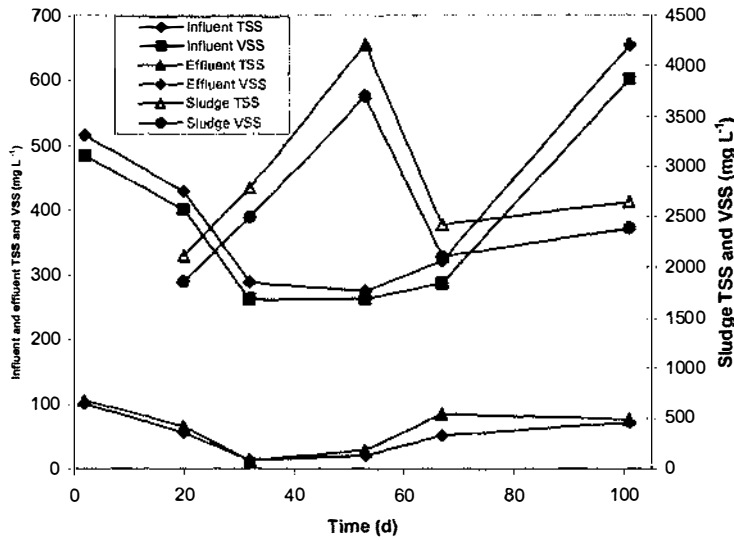


Figure 5.4 Influent, effluent and sludge solids during Run I

Figure 5.5 shows soluble COD, $\text{NH}_3 - \text{N}$, $\text{NO}_2 - \text{N}$, $\text{NO}_3 - \text{N}$ and $\text{PO}_4 - \text{P}$ profiles in a cycle study after 2 months' operation of this run. Influent TCOD, TKN, $\text{NH}_3 - \text{N}$ and $\text{PO}_4 - \text{P}$ were 1506, 160, 80 and 20 mg L^{-1} respectively. The COD and N removal efficiencies were greater than 93 and 87 % respectively from this cycle study. The COD and N removal efficiencies were calculated using the Equations 5.2 and 5.3. Phosphorus profile during the cycle shows no enhanced biological P uptake or release.

$$\% \text{ COD removal efficiency} = \frac{(\text{TCOD}_{\text{inf}} - \text{SCOD}_{\text{eff}})}{\text{TCOD}_{\text{inf}}} \times 100 \quad (5.2)$$

$$\% \text{ N removal efficiency} = \frac{(\text{TKN} + \text{NO}_x - \text{N})_{\text{inf}} - (\text{NH}_3 - \text{N} + \text{NO}_x - \text{N})_{\text{eff}}}{(\text{TKN} + \text{NO}_x - \text{N})_{\text{inf}}} \times 100 \quad (5.3)$$

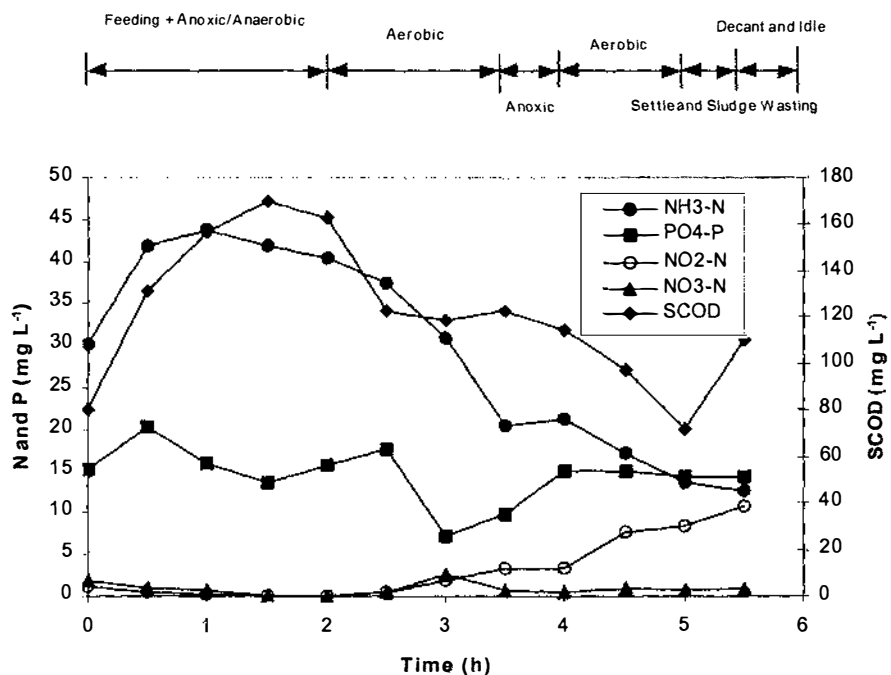


Figure 5.5 SCOD, N and P profiles in a cycle study during Run I

Figure 5.6 shows the DO and pH profiles during this cycle. The DO was less than 1.0 mg L^{-1} , which shows that there was inadequate aeration to biodegrade the slowly biodegradable COD and to prevent the filamentous bacteria growth (Travers & Lovett, 1984). The pH during the anoxic/anaerobic period increased probably due to denitrification and an increase in $\text{NH}_3 - \text{N}$ due to anoxic/anaerobic hydrolysis (Henze, 2002). During the aerobic period pH reduced. This is attributed to nitrification.

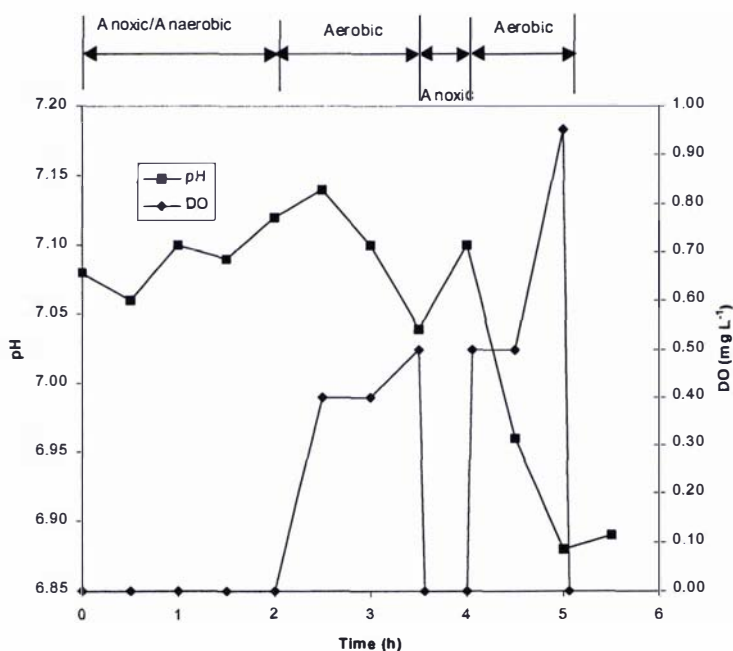


Figure 5.6 DO and pH profiles in a cycle study during Run I

5.3 Performance of the SBR during Run II

In this run, the HRT was increased to 2.5 d and the DO concentration in the mixed liquor was controlled. The airflow rate was controlled between 4.8 and 6 L air (L volume. h)⁻¹. The influent feed time was 20 minutes. The operating cycle for this run was as shown in Table 5.2.

Table 5.2 Operating cycle of Run II (6-h cycle)

Reactor Sequence	Time (h)	DO (mg L ⁻¹)
Fill and non-aerated mix	2.0	0.0
Aerated mixed react 1	1.5	2.5 ± 0.25
Non-aerated mixed react (anoxic)	0.5	0
Aerated mixed react 2	1.0	2.5 ± 0.25
Settle	0.75	0
Decant and Idle	0.25	0

Figure 5.7 shows the cycle study results after one week with HRT of 2.5 d. During this cycle study the OLR was 0.63 kg COD (m³.d)⁻¹ which is within the recommended design value. Influent TCOD, TKN, NH₃ – N and TP were 1570, 160, 110 and 27 mg L⁻¹

¹ respectively. The COD, N and P removal efficiencies were 88, 96 and 83 % respectively.

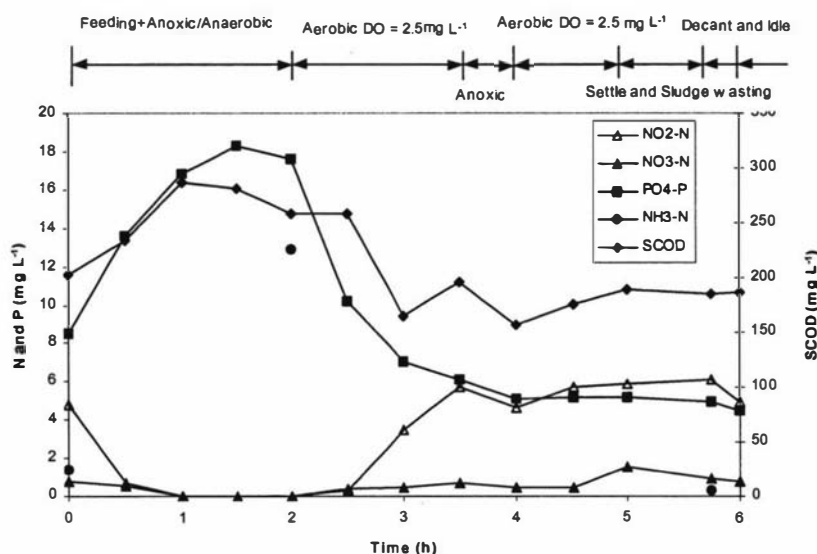


Figure 5.7 SCOD, N and P profiles in a cycle study during Run II

Within the first half an hour of the first aerobic period there was no significant oxidised nitrogen ($\text{NO}_x - \text{N}$) concentration observed. An increase in $\text{NO}_x - \text{N}$ was observed after half an hour of aeration. The average nitrification rate during the first aerobic period was $1.65 \text{ mg NO}_x - \text{N (g VSS.h)}^{-1}$ and this is comparable to the nitrification rate of $1.97 \text{ mg NO}_x - \text{N (g VSS. h)}^{-1}$ reported for meat processing balance pond effluent by Bickers (1996a). The $\text{NO}_x - \text{N}$ carry over from the previous cycle was denitrified rapidly during the feed time. The average denitrification rate was $2.07 \text{ mg NO}_3 - \text{N (g VSS.h)}^{-1}$ during the initial half an hour of the anaerobic/anoxic period. The initial denitrification rate was less than the maximum denitrification rate in the presence of RBCOD and was comparable to the denitrification rate when only slowly biodegradable COD was present. During the anoxic period $0.82 \text{ mg L}^{-1} \text{ NO}_x - \text{N}$ was denitrified at the rate of $0.71 \text{ mg NO}_3 - \text{N (g VSS.h)}^{-1}$. This anoxic denitrification rate was slightly higher than the endogenous denitrification rate determined from batch tests in this study. This indicates that most of the biodegradable COD was consumed before the anoxic period. Effluent $\text{NH}_3 - \text{N}$ was less than 0.2 mg L^{-1} indicating a complete removal of $\text{NH}_3 - \text{N}$.

Lakay *et al.* (1999) observed that filamentous organisms proliferate in systems with sludge exposed to alternating anoxic and aerobic conditions in which NO_3 and/or NO_2

exceeded 5 or 1 mg N L⁻¹ and are present throughout the anoxic period. Nitrite N concentration was above 1 mg L⁻¹ in the anoxic period of this cycle study, indicating possible proliferation of filamentous organisms. The proliferation of filamentous bulking did occur occasionally during this run.

Figure 5.8 shows the pH profile during this cycle study. The pH was less than 7.4. According to the chart provided by Anthonisen *et al.* (1976) for determination of unionised NH₃ – N concentrations, less than 2 % of free NH₃ – N was expected in the reactor. Since low NH₃ – N was present in the reactor (up to 8 mg L⁻¹), the loss of N due to NH₃ volatilisation could be assumed to be negligible (Philips & Verstraete, 2001). A mass balance on influent N removal showed about 37.3, 33.5 and 21.1 % of influent N was removed by denitrification, simultaneous nitrification and denitrification (SND) and assimilation respectively.

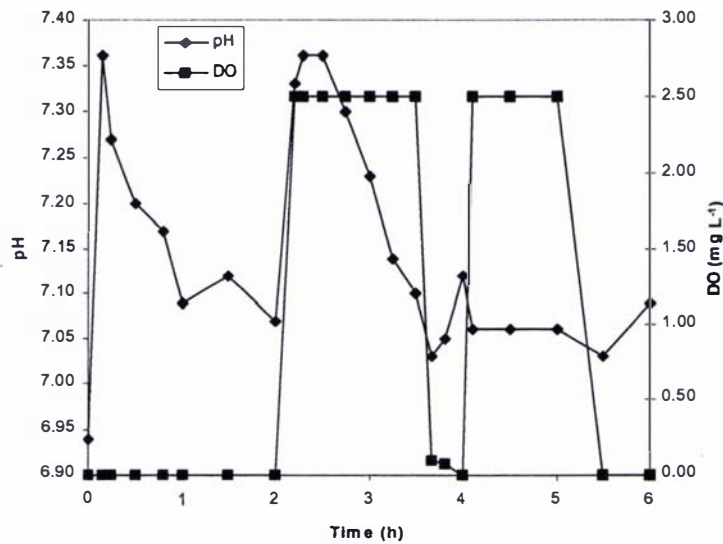


Figure 5.8 pH and DO profiles during a cycle study during Run II

The P profile in Figure 5.7 shows the P release and uptake during the anaerobic and aerobic periods respectively. The average P release of 2.85 mg P (g VSS.h)⁻¹ was observed in the first one and a half hours of the anoxic/anaerobic period and an average uptake rate of 3.33 mg P (g VSS.h)⁻¹ was observed in the first aerobic period. The anoxic P uptake rate was 0.84 g P (g VSS.h)⁻¹ which shows a reduced level of about 25 % of the aerobic uptake (Henze *et al.*, 1999). The sludge P content was 2.6 % of VSS at the end of the aerobic period, which suggests EBPR (Orhon & Artan, 1994, Leonard, 1996).

Phosphorus uptake continued during the anoxic period. Bio-P bacteria might have used NO_3 as an electron acceptor for their growth instead of oxygen (Kuba *et al.*, 1993). Denitrification by bio-P bacteria does not require an external carbon source instead they use stored carbon in the anaerobic period. Hence they reduce the requirement of COD needed for denitrification (Comeau *et al.*, 1987; Gerber *et al.*, 1987).

Figure 5.8 also shows the DO profile during this cycle study. DO profile shows the intrusion of DO into the anoxic period. This might have caused the reduced anoxic activity of the microorganisms. The pH increased in the SBR during the fill period and this was probably due to influent alkalinity as well as by rapid denitrification. However the observed decrease in the pH toward the end of the anoxic/anaerobic period was probably due to P release (Henze, 2002). The pH increased immediately after the aeration started, presumably due to stripping of CO_2 from the tank. However, net decrease in the pH toward the end of first aerobic period may be because of nitrification. During the anoxic period the pH increased as denitrification progressed.

The characteristics of the influent and the effluent from continuous operation of the SBR at this operating condition are shown in Figures 5.9 and 5.10. The influent wastewater characteristics were less than the average wastewater characteristics of this study. The effluent wastewater characteristics showed no quasi steady state, which was probably because the biomass escape through the effluent due to filamentous bulking. Occasionally some pinpoint flocs were also observed from microscopic observation. The effluent SCOD was within 5.8 – 10.1 % of the influent TCOD. The effluent $\text{NH}_3 - \text{N}$ concentration was above 7 mg L^{-1} indicating incomplete nitrification. The effluent $\text{PO}_4 - \text{P}$ as well as $\text{NO}_3 - \text{N}$ was below 5 mg L^{-1} . The effluent alkalinity was lower than the influent alkalinity but above 100 mg L^{-1} (CaCO_3). COD, N and P could be removed under the operating conditions of Run II but the performance could not be maintained for a long period because of the occasional escape of biomass.

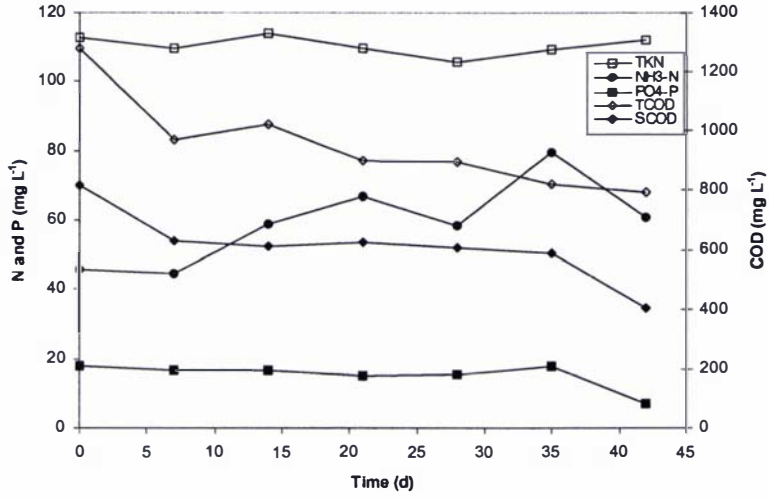


Figure 5.9 Influent COD, N and P profiles during Run II

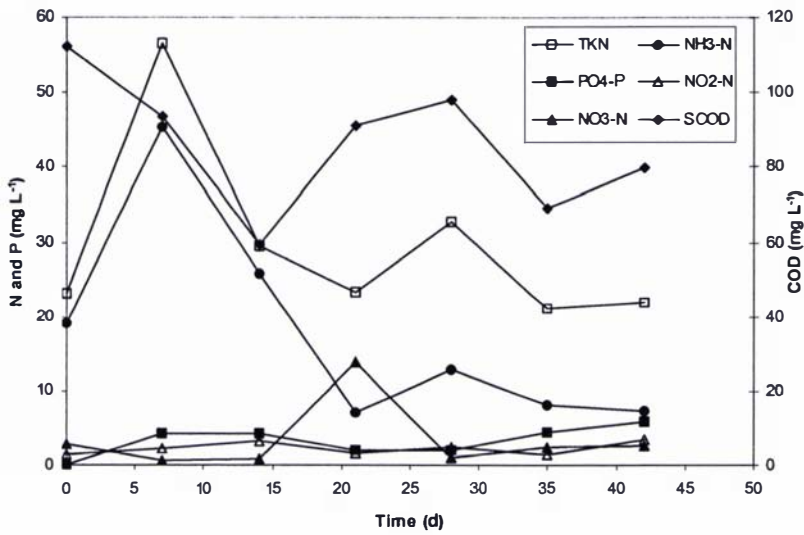


Figure 5.10 Effluent soluble COD, N and P profiles during Run II

5.4 Performance of the SBR during Run III (Centrifuged wastewater)

In Run III centrifuged wastewater was treated in a 10 L SBR. The operating cycle was the same as that shown in Table 5.2 except that the DO concentration was controlled between $2.0 \pm 0.25 \text{ mg L}^{-1}$. The influent feed time was 7 minutes. The centrifuged wastewater was obtained by centrifuging the primary treated meat processing wastewater at 6000 G for 0.25 h (Sorvall GS3 rotor, RC5C centrifuge, Dupont, USA). The OLR on volumetric basis was between $0.21 - 0.28 \text{ kg COD (m}^3 \cdot \text{d)}^{-1}$ which is below the recommended design value.

The influent and effluent characteristics are shown in Figures 5.11 and 5.12. The influent COD reduced with time in the feed tank. The influent $\text{NH}_3 - \text{N}$ in the feed also increased and TKN remained approximately constant, suggesting that $\text{NH}_3 - \text{N}$ was produced due to hydrolysis in the storage tank. During this run the wastewater storage refrigerator temperature was slightly higher than 4°C , which might have resulted in increased anaerobic activity. The influent COD:TKN ratio was between 5.8 – 7.8 which is below the ratio of 8 suggested for denitrification (Keller *et al.*, 1997). The effluent characteristics improved during the first three weeks, but the effluent pH and alkalinity decreased with time (data not shown).

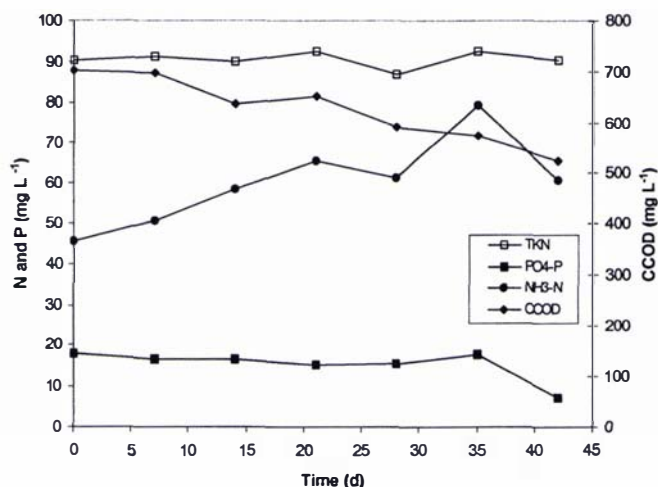


Figure 5.11 Influent centrifuged COD, N and P profiles during Run III

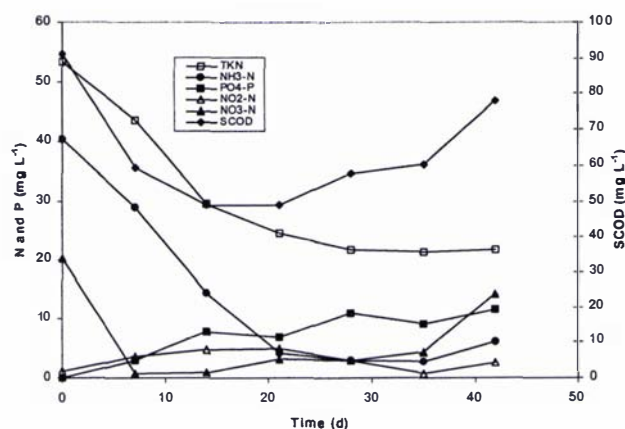


Figure 5.12 Effluent SCOD, N and P profiles during Run III

Good sludge settling was observed but the reactor failed to operate well for a prolonged period due to unfavourably low pH in the reactor. When the centrifuged wastewater contained less than $250 \text{ mg L}^{-1} \text{ CaCO}_3$ alkalinity, the pH and the alkalinity during this run dropped below 6.3 and $10 \text{ mg L}^{-1} \text{ CaCO}_3$ alkalinity respectively. The reduced pH and the alkalinity were probably due to nitrification and reduced denitrification activity due to low COD:TKN ratio in the centrifuged feed. The gain of alkalinity by $\text{NH}_3 - \text{N}$ release during hydrolysis (Henze *et al.*, 1999) of the particulate organic matter in the SBR was eliminated in the centrifuged wastewater. This could also be a reason for the reduced alkalinity and the pH in the effluent. According to Dold and Marais (1987) nitrification, when it occurs, is the biological process with the largest impact, to the extent that the magnitude of the alkalinity change can cause a decrease in pH values to as low as 4. The alkalinity of the wastewater was then increased by the addition of $1 \text{ M Na}_2\text{CO}_3$ (2 ml / L wastewater) on the 21st day. Later, the alkalinity was not adjusted and the performance of the reactor declined. The effluent $\text{NO}_3 - \text{N}$ increased (accumulated) probably due to insufficient RBCOD in the feed for sufficient denitrification in a cycle. The effluent $\text{NO}_3 - \text{N}$ and $\text{PO}_4 - \text{P}$ were above 10 mg L^{-1} in 42 d. Due to the failure of the centrifuge, the reactor was continuously operated with low COD wastewater with occasional alkalinity adjustment to see the performance of the SBR.

The SBR's performance is shown in Figure 5.13. During this cycle the TCOD, TKN and TP of the influent were 365 mg L^{-1} , 88.5 mg L^{-1} and 9.3 mg L^{-1} , respectively. The SCOD in the effluent was about 40 mg L^{-1} . The effluent SCOD was about 10.9 % of the

influent TCOD. Effluent $\text{NH}_3 - \text{N}$ was greater than 2.0 mg L^{-1} , which indicates incomplete nitrification. Part of $\text{NO}_3 - \text{N}$ carried over from the previous cycle was denitrified using the RBCOD available in the feed. The nitrogen mass balance showed that 80 % of influent N was removed by denitrification during the initial anoxic period. Only 4 % of influent N was removed by SND and the remaining 10 % of the influent N was incorporated into the biomass and 6 % was in the effluent.

Figure 5.13 also shows the $\text{NO}_3 - \text{N}$ and $\text{NO}_2 - \text{N}$ profiles. The $\text{NO}_2 - \text{N}$ was not significantly changed during the cycle. However, the $\text{NO}_3 - \text{N}$ dropped during the feed cycle due to dilution and denitrification. After the end of the feed cycle, a faster denitrification rate of $11.93 \text{ mg NO}_3 - \text{N (g VSS.h)}^{-1}$ and during the remaining anoxic/anaerobic period a slower denitrification rate of $1.98 \text{ mg NO}_3 - \text{N (g VSS.h)}^{-1}$ were obtained from the profiles. These denitrification rates are similar to the rates found by batch tests on readily and slowly biodegradable COD of the wastewater in this study. The $\text{PO}_4 - \text{P}$ concentration did not change much throughout the cycle. This revealed that there was minimal biological P activity. Phosphorus balance during this cycle study revealed that the P removal by precipitation was negligible.

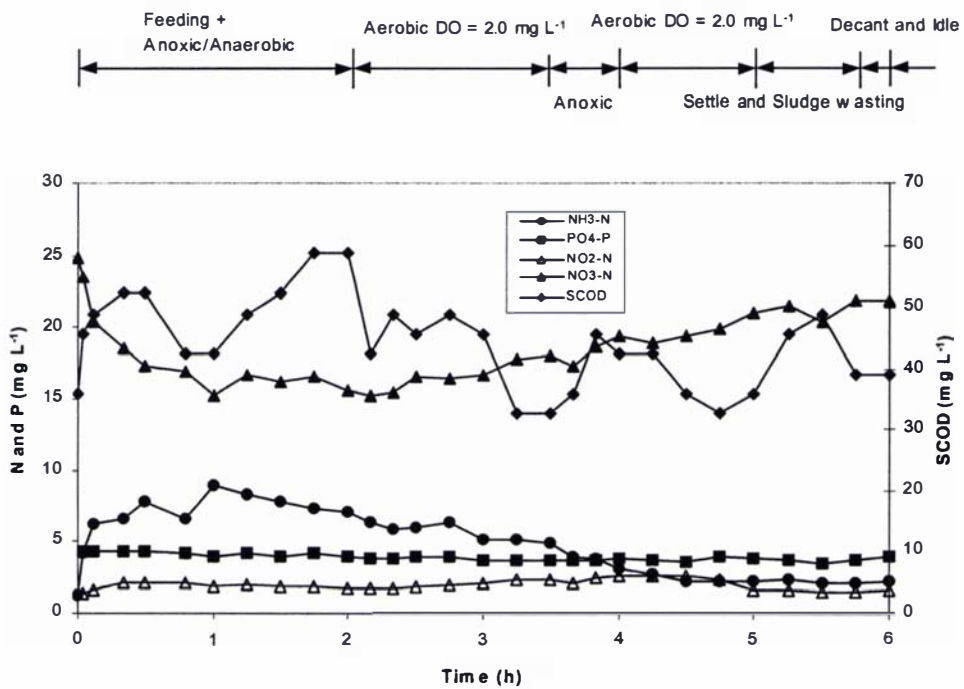


Figure 5.13 Soluble COD, N and P profiles in a cycle study during Run III

Figure 5.14 shows the DO and pH profiles. The DO profile shows the intrusion of DO into the anoxic period, which might have reduced the anoxic activity. The intrusion of DO during the settling period indicates that DO has to be controlled at a low level before the settling period to prevent the DO from carrying over to the subsequent anoxic/anaerobic cycle. The pH profile shows an increase in pH during the initial anoxic period because of denitrification and an increase in $\text{NH}_3 - \text{N}$.

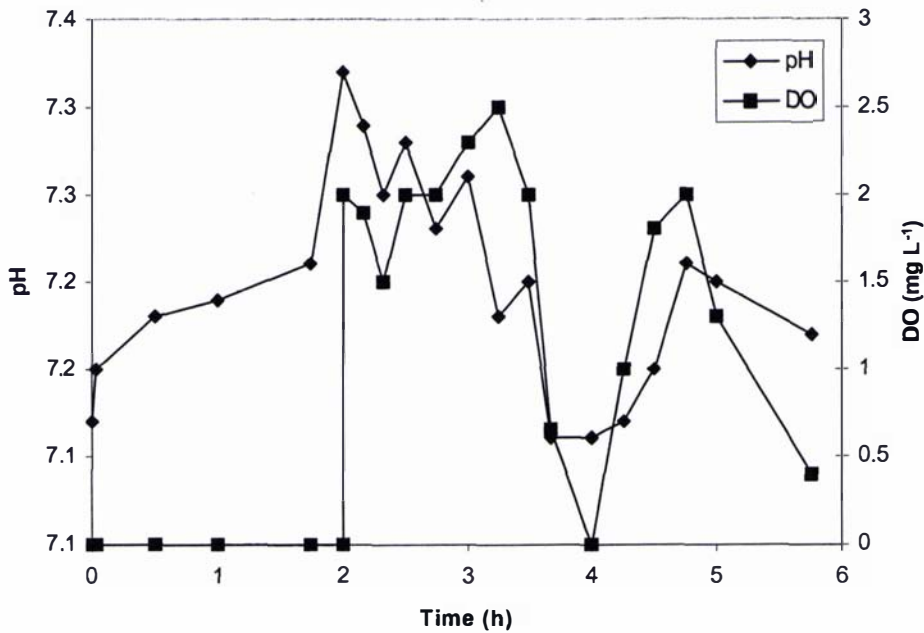


Figure 5.14 DO and pH profiles in a cycle study during Run III

5.5 Performance of the SBR during Run IV

Based on the results from the previous runs, the operating conditions for Run IV were determined according to the following. (1) DO before the anoxic and settling periods must be kept low to prevent DO intrusion into the anoxic phase as well as into the anoxic/anaerobic phase of the subsequent cycle. (2) Solids in the influent could enhance the alkalinity as well as COD:TKN ratio in the reactor. Travers and Lovett (1984) reported that at low DO ($< 0.5 \text{ mg L}^{-1}$), fat degradation was inhibited (56 % removal), leading to poorly settling sludge (sludge volume index (SVI) $> 250 \text{ ml/g}$) with a high fat content and an excessive number of filamentous microorganisms. They also reported that in contrast to low DO, high DO concentrations (up to 4 mg L^{-1})

correlated with rapid fat degradation (90 % removal), better settling sludge and fewer filamentous organisms. Münch *et al.* (1996) found that the DO concentration must be kept low to achieve SND and at about 0.5 mg L^{-1} the nitrification and the denitrification rates were equal. Considering all these factors, the operating conditions for Run IV were set as shown in Table 5.3. The influent feed time was 8 minutes. The SRT and the HRT were kept at 15 d and 2.5 d respectively.

Table 5.3 Operating cycle of Run IV (6-h cycle)

Reactor Sequence	Time (h)	DO (mg L^{-1})
Fill and non-aerated mix	2.0	0.0
Aerated mixed react 1	1.0	0.5 ± 0.25
Non-aerated mixed react (anoxic)	0.5	0
Aerated mixed react 2	1.0	3.75 ± 0.25
Aerated mixed react 3	0.5	0.5 ± 0.25
Settle	0.75	0
Decant and Idle	0.25	0

The wastewater characteristics during this run are shown in Figures 5.15 – 5.16. The OLR was between $0.56 - 0.72 \text{ kg COD (m}^3\cdot\text{d)}^{-1}$ which is within the recommended design value. The TCOD:TKN and TCOD:TP ratios were 9 and 46 respectively. These ratios were adequate to remove N and P simultaneously by biological process alone in this study.

The ratio of the effluent SCOD to the influent TCOD was between $0.05 - 0.07$. This ratio is similar to the total inert SCOD of wastewater origin (4 %) and biomass origin (2 %) as discussed in Chapter IV. These results suggest more than 99 % of biodegradable SCOD was removed under these operating conditions.

Effluent $\text{NH}_3 - \text{N}$ was less than 0.6 mg L^{-1} , which indicates greater than 99 % $\text{NH}_3 - \text{N}$ removal from the system. Effluent and anoxic $\text{NO}_3 - \text{N}$ and $\text{NO}_2 - \text{N}$ was less than 5 and 1 mg L^{-1} respectively during the experiments. The measured SVI was within $100 - 200 \text{ ml (g TSS)}^{-1}$ as shown in Figure 5.17, indicating good sludge settling.

The effluent $\text{PO}_4 - \text{P}$ was less than 0.1 mg L^{-1} in this run yielding more than 99 % of P removal. The reduction of the VSS:TSS ratio from the anaerobic stage to the end of the aerobic stage (Figure 5.17) may be explained by the release of P during the

anaerobic period and P storage in the aerobic stage with little change in the biomass concentration. The influent TSS of 480 – 655 mg L⁻¹ was reduced to 11 – 45 mg L⁻¹ in the effluent. This shows more than 90 % of TSS removal.

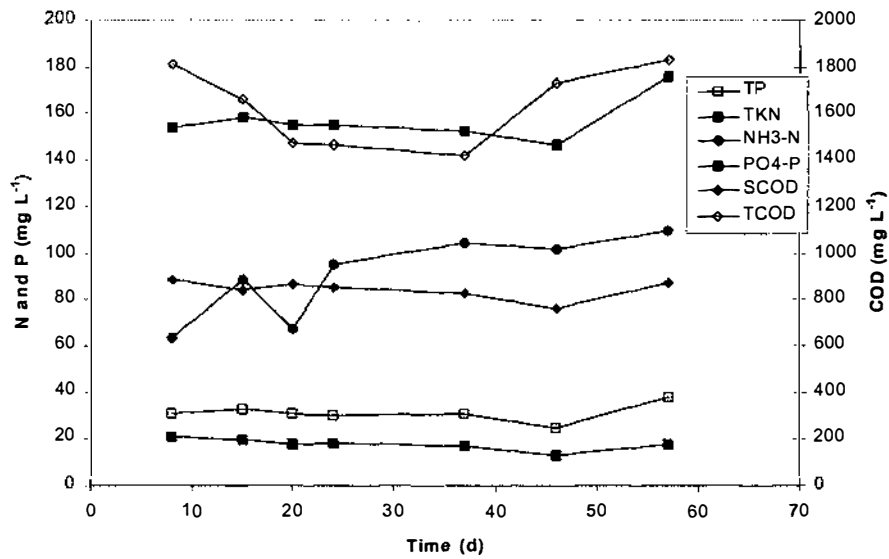


Figure 5.15 Influent COD, N and P profiles during Run IV

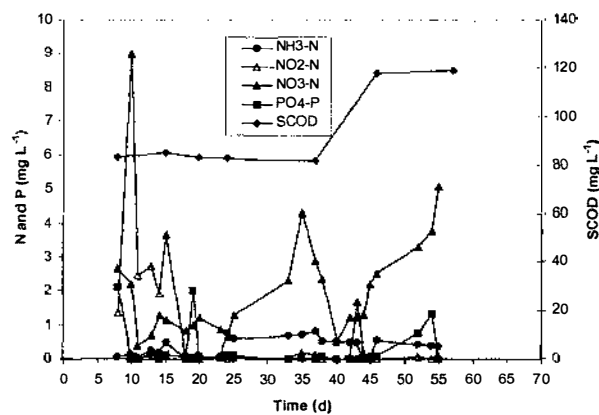


Figure 5.16 Effluent SCOD, N and P profiles during Run IV

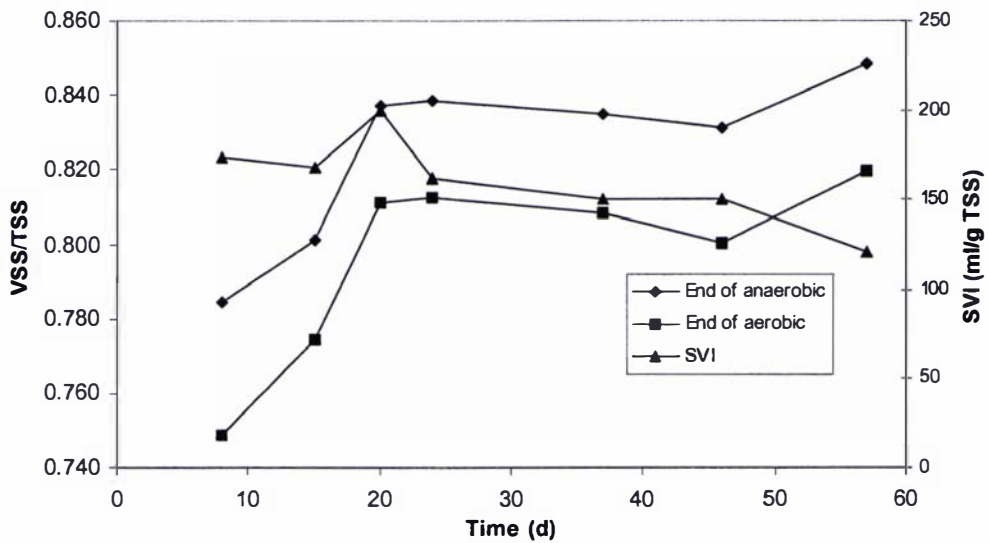


Figure 5.17 VSS to TSS ratio at the end of the anaerobic and aerobic phases during Run IV

Figure 5.18 shows COD, N and P profiles in a cycle study after the system reached a quasi steady state (where mixed liquor VSS, effluent soluble COD, $\text{NO}_3 - \text{N}$ and $\text{PO}_4 - \text{P}$ were relatively stable). The calculated SCOD was above 200 mg L^{-1} after the influent feeding time, but the observed SCOD was only 133.9 mg L^{-1} . This is probably due to adsorption or absorption and storage (Van Loosdrecht *et al.*, 1997). The ratio of effluent SCOD to the influent TCOD was 0.06. This ensured complete removal of the biodegradable SCOD. The anaerobic hydrolysis rate could be assumed to be very low as only a slight increase in $\text{NH}_3 - \text{N}$ concentration was observed during the anoxic/anaerobic period. The effluent $\text{NH}_3 - \text{N}$ concentration was slightly higher than at the end of the aerobic period. This might be due to the resynthesis of $\text{NH}_3 - \text{N}$ from $\text{NO}_3 - \text{N}$ or hydrolysis of N from endogenous biomass (Henze, 2002). The $\text{NO}_2 - \text{N}$ and $\text{NO}_3 - \text{N}$ were less than 1 and 5 mg L^{-1} respectively during the anoxic phase and good settling of sludge was observed. This is in line with the results of Lakay *et al.* (1999).

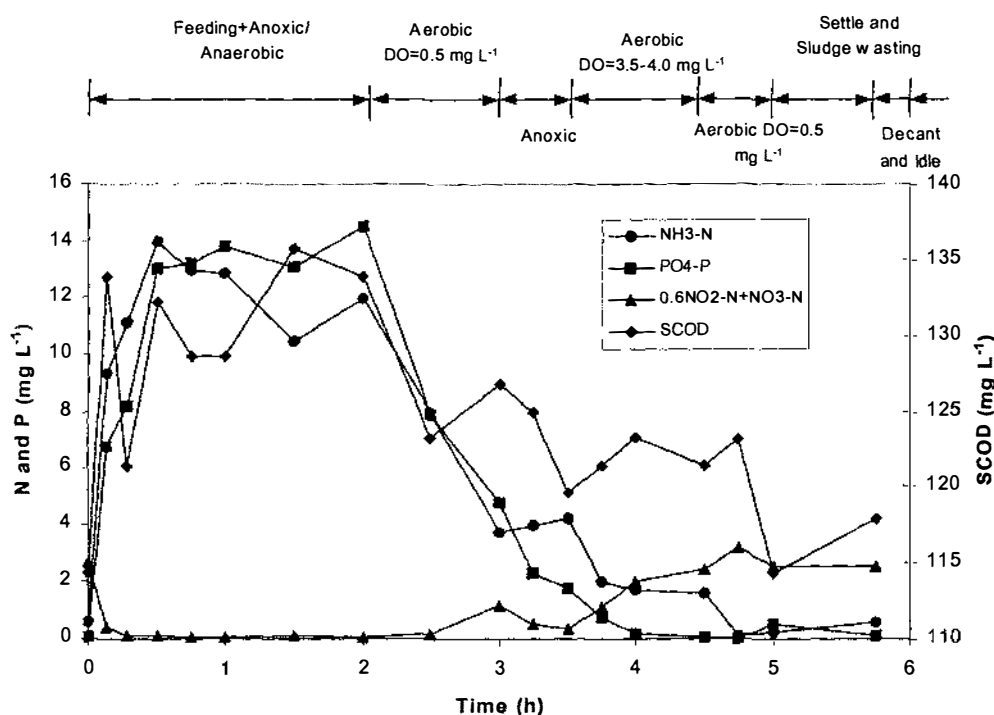


Figure 5.18 Soluble COD, N and P profiles in a cycle study during Run IV

The pH (Figure 5.20) was between 6.9 - 7.6 during this cycle, therefore less than 2 % of free $\text{NH}_3 - \text{N}$ was expected in the reactor (Anthonisen *et al.*, 1976). Since low $\text{NH}_3 - \text{N}$ was present in the reactor (12 mg L^{-1}), the loss of N due to NH_3 volatilisation could be assumed negligible (Philips & Verstraete, 2001). During the first aerobic period $8.18 \text{ mg L}^{-1} \text{ NH}_3 - \text{N}$ was removed, however only $1.87 \text{ mg L}^{-1} \text{ NO}_x - \text{N}$ was formed. This indicates that most of the N was removed by SND. The low DO concentration of $0.5 \pm 0.25 \text{ mg L}^{-1}$ during first aerobic period permitted SND. This result is similar to that reported by Münch *et al.* (1996). During the anoxic period $\text{NH}_3 - \text{N}$ was formed at an average rate of $0.33 \text{ mg NH}_3 - \text{N (g VSS. h)}^{-1}$ due to anoxic hydrolysis, and the $\text{NO}_3 - \text{N}$ was denitrified at the rate of $0.63 \text{ mg NO}_3 - \text{N (g VSS. h)}^{-1}$. The denitrification rate in the anoxic period is comparable to the endogenous denitrification rate. This shows that most of the biodegradable COD was removed prior to this period. Figure 5.19 shows N balance in this cycle study. The N balance revealed that 25.8 % of influent N was removed by denitrification during the anoxic periods and 43.3 % was removed by SND-probably in the initial aerobic period.

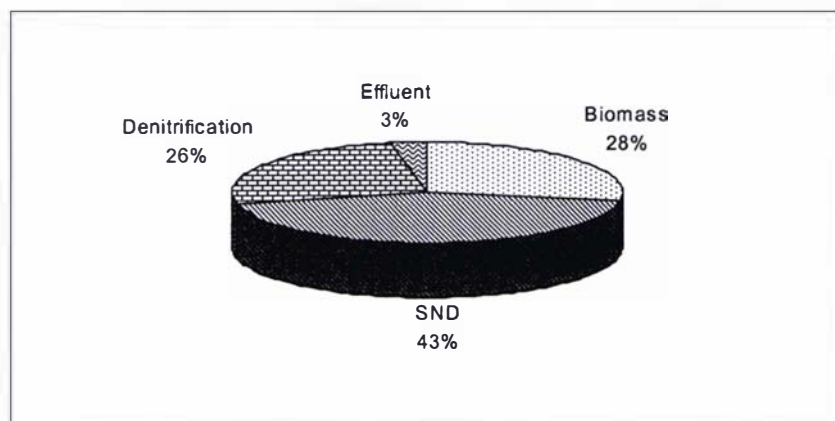


Figure 5.19 N balance in a cycle study during Run IV

A higher percentage of SND indicates that the reactor operation is efficient. A considerable amount (about 27.9 %) of influent N was in the sludge waste. The influent $\text{NH}_3 - \text{N}$ was reduced from 101.8 mg L^{-1} to 0.57 mg L^{-1} in the effluent.

The $\text{PO}_4 - \text{P}$ in the influent was 13.3 mg L^{-1} , which was reduced to 0.11 mg L^{-1} in the effluent, that is greater than 99 % of $\text{PO}_4 - \text{P}$ removal in the system. The maximum P release rate was $11.4 \text{ mg P (g VSS.h)}^{-1}$ in the anoxic/anaerobic period and the highest P uptake rate was $4.78 \text{ mg P (g VSS.h)}^{-1}$ in the first aerobic period. The P uptake rate during the first aerobic period was $3.55 \text{ mg P (g VSS.h)}^{-1}$. The anoxic P uptake rate was $2.14 \text{ mg P (g VSS.h)}^{-1}$ which is about 60 % of the aerobic P uptake rate and is similar to the level suggested in Activated Sludge Model 2d (Henze *et al.*, 1999). The anoxic P uptake reduces the oxygen as well as the COD required for N removal. The measured sludge P content at the end of the aerobic period (4.58 %) confirms EBPR (Arun *et al.*, 1988; Orhon & Artan, 1994).

The alkalinity profile during this cycle is shown in Figure 5.20. The alkalinity during the anoxic/anaerobic period increased probably due to removal of fermentation products during P release. During the initial aeration the alkalinity was reduced and this is attributed to nitrification. During the anoxic/anaerobic period even though the alkalinity increased, the pH decreased (Figure 5.20). This is probably due to CO_2 increase in the mixed liquor. The reverse phenomenon occurred during the aerobic period when alkalinity decreased and pH increased as the CO_2 concentration decreased in the mixed liquor due to CO_2 stripping from the reactor (Dold & Marais, 1987). The increase in the CO_2 concentration in the mixed liquor is due to fermentation, partial

functioning of the TCA (tricarboxylic acid) cycle and utilisation of glycogen for energy production during PHB formation (Henze, 2002; Hesselmann *et al.*, 2000). During the anoxic period the pH and alkalinity increase during denitrification.

Total suspended solids were reduced from 505 mg L⁻¹ in the influent to 33 mg L⁻¹ in the effluent giving 94 % removal. Figure 5.21 shows a typical oxygen uptake rate (OUR) profile during one cycle. The initial OUR was 25 mg O₂ (g VSS. h)⁻¹. This high value suggests rapid RBCOD utilisation immediately after the aeration started. During the anoxic/anaerobic period most of the RBCOD in the influent would have been used up for denitrification and during P release. The second level of the OUR profile was 17 mg O₂ (g VSS. h)⁻¹ which is attributed to the slowly hydrolysable COD. The third lower level was observed at about 7.5 mg O₂ (g VSS. h)⁻¹, which is probably due to the utilisation of storage compounds during maintenance (Brdjanovic *et al.*, 1998b). The higher DO concentration between 3.75 ± 0.25 mg L⁻¹ increased the rate of degradation of slowly biodegradable COD as suggested by Travers and Lovett (1984). The prolonged aeration under starvation conditions might have helped to achieve good settling sludge. This was also reported by Wilderer *et al.* (2001). The third aerobic phase at a low DO of 0.5 mg L⁻¹ ensured complete removal of NH₃ – N and enhanced denitrification.

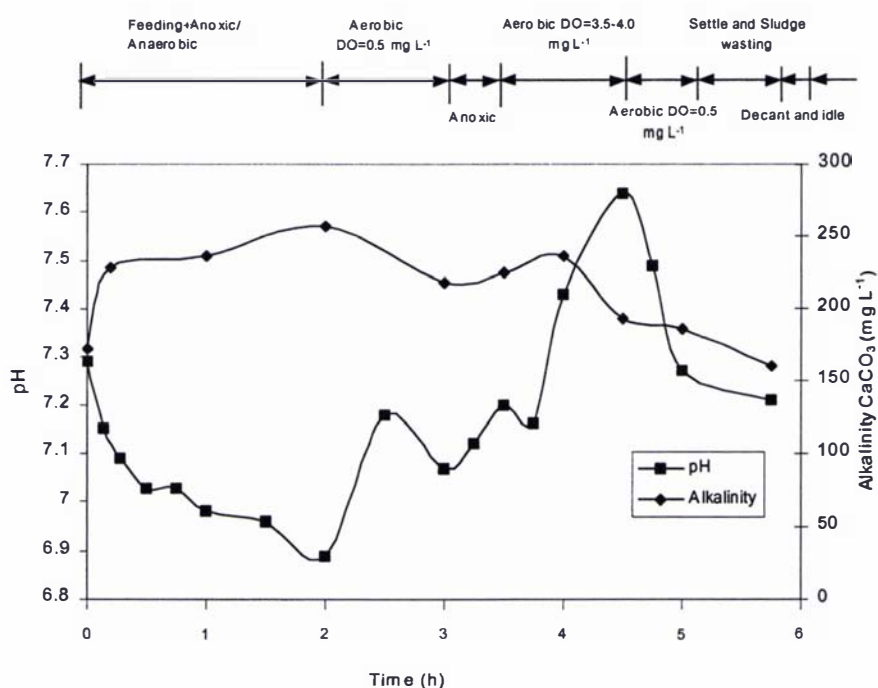


Figure 5.20 Alkalinity and pH profiles in a cycle during the Run IV

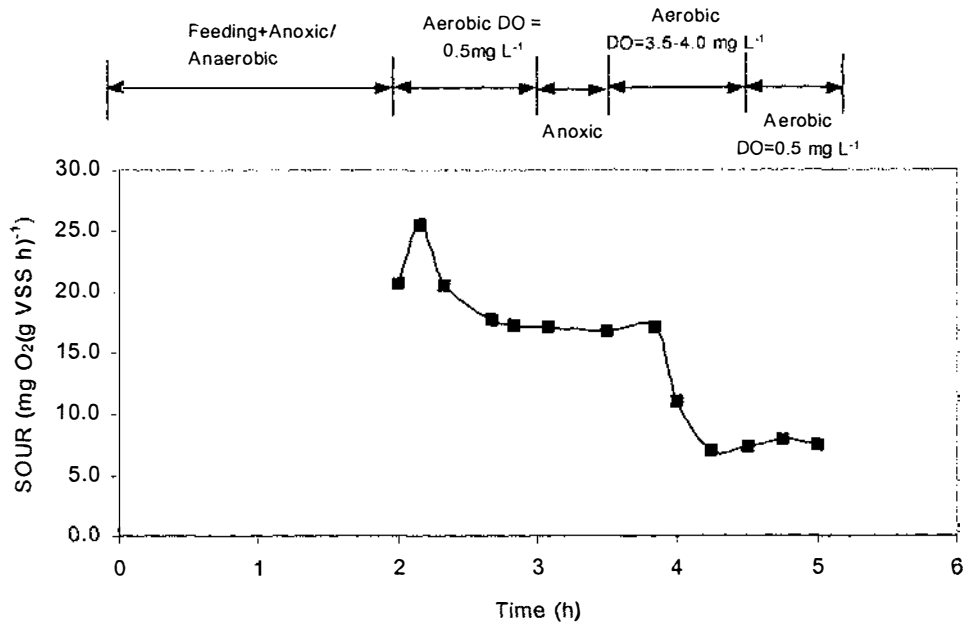


Figure 5.21 Typical oxygen uptake rate profile during Run IV

5.6 Summary

In Run I low DO concentration in the mixed liquor resulted in proliferation of filamentous bacteria. Inadequate aeration coupled with high OLR of $1 \text{ kg COD (m}^3 \cdot \text{d)}^{-1}$ caused incomplete nitrification. High OLR and inadequate aeration inhibit the nitrite oxidation. The COD and N removal efficiencies achieved were 93 and 87 % respectively in Run I. The RBCOD content of the meat processing wastewater was insufficient for combined N and P removal when effluent $\text{NO}_3 - \text{N}$ was above 7.4 mg L^{-1} .

The operating conditions in Runs II and III did not allow near neutral pH to be maintained. The first aerobic period of one hour and a half at DO level of $2.5 \pm 0.25 \text{ mg L}^{-1}$ appeared to have reduced the anoxic activity in these runs. Anoxic P uptake was observed in Run II but the uptake rate was only 25 % of the aerobic P uptake rate. The concentrations of $\text{NO}_3 - \text{N}$ and $\text{NO}_2 - \text{N}$ were above 5 and 1 mg L^{-1} , respectively during the anoxic period, and proliferation of filamentous bacteria was observed. COD, N and P removal efficiencies of 88, 96 and 83 % were achieved during this run. However, the performance could not be maintained for a long period because there was occasional biomass escape.

In the centrifuged wastewater treatment, there was a net loss of alkalinity during nitrification and denitrification. It appears that the alkalinity consumed during

nitrification was only partially recovered during denitrification. The overall performance in terms of organic carbon, N and P removal was also poor. Alkalinity in the effluent was decreased below 10 mg L^{-1} as CaCO_3 . Incomplete nitrification was observed during this run. The DO concentration at $2 \pm 0.25 \text{ mg L}^{-1}$ during the second aerobic period resulted in carry over of DO into the subsequent cycle's anoxic/anaerobic period.

The operating conditions in Run IV were suitable for simultaneous biological nutrient and COD removal from meat processing wastewater with the SRT of 15 d and HRT of 2.5 d. The effluent SCOD was found to be non-biodegradable as reflected by the fact that there was no further SCOD removal following prolonged aeration. The TN in the wastewater was reduced to less than 10 mg L^{-1} , while the TP decreased from a range of 20 - 40 mg L^{-1} in the wastewater to less than 1.0 mg L^{-1} . Removal of biodegradable SCOD, $\text{NH}_3 - \text{N}$ and $\text{PO}_4 - \text{P}$ of greater than 99 % was achieved in the SBR. The N balance revealed that 25.8 % of influent N was removed by denitrification during the anoxic period and 43.3 % was removed by SND probably in the initial aerobic period. A considerable amount (about 27.9 %) of influent N was present in the sludge waste. Total suspended solids were reduced from 505 mg L^{-1} in the influent to 33 mg L^{-1} in the effluent giving 94 % removal. The maximum phosphate uptake rate was $4.78 \text{ mg P (g VSS.h)}^{-1}$ while the average aerobic phosphate uptake rate was $3.55 \text{ mg P (g VSS.h)}^{-1}$. The average anoxic phosphate uptake rate was 60 % of the aerobic phosphate uptake rate. The OUR related to RBCOD, slowly biodegradable COD and the biomass storage compounds were 25, 17 and $7.5 \text{ mg O}_2 \text{ (g VSS.h)}^{-1}$. Mixed liquor pH was decreased during nitrification and anaerobic P release but increased during denitrification. Alkalinity in the mixed liquor increased during the anaerobic period.

CHAPTER VI

KINETIC CHARACTERISATION OF WASTEWATER

6.1 Introduction

The development of an effective SBR operating cycle to treat meat processing wastewater for simultaneous COD and nutrient removal was discussed in Chapter V. The results from the effective cycle showed a removal of more than 99 % of soluble biodegradable organic carbon, $\text{NH}_3 - \text{N}$ and $\text{PO}_4 - \text{P}$.

The use of mechanistic models such as the ASM 1 and ASM 2 is a key tool for finding potentially feasible solutions in designing a treatment system for the removal of organic carbon and nutrients. Realistic prediction from these models, however, requires the key kinetic and stoichiometric parameters specific to the wastewater. The default parameters given in the ASM 1 and ASM 2 are specific to domestic wastewater. These parameters have to be determined for meat processing wastewater for prediction of biological organic carbon and nutrient removal in the SBR. Also, characterisation of the wastewater gives the key processes involved in the treatment of meat processing wastewater, particularly in biological P removal.

In this chapter, the determination of key kinetic and stoichiometric parameters required for the simulation of ASM 1 and ASM 2 models applied to SBR treatment of meat processing wastewater is discussed. The variation in PHA, glycogen, organic substrate and $\text{PO}_4 - \text{P}$ during anaerobic and aerobic conditions is discussed in detail. Anoxic phosphorus removal and magnesium limitation in meat processing wastewater treatment affecting phosphorus uptake are considered.

6.2 Kinetic and stoichiometric parameters in biological organic carbon and nitrogen removal

6.2.1 Heterotrophic yield coefficient

The heterotrophic yield coefficient allows the estimation of sludge production and oxygen demand. The yield coefficient was determined following the method described by Henze *et al.* (1987a). The methodology was discussed in Chapter III. The most important parameter in batch cultivation of mixed cultures is the ratio of the initial substrate concentration to the initial biomass concentration (S_0/X_0). When the ratio is sufficiently low (below 2 - 4 depending on the mixed culture history) no cell multiplication takes place during the exogenous substrate removal. Under these conditions, a biomass increase is mostly due to the synthesis of storage polymers (Chudoba *et al.*, 1992). Since the SBR was operated at a lower S_0/X_0 ratio, it is necessary to do the kinetics parameter estimation at a lower S_0/X_0 ratio. Higher S_0/X_0 ratios cause cell multiplication of mixed culture that changes in the proportion among slow growers and fast growers (Chudoba *et al.*, 1992).

The effect of different initial S_0/X_0 ratios on substrate removal is illustrated in Figure 6.1. When the S_0/X_0 ratio was low, the substrate removal follows an exponential decay profile. When the S_0/X_0 ratio was 0.42, only 2.5 h were required for complete removal of the biodegradable soluble COD. Therefore, low S_0/X_0 ensures a complete removal of biodegradable soluble COD when the SBR is operated below the specific loading of 0.4 mg SCOD/mg VSS. The measurement of the TCOD was a problem during low S_0/X_0 ratios employed for yield coefficient measurement due to difficulties in obtaining homogenous samples. Figure 6.2 shows the biomass growth when S_0/X_0 was 2.

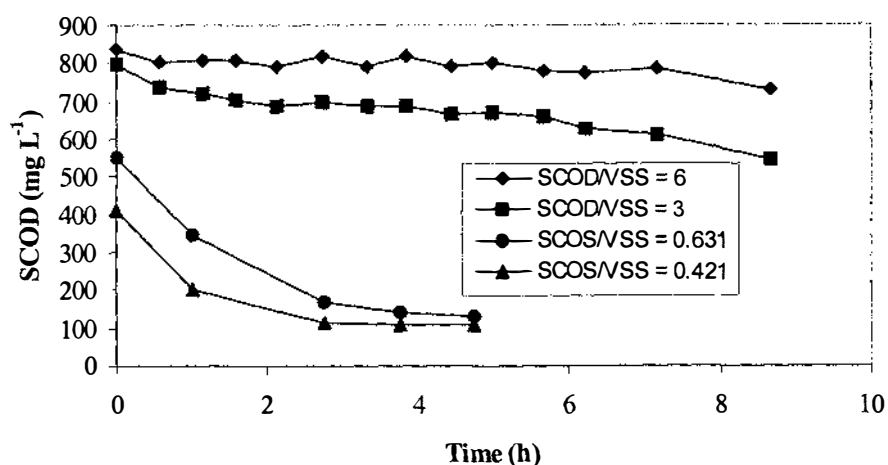


Figure 6.1 Substrate removal with different S_0/X_0

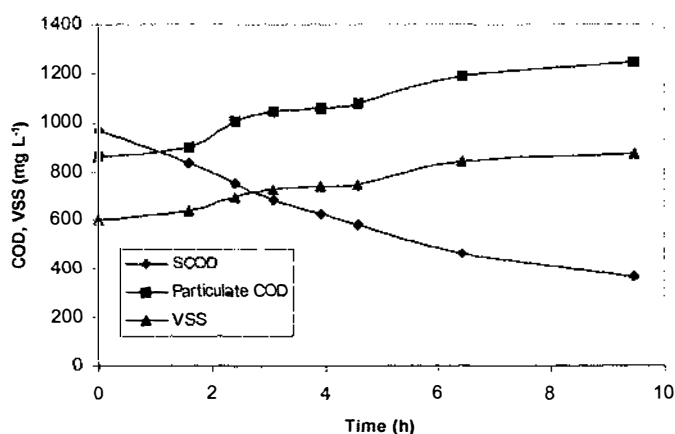


Figure 6.2 Yield coefficient with $S_0/X_0 = 2$

Observed yield coefficient was $0.63 \text{ biomass COD (mg SCOD)}^{-1}$ and the average biomass COD to biomass ratio was 1.42. The initial SCOD and particulate COD were calculated from the COD measurements before mixing the soluble wastewater and mixed liquor. Chang (1999) observed similar results by using the biomass prepared by serial dilution. The COD of unit biomass cell could be obtained from the stoichiometric equation of 1 mole of biomass needs 5 moles of oxygen as electron acceptors during oxidation ($5O_2/C_5H_7NO_2 = 1.42$).

6.2.2 Maximum specific growth rate and half saturation constant of heterotrophs

The method used for finding the maximum specific growth rate and half saturation constants in this study was developed by Cech *et al.* (1984). Previously, either batch cultivation or continuous cultivation without biomass recycling (chemostats) was used. Batch cultivation can be carried out with both high and low initial concentrations of biomass. Though this method is simple and rapid, the main disadvantage is its limited accuracy when K_s values are small (less than 20 mg L^{-1}) because of the large analytical errors associated with measuring low substrate concentrations (Williamson & McCarty, 1975). In continuous chemostat method, a relatively long period is generally required to reach a steady state, especially for organisms with long generation periods. Moreover, application of this method to mixed cultures containing species with substantially different generation periods is questionable. The infinite dilution method developed by McCarty needs a simple, sufficiently specific and accurate analytical method for determination of a substrate tested. This can be overcome by a simple respirometric method (Cech *et al.*, 1984). For this experiment, the respirometer-which was used by Leonard (1996)-was used. During the OUR recording time re-aeration was assumed to be negligible. Figure 6.3 shows a typical respirogram.

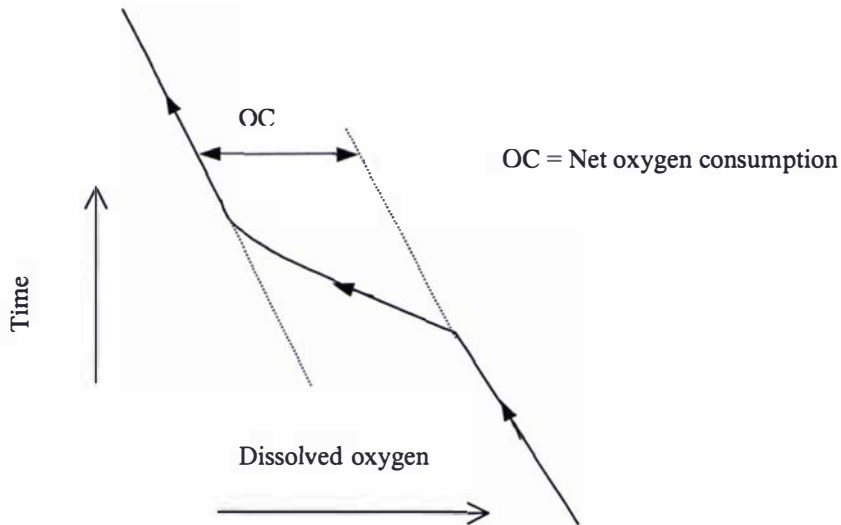


Figure 6.3 A typical respirogram

The specific substrate removal rate (r_X) at concentration S is given by the Equation 6.1. The coefficient of biomass yield (Y_{obs}) was obtained using the Equation 6.2 (Cech *et al.*, 1984).

$$r_X = \frac{\mu_{max}}{Y_{obs}} \cdot \frac{S}{K_S + S} \quad (6.1)$$

$$Y_{obs} = 1 - \frac{OC}{S} \quad (6.2)$$

Three methods exist for the linearisation of Equation 6.1. Linear Equation 6.3 was used in this study for computing maximum specific growth rate (μ_{max}) and half saturation constant (K_S).

$$r_X = \frac{\mu_{max}}{Y_{obs}} - \frac{r_X}{S} \cdot K_S \quad (6.3)$$

For respirometric measurements, unwashed biomass was used with the initial concentrations between 750 – 2680 mg VSS L⁻¹. Figure 6.4 shows the profile of r_X change with S in four different trials. They all followed the Monod saturation kinetics. Figure 6.5 shows the linear profile of r_X with r_X/S for the Trial III.

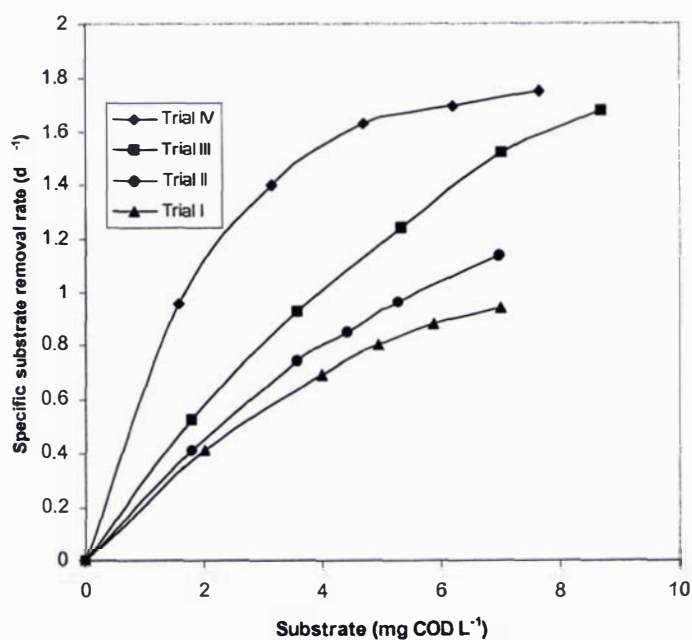


Figure 6.4 Relationship between specific substrate removal rate and substrate in soluble meat processing wastewater

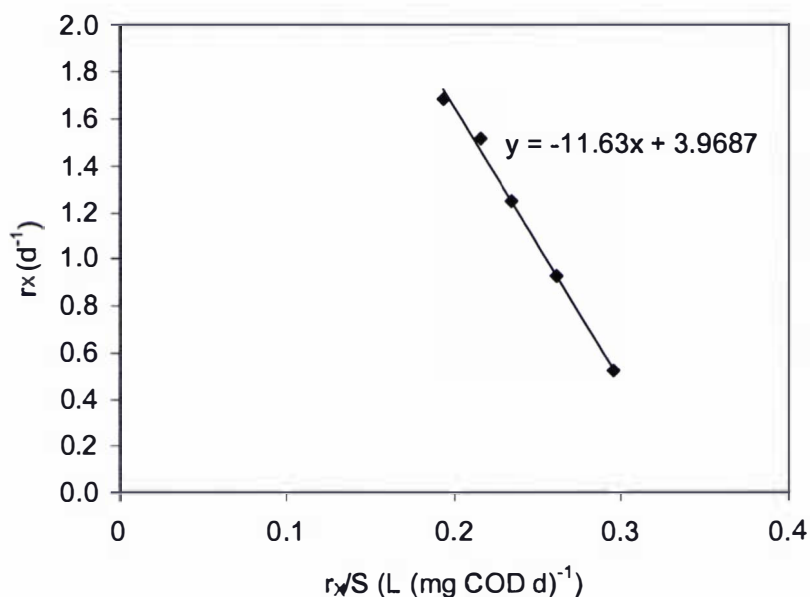


Figure 6.5 Linear profile of r_x with r_x/S

The K_S value was obtained from the slope of the linear curve (Figure 6.5). The maximum specific growth rate of heterotrophs was obtained from the intercept of the linear curve multiplied by the observed average yield coefficient. Table 6.1 shows the maximum specific growth rate, half saturation constant and the average yield coefficients in different trials.

Table 6.1 Heterotrophic growth kinetic and stoichiometric constants

Trial No.	Maximum specific growth rate (d ⁻¹)	Half saturation constant (mg L ⁻¹)	Yield coefficient (COD basis)
I	1.24	7.44	0.63
II	1.87	10.85	0.634
III	2.51	11.63	0.633
IV	1.49	2.11	0.651
Average	2	8	0.637

Maximum specific growth rates and half saturation constants were in the range of 1.24 - 2.51 d⁻¹ and 2.11 – 11.63 mg L⁻¹ respectively in the GF/C filtered wastewater in this study. The S_0/X_0 ratio was very low (< 0.01) during these experiments. Chang (1999) reported values for maximum specific growth rate and the half saturation

constant of 3.3 d^{-1} and 10 mg COD L^{-1} for soluble meat processing wastewater. Values reported by Annachatre and Bhamidimarri (1993) are higher for half saturation constant ($176 \text{ mg COD L}^{-1}$) and lower for maximum specific growth rate (1.14 d^{-1}) compared to this study. They, however, used the tedious chemostat method. The yield coefficient averaged 0.637 on the COD basis. When the substrate concentration was high it took a longer time to return to the endogenous phase. Substrate could be adsorbed on the biomass surface, thus lowering its actual concentration in the solution. Substrate concentration was calculated based on the initial concentration, not measured.

6.2.3 Maximum specific growth rate of autotrophs

The maximum specific growth rate for autotrophic biomass, $\mu_{\max,A}$ is the most critical parameter in the modelling and design of nitrification systems. A number of different procedures have been suggested to estimate the value of $\mu_{\max,A}$ in activated sludge, which involve either activity measurements such as oxygen uptake rate (OUR), or monitoring related model components such as ammonia nitrogen ($\text{NH}_3 - \text{N}$) or oxidised nitrogen forms ($\text{NO}_2 - \text{N}$ and $\text{NO}_3 - \text{N}$).

In the procedure involving autotrophic activity, the OUR is measured in a reactor sustaining both autotrophic and heterotrophic biomass, before and after the inhibition of nitrifiers (Nowak & Svoldal, 1993); the difference between the two measurements is interpreted as a direct indication of the OUR associated with nitrification. The use of $\text{NH}_3 - \text{N}$ for evaluating the value of $\mu_{\max,A}$ is limited since ammonia nitrogen also serves as the basic nitrogen source and is incorporated into the biomass at the same time as it is oxidised to $\text{NO}_3 - \text{N}$. Consequently, the concentration of oxidised nitrogen, S_{NO} , is a much more convenient parameter for this purpose, mainly because S_{NO} is the model component solely related to autotrophic growth.

The conceptual basis for determination of $\mu_{\max,A}$ was outlined by Sozen *et al.* (1996). The value of $\mu_{\max,A} - b_A$ in this study was determined by a non-linear curve fitting to Equation 6.4 using Matlab 5.3.

$$S_{\text{NO}} = S_{\text{NO}0} + \frac{1}{k} [e^{at} - 1] \quad (6.4)$$

where $a = \mu_{\max,A} - b_A$

$$\text{and } k = \frac{Y_A (\mu_{\max,A} - b_A)}{\mu_{\max,A} X_{A0}} \quad (6.5)$$

Codes for script and function file in Matlab 5.3, for finding the best k value and the initial oxidised nitrogen concentration from the Equation 6.4 are given in Appendix B.

Figure 6.6 shows the $\text{NO}_3 - \text{N}$ ($\text{NO}_3 - \text{N} + 0.6 \text{NO}_2 - \text{N}$) profile in three different runs. The $\mu_{\text{max,A}} - b_A$ values were 0.66 d^{-1} , 0.60 d^{-1} and 0.61 d^{-1} respectively in three runs. The decay coefficient for autotrophs, b_A , is not as critical as heterotrophic biomass endogenous decay rate in the evaluation of sludge production and oxygen utilisation, especially for combined systems for carbon and nutrient removal, since autotrophs constitute only a small fraction of the total biomass (Orhon & Artan, 1994). The recommended value for b_A is in the range between 0.05 and 0.15 d^{-1} (Henze *et al.*, 1987a). The maximum specific growth rate of autotrophs was calculated to be between 0.65 d^{-1} to 0.8 d^{-1} at 22°C . The $\mu_{\text{max,A}}$ values were comparable to those values reported by Sözen *et al.* (1996) and Chang (1999) for meat processing wastewater.

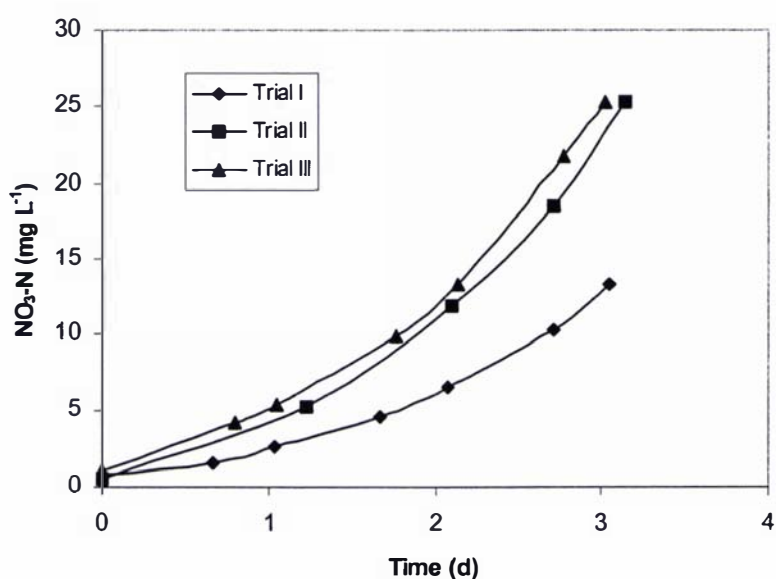


Figure 6.6 Maximum specific growth rate of autotrophs

6.2.4 Heterotrophic decay coefficient

The decay coefficient for heterotrophic biomass is a significant kinetic parameter for evaluation of sludge production and oxygen utilisation. The heterotrophic biomass endogenous decay rate (b'_H) was estimated using a respirometric batch test method as outlined in Ekama *et al.* (1986) and Henze *et al.* (1987a). The observed OUR profile is shown in Figure 6.7.

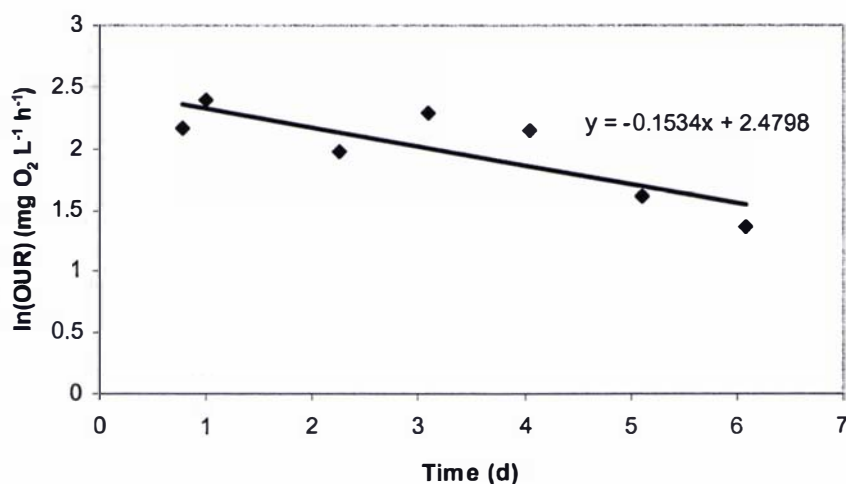


Figure 6.7 Heterotrophic decay coefficient

The heterotrophic decay rate coefficient (b'_H) was calculated from the gradient of the linear curve (Figure 6.7) as 0.15 d^{-1} . The Task Group model decay coefficient (b_H) (Henze *et al.*, 1987a; Orhon & Artan, 1994) was determined from b'_H in the following manner:

$$b_H = \frac{b'_H}{1 - Y_H(1 - f_p)} = \frac{0.15}{1 - 0.63(1 - 0.08)} = 0.36 \text{ d}^{-1} \quad (6.6)$$

$$\text{where, } f_p = \frac{(1 - Y_H)}{(1 - Y_H f_{EX})} f_{EX} = \frac{(1 - 0.63)}{(1 - 0.63 \times 0.17)} \times 0.17 = 0.08 \quad (6.7)$$

The decay coefficient value of 0.36 d^{-1} is lower than the Task Group's value for domestic wastewater, and was slightly lower than the range of $0.38 - 0.49 \text{ d}^{-1}$ reported by Chang (1999) for meat processing wastewater. Gorgun *et al.* (1995) reported a much lower value of 0.24 d^{-1} . Ekama *et al.* (1986) found the decay rate to be constant even with different sludge ages, varying only slightly at different temperatures. Predators such as protozoa and rotifers may influence the decay rate to some extent (Huisman & Mino, 2002).

6.3 Stoichiometric and kinetic parameters in biological phosphorus removal

The stoichiometric relationship among the acetic acid (HAc), phosphorus (P), PHA and glycogen for the anaerobic P metabolism as set out in the literature is shown in Table 6.2. The stoichiometry of g P release to g HAc COD consumed varied from 0.16 – 0.48 in models. The variation in the stoichiometry is due to the dependency of Bio-P bacteria on polyphosphate (poly-P) as an energy source (Mino *et al.*, 1998). Also, the variation could be due to the energy derived from utilisation of stored glycogen for anaerobic substrate uptake. Models other than the Comeau/Wentzel model suggest that glycogen is utilised for the production of PHA during the anaerobic P metabolism.

Table 6.2 Stoichiometric relationships among HAc, P, PHA and glycogen during anaerobic P metabolism

Reference	HAc COD (g)	PHA COD (g)	P (g)	Glycogen COD (g)
Mino's model (Pereira <i>et al.</i> , 1996)	1.0	1.50	0.24	0.50
Adapted Mino's model (Pereira <i>et al.</i> , 1996)	1.0	1.50	0.32	0.5
Smolders <i>et al.</i> (1995a, b)	1.0	1.49	0.48 (pH = 7.0)	0.50
Comeau/Wentzel model (Pereira <i>et al.</i> , 1996)	1.0	1.0	0.48	
Pereira <i>et al.</i> (1996)	1.0	1.67	0.16	0.70

6.3.1 Kinetic and stoichiometric parameters for meat processing wastewater

To determine the kinetic and stoichiometric parameters, SBR and batch tests with meat processing wastewater were performed. Also, to determine the stoichiometric relationships among HAc, P, PHA and glycogen batch tests were conducted with acetate using the acclimated sludge obtained from the SBR.

6.3.1.1 SBR cycle study

Run IV of the SBR cycle described in Section 5.4 was used to characterise the sludge and to determine the kinetic and stoichiometric parameters. In order to do that, 1.5 L of wastewater was fed at the beginning of the cycle within 1 minute instead of normal feeding with the pump for 8 minutes. The wastewater characteristics were 1718 mg L⁻¹ total COD, 916 mg L⁻¹ soluble COD, 19.3 mg L⁻¹ PO₄ – P, 1.37 mg L⁻¹ NO₃ – N,

329.6 mg COD L⁻¹ SCFA and 121 mg L⁻¹ NH₃ - N. In this study, the NO₃ - N was taken as equivalent to 0.6NO₂ - N + NO₃ - N. The reactor pH was near neutral. Samples were taken every 0.25 h for SCFA measurement during the anaerobic period. Oxidised nitrogen (NO_x - N) and PO₄ - P were also measured at 0.25-h intervals. PHB, PHV and glycogen were measured at 0.5 h intervals. The first sample was taken 1 minute after experiment started.

Figure 6.8 shows the PO₄ - P, NO₃ - N, SCFA, PHA and glycogen COD profiles during this cycle study. Although the calculated SCFA COD after the addition of feed was 33 mg L⁻¹, only 13.7 mg L⁻¹ SCFA COD was measured in the initial sample. This reduction in the measured SCFA COD could be due to rapid adsorption or absorption and storage (Van Loosdrecht, *et al.*, 1997). The rapid removal of the SCFA COD occurs because the microorganisms are exposed to a pronounced feast and famine regime (Van Loosdrecht *et al.*, 1997).

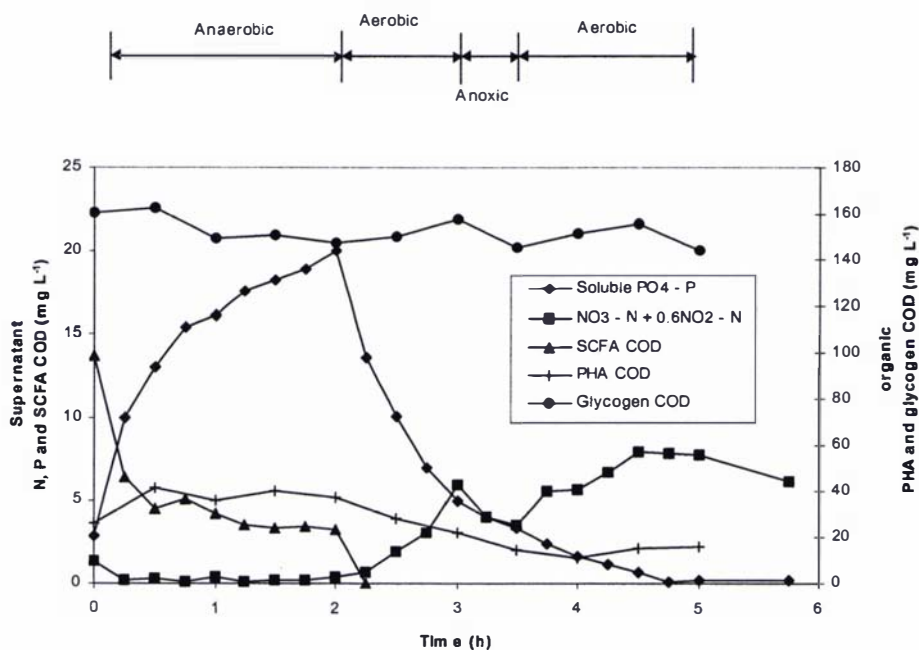


Figure 6.8 Soluble phosphate phosphorus, nitrate nitrogen, SCFA COD, PHA COD and glycogen COD profiles during an SBR cycle

The phosphorus profile shows an initial fast release followed by a slow release during the anaerobic period. During the subsequent aerobic and anoxic periods P was restored completely. The highest P release rate of 10.4 mg P (gVSS.h)⁻¹ was observed during the initial anoxic/anaerobic period. The P release depends on SCFA

concentration, poly-P and glycogen fraction in Bio-P (Mino *et al.*, 1998). Hessleman *et al.* (2000) indicated that the energy required for anaerobic uptake of organic substrates by Bio-P is not only supplied by glycolysis and hydrolysis of poly-P but probably also by hydrolysis of pyrophosphate and the efflux of $MgHPO_4$.

Table 6.3 TSS, VSS and sludge phosphorus content during the SBR and batch studies

Experiment	End of anaerobic period			End of final aerobic period				
	Initial anaerobic period*			TSS (mg L ⁻¹)	VSS (mg L ⁻¹)	VSS/ TSS (%)	Sludge Phosphorus	
	TSS (mg L ⁻¹)	VSS (mg L ⁻¹)	VSS/ TSS (%)				(mg L ⁻¹)	% of VSS
SBR cycle With wastewater	3435*	2820*	82.0	3360	2755	82.0	114.9	4.17
Batch test with wastewater	2455*	2020*	82.3	2385	2000	83.9	57.81	2.89
Batch test with acetate Trial I	3165*	2565*	81.0	3145	2575	81.9	76.4	2.97
Batch Test with acetate Trial II	1715	1470	85.7	1815	1445	79.6	53.2	3.68

The solids concentrations and sludge P contents during the SBR cycle study and the batch tests are shown in Table 6.3. The sludge P concentration was 4.17 % of VSS at the end of the aerobic period, whereas it was 3.4 % of VSS at the end of the anaerobic period. A high P content in the sludge suggests that the poly-P was not a limiting factor for SCFA uptake in this study (Arun *et al.*, 1988; Orhon & Artan, 1994). The glycogen concentration of 146 mg COD L⁻¹ (about 29 % of active Bio-P) measured at the end of anaerobic period suggests that glycogen was not the limiting factor for the SCFA uptake (Mino *et al.* 1995; Mino *et al.*, 1998). Although the poly-P and glycogen do not seem to be the limiting factors, about 3 mg L⁻¹ HAc COD was present during the last one hour of the anaerobic period while there was a continuous release of $PO_4 - P$. During this period PHA COD was almost stable. This suggests that HAc COD could be produced by fermentation, however, the removed HAc COD was not utilised for PHA formation. This could be due to diffusion limitation (Fleit, 1995). A part of the energy produced by hydrolysis of poly-P could also be used for glycogen storage as shown in Figure 6.8. Also, the uptake of some other organic acids in the meat processing wastewater might

have utilised the energy derived from the hydrolysis of poly-P (Mino *et al.*, 1998; Nakamura *et al.*, 1991; Wang *et al.*, 2002). Sato *et al.* (2000) reported that some of the fermentation related COD or soluble COD remained without being utilised by Bio-P bacteria in activated sludge treatment of sewage wastewater during the anaerobic period. Wang *et al.* (2002) reported that lactic acid was produced by fermentation in the EBPR of glucose dominant substrate. According to Wentzel *et al.* (1991) and Brodisch (1985), the anaerobic/aerobic EBPR systems could develop organisms which convert sugars and similar organic compounds to SCFA under anaerobic conditions. The reason for the presence of unused HAc in this study is unclear and has to be further clarified in future studies.

The highest P uptake rate of $9.3 \text{ mg P (g VSS.h)}^{-1}$ was observed in the first aerobic period. Phosphorus uptake continued during the anoxic period. Similar anoxic P uptake was reported in the literature (Kuba *et al.*, 1993; Lee *et al.*, 2001).

The glycogen profile shows a slight increase in concentration in the 0.5 h sample compared to the first sample probably due to the immediate storage of glycogen (Figure 6.8). The storage of glycogen is possible using the energy obtained from the hydrolysis of poly-P (Nakamura *et al.*, 1991; Mino *et al.*, 1998), by oxidising some of the carbohydrate using prevailed $\text{NO}_3 - \text{N}$ at the initial anoxic/anaerobic period (Van Loosdrecht *et al.*, 1997) or from the fermentation of glycogen (Wang *et al.*, 2002). There was a progressive decrease in glycogen during P release during the anoxic/anaerobic period. This indicates that glycogen was utilised for PHA storage and/or fermented during the anaerobic period (Hesselmann *et al.*, 2000; Mino *et al.*, 1998; Pereira *et al.*, 1996). During the anoxic period, glycogen decreases slightly. One of the explanations may be that the glycogen was utilised for reducing power during the anoxic period (about $5 \text{ mg L}^{-1} \text{ NO}_3 - \text{N}$ was available). A second, more likely, explanation is that the glycogen was utilised for P uptake (Mino *et al.*, 1998; Nakamura *et al.*, 1991). The observed decrease in glycogen in the final aerobic period was probably due to glycogen utilisation by Bio-P bacteria for maintenance (Brdjanovic *et al.* 1998b). Approximately 12.5 mg L^{-1} glycogen COD ($4.5 \text{ mg glycogen COD per g VSS}$) was utilised in the anaerobic period.

The net increase observed in the PHA during the anaerobic period, as shown in Figure 6.8, indicates PHA storage by Bio-P bacteria. Other forms of PHA such as 3-hydroxy-2-methylbutyrate (3H2MB) and 3-hydroxy-2-methylvalerate (3H2MV) might

also have been formed during the anaerobic period as the wastewater contains mixed SCFA (Satoh *et al.*, 1992). PHB and PHV CODs were about 65 and 35 % respectively of the total PHA COD measured. The PHV content was little higher than the reported value of 26 % by Pereira *et al.* (1996) for a mixed SCFA substrate. Satoh *et al.* (1992) also found higher PHV fractions when substrates such as lactate or propionate were used as the carbon source. An average PHA COD of 14.1 mg L⁻¹ (5.1 mg L⁻¹ of PHA COD per g VSS) was observed at the end of aerobic periods with the highest value of 38.6 mg L⁻¹ during the anaerobic periods in this cycle study. The observed PHA COD at the end of the aerobic period is slightly higher than the 2.11 and 2.5 mg COD per g VSS reported by Brdjanovic *et al.* (1998b) and Temmink *et al.* (1996) respectively. This amount of PHA COD may not be available for the P uptake or growth of Bio-P.

Carbon flow estimation in the anaerobic P metabolism is shown in Table 6.4. In order to find out the available SCFA/acetate COD for anaerobic P metabolism, the SCFA/ acetate COD (in this study, it was assumed that the RBCOD of the wastewater was equivalent to SCFA COD) required for denitrification of the available NO₃ – N at the beginning of the test was subtracted. The COD removed from the mixed liquor via denitrification can be calculated from the oxygen reduction equivalent (R_{EQ}) of the NO₃ – N to be reduced and the yield coefficient Y_H (Leonard, 1996; Siegrist & Gujer, 1994) as shown in Equation 6.8.

$$\text{g COD required for g N oxidised} = \frac{R_{EQ}}{1 - Y_H} \quad (6.8)$$

The reduction equivalent of nitrate is 2.86. The average value for Y_H in this study was 0.63. Denitrification, therefore, requires 7.7 g COD per g of NO₃ – N. This value is consistent with the substrate requirement values of 7 to 8 g COD per g of NO₃ – N reported by Argaman and Brenner (1986) and Siegrist and Gujer (1994). Table 6.5 shows the COD conversion factors (Smolders *et al.*, 1995b) used in the calculations in Table 6.4.

Table 6.4 Carbon balance in anaerobic phosphorus metabolism

Experiment	Consumed SCFA COD (mg L ⁻¹)	Initial Nitrate nitrogen		Remaining SCFA COD		Consumed Glycogen	Stored PHA	Released phosphorus		Released g P _{org} /g SCFA COD	Consumed g Glycogen COD/g SCFA COD	Stored g PHA COD/g SCFA COD
		at the beginning (mg L ⁻¹)	Consumed SCFA COD (mg L ⁻¹)	(mg L ⁻¹)	mg COD/ g TSS	mg COD/ g dry mass	mg COD/ g dry mass	(mg L ⁻¹)	mg P/g TSS			
SBR cycle with wastewater	29.692	1.369	10.582	19.110	5.563	3.712	6.96	17.203	5.008	0.900	0.667	1.251
Batch test with wastewater	71.608	4.798	37.089	34.519	14.061	10.944	17.513	33.28	13.392	0.952	0.778	1.246
Batch test with acetate Trial I	134.19	5.536	42.793	91.397	28.877	13.536	25.721	44.469	14.140	0.490	0.469	0.891
Batch test with acetate Trial II	78.98	2.839	21.945	57.035	31.424	12.512	46.438	27.326	15.056	0.479	0.398	1.478

Note : a. Initial nitrate nitrogen was calculated using added mixed liquor nitrate nitrogen and the added substrate nitrate nitrogen
 b. Initial glycogen and PHA was taken as similar to the glycogen and PHA of immediate sample
 c. In the SBR study initial PHA was taken as the PHA obtained at the end of aerobic period

Table 6.5 COD conversion factors for some components in the P metabolism (Smolder *et al.*, 1995b)

Component	Chemical formulae	Unit	Mass (g)	COD (g)
Acetate	CH ₃ COOH	1C-mol	30.0	32.0
PHB	(C ₄ H ₆ O ₂) _n	1C-mol	21.5	36.0
PHV	(C ₅ H ₈ O ₂) _n	1C-mol	20.0	38.4
Glycogen	C ₆ H ₁₀ O ₅	1C-mol	27.0	32.0
Phosphate	PO ₄ ³⁻	1P-mol	31.0	0.0

PHA and glycogen were measured in dry mass (TS) but the released phosphorus and utilised HAc were calculated on a TSS basis. For the stoichiometry comparisons, both dry mass (TS) and the TSS were assumed to be equal. Table 6.6 shows the summary of the stoichiometric relationship determined among SCFA, P, PHA and glycogen during anaerobic P metabolism in this study.

Table 6.6 Stoichiometric relationships among HAc, P, PHA and glycogen during anaerobic P metabolism

Experiment	Released P (g)	Consumed glycogen (g COD)	Stored PHA (g COD)	HAc/SCFA (g COD)
SBR cycle With wastewater	0.90	0.67	1.25	1.00
Batch test with wastewater	0.95	0.78	1.25	1.00
Batch test with acetate Trial I	0.49	0.47	0.89	1.00
Batch Test with acetate Trial II	0.48	0.40	1.48	1.00

The released P of 0.9 g P(g SCFA COD)⁻¹ in this study is higher than the literature values shown in Table 6.2. Lower P release was expected as the stoichiometry was derived from mixed SCFA. For equivalent amounts of COD taken up, the uptake of propionate and butyrate was shown to result in a lower release of phosphorus (Abu-Ghararah & Randall, 1991) than for the uptake of acetate. This suggests that more SCFA COD could be produced from fermentation of rapidly hydrolysable COD in the wastewater and/or from stored glycogen and/or energy derived from released P was utilised for storage of glycogen or other organic acids. The consumed glycogen COD per g SCFA COD removed was higher in wastewater than in the acetate batch test

result, which reflects the fermentation of glycogen. The stored PHA COD was lower than the consumed total glycogen and HAc COD. According to Mino *et al.* (1998); Smolders *et al.* (1995b) and Pereira *et al.* (1996) models the total of glycogen and HAc COD consumed is equivalent to stored PHA COD. This indicates that some of the SCFA COD and glycogen COD was not converted to PHA COD or stored as some other forms of PHA other than PHB and PHV (Satoh *et al.*, 1992).

6.3.1.2 Stoichiometric coefficients using batch test

The meat processing wastewater was also characterised for biological P removal with a higher substrate to biomass ratio than in the SBR cycle study described in Section 6.3.1.1.

To do this, 1.1 L of mixed liquor was withdrawn from the SBR at the end of the aerobic period and mixed using a magnetic stirrer in a 2 L cylindrical batch reactor. The DO was brought to zero by purging with nitrogen gas. Then 0.4 L of meat processing wastewater was added to the reactor. The pH in the mixed liquor was controlled between 7 and 7.5 using 0.5 N HCl and NaOH. A pH controller (HORIZON ecology co., Model 5997-20) was used. Nitrogen gas was purged continuously during the anaerobic period. An aerobic period of 3 h followed the 2 h of anaerobic period. During the aerobic period DO was controlled between 3.5 – 4 mg L⁻¹. The reactor was kept at a temperature of 22 ± 2° C. Samples were taken every 0.25 h for SCFA measurement during the anaerobic and initial aerobic periods. Oxidised nitrogen and PO₄ – P were also measured every 0.25 h during this batch test. PHB, PHV and glycogen were measured at 1 h intervals.

Figure 6.9 shows the PO₄ – P, NO₃ – N, SCFA, PHA and glycogen COD profiles during this batch test. The P profile shows a release of P during the anaerobic period and a storage of P during the aerobic period. The observed 18.9 mg L⁻¹ PO₄ – P at the end of the aerobic period shows an incomplete uptake of P. The P uptake depends on the presence of an external carbon source, PO₄ – P, SCFA concentration, poly-P fraction of Bio-P, unsaturated storage capacity of intracellular phosphorus, DO concentration and also soluble magnesium concentration (Henze *et al.*, 1999; Hesselmann *et al.*, 2000; Ky *et al.*, 2001; Mino *et al.*, 1998; Somiya *et al.*, 1988). The carry over of SCFA from the anaerobic period could be a reason for a slow down in the aerobic P uptake. Figure 6.9 shows an increase in PHA and glycogen COD during the initial aerobic period.

Somiya *et al.* (1988) and Brdjanovic *et al.* (1998b) also observed a release of phosphorous and storage of carbohydrate and PHA during the aerobic period when a sufficient amount of extracellular organic substrate was available.

The SCFA COD was reduced from 87.9 mg L⁻¹ to about 16 mg L⁻¹ in the first hour and was almost stable during the remaining anaerobic period. The possible reasons for the incomplete removal of SCFA COD during the anaerobic period were discussed above in Section 6.3.1.1. Sludge P content was about 1.92 % of VSS at the end of the anaerobic period as shown in Table 6.7. This shows that poly-P could also be a limiting factor for acetate uptake.

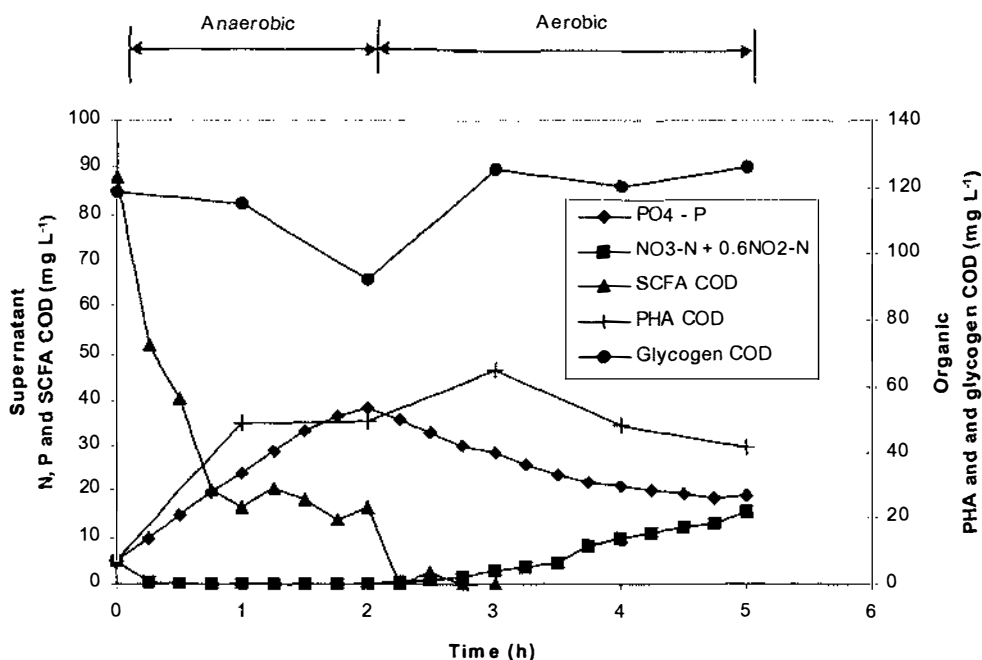


Figure 6.9 Soluble phosphate phosphorus, nitrate nitrogen, SCFA COD, PHA COD and glycogen COD profiles during a batch test with wastewater

The glycogen profile shows a slow decrease in the first hour of the anaerobic period and a sudden decrease in the remaining anaerobic period. The slow decrease was probably due to glycogen storage from the wastewater carbohydrate. Glycogen could be utilised for PHA formation and fermentation during this period. During the aerobic period glycogen increases with the PHA increase. During the final aerobic period glycogen replenishment was negligible while PHA decreased. Somiya *et al.* (1988) reported carbohydrate decreases with decreases in PHA during the aerobic period.

Table 6.6 shows that the released P was $0.95 \text{ g P(g SCFA COD)}^{-1}$. The released P was higher than the literature values shown in Table 6.2. The consumed glycogen COD per g SCFA COD removed was also higher than for acetate batch tests results. The stored PHA COD was lower than the total glycogen COD and SCFA COD consumed. The reasons for the discrepancy are likely to be similar to the reasons discussed previously (Section 6.3.1.1).

6.3.1.3 Stoichiometric coefficients with acetate batch tests

As discussed in Sections 6.3.1.1 and 6.3.1.2, it was not possible to determine the exact stoichiometry among SCFA, PHA, glycogen and $\text{PO}_4 - \text{P}$ using the experimental results with wastewater. To determine a reliable stoichiometry, two batch tests were carried out with acetate and acclimatised sludge obtained from the SBR.

Two 2 L cylindrical batch reactors were set up in a $22 \pm 2^\circ\text{C}$ controlled room. At the end of the aerobic period 1.5 L and 0.75 L of mixed liquor were added to the first and second reactors respectively. The mixed liquor was transferred from the SBR and mixed by a magnetic stirrer. The DO was brought to zero by purging with nitrogen gas. Both Trials I and II were conducted with acetate. In Trial II, 0.75 L of distilled water was added. In both trials sodium acetate was added such that the final HAc concentration was 200 and 75 mg L^{-1} respectively. The pH in the mixed liquor was controlled between 7 – 7.5 using 0.5 N HCl and NaOH, and the pH was measured using the pH controller. Nitrogen gas was also purged continuously during the anaerobic period. Three hours of aeration followed the 2-h anaerobic period. During the aerobic period DO was controlled between $3.5 - 4.0 \text{ mg L}^{-1}$. Samples were taken every 0.25 h for HAc measurement during the anaerobic and initial aerobic periods. $\text{NO}_3 - \text{N}$ and $\text{PO}_4 - \text{P}$ were also measured every 0.25 h during this batch test. PHB, PHV and glycogen were measured at 1 h intervals. The trials were conducted on different days.

TRIAL I (200 mg HAc L⁻¹): Figure 6.3 shows the $\text{PO}_4 - \text{P}$, $\text{NO}_3 - \text{N}$, HAc, PHA and glycogen COD profiles during Trial I. The phosphorus profile shows that the P was released at a reducing rate during the anaerobic period. This was probably due to poly-P limitation. Table 6.7 shows the sludge P and stored P content for the four different experiments discussed in Section 6.3.1. Minimum P content in the activated sludge was taken as 1.37 % of VSS, which was determined during this batch test. Minimum activated sludge P content is reported in the range of 1 – 1.5 % of VSS in the literature

(Bickers *et al.*, 2001; Henze, 2002; Orhon & Artan, 1994). Stored P content at the beginning of the test was calculated from Equation 6.10.

Stored sludge P content in the beginning of the test =

$$\text{Released P} + \text{stored P of the sludge at the end of anaerobic period} \quad (6.10)$$

It was assumed that the stored P content of the sludge was depleted at the end of the anaerobic period of this batch test. According to Mino *et al.* (1998), under normal conditions poly-P is not totally depleted at the end of the anaerobic phase. Brdjanovic *et al.* (1998c) reported that poly-P would be limiting at high pH, since more energy is required for acetate transport through membrane at high pH (Smolders *et al.*, 1994a). Net phosphorus uptake did not start until half an hour after aeration started. This was due to the HAc carry over from the anaerobic period. A similar result was reported by Brdjanovic *et al.* (1998b).

Table 6.7 Sludge P and stored P content

Experiment	Sludge P content (% of VSS)		% of stored P content In the beginning of the anaerobic period
	End of aerobic period	End of anaerobic period	
SBR cycle with wastewater	4.17	3.45	2.70
Batch test with wastewater	2.89	1.92	2.20
Batch test with acetate Trial I	2.97	1.37	1.85
Batch test with acetate Trial II	3.68	1.66	2.20

The HAc profile followed almost a linear trend during the anaerobic period after denitrification (Figure 6.10). About 50 mg L⁻¹ of HAc COD was carried over from the anaerobic period to the aerobic period. However, this excess HAc COD disappeared within one hour after the aerobic period started. A similar result was reported by Somiya *et al.* (1988). The PHA profile shows a fast increase in the first hour and a slower increase in the second hour during the anaerobic period. The slower increase in PHA was probably due to poly-P limitation in the sludge. Smolders *et al.* (1994a)

reported that a very slow conversion of glycogen to PHA was possible for the maintenance energy need for the cells in the poly-P limited condition. The increase in PHA during the anaerobic period continued to the initial aerobic period. In the initial aerobic period, an increase was observed in glycogen and PHA concentration. A similar result was reported by Somiya *et al.* (1988). The increase in both glycogen and PHB during the initial aerobic period suggests that glycogen involvement in aerobic PHA formation is negligible. After an hour of aeration, glycogen replenishment was negligible. An almost complete uptake of P was observed within 3 h of aeration, though the excess acetate delayed the net P uptake in the initial aerobic period.

The stoichiometry among glycogen, HAc COD and P shown in Table 6.6 were comparable to the stoichiometry reported by Smolders *et al.* (1995b). In this study, however, a lower PHA COD was produced per g of HAc COD removed. This was probably due to poly-P limitation as suggested by Brdjanovic *et al.* (1998c) that glycogen cannot replace poly-P for PHA storage under poly-P limited condition.

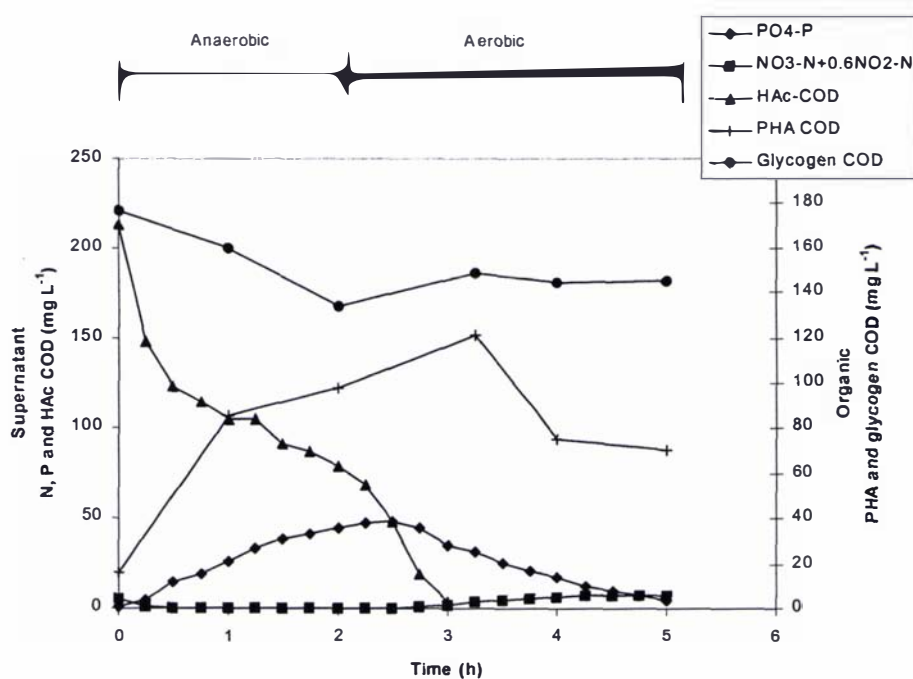


Figure 6.10 Soluble phosphate phosphorus, nitrate nitrogen, SCFA COD, PHA COD and glycogen COD profiles during a batch test with acetate (Trial I)

TRIAL II (75 mg HAc L⁻¹): Figure 6.11 shows the NO₃ – N and PO₄ – P, HAc, PHA and glycogen COD profiles during Trial II. The P profile shows a “bell” shaped P

release and uptake profile during the acetate limiting condition. At the beginning, a reduced P release was observed while $\text{NO}_3 - \text{N}$ was available, showing the simultaneous uptake and release of P as reported by Gerber *et al.* (1987). The P release rate decreased at the end of the anaerobic period-which was probably due to poly-P limitation as shown by the 1.67 % of sludge P content at the end of the anaerobic period (Table 6.7). HAc COD was completely removed during the anaerobic period. The sudden decrease in HAc COD in the initial anaerobic period was most probably due to uptake for denitrification. PHA that was formed during the anaerobic period was utilised during the aerobic period resulting in P uptake. The decrease in glycogen during the anaerobic period suggests that there was an involvement of glycogen in anaerobic PHA formation (Mino *et al.*, 1998). During the initial aerobic period the glycogen was stored rapidly. The average PHA storage rate of $47 \text{ mg PHA COD (g VSS h)}^{-1}$ was observed in the first 1 h of the anaerobic period.

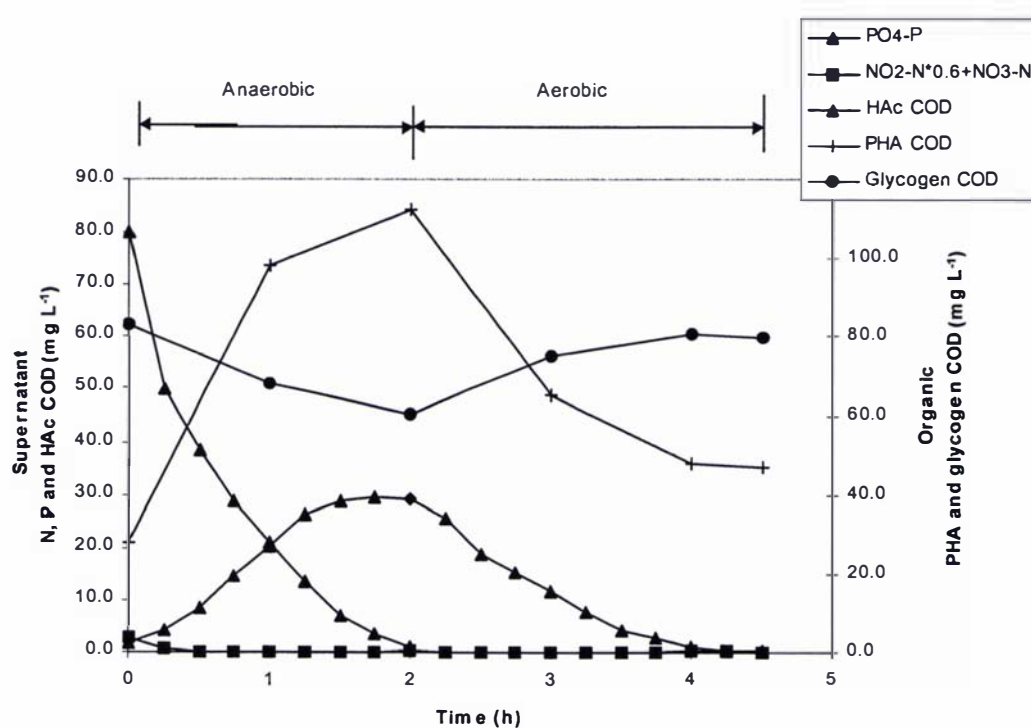


Figure 6.11 Soluble phosphate phosphorus, nitrate nitrogen, SCFA COD, PHA COD and glycogen COD profiles during a batch test with acetate (Trial II)

Table 6.6 shows that 1 g of PHA COD was produced from 0.68 g of HAc COD and 0.27 g of glycogen COD while 0.33 g of P was released during the anaerobic metabolism. The stoichiometry ratios are comparable to the stoichiometry reported by

Smolders *et al.* (1995b). Table 6.8 shows the carbon balance during the aerobic period in Trial II. Using 1g of PHA COD, 0.49 g P and 0.3 g of glycogen COD were stored. The amount of stored P was higher than 0.35 g P and the stored glycogen was slightly lower than the 0.37 g glycogen COD reported by Smolders *et al.* (1995b). This is possibly due to the uptake of P utilising glycogen (Nakamura *et al.*, 1991). The average glycogen storage rate over the first 1 h aeration was 9.97 mg glycogen COD (g VSS h)⁻¹.

Table 6.8 Carbon balance in aerobic P metabolism

Consumed PHA mg COD (g dry mass) ⁻¹	Stored phosphorus mg P (g TSS) ⁻¹	Stored glycogen COD (g dry mass) ⁻¹	g P (g PHA COD) ⁻¹	g Glycogen COD (g PHA COD) ⁻¹
35.99	17.53	10.88	0.49	0.30

6.4 Influence of cations on phosphorus removal

6.4.1 Magnesium, potassium and calcium ions in phosphorus removal

The role of chemical precipitation in P removal has been discussed by Marais *et al.* (1983) and Arvin, (1983). This has not been fully resolved, and the role of cations - especially calcium (Ca²⁺) - in the influent, is still under debate (Carlsson *et al.*, 1997). The chemical precipitation of phosphate in activated sludge systems is a very complicated process as inorganic and organic materials and biological activity are present together. It has been shown in numerous studies that potassium (K⁺) and magnesium (Mg²⁺) are released and taken up together with phosphate under anaerobic and aerobic conditions, respectively (Wentzel *et al.*, 1991). These cations and possibly small amounts of Ca²⁺, function as counter ions in the intracellular polyphosphate granules (Carlsson *et al.*, 1997). Cation involvement in phosphorous metabolism observed in this study is discussed below.

Experiments discussed in Section 6.3.1.1, 6.3.1.2 and 6.3.1.3 were used to analyse the cation involvement in P removal. Figure 6.12 shows the soluble Mg²⁺, K⁺ and Ca²⁺ concentrations in mixed liquor during the SBR cycle and the batch test studies.

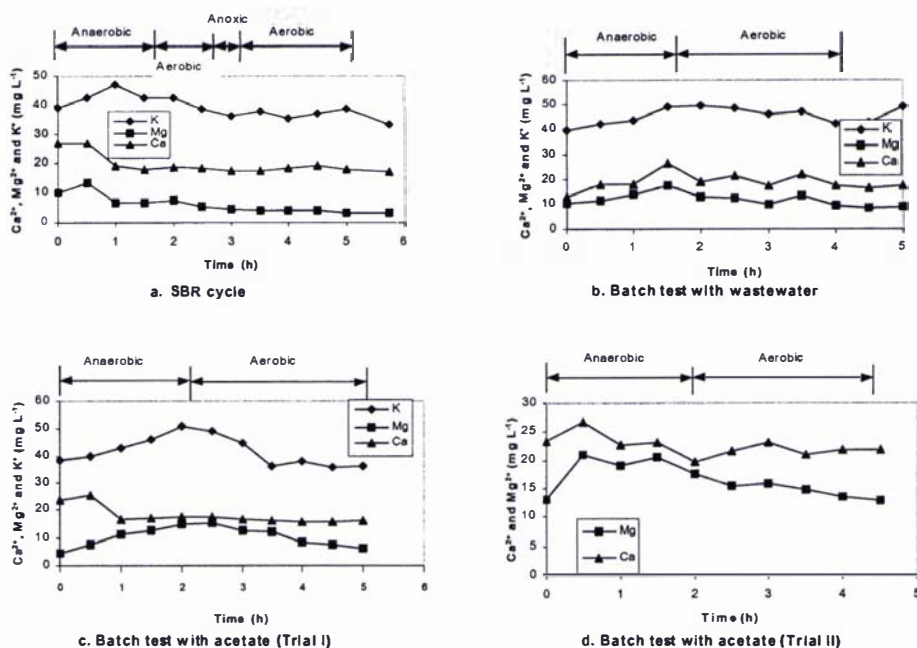


Figure 6.12 Mg^{2+} , K^+ and Ca^{2+} profiles during the SBR cycle and batch tests

In the SBR study, the Ca^{2+} concentration in the mixed liquor increased up to 0.5 h during the anoxic/anaerobic period. The increase in Ca^{2+} was probably from the stabilising divalent cations in bacterial cell walls during the release of P as stated by Comeau *et al.* (1987). There could have been some contribution of Ca^{2+} from the solubilisation of solid magnesium calcium carbonate due to a sudden increase in Mg^{2+} concentration from the feed in the SBR cycle study. A similar result was observed during the addition of $10 \text{ mg L}^{-1} \text{ Mg}^{2+}$ in a batch test (Section 6.4.2). Snoeyink and Jenkins (1980) reported that when CaCO_3 precipitation takes place from solutions containing high Mg^{2+} concentrations, a more soluble solid – a so-called magnesium calcium carbonate – is formed. The Ca^{2+} concentration dropped in the sample taken at 1 h, but did not change much either in the remaining anaerobic period or during the aerobic period. The observed drop in Ca^{2+} could be either from Ca^{2+} phosphate or calcite precipitation as reported by Carlsson *et al.* (1997). But precipitation of Ca^{2+} phosphate seems unlikely as indicated by the low amount of Ca^{2+} and $\text{PO}_4 - \text{P}$ concentrations measured (maximum of 30 and 40 mg L^{-1}) during the anaerobic period in this study. According to Carlsson *et al.* (1997), at near neutral pH the phosphate concentrations must be at least 50 mg P L^{-1} at a Ca^{2+} concentration of 100 mg Ca L^{-1} , before precipitation starts. The drop in Ca^{2+} concentration could not be due to the utilisation of these ions for cell growth as no significant increase in biomass

concentration was observed. Typical composition of Mg^{2+} , Ca^{2+} and K^+ in the bacterial cells is 0.5, 0.5 and 1 % of dry mass (Metcalf & Eddy, 1991).

Mg^{2+} and K^+ are relatively more important than Ca^{2+} in polyphosphate formation, principally due to the higher concentrations of these cation species than Ca^{2+} within the intracellular fluid of organisms equipped with a polyphosphate storage mechanism (Harper, 1969). According to Schönborn *et al.* (2001) “reactive” Mg^{2+} and K^+ stabilised polyphosphates, taking part in P release and uptake processes, and “inert” Ca^{2+} stabilised polyphosphates seemed to be very stable against changes in the redox conditions. The concentration of Mg^{2+} was low at the end of the aerobic period in the SBR cycle, potentially resulting in limitation in the removal of P from meat processing wastewater. Imai *et al.* (1988) found that Mg^{2+} was the limiting factor of EBPR at an influent concentration of less than 8 mg L^{-1} . The Mg^{2+} limitation in P uptake rate is discussed in Section 6.4.2. According to Schönborn *et al.* (2001) the Mg^{2+} content and the Mg^{2+} to Ca^{2+} ratio in the influent wastewater are important deciding factors in maintaining long-term stability in the EBPR process. However, Ca^{2+} was more involved than Mg^{2+} in sludge flocculation through cationic bridging (Sanin & Vesilind, 2000). Figure 6.13 shows the relationship amongst the molar concentrations of soluble Mg^{2+} , K^+ and Ca^{2+} with $PO_4 - P$ during the anaerobic and aerobic periods. Molar ratios of these cations with phosphate are tabulated in Table 6.9.

Table 6.9 Molar ratios of cations with phosphate

Molar ratio (mol/mol)		
Cation/Phosphorus	Anaerobic period	Aerobic period
K^+/P	0.21	0.23
Mg^{2+}/P	0.21	0.33
Ca^{2+}/P	-0.07	0.01
Sum of charges/P	$= 0.21 + 2 \times (0.21 - 0.07) = 0.49$	$= 0.23 + 2 \times (0.33 + 0.01) = 0.91$

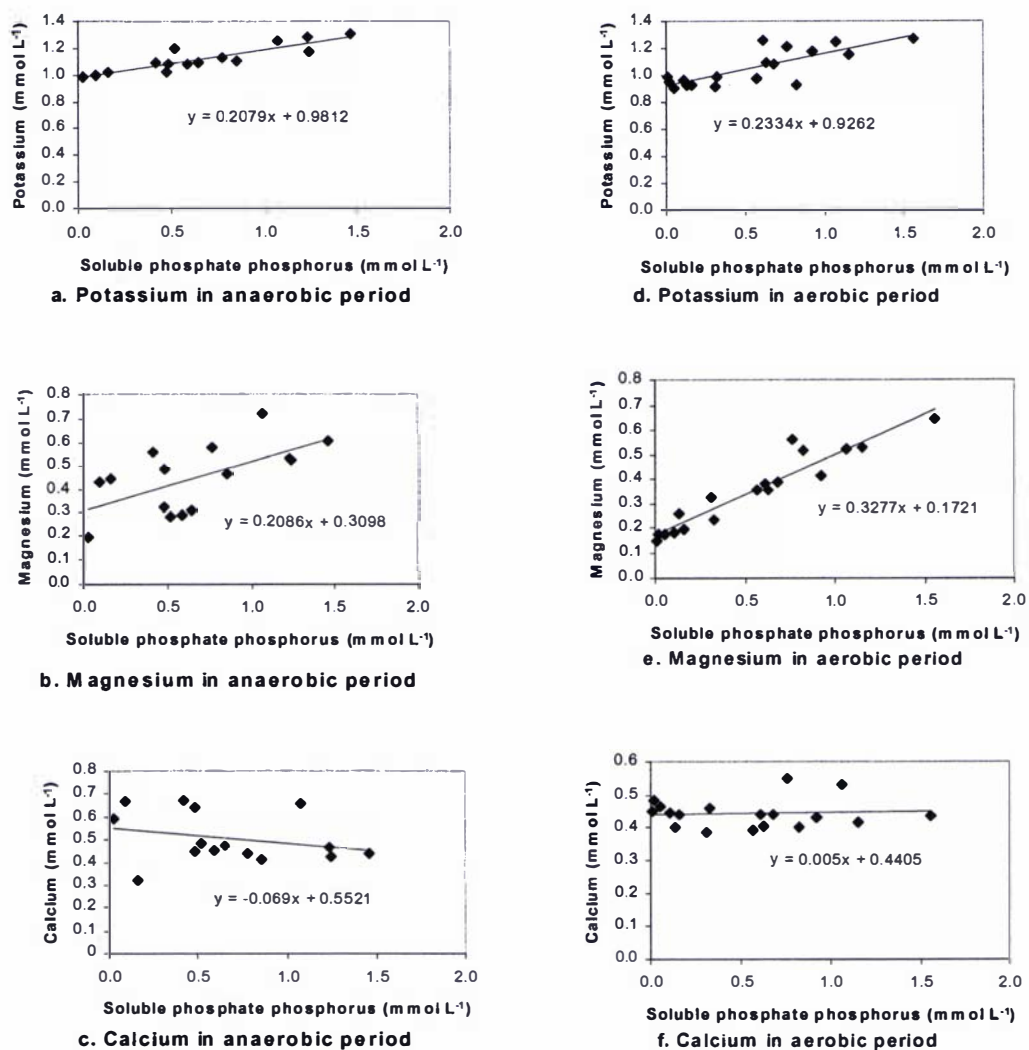


Figure 6.13 Relationships between the molar concentrations of Mg²⁺, K⁺ and Ca²⁺ with PO₄-P

The K⁺, Mg²⁺ and Ca²⁺ cations with phosphate molecules were in a total ionic charge ratio of about 0.49:1 and 0.91:1 in the anaerobic and aerobic periods, respectively in this study. However, Comeau *et al.* (1987) and Wentzel *et al.* (1991) reported that they were co-transported with phosphate molecules in a total ionic charge ratio of about 1:1. The lower ratio observed in this study, especially during the anaerobic period, was probably due to calcite precipitation (Carlsson *et al.*, 1997). Further, the formation of magnesium calcium carbonate was also possible in the anaerobic period as the Mg²⁺ concentration increased during the P release (Snoeyink & Jenkins, 1980). The molar ratio of K⁺ to PO₄-P during anaerobic release and aerobic uptake was comparable to the value of 0.23 reported by Rickard and McClintock (1992). The observed molar ratio of Mg²⁺ to PO₄-P during the anaerobic period was

slightly lower than the value of 0.3 reported by Rickard and McClintock (1992), however it was similar to the value of 0.20 in cheese factory effluent treatment reported by Ky *et al.* (2001). Precipitation of magnesium ammonium phosphate (struvite) was not likely to take place in this study since the value of the product of $[Mg^{2+}][NH_4][PO_4]$ was always less than 10^{-9} . Snoeyink and Jenkins (1980) reported that if the value of the product of $[Mg^{2+}][NH_4][PO_4]$ is less than 10^{-9} , the chance of the precipitation of magnesium ammonium phosphate will be low.

6.4.2 Magnesium ion influence in phosphorus uptake

Among many factors that affect biological excess phosphate uptake metal ions such as Mg^{2+} and K^+ are important (Imai *et al.*, 1988). The presence of sufficient soluble Mg^{2+} in the mixed liquor is necessary for P uptake (Imai *et al.*, 1988; Ky *et al.*, 2001). Soluble Mg^{2+} in the effluent was about 3.5 mg L^{-1} in the SBR cycle study and it is thought that Mg^{2+} could have influenced the P uptake in this study.

Three batch trials were conducted using acetate to assess the influence of Mg^{2+} in phosphorous uptake. Trial II and III were conducted simultaneously 3 d after Trial I. In all trials, sodium acetate was added such that the final HAc concentration was 75 mg L^{-1} . In Trial I, $10 \text{ mg L}^{-1} \text{ Mg}^{2+}$ was added in the form of $MgSO_4 \cdot 7H_2O$. In Trial II 5 mg L^{-1} of Mg^{2+} was added in the form of $MgCl_2 \cdot 6H_2O$. In Trial III there was no Mg^{2+} added. The pH in the mixed liquor was controlled between 7 – 7.5 using 0.5 N HCl and NaOH. Nitrogen gas was purged continuously during the anaerobic period. After 2 h of anaerobic conditions, 3 h of aeration followed. During the aerobic period the DO was controlled at $3.5 - 4 \text{ mg L}^{-1}$. The reactors were kept in a $22 \pm 2^\circ\text{C}$ controlled temperature room. The concentrations of $PO_4 - P$ and metals were measured by samples taken every 0.5 h.

Figure 6.14 and Table 6.10 show the P uptake and release during Trials I, II and III. The highest rate of P release was lower in Trial I compared to the rates in Trials II and III. This may occur if the added Mg^{2+} of 10 mg L^{-1} retarded the P release. According to Fleit (1995), the maximum acetate penetration rate is set by the proton removal rate. Therefore, the higher concentration of soluble Mg^{2+} in the mixed liquor may have retarded the proton removal rate. As the added HAc and the initial $NO_3 - N$ concentrations were similar in all three trials, a similar amount of P release was expected, assuming that the poly-P and glycogen fraction were similar in these three

trials. However, the amount of released P was lower in Trial I than in the other two trials. In Trial II, the added Mg^{2+} of 5 mg L^{-1} did not significantly affect the P release.

The highest P uptake rate in Trial II was greater than the highest in Trial III. This indicates the influence of Mg^{2+} on the P uptake rate during the aerobic period. The highest uptake rate of P in Trial I was lower than the highest in Trial II. This was probably due to the lower amount of P released during the anaerobic period. During the anaerobic period per g of P release 2.04 g of HAc COD was utilised (Section 6.3.1.3). The carry over HAc COD is first used for PHA storage then P uptake (Mino *et al.*, 1998). The uptake of P during the aerobic period is co-related to the release of P during the anaerobic period (Henze *et al.*, 1999; Randall *et al.*, 2002).

Table 6.10 Magnesium influence in P uptake and release

Trial	Mg^{2+} added (mg L^{-1})	VSS (mg L^{-1})	Highest P Release rate ($\text{mg P (g VSS h)}^{-1}$)	Highest P Uptake rate ($\text{mg P (g VSS h)}^{-1}$)
I	10	3190	3.23	7.0
II	5	1010	10.6	9.8
III	0	980	11.4	6.5

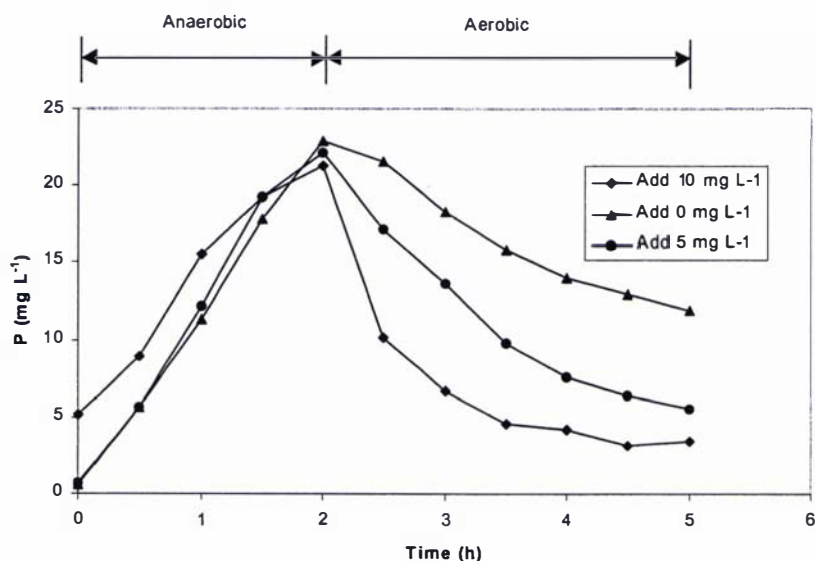


Figure 6.14 Mg influence on phosphate uptake

Figure 6.15 shows the soluble Mg^{2+} , K^+ and Ca^{2+} profiles during Trial I. The calcium profile shows that it increases with time. The increase in Ca^{2+} was probably from solubilisation of solid magnesium calcium carbonate as discussed in Section 6.4.1. The added Mg^{2+} may have enhanced this process (Snoeyink and Jenkins, 1980). The Mg^{2+} profile also shows a slight increase with Ca^{2+} during the anaerobic period. These results show the likelihood of precipitated magnesium calcium carbonate in the sludge. The Mg^{2+} concentration in the aerobic period decreases-probably due to the uptake of P. The K^+ profile remains relatively steady through out.

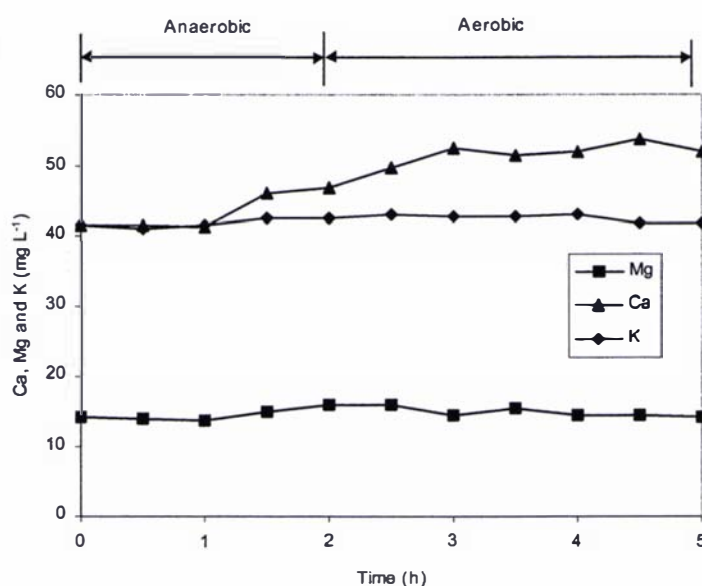


Figure 6.15 Soluble Mg^{2+} , K^+ and Ca^{2+} in mixed liquor in a batch test with $10 \text{ mg L}^{-1} Mg^{2+}$ addition

Polyphosphate storage rate is a key kinetic parameter in the ASM 2 model for the simulation of biological phosphorous removal. Mg^{2+} is a limiting factor for P uptake in meat processing wastewater treatment. Imai *et al.* (1988) found that when Mg^{2+} was less than 8 mg L^{-1} , the effluent P concentration decreased linearly with increases of Mg^{2+} in the feed (artificial wastewater). When influent Mg^{2+} was more than 8 mg L^{-1} , P in the effluent was almost constant (Imai *et al.*, 1988). Ky *et al.* (2001) also reported the limitation of Mg^{2+} in P uptake in a cheese factory effluent treatment. The limitation of Mg^{2+} in the P storage rate is given in a Monod function $MS_{Mg} = S_{Mg}/(S_{Mg} + K_{Mg})$, where S_{Mg} represents the soluble Mg^{2+} concentration and K_{Mg} , the half saturation constant (Ky *et al.*, 2001). The half saturation constant for Mg^{2+} was determined in this study as described below.

$$q = q_{\max} \left[\frac{S_{Mg}}{K_{Mg} + S_{Mg}} \right] \quad (6.11)$$

where q = P uptake rate and q_{\max} = maximum P uptake rate

Other limitations in the P uptake were assumed to be similar for both Trials II and III. Table 6.11 shows the Mg^{2+} concentration at the beginning of the anaerobic period and the P storage rate. Only Trial II and III data were considered for the half saturation constant calculation. In both trials the same amount of P was released in the anaerobic period. The P uptake rate was assumed to be zero when there was no Mg^{2+} in the initial anaerobic period (Rickard & McClintock, 1992).

Table 6.11 Relationship between Mg^{2+} concentration at the beginning of the anaerobic period and the P storage rate.

Mg^{2+} concentration (mg L ⁻¹)	P uptake rate (mg P (g VSS d) ⁻¹)
0	0
3.5	156
8.5	235

Figure 6.16 shows the P uptake rate is increased with soluble Mg^{2+} concentration in the mixed liquor, in the Monod saturation kinetic. By linearising the Monod curve K_{Mg} was found to be 4.7 mg L⁻¹.

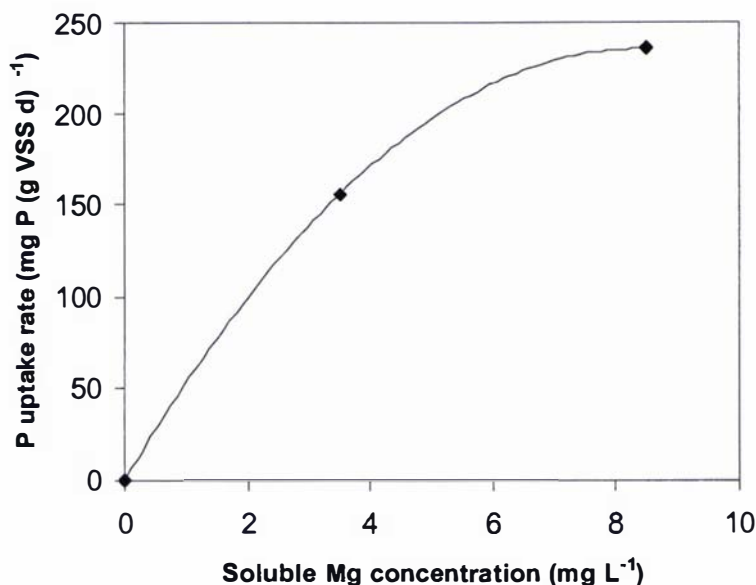


Figure 6.16 Relationship between Mg^{2+} concentration at the beginning of the anaerobic period and the P storage rate

6.5 Anoxic phosphorus uptake and release

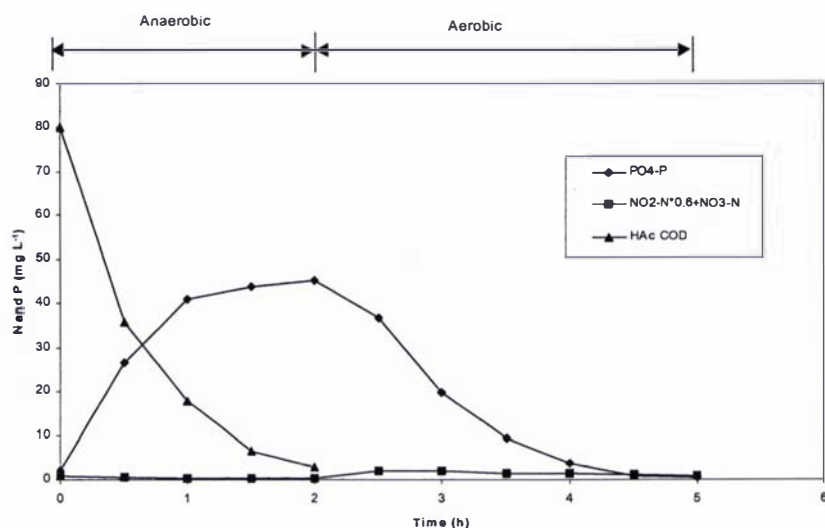
In the early stages of biological nutrient removal processes, it was assumed that the Bio-P bacteria could not use nitrate as an electron acceptor and, hence, could grow and accumulate phosphate only under aerobic conditions (Wentzel *et al.*, 1989). However, later researchers have claimed that a significant fraction of Bio-P bacteria could take up phosphate in the anoxic phase too (Kerrn-Jespersen & Henze, 1993; Kuba *et al.*, 1993; Mino *et al.*, 1998). The anaerobic anoxic P removal system has potential for saving energy, reducing biomass production and maximising the COD available for N and P removal (Kuba *et al.*, 1993). The presence of nitrate reduces phosphate release in the anaerobic phase and diminishes its uptake in the aerobic phase (Comeau *et al.*, 1986; Hascoet & Florentz, 1985). A possible reason for the reduction of phosphate release by nitrate is that phosphate release and uptake occur simultaneously in the presence of nitrate and an organic substrate (Gerber *et al.*, 1987).

The denitrifying capability of Bio-P bacteria is also important in modelling for the better prediction of the behaviour of P and N compounds like $PO_4 - P$, $NH_3 - N$ and $NO_3 - N$. They can be predicted only by introducing denitrifying Bio-P bacteria in mathematical modelling of EBPR (Henze *et al.*, 1999; Kuba *et al.*, 1996; Mino *et al.*, 1995; Mino *et al.*, 1998). In the ASM 2d, the denitrifying Bio-P fraction is accounted for by a reduced anoxic activity of Bio-P in the anoxic condition (60 % of the aerobic

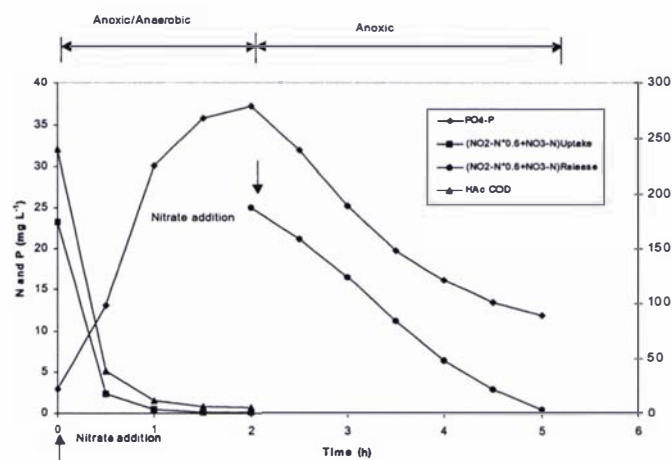
activity). In order to verify the existence of denitrifying Bio-P bacteria in the SBR sludge in this study the following experiment was carried out.

One anoxic-anoxic batch reactor (AA) and one anaerobic-aerobic batch reactor (AO) were set up. In the AA reactor sodium acetate and potassium nitrate were added so that final HAc and nitrate nitrogen were 225 and 25 mg L⁻¹ respectively. In the AO reactor only sodium acetate was added so that the final HAc was 75 mg L⁻¹. The pH of the mixed liquor was controlled between 7 – 7.5 using 0.5 N HCl and NaOH. Nitrogen gas was purged continuously during the anaerobic period in the AO reactor. The anoxic/anaerobic period was 2 h followed by 3 h of anoxic/aerobic conditions. After 2 h 25 mg L⁻¹ nitrate nitrogen was again added to the AA reactor. Nitrogen gas was sparged continuously through the AA reactor. The AO reactor DO was controlled between 3.5 – 4 mg L⁻¹ during the aerobic period. The reactors were kept in a 22 ± 2°C controlled temperature room. Samples were taken at 0.5 h intervals for HAc, NO₃ – N and PO₄ – P measurements.

Figure 6.17 shows the P uptake and release in the AA and AO reactors. The initial P release rate in the AO and AA reactors were 14.3 and 5.8 mg P (g VSS h)⁻¹ and the HAc COD removal rates were 25.5 and 115.2 mg COD (g VSS h)⁻¹. The P release rate was lower in the anoxic condition than in the anaerobic condition. This demonstrates the kinetic competition for the available acetate under anoxic condition. Nitrate would reduce the phosphorus release rate and increase acetate removal rate simultaneously (Chuang *et al.*, 1996). According to Chuang *et al.* (1996), when the substrate is abundant under anoxic conditions, the sludge is under a ‘releasable phosphorus limited’ condition. The anoxic P release rate was 40 % of the anaerobic P release rate in this study. A denitrification rate of 11.9 mg NO₃ – N (g VSS h)⁻¹ was also observed in this study. This simultaneous release of phosphorous and denitrification observed in the AA reactor in this study demonstrates simultaneous uptake and release of P (Filipe & Daigger, 1999; Gerber *et al.*, 1987). The total P release in the AA reactor (34.33 mg L⁻¹) was 80 % of that of the AO reactor (42.85 mg L⁻¹).



a. Anaerobic – aerobic batch test



b. Anoxic – anoxic batch test

Figure 6.17 Anoxic – anoxic and anaerobic – aerobic batch tests

It has been shown that the contribution of phosphate removal by denitrifying Bio-P to the total P removal could be calculated from the ratio of the anoxic phosphate uptake rate to the aerobic phosphate uptake rate (Wachtmeister *et al.*, 1997). This is based on the fact that the denitrifying Bio-P can take up the phosphate at nearly the same rate under both aerobic and anoxic conditions, whereas aerobic Bio-P are inactive under the anoxic condition (Lee *et al.*, 2001). The average anoxic and aerobic P uptake rates were 3.3 and 6.8 mg P (g VSS h)⁻¹ during the first hour in this study. Therefore, the

denitrifying Bio-P fraction was 48 % of the total Bio-P. However, there was about an 80 % P release observed in the AA reactor. This could reduce the analytical fraction of the denitrifying Bio-P. The denitrification rate during the anoxic P uptake was $2.3 \text{ mg NO}_3 - \text{N (g VSS h)}^{-1}$. This is similar to the denitrification rate obtained with the slowly biodegradable COD of meat processing wastewater as discussed in Chapter IV.

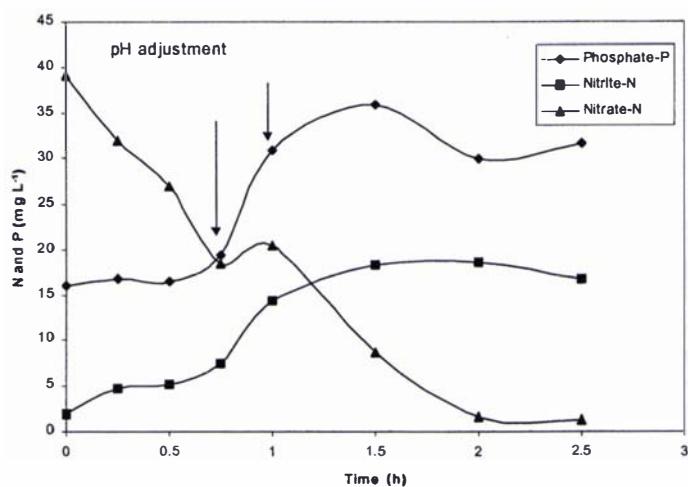
6.6 Phosphorus release during the pH adjustment

The phosphorus release during the anaerobic period depends on the $\text{NO}_3 - \text{N}$ concentration and pH (Smolders *et al.*, 1995a, b). The effect of pH adjustment on the P release was checked using one of the anoxic batch tests discussed in Chapter IV. In this test, pH was not regulated until it increased above 8. At 0.7 h the pH was 8.05 and immediately after that the pH was brought to 7 by 0.5 N HCl. At 0.93 h the pH increased above 8 and was readjusted to 7.

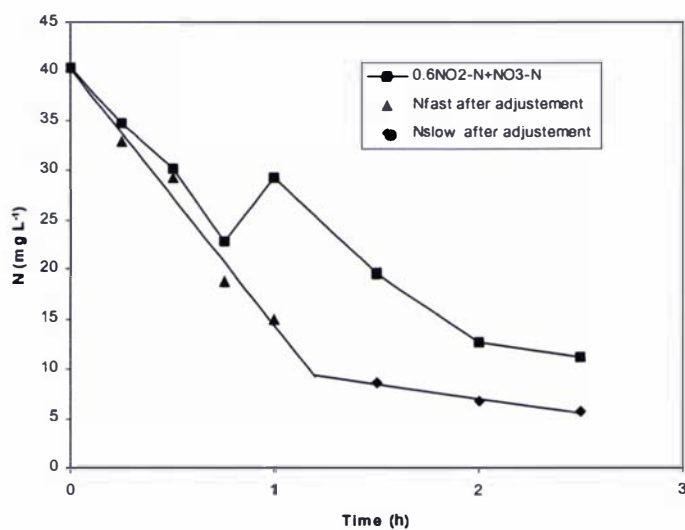
Figure 6.18(a) shows the $\text{NO}_2 - \text{N}$, $\text{NO}_3 - \text{N}$ and $\text{PO}_4 - \text{P}$ profiles during the anoxic batch test. The $\text{NO}_2 - \text{N}$ profile shows an accumulation of $\text{NO}_2 - \text{N}$ with time. Although partial denitrification to nitrite is rarely detected in traditional activated sludge processes, it is often reported when the biomass is exposed to highly transient conditions (Almeida *et al.*, 1995 a, b ; Beun *et al.*, 2000; Wilderer *et al.*, 1987). Due to the higher nitrite concentration, an equivalent amount of nitrate ($0.6 \text{ NO}_2 - \text{N} + \text{NO}_3 - \text{N}$) was used to determine the denitrification profile (Henze, 1986). However, the denitrification profile was not linear with time, as shown in Figure 6.18 (b). The P profile shows a sudden release of P after the pH adjustment. This was also reported by Comeau *et al.* (1986). The observed non-linear denitrification profile was probably due to the sudden release of P. Using the energy derived from hydrolysis of poly-P, Bio-P bacteria could consume some of the available RBCOD, which might have affected the denitrification profile. Interestingly, when the equivalent $\text{NO}_3 - \text{N}$ was decreased in proportion to the increased P, the denitrification profile was linear (Figure 6.18 (b)). This indicates that an equivalent amount of RBCOD is required for 1 g of $\text{NO}_3 - \text{N}$ to be denitrified and also for the release of 1 g of $\text{PO}_4 - \text{P}$. As discussed in Equation 6.9, the required COD for 1 g of $\text{NO}_3 - \text{N}$ to be denitrified is about 7.7 g. This is shown below, where RBCOD is assumed as SCFA COD.

$$\frac{7.7 \text{ g COD}}{\text{g PO}_4 - \text{P}} \Rightarrow \frac{0.13 \text{ g P}}{1 \text{ g SCFA COD}}$$

In other words, 0.13 g P was released per g of SCFA COD removed in the anoxic conditions at sudden pH adjustment. This clearly shows that pH and oxidised nitrogen influence the anaerobic P release.



a. Nitrogen and phosphorus profiles



b. Modified nitrogen profiles

Figure 6.18 N and P profiles in an anoxic batch test

6.7 Summary

In the chapter, the meat processing wastewater was characterised to determine the key kinetic and stoichiometric parameters required in the ASM 1 and ASM 2 models. Also

key processes involved in biological P removal were identified. The maximum specific growth rate of heterotrophs, half saturation constant and yield coefficient (COD basis) were $1.2 - 2.5 \text{ d}^{-1}$, $2 - 12 \text{ mg L}^{-1}$ and 0.63 respectively. The maximum specific growth rate of autotrophs was $0.65 - 0.8 \text{ d}^{-1}$. The heterotrophic Task Group model decay coefficient was 0.36 d^{-1} .

The highest phosphorous release rate of $10.4 \text{ mg P (g VSS. h)}^{-1}$ and a highest poly-P storage rate of $9.3 \text{ mg P (g VSS. h)}^{-1}$ were determined from the SBR cycle study. The average PHA storage rate of $47 \text{ mg PHA COD (g VSS h)}^{-1}$ was observed in the first hour of the anaerobic period in an acetate batch study with 75 mg L^{-1} HAc concentration. The average glycogen storage rate was $9.97 \text{ mg glycogen COD (g VSS h)}^{-1}$ during the first hour of the aerobic period in the same acetate batch study. During this SBR cycle study the sludge P concentration was 4.17% of VSS at the end of the aerobic period. A low sludge P content of 1.37% of VSS was observed in the acetate batch test with 200 mg L^{-1} HAc concentration at the end of the anaerobic period.

The anaerobic P release in the SBR treatment of meat processing wastewater was not limited by the stored glycogen and poly-P; however the available SCFA COD in the meat processing wastewater limited the anaerobic P release. During the anaerobic period unutilised HAc COD by Bio-P bacteria were found. The glycogen concentration increased in the initial anaerobic period and then decreased during the remaining anaerobic period. The glycogen concentration decreased during the anoxic as well as in the final aerobic period. PHB and PHV COD were about 65 and 35% respectively of the total PHA COD measured in the meat processing wastewater sludge. The PHA concentration increased during the fast release of P but was almost constant during the slow release of P. A low PHA COD of $5.1 \text{ mg L}^{-1} \text{ PHA COD (g VSS)}^{-1}$ was observed towards the end of aerobic periods.

The P release per g SCFA COD utilised in meat processing wastewater was $0.9 - 0.95 \text{ g}$ during the anaerobic period. Also, while for 1 g of SCFA COD removed, 1.25 g PHA COD was produced. These stoichiometric parameters were considered unrealistic due to the unknown storage components other than PHB and PHV and glycogen. The stoichiometric relationship was determined in a batch test using limited acetate and the acclimatised sludge obtained from meat processing wastewater treatment by the SBR. In this batch test, 1 g of PHA COD was produced from 0.68 g of HAc COD and 0.27 g of glycogen COD, while 0.33 g of P was released during the anaerobic period. In the

aerobic period, for every 1 g of PHA COD utilised, 0.49 g P and 0.3 g glycogen COD were stored.

In the batch test with excess substrate, despite the presence of a substantial amount of extracellular acetate, the release of P under the anaerobic condition appeared to be limited once a fixed portion of intracellular P had been released. The amount of intracellular PHA increased in the subsequent aerobic condition in the presence of a sufficient amount of extracellular acetate, but the amount decreased when the extracellular acetate had been depleted. Similarly, the amount of intracellular glycogen initially increased, and then remained constant following the decrease in PHA content. In the poly-P limited condition a lower PHA COD was stored per g of HAc COD removed.

The mol ratios of K^+ with $PO_4 - P$ were 0.21 during the anaerobic period, and 0.23 during the aerobic period. The mol ratios of Mg^{2+} with $PO_4 - P$ were 0.21 during the anaerobic period, and 0.33 during the aerobic period. Calcite and magnesium calcium carbonate solids were possibly formed during the meat processing wastewater treatment by an SBR. Mg^{2+} was a limiting factor for the P uptake and the uptake rate could be explained by a Monod kinetic. In the Monod kinetic expression the magnesium half saturation constant was found to be 4.7 mg L^{-1} .

In the presence of an external carbon source simultaneous P uptake and release and denitrification were observed in the anoxic batch test. This indicates the presence of a competition between denitrifiers and Bio-P for the carbon source during the anoxic period. Reduced anoxic P uptake rate compared to the oxic P uptake rate indicates that a fraction of Bio-P bacteria had a denitrifying capacity in the meat processing wastewater treatment by an SBR.

The P release per g HAc COD removal depends on the pH, $NO_3 - N$ concentration and Mg^{2+} concentration (under a non-steady state) in the mixed liquor. The sudden adjustment of pH caused P release in the anoxic batch test. During this period 0.13 g P was released per 1 g of SCFA COD removed.

CHAPTER VII

APPLICATION OF ACTIVATED SLUDGE MODELS

7.1 Introduction

Mathematical models are powerful tools by which the designers of biological wastewater treatment systems can investigate the performance of potential systems under a variety of conditions. Using mechanistic models, many potentially feasible solutions may be evaluated quickly and inexpensively, thereby only the more favourable ones will be selected for actual testing by a physical model. Models may also be used for controlling the reactor operations. Such a model should be simple to use and capable of predicting performance accurately.

The development of the Activated Sludge Model No. 1 (ASM 1) by the IAWPRC Task Group allowed prediction of organic matter degradation, nitrification and denitrification in suspended sludge systems (Henze *et al.*, 1987a). The ASM 1 model is a major step forward in modelling activated sludge systems. Deeper understanding of the biological phosphorus removal mechanism has led to the development of more comprehensive models for biological carbon, nitrogen and phosphorus removal in activated sludge systems. Phosphorus removal was included in ASM 2 by the IAWQ Task Group (Henze *et al.*, 1995). The ASM 2 model is based on the TCA cycle for deriving the reducing power required for PHA formation (Mino *et al.*, 1998; Smolders *et al.*, 1995b). Also, the denitrification capability of Bio-P is not considered in the ASM 2 model. The subsequent ASM 2d model (Henze *et al.*, 1999) incorporates the denitrification process by Bio-P bacteria.

Key kinetic and stoichiometric parameters are discussed in Chapter VI for simulation of Sequencing Batch Reactor (SBR) treatment of meat processing wastewater by the ASM 1 and ASM 2 models. Also in Chapter VI the anoxic phosphorus uptake process, glycogen involvement in PHA storage process and Mg^{2+} requirement in phosphorus uptake were identified during the SBR treatment of meat processing wastewater. Most of the biologically active phosphate esters are, for instance, present in the cell as magnesium complexes. Also the phospho-lipoproteins of bacterial cell walls are chelated with magnesium ions (Gottschalk, 1979).

Even though the applicability of ASM 2 model was tested for domestic wastewater by several workers, it has not yet been tested for meat processing wastewater. For the prediction of glycogen and Mg^{2+} concentration during the SBR treatment the activated sludge model No. 2 was modified. The modified model can predict the glycogen and Mg^{2+} profiles during different scenarios of operating condition.

In this chapter, the modifications made to the ASM 1 and ASM 2 models to incorporate all the major processes that take place in an SBR cycle during the treatment of meat processing wastewater, calibration and validation of the models are discussed. The optimisation of phases in a 6-h cycle for COD and nutrients removal is also considered.

7.2 Activated Sludge Model No. 1 (ASM 1)

7.2.1 Model description

The development of mechanistic mathematical models to describe biological wastewater treatment has been evolutionary. The key to successful modelling of the oxygen consumption pattern in activated sludge was the recognition that part of the substrate is used directly for synthesis, with a direct coupling between substrate consumption, biomass growth and oxygen utilisation. Another portion of the substrate is removed rapidly from the liquid phase through storage processes that do not require oxygen consumption (Cliff & Andrews, 1981). The substrate storage mechanism suggested by Cliff and Andrews is illustrated in Figure 7.1. The IAWPRC task group recognised the substrate storage mechanism, but they were unconvinced of the generality of the storage process (Grady, 1989). A flow diagram for the ASM 1 model produced by the IAWPRC is given in Figure 7.2.

The ASM 3 model (Gujer *et al.*, 1999) has evolved from the ASM 1 model. The ASM 3 corrects some deficiencies in the ASM 1 (Henze *et al.*, 1987a). It includes the storage of organic substrates as a new process. However, the storage components are difficult to identify and quantify for real wastewater. Further experiments will have to be performed specifically for calibrating ASM 3 more accurately (e.g. heterotrophic storage of organic substrate) (Koch *et al.*, 2000). Also phosphorus removal processes were not included in the ASM 3. But the ASM 2 can simulate organic carbon and nutrient removal, and overcome most of the limitations in the ASM 1. The concept of

death-regeneration is used in the ASM 1 and ASM 2 models, whereas the concept of endogenous respiration is used in the ASM 3. Therefore, in this study model simulations were carried out using both the ASM 1 and ASM 2, and the results were compared.

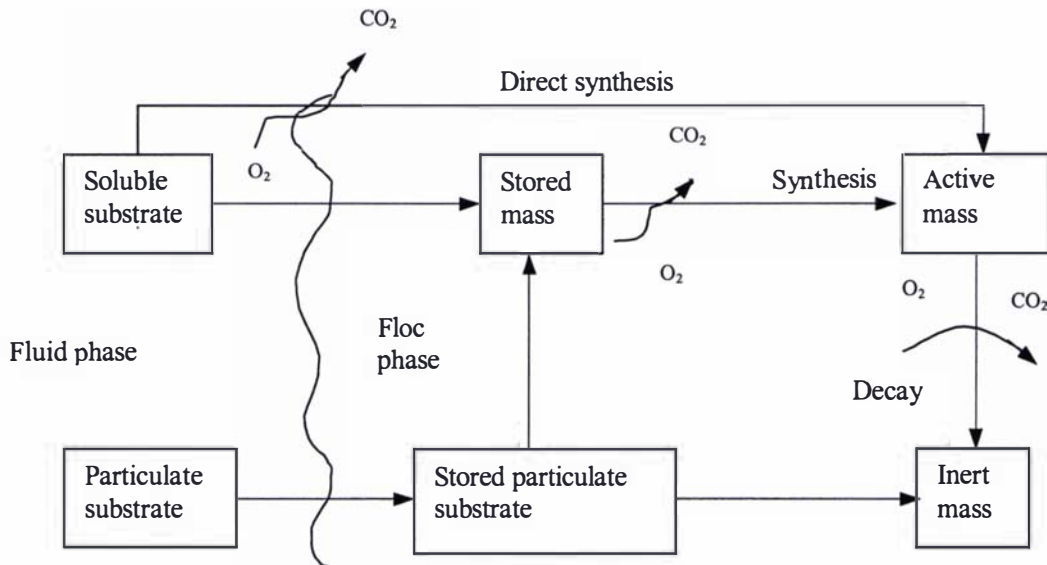


Figure 7.1 Flow diagram for model used by Clift and Andrews (1981)

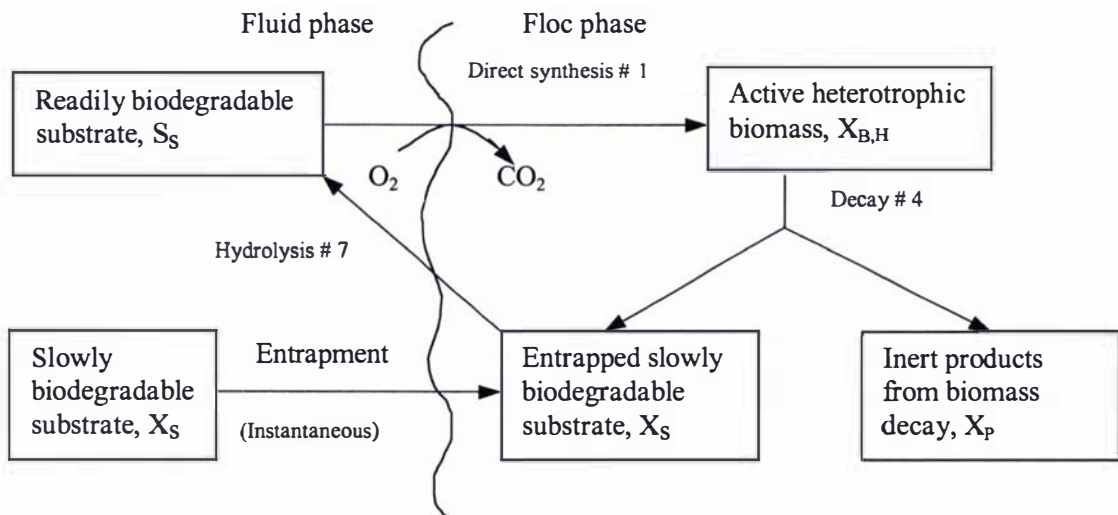


Figure 7.2 Flow diagram for the ASM 1 model (Grady, 1989)

A detailed description of the ASM 1 model can be found in Henze *et al.* (1987b) and Grady (1989). The key features of the model are outlined below. The processes incorporated into the ASM 1, and the procedures for its use, are in Table 7.1. All components in the model are listed by symbols across the top of the table, while their definitions are given in the bottom row. The fundamental processes which are important

in single sludge systems are listed down the extreme left column, while the rate expressions chosen to represent them are listed on the extreme right. The parameters in these rate expressions are defined in the lower right hand corner. The body of the matrix contains the stoichiometric coefficients, which are defined in the lower left corner. If a particular process has no impact upon a given component, then the box formed by the intersection of the process row and component column is blank.

The concentrations of all organic components, whether soluble (S) or particulate (X), are given in units of chemical oxygen demand (mg L^{-1} COD). The concentrations of all nitrogen species are given as nitrogen (mg N L^{-1}). Consequently, two conversion factors 2.86 and 4.57 are used in the matrix to convert nitrate nitrogen and ammonia nitrogen concentrations respectively, to an equivalent COD basis for calculating nitrate or oxygen utilisation rates.

Construction of the observed conversion rate for a component is accomplished by moving down the column i corresponding to that component and summing the product of each process rate ρ_j times the appropriate stoichiometric coefficient v_{ij} , as shown in Equation 7.1.

$$r_i = \sum_{j=1 \rightarrow 8} v_{ij} \rho_j \quad \text{for } i = 1 \rightarrow 13 \quad (7.1)$$

For example, the observed conversion rate for readily biodegradable substrate (S_S) (component 2) is given by Equation 7.2.

$$r_2 = v_{21} \rho_1 + v_{22} \rho_2 + v_{27} \rho_7 \quad (7.2)$$

Table 7.1 Activated sludge model No. 1 (Henze *et al.*, 1987a, b)

j	Component → i Process ↓	1	2	3	4	5	6	7	8	9	10	11	12	13	Process rate, ρ_j ($ML^{-3}T^{-1}$)
1	Aerobic growth of heterotrophs		$-\frac{1}{Y_H}$			1			$\frac{1-Y_H}{Y_H}$		$-i_{XB}$			$-\frac{i_{XB}}{14}$	$\hat{\mu}_H \frac{S_S}{K_S+S_S} \frac{S_O}{K_{O,H}+S_O} X_{B,H}$
2	Anoxic growth of heterotrophs		$-\frac{1}{Y_H}$			1			$\frac{1-Y_H}{2.86Y_H}$		$-i_{XB}$			$\frac{1-Y_H}{14 \cdot 2.86Y_H} - \frac{i_{XB}}{14}$	$\hat{\mu}_H \frac{S_S}{K_S+S_S} \frac{K_{O,H}}{K_{O,H}+S_O} \frac{S_{NO}}{K_{NO}+S_{NO}} \eta_g \cdot X_{B,H}$
3	Aerobic growth of autotrophs						1		$\frac{4.57-Y_A}{Y_A}$	$\frac{1}{Y_A}$	$-i_{XB} \frac{1}{Y_A}$			$-\frac{i_{XB}}{14} \frac{1}{7Y_A}$	$\hat{\mu}_A \frac{S_{NH}}{K_{NH}+S_{NH}} \frac{S_O}{K_{O,A}+S_O} X_{B,A}$
4	“Decay” of heterotrophs				$1-f_P$	-1		f_P						$i_{XB} - f_P \cdot i_{XP}$	$b_H \cdot X_{B,H}$
5	“Decay” of autotrophs				$1-f_P$		-1	f_P						$i_{XB} - f_P \cdot i_{XP}$	$b_A \cdot X_{B,A}$
6	Ammonification of soluble organic nitrogen										1	-1		$\frac{1}{14}$	$k_a \cdot S_{ND} \left[\frac{S_O}{K_{O,H}+S_O} + \eta_g \frac{K_{O,H}}{K_{O,H}+S_O} \frac{S_{NO}}{K_{NO}+S_{NO}} \right] X_{B,H}$
7	“Hydrolysis” of entrapped organics		1		-1										$k_h \frac{X_S/X_{B,H}}{K_X+X_S/X_{B,H}} \left[\frac{S_O}{K_{O,H}+S_O} + \eta_h \frac{K_{O,H}}{K_{O,H}+S_O} \frac{S_{NO}}{K_{NO}+S_{NO}} \right] X_{B,H}$
8	“Hydrolysis” of entrapped organic nitrogen											1	-1		$\rho_7 \frac{X_{ND}}{X_S}$
Observed conversion rates ($ML^{-3}T^{-1}$)		$r_i = \sum_j v_{ij} \rho_j$													Kinetic parameters:
Stoichiometric parameters: Heterotrophic yield: Y_H Autotrophic yield: Y_A Fraction of biomass yielding particulate products: f_P Mass N/mass COD in biomass: i_{XB} Mass N/mass COD in products from biomass: i_{XP}		Soluble inert organic matter-M(COD)L ⁻³	Readily biodegradable substrate -M(COD)L ⁻³	Particulate inert organic matter -M(COD)L ⁻³	Slowly biodegradable substrate -M(COD)L ⁻³	Active heterotrophic biomass -M(COD)L ⁻³	Active autotrophic biomass -M(COD)L ⁻³	Particulate products arising from biomass decay -M(COD)L ⁻³	Oxygen (negative COD) -M(COD)L ⁻³	Nitrate and Nitrite nitrogen -M(N)L ⁻³	NH ₄ ⁺ + NH ₃ nitrogen -M(N)L ⁻³	Soluble biodegradable organic nitrogen -M(N)L ⁻³	Particulate biodegradable organic nitrogen -M(N)L ⁻³	Alkalinity – molar units	Heterotrophic growth and decay $\hat{\mu}_H \cdot K_S, K_{O,H}, K_{NO}, b_H$ Autotrophic growth and decay $\hat{\mu}_A \cdot K_{NH}, K_{O,A}, b_A$ Correction factor for anoxic growth of heterotrophs: η_g Ammonification: k_a Hydrolysis: k_h, K_X Correction factor for anoxic hydrolysis: η_h

Note : The process rate 6 is modified according to Oles and Wilderer, 1991

The observed reaction rates can be substituted into the mass balance Equation 2.8 or Equation 2.9 to formulate a model of the SBR to depict the fate of the components (Oles & Wilderer, 1991). The components and the process rate equations in Table 7.1 are essential to a realistic simulation. However, the expressions might not depict perfectly the actual reactions occurring within a system (Henze *et al.*, 1987b; van Loosdrecht & Henze, 1999).

Switching functions: The ASM 1 incorporated switching functions for some processes, to turn them on and off as environmental conditions change. These are introduced so that the functions are mathematically continuous to help to eliminate problems of numerical instability, which can occur during simulation with models that include rate equations that are switched on and off discontinuously.

Organic matter COD: In the ASM 1, the organic matter COD in wastewater is subdivided as shown in Figure 7.3. Inert organic matter passes through an activated sludge system unchanged. Inert soluble organic matter leaves the system at the same concentration as it enters. Inert suspended organic matter becomes enmeshed in the activated sludge and is removed from the system through sludge wastage. The readily biodegradable substrate (S_S) which consists of simple molecules is treated as if it were soluble, whereas the slowly biodegradable material (X_S), consisting of complex molecules, is treated as if it were particulate, although some may indeed be soluble.

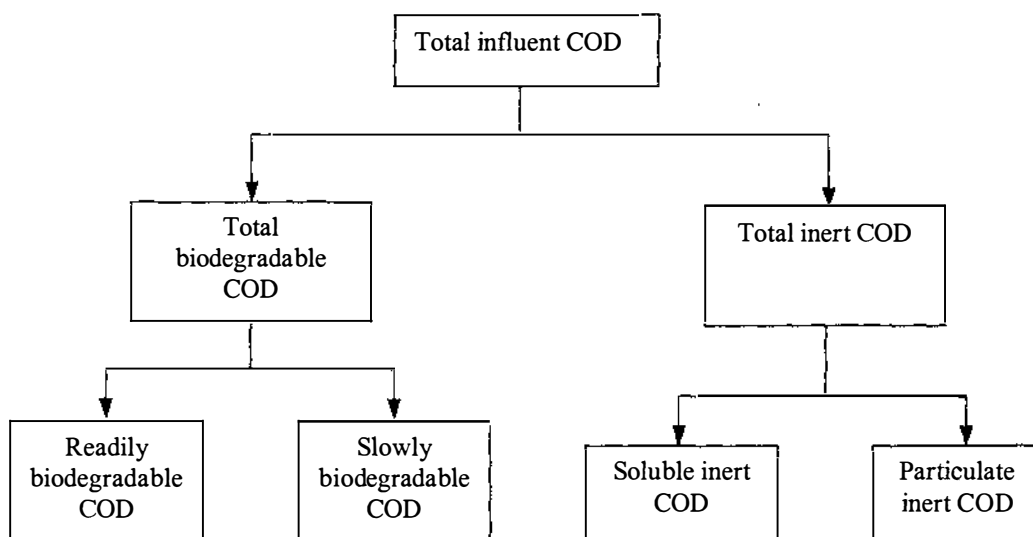


Figure 7.3 Distribution of COD fractions in wastewater

S_S is considered to be the only substrate for the growth of heterotrophic biomass, which can convert it into new biomass under either aerobic or anoxic conditions. The electrons associated with the expenditure of energy for cell synthesis are transferred to the exogenous electron acceptors (oxygen or nitrate).

X_S is considered in the model to be removed from suspension instantaneously by entrapment in the bioflocs. However, once there, it must be acted upon extracellularly and converted into S_S before it can be used by the heterotrophic biomass for growth. The reactions involved in this conversion are called “hydrolysis” in the model, although in reality they are likely to be more complex. It is assumed that hydrolysis involves no energy utilisation, and thus there is no utilisation of an electron acceptor associated with it.

The degradation of X_S is very important to the realistic modelling of activated sludge systems, because it is primarily responsible for the attainment of realistic space-time and real-time dependent electron acceptor profiles. In the ASM 1, the hydrolysis process is modelled so that the rate appears to saturate, as the amount of entrapped substrate becomes large in proportion to the biomass. In addition, the rate of hydrolysis is usually considerably lower than the specific rate of utilisation of S_S , so it becomes the rate-limiting factor in the growth of biomass when only X_S is present. Furthermore, because of the need for enzyme synthesis, it was reasoned that the rate would be dependent on the concentration of the electron acceptor present and would be lower under anoxic conditions than under aerobic conditions. The anaerobic hydrolysis is assumed to be negligible in the ASM 1 model.

Heterotrophic biomass: Heterotrophic biomass is generated by growth in S_S under either aerobic or anoxic conditions, but its generation is assumed to stop under anaerobic conditions. Biomass is lost by decay, which incorporates a large number of mechanisms, including endogenous metabolism, death, predation and lysis (Henze *et al.*, 1987 a, b; van Loosdrecht & Henze, 1999). The most common technique used for modelling decay under aerobic conditions is to incorporate all of the mechanisms into a single rate expression, which is first order with respect to the concentration of the active biomass. Also, each unit of biomass COD lost results in the utilisation of an equivalent amount of oxygen. This approach, however, causes problems when other electron acceptors are considered. To avoid the problem, the death regeneration model of Dold *et*

al. (1980) was adopted, and is depicted in row 4 of Table 7.1. Both endogenous decay and death-regeneration approaches are illustrated in Figure 7.4.

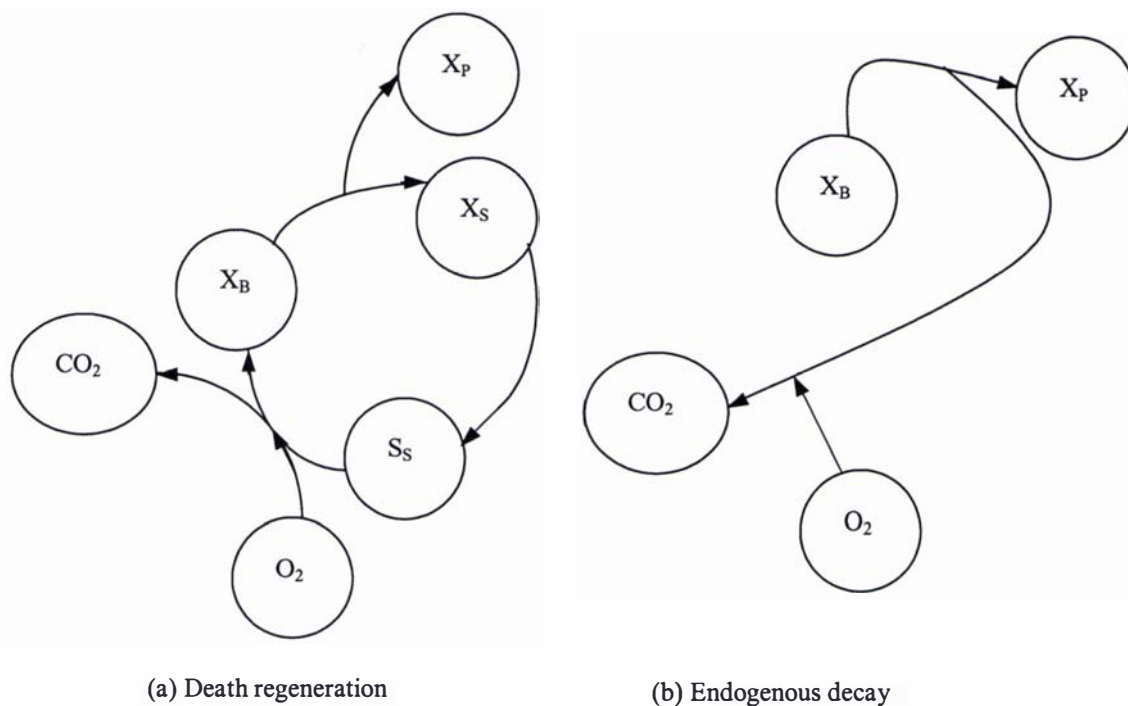


Figure 7.4 Illustration of death-regeneration and endogenous decay models (Orhon & Artan, 1994)

In the regeneration model, decay converts the biomass into a combination of X_S and particulate inert products. The inert particulate biomass products act to reduce the viability of the suspended solids in a bioreactor. No loss of COD is involved in this reaction. Furthermore, decay continues at a constant rate regardless of the type of electron acceptor present. The use of an electron acceptor that is normally associated with decay occurs as a result of cell growth on the S_S , which arises from hydrolysis of the X_S released by decay. If conditions are aerobic, oxygen will be used. If conditions are anoxic, nitrate will be used. If neither oxygen nor nitrate is available, no conversion occurs and the X_S accumulates. When an electron acceptor becomes available, the X_S will be converted and used. A portion of the biomass lost by decay is reconverted into new biomass via the use of the S_S resulting from the X_S released. Because of this conversion, the decay rate coefficient must be higher, so that the same net loss of biomass is achieved as in the conventional method of modelling decay.

Nitrogenous matter: Nitrogenous matter in wastewater is subdivided in the model as shown in Figure 7.5 (Orhon & Artan, 1994). With respect to the non-biodegradable

fraction, the particulate and soluble portions are those associated with the non-biodegradable particulate and soluble COD respectively.

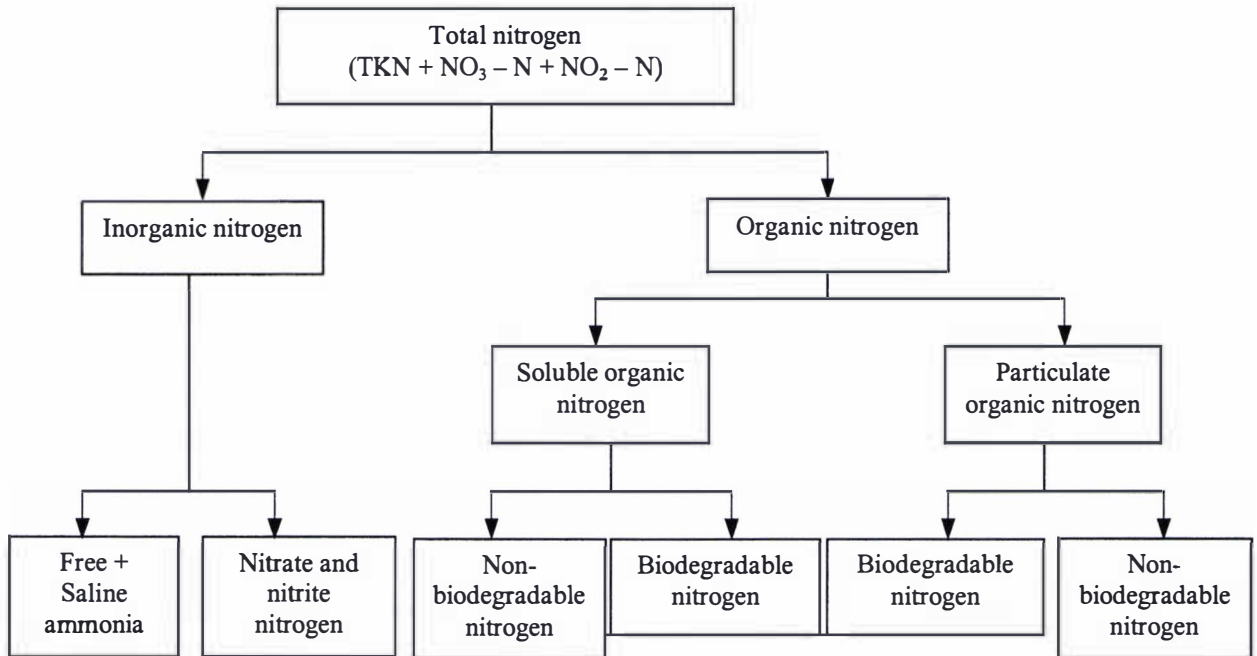


Figure 7.5 Wastewater characterisation for nitrogenous components (Orhon & Artan, 1994)

Particulate biodegradable organic nitrogen (X_{ND}) is hydrolysed to soluble biodegradable organic nitrogen (S_{ND}) in parallel with the hydrolysis of X_S . The S_{ND} is converted to ammonia by heterotrophic bacteria. Oles and Wilderer (1991) modified the ammonification of S_{ND} process rate by assuming that it depends on terminal electron acceptor conditions. The modification was obtained by adding switching functions for aerobic and anoxic conditions to the ammonification process rate. Anoxic ammonification activity is assumed to be governed by the same limiting factors as anoxic growth activity. The ammonia serves as the nitrogen source for synthesis of heterotrophic and autotrophic biomass, and as the energy supply for the growth of autotrophic nitrifying bacteria. For simplicity, the autotrophic conversion of ammonia to nitrate nitrogen is considered to be a single-step process, which requires oxygen. The nitrate formed may serve as a terminal electron acceptor for heterotrophic bacteria under anoxic conditions, yielding nitrogen gas. Cell decay of either autotrophic or heterotrophic biomass leads to the release of X_{ND} which re-enters the cycle.

Autotrophic biomass: Autotrophic biomass is formed by growth at the expense of ammonia nitrogen under aerobic conditions. The decay of autotrophs follows the same pattern as the decay of heterotrophs.

Alkalinity: The processes are assumed to be independent of alkalinity. Inclusion of the alkalinity in the ASM 1 provides information on any undue changes in pH. All reactions involving addition or subtraction of protons will cause changes in alkalinity. The primary reactions affecting alkalinity involve nitrogen and are shown in Table 7.1.

7.2.2 Calibration of the modified ASM 1 model

The process of ammonification of soluble organic nitrogen in the ASM 1 model was modified as discussed in Section 7.2.1 in this chapter for the $\text{NO}_3 - \text{N}$ observed in the initial anoxic/anaerobic period of the SBR cycle study. In the modelling $\text{NO}_3 - \text{N}$ was taken as the equivalent of $\text{NO}_3 - \text{N}$ plus $0.6 \text{NO}_2 - \text{N}$. The model with the modification will be referred to as the *modified ASM 1 model*. The SBR cycle study described in Section 6.3.1.1 in Chapter VI was used to calibrate the ASM 1 model.

The characteristics of the wastewater used for the model calibration are described in Section 6.3.1.1. The short chain fatty acid COD (SCFA COD) of the wastewater was taken as the readily biodegradable COD (RBCOD), as RBCOD was not measured during the SBR cycle study. The RBCOD or the SCFA COD of the wastewater was not determined during the cycle study described in Section 5.5. Therefore the RBCOD was taken as the average RBCOD found in Chapter IV (17 % of the TCOD). In general, for the validation of the calibrated models it is necessary to have several data sets that have been obtained independently from the data used for calibration. In this study the experimental data were all obtained from the same SBR reactor, but cycle studies were carried out at periods of time some three months apart. The data sets from such cycle studies were assumed to be independent data sets. The soluble and particulate biodegradable organic nitrogen were taken as 42 % and 53 % respectively corresponding to the rapidly hydrolysable and slowly hydrolysable COD fraction found in Chapter IV. The influent heterotrophic biomass was not determined in this study but was assumed to be negligible compared to the reactor biomass.

Most of the key kinetic and stoichiometric constants were determined from the experimental results discussed in Chapter VI. Other parameters necessary for the model

simulation were obtained by adjusting the default values of the ASM 1 model to best fit (eye observation) the SBR cycle study results described in Section 6.3.1.1. In order to do that, model calibration was initialised with the default values proposed in the ASM 1 model (Henze *et al.*, 1987a). Then the parameters were adjusted to fit the experimental data.

Kinetic and stoichiometric parameters: All kinetic and stoichiometric parameters for the calibrated model are shown in Table 7.2. The values in bold type are those different from the default values stipulated in ASM 1 (Henze *et al.*, 1987a) for domestic wastewater.

The values for parameters Y_H , $\hat{\mu}_H$, K_S and $\hat{\mu}_A$ were determined using experimental results as described in Chapter VI. The heterotrophic decay coefficient was also estimated using the experimental results as described in Chapter VI and, it was adjusted to fit the calibration cycle experimental results. Predators such as protozoa and rotifers influence the decay rate, therefore it may have to be adjusted to some extent during model calibration (Huisman & Mino, 2002). The value of 0.24 d^{-1} thus obtained by calibration was similar to the value reported by Görgün *et al.* (1995). The value used for k_a was from Oles and Wilderer (1991). Other parameters were obtained by calibrating the model to SBR cycle data, and the values thus obtained were within the range of values reported by Henze *et al.* (1987a). Temperature correction was not made for these parameters, as the SBR was operated at $22 \pm 2^\circ\text{C}$.

The total active biomass was calculated as 68 % of the measured volatile suspended solids (VSS) at the end of the aerobic phase, using the expressions presented by Ekama *et al.* (1986). A nitrifier fraction of 4.5 % of the total active biomass was assumed, following Metcalf and Eddy (1991). This corresponds to a 5 d biochemical oxygen demand (BOD_5) to TKN ratio of 5 – 6, where BOD_5 was taken as 50 % of TCOD (Cooper & Russell, 1991).

The code for the ASM1 model was written in Matlab 5.3 (The Math Works, Natick, MA, USA). The equations were solved using the Matlab function “ode45” for ordinary differential equations systems. Codes for the script and function files in Matlab 5.3 are given in Appendix C.

Table 7.2 Kinetic and stoichiometric parameter values used after the calibration of ASM 1 model

Symbol	Description	Units	Default value in ASM 1	Values used in model
Y_A	Yield of autotrophic biomass	g COD (g N) ⁻¹	0.24	0.20 (adjusted)
Y_H	Yield of heterotrophic biomass	g COD (g COD) ⁻¹	0.67	0.63 (measured)
i_{XB}	Mass of nitrogen per mass of COD in biomass	g N (g COD) ⁻¹ in biomass	0.086	0.086
f_P	Fraction of biomass leading to particulate products	-	0.08	0.08
i_{XE}	Mass of nitrogen per mass of COD in products from biomass	g N (g COD) ⁻¹ in products from biomass	0.06	0.06
$\hat{\mu}_H$	Maximum specific growth rate of heterotrophic biomass	d ⁻¹	6.0	2.0 (measured)
K_S	Half saturation coefficient for heterotrophic biomass	g COD m ⁻³	20.0	8.00 (measured)
$K_{O,H}$	Oxygen half saturation coefficient for heterotrophic biomass	g O ₂ m ⁻³	0.20	0.20
K_{NO}	Nitrate half saturation coefficient for denitrifying heterotrophic biomass	g NO ₃ - N m ⁻³	0.50	0.50
b_H	Decay coefficient for heterotrophic biomass	d ⁻¹	0.62	0.24 (measured and adjusted)
η_g	Correction factor for heterotrophic growth rate under anoxic conditions	-	0.80	0.80
η_h	Correction factor for hydrolysis under anoxic conditions	-	0.40	0.40
K_h	Maximum specific hydrolysis rate	g slowly biodegradable COD (cell COD.d) ⁻¹	3.00	3.00
K_X	Half saturation coefficient for hydrolysis of slowly biodegradable substrate	g slowly biodegradable COD (cell COD) ⁻¹	0.03	0.03
$\hat{\mu}_A$	Maximum specific growth rate of autotrophic biomass	d ⁻¹	0.80	0.75 (measured)
K_{NH}	Ammonia half saturation coefficient for autotrophic biomass	g NH ₃ - N m ⁻³	1.00	1.00
K_{OA}	Oxygen half saturation coefficient for autotrophic biomass	g O ₂ m ⁻³	0.40	1.2 (adjusted)
B_a	Decay coefficient for autotrophic biomass	d ⁻¹	0.15	0.1 (adjusted)
K_a	Ammonification rate	m ³ (g COD d) ⁻¹	0.08	0.40 (adjusted)

Figure 7.6 shows the simulated and experimental $\text{NH}_3 - \text{N}$ and $\text{NO}_3 - \text{N}$ profiles of the SBR cycle described in Section 6.3.1.1. The measured $\text{NO}_3 - \text{N}$ was slightly higher than the model prediction during the anoxic period. This could be due to the observed fast nitrification during the first aerobic period which was not simulated well by the model.

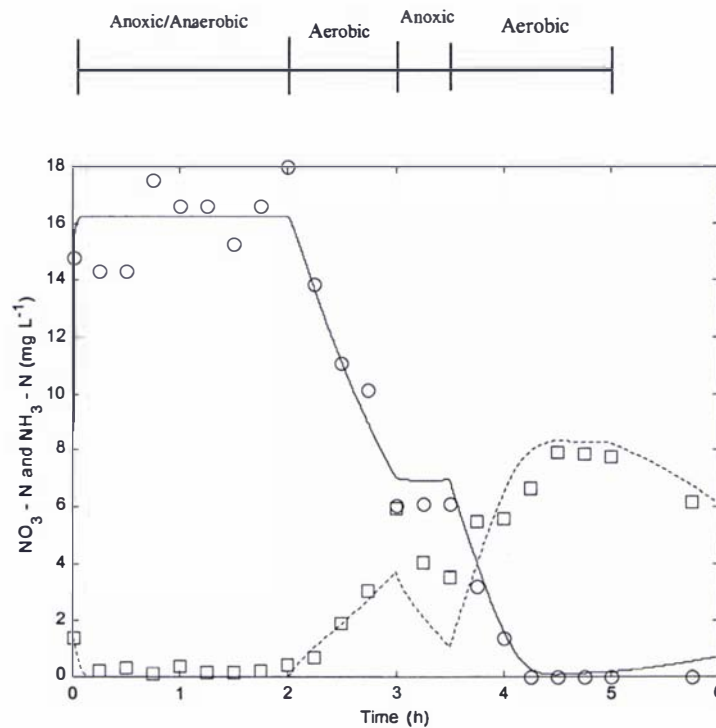


Figure 7.6 Simulated and experimental $\text{NH}_3 - \text{N}$ (—, ○) and $\text{NO}_3 - \text{N}$ (---, □) during the SBR cycle described in Section 6.3.1.1

7.2.3 Simulation of the SBR cycle described in Section 5.5

Using the calibrated ASM 1 model the experimental results described in Section 5.5 were simulated. Figure 7.7 shows the simulated and experimental $\text{NO}_3 - \text{N}$ and $\text{NH}_3 - \text{N}$ profiles. The simulated results in general are in good agreement with the experimental results. The simulated $\text{NO}_3 - \text{N}$ profile shows a steady increase during the first aerobic period. However the experimental $\text{NO}_3 - \text{N}$ increases at a slower rate. This was probably due to greater nitrogen removal by the simultaneous nitrification and denitrification (SND) process than in the calibration cycle during the first aerobic period. The model slightly over-predicted the $\text{NO}_3 - \text{N}$ during the second aerobic period. The over-predicted $\text{NO}_3 - \text{N}$ is almost equal to the over predicted removal of $\text{NH}_3 - \text{N}$ as shown in Figure 7.7 ($1.75 \text{ mg L}^{-1} \text{ NH}_3 - \text{N}$). The fast removal of $\text{NH}_3 - \text{N}$ in the simulated results could be due to the assumed step increase in the DO (from 0 to

3.75 mg L⁻¹) in the model, as in the experiment the DO increased gradually over a 0.17 h period.

The simulation results suggest that the selected kinetic and stoichiometric parameters for the modified ASM 1 simulation of meat processing wastewater treatment of the SBR are reasonably reliable.

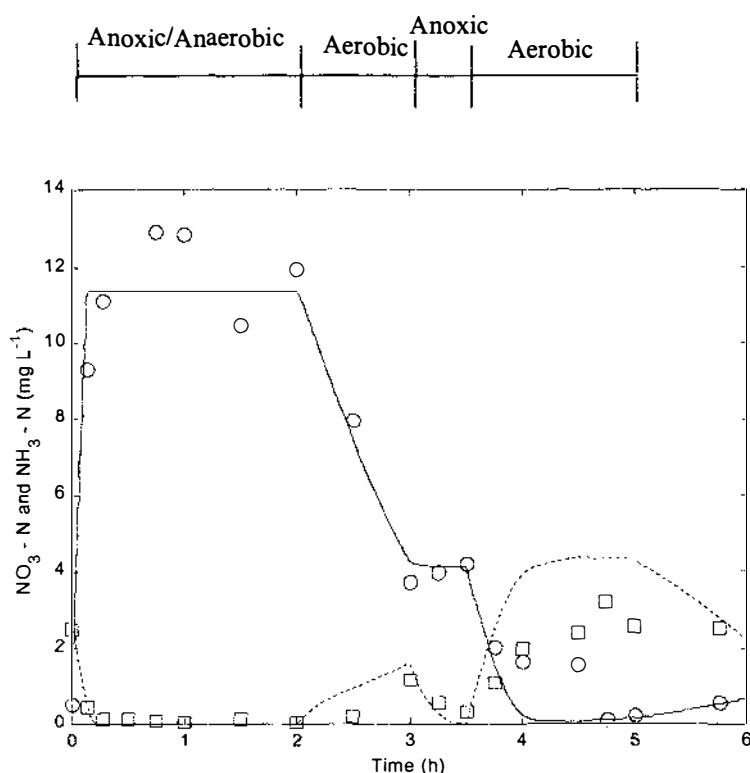


Figure 7.7 Simulated and experimental NH₃ – N (—, ○) and NO₃ – N (-----, □) of the SBR cycle described in Section 5.5

7.2.4 Sensitivity of the model parameters in ASM 1

Uncertainty in kinetic and stoichiometric experiments can lead to errors in simulating wastewater treatment. Since the parameters differ in their contribution to the model, error in each parameter will affect the simulation in a different way. A sensitivity analysis was performed, therefore, on the effect of varying several kinetic and stoichiometric parameters on simulated NH₃ – N and NO₃ – N. The sensitivity (s) of the parameters (p) with respect to the state variables, y (being effluent NH₃ – N and NO₃ – N) is a dimensionless number and was calculated as

$$s = \frac{\Delta y}{y} \cdot \frac{p}{\Delta p} \quad (7.4)$$

Where Δp is the change in the parameter value p , and Δy the change in the output y (Van Veldhuizen *et al.*, 1999).

In this study parameter values were changed by a factor of $\Delta p = \pm 0.2 p_{nom}$ to assess the sensitivity to the parameters in the effluent $\text{NH}_3 - \text{N}$ and $\text{NO}_3 - \text{N}$. Here, p_{nom} is the model parameter value. The parameters, which have high sensitivity (s) values are considered as more sensitive during the simulation of the effluent $\text{NH}_3 - \text{N}$ and $\text{NO}_3 - \text{N}$. Table 7.3 shows the more sensitive parameters and their sensitivity. The positive or negative numbers show an increase or decrease in the state variables when the parameters were perturbed.

Table 7.3 Sensitive kinetic and stoichiometric parameters of the ASM 1 model

Symbol	Units	Model value	Ammonia nitrogen		Oxidised nitrogen	
			-20 % model value	+20 % model value	-20 % model value	+20 % model value
Stoichiometric parameters						
Y_A	g COD (g N) ⁻¹	0.20	-0.3	0.3	-1.3	1.6
Y_H	g COD (g COD) ⁻¹	0.63	1.9	-1.6	2.1	0.7
i_{XB}	g N (g COD) ⁻¹ in biomass	0.086	-1.1	1.0	1.4	-1.3
Kinetic parameters						
K_{OH}	g O ₂ m ⁻³	0.20	0.0	0.0	1.1	-0.8
b_H	d ⁻¹	0.24	-1.0	1.0	0.2	-0.1
η_g	-	0.80	0.0	0.0	1.0	-0.6
η_h	-	0.40	-0.5	0.4	0.6	-0.4
$\hat{\mu}_A$	d ⁻¹	0.75	0.4	-0.3	2.1	-1.2
K_{OA}	g O ₂ m ⁻³	1.20	-0.2	0.2	-0.9	1.1

Table 7.3 shows that in this study both $\text{NH}_3 - \text{N}$ and $\text{NO}_3 - \text{N}$ were sensitive to the heterotrophic yield coefficient, and the $\text{NO}_3 - \text{N}$ is most sensitive to the autotrophic growth rate. Both of these parameters were determined from the experimental results. The heterotrophic decay coefficient has a significant effect on the effluent $\text{NH}_3 - \text{N}$, the value was adjusted during calibration to best fit the experimental results.

7.3 Activated Sludge Model No. 2 (ASM2)

7.3.1. ASM 2 model description

The ASM 2 model is an extension of the ASM 1 and overcomes most of the limitations in the ASM 1 (Gujer *et al.*, 1999; Henze *et al.*, 1995).

- ASM 1 does not include kinetic expressions, which can deal with the nutrient and alkalinity limitations of heterotrophic organisms.
- ASM 1 includes biodegradable soluble and particulate organic nitrogen as model components. These cannot easily be measured.
- The kinetics of ammonification in ASM 1 cannot really be quantified. This process is eliminated in the ASM 2 by assuming a constant composition of all organic components (constant N to COD ratio).
- ASM 1 differentiates inert particulate organic material depending on its origin, as either wastewater inflow or biomass decay. It is impossible, however, to differentiate these two fractions in reality.
- ASM 1 does not allow for the modelling of directly measurable mixed liquor suspended solids.

The ASM 2 is more complex and includes many more components, which are required in order to characterise the wastewater as well as the activated sludge. Additionally, more biological processes are included, primarily for phosphorus removal. In order to include biological phosphorus removal in the model, the biomass is considered to have internal stored components such as poly- β -hydroxyalkanoate (PHA) and polyphosphate (poly-P). An example of the relationship between MLSS, VSS, ash, storage compounds and active biomass is illustrated in Table 7.4 (Smolders *et al.*, 1995b). Activated Sludge Model No. 2 (ASM 2) (Henze *et al.*, 1995) also has some limitations.

The important limitations in the ASM 2 are

- Anoxic phosphorus uptake is not included
- Wastewater must contain sufficient Mg^{2+} and K^+

- Processes with overflow of substantial readily biodegradable substrate to the aerobic phase cannot be modelled
- It is assumed that there is no limitation of glycogen
- It is assumed that the pH remains near neutral
- Temperature is expected to be in the range of 10 – 25°C

Table 7.4 Composition of the biomass and the relation with MLSS and VSS

MLSS (100 %)								
VSS (80 %)					Ash (20 %)			
Active heterotrophs (51 %)	Bio-P (18 %)			Active autotrophs (3 %)	Inert organics (28 %)	Ash from active biomass (5-10 %)	Poly-P (25 - 35 %)	Inorganic (55 – 70 %)
	PHB (6 %)	Glycogen (25 %)	Active Bio-P (69 %)					

The anoxic phosphorous uptake and glycogen storage capability of Bio-P bacteria were later on included in Mino *et al.* (1995) sub-models. Important characteristics of Bio-P and their implication in ASM 2 are summarised below and graphically shown in Figure 7.8 (Mino *et al.*, 1995).

1. Under anaerobic conditions, Bio-P takes up organic substrates and synthesises PHA, with concurrent $\text{PO}_4 - \text{P}$ release as a result of poly-P degradation. Bio-Ps are supposed to prefer low molecular fatty acids like acetate (Wentzel *et al.*, 1985), and are modelled in the ASM 2 to take up only fermentation products (S_A).
2. Under aerobic conditions, Bio-P utilises PHA in the sludge as the energy and carbon source for their own growth and polyphosphate recovery. Therefore the PHA, which has been accumulated in the sludge during the preceding anaerobic phase, decreases and $\text{PO}_4 - \text{P}$ in the bulk solution is taken up by Bio-P. These aerobic processes are taken into account in the ASM 2.
3. There was an experimentally observed decrease in glycogen in the sludge under anaerobic conditions, and a recovery under aerobic conditions. These observations, imply that intracellular glycogen, which was analytically determined as glucose, is utilised for anaerobic PHA synthesis and that a part of the accumulated PHA can be converted to glycogen aerobically. Such a glycogen economy is not considered in the ASM 2.

4. The fact that $\text{PO}_4 - \text{P}$ is sometimes taken up in the sludge under anoxic conditions indicates that Bio-P has denitrification capability. Bio-P in ASM 2 is modelled to be unable to denitrify.

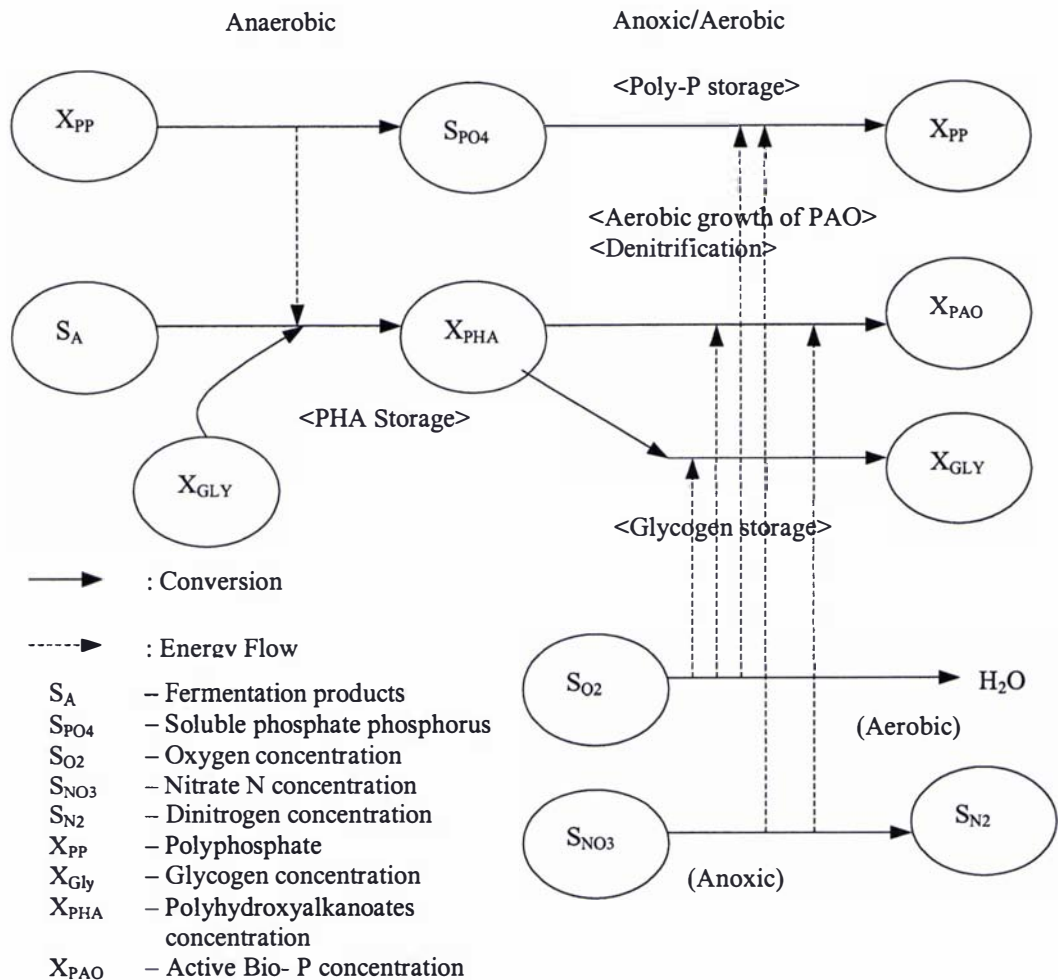


Figure 7.8 Metabolism of polyphosphate accumulating organisms (Mino *et al.*, 1995)

7.3.2 ASM 2 model modification

As discussed in Chapters V and VI, anoxic phosphorus uptake was observed in this study. In order to take into account these observations, four additional processes were included in the ASM 2 for anoxic phosphorus storage and glycogen storage capability of Bio-P from Mino's sub-models (Mino *et al.*, 1995). However, anoxic glycogen storage was not thought to be significant in this study and was not included in the modification.

Also the meat processing wastewater treatment showed a potential limitation of Mg^{2+} for the EBPR process, as discussed in Chapter VI. The effect of a limitation of

Mg^{2+} in meat processing wastewater treatment was taken into account by multiplying the aerobic and anoxic polyphosphate synthesis rates by a Monod type of saturation function, $\frac{S_{Mg}}{K_{Mg} + S_{Mg}}$, where S_{Mg} represents the soluble Mg^{2+} concentration and K_{Mg} , the half saturation constant (Ky *et al.*, 2001).

Table 7.5 shows the conversion factors, i_{ci} , to be applied in the continuity equations of modified ASM 2. Polyphosphates are assumed to have the composition of $(K_{0.33}Mg_{0.33}PO_3)_n$ in the ASM 2 model. Since the ASM 2 does not account for K^+ and Mg^{2+} , the charge factor of $-1/31$ is added in the conversion factor table (Henze *et al.*, 1999). Components X_{GLY} and S_{Mg} were also added in the ASM 2 conversion factor table as shown in Table 7.5. For the component Mg^{2+} , a charge factor of $+2/24$ is added in the conversion table. The complete process rate equations of the ASM 2 model and Mino's sub-models are shown in Table 7.6. Processes 11 and 12 were modified for Mg^{2+} limitation. Tables 7.7 – 7.11 show the stoichiometric coefficients for component i in process j . A continuity equation, which is valid for all processes j and all materials c subject to continuity, may be written as Equation 7.3 (Henze *et al.*, 1995).

$$\sum v_{ji} \cdot i_{ci} = 0 \text{ for over all components } i \quad (7.3)$$

Detailed descriptions of the components and the processes are given in Henze *et al.* (1995); Mino *et al.* (1995) and Henze *et al.* (1999).

In addition to the biological processes, the ASM 2 also includes two 'chemical processes' to model the chemical precipitation of phosphorus. However, as discussed in Chapters IV and VI, in meat processing wastewater chemical precipitation can be assumed to be negligible. Further, simultaneous precipitation of P via addition of iron or aluminium salts is not considered in this study, and hence the processes 20 and 21 are not included in the model. The pH in this study was near neutral and the temperature was in the range of $22 \pm 2^\circ C$.

The ASM 2 model with the additional processes added is hence hereinafter referred to as the *modified ASM 2 model*.

Table 7.5 Conversion factors i_{ci} to be applied in the continuity equations of the modified ASM 2 model. Missing values are equal to 0. The units of i_{ci} are $M_c M_i^{-1}$ (Henze *et al.*, 1999)

Index c: Continuity for			COD	N	P	Charge	Mass
Factor:			$I_{COD,i}$	$i_{N,i}$	$i_{P,i}$	$i_{Charge,i}$	$i_{TSS,i}$
I	Component	Units	g COD	g N	g P	Mole ⁺	g TSS
1	S_{O_2}	g O ₂	-1				
2	S_F	g COD	1	i_{NSF}	i_{PSF}		
3	S_A	g COD	1			-1/64	
4	S_{NH_4}	g N		1		+1/14	
5	S_{NO_3}	g N	-64/14	1		-1/14	
6	S_{PO_4}	g P			1	-1.5/31	
7	S_I	g COD	1	i_{NSI}	i_{PSI}		
8	S_{ALK}	Mole HCO ₃ ⁻				-1	
9	S_{N_2}	g N	-24/14	1			
10	X_I	g COD	1	i_{NXI}	i_{PXI}		i_{TSSXI}
11	X_S	g COD	1	i_{NXS}	i_{PXS}		i_{TSSXS}
12	X_H	g COD	1	i_{NBM}	i_{PBM}		i_{TSSBM}
13	X_{PAO}	g COD	1	i_{NBM}	i_{PBM}		i_{TSSBM}
14	X_{PP}	g P			1	-1/31 ^{b)}	3.23
15	X_{PHA}	g COD	1				0.6
16	X_{AUT}	g COD	1	i_{NBM}	i_{PBM}		i_{TSSBM}
17	X_{TSS}	g TSS					-1 ^{a)}
18	X_{MeOH}	g TSS					1
19	X_{MeP}	g TSS			0.205		1
20	X_{GLY}	g COD	1				0.84
21	S_{Mg}	g Mg				+2/24	

Note: a) Since TSS is counted twice this factor must be negative.

b) Since the ASM 2 does not account for K⁺ and Mg²⁺ this factor must compensate for their charge.

Nomenclature:

S_A	Fermentation products (mg COD L ⁻¹)
S_{ALK}	Alkalinity of the wastewater (mol HCO ₃ L ⁻¹)
S_F	Fermentable, readily biodegradable organic substrates (mg COD L ⁻¹)
S_I	Inert soluble organic material (mg COD L ⁻¹)
S_{N_2}	Dinitrogen (mg N L ⁻¹)
S_{NH_4}	Ammonium plus ammonia nitrogen (mg N L ⁻¹)
S_{NO_3}	Nitrate plus 0.6 times the nitrite nitrogen (mg N L ⁻¹)
S_{O_2}	Dissolved oxygen (mg O ₂ L ⁻¹)
S_{PO_4}	Inorganic soluble phosphorus (mg P L ⁻¹)
S_{Mg}	soluble magnesium concentration (mg Mg L ⁻¹)
X_{AUT}	Nitrifying organisms (mg COD L ⁻¹)
X_H	Heterotrophic organisms (mg COD L ⁻¹)
X_I	Inert particulate organic material (mg COD L ⁻¹)
X_{PAO}	Phosphate accumulating organisms (mg COD L ⁻¹)
X_{PHA}	A cell internal storage product of Bio-P (mg COD L ⁻¹)
X_{PP}	Polyphosphate (mg P L ⁻¹)
X_S	Slowly biodegradable substrates (mg COD L ⁻¹)
X_{TSS}	Total suspended solids (mg TSS L ⁻¹)
X_{Gly}	A cell internal storage product of Bio-P (mg COD L ⁻¹)
i_{NSF}	N content of fermentable substrate S_F , gN(g COD) ⁻¹
i_{NSI}	N content of inert soluble COD S_I , gN(g COD) ⁻¹
i_{NXI}	N content of inert particulate COD X_I , gN(g COD) ⁻¹

i_{NXS}	N content of slowly biodegradable substrate X_S , $\text{gN}(\text{g COD})^{-1}$
i_{NBM}	N content of biomass X_H, X_{PAO}, X_{AUT} , $\text{gN}(\text{g COD})^{-1}$
i_{PSF}	P content of fermentable substrate S_F , $\text{gP}(\text{g COD})^{-1}$
i_{PSI}	P content of inert soluble COD S_i , $\text{gP}(\text{g COD})^{-1}$
i_{PXI}	P content of inert particulate COD X_i , $\text{gP}(\text{g COD})^{-1}$
i_{PXS}	P content of slowly biodegradable substrate X_S , $\text{gP}(\text{g COD})^{-1}$
i_{PBM}	P content of biomass X_H, X_{PAO}, X_{AUT} , $\text{gP}(\text{g COD})^{-1}$
i_{TSSXI}	TSS to X_i ratio, $\text{gTSS}(\text{g COD})^{-1}$
i_{TSSXS}	TSS to X_S ratio, $\text{gTSS}(\text{g COD})^{-1}$
i_{TSSBM}	TSS to biomass ratio for X_H, X_{PAO}, X_{AUT} , $\text{gTSS}(\text{g COD})^{-1}$

Table 7.6 Process rate equations (Henze *et al.*, 1995; Mino *et al.*, 1995)

	Process	Process rate equation ρ_j $\rho_j > 0$ [ML ⁻³ T ⁻¹]
Hydrolysis Processes:		
1	Aerobic hydrolysis	$K_h \frac{S_{O_2}}{K_{O_2} + S_{O_2}} \frac{X_S/X_H}{K_X + X_S/X_H} \cdot X_H$
2	Anoxic hydrolysis	$K_h \cdot \eta_{NO_3H} \frac{K_{O_2}}{K_{O_2} + S_{O_2}} \frac{S_{NO_3}}{K_{NO_3} + S_{NO_3}} \frac{X_S/X_H}{K_X + X_S/X_H} \cdot X_H$
3	Anaerobic hydrolysis	$K_h \cdot \eta_{fe} \frac{K_{O_2}}{K_{O_2} + S_{O_2}} \frac{K_{NO_3}}{K_{NO_3} + S_{NO_3}} \frac{X_S/X_H}{K_X + X_S/X_H} \cdot X_H$
Heterotrophic organisms: X_H		
4	Growth on fermentable Substrates, S_F	$\mu_h \cdot \frac{S_{O_2}}{K_{O_2} + S_{O_2}} \cdot \frac{S_F}{K_F + S_F} \cdot \frac{S_F}{S_F + S_A} \cdot \frac{S_{NH_4}}{K_{NH_4} + S_{NH_4}} \cdot \frac{S_{PO_4}}{K_P + S_{PO_4}} \cdot \frac{S_{ALK}}{K_{ALK} + S_{ALK}} \cdot X_H$
5	Growth on fermentation products, S_A	$\mu_h \frac{S_{O_2}}{K_{O_2} + S_{O_2}} \frac{S_A}{K_A + S_A} \frac{S_A}{S_F + S_A} \frac{S_{NH_4}}{K_{NH_4} + S_{NH_4}} \frac{S_{PO_4}}{K_P + S_{PO_4}} \frac{S_{ALK}}{K_{ALK} + S_{ALK}} \cdot X_H$
6	Denitrification with Fermentable substrates, S_F	$\mu_h \cdot \eta_{NO_3} \frac{K_{O_2}}{K_{O_2} + S_{O_2}} \frac{S_{NO_3}}{K_{NO_3} + S_{NO_3}} \frac{S_F}{K_F + S_F} \frac{S_F}{S_F + S_A} \frac{S_{NH_4}}{K_{NH_4} + S_{NH_4}} \frac{S_{PO_4}}{K_P + S_{PO_4}} \frac{S_{ALK}}{K_{ALK} + S_{ALK}} \cdot X_H$
7	Denitrification with fermentation products, S_A	$\mu_h \cdot \eta_{NO_3} \frac{K_{O_2}}{K_{O_2} + S_{O_2}} \frac{S_{NO_3}}{K_{NO_3} + S_{NO_3}} \frac{S_A}{K_A + S_A} \frac{S_A}{S_F + S_A} \frac{S_{NH_4}}{K_{NH_4} + S_{NH_4}} \frac{S_{PO_4}}{K_P + S_{PO_4}} \frac{S_{ALK}}{K_{ALK} + S_{ALK}} \cdot X_H$
8	Fermentation	$q_{fe} \frac{K_{O_2}}{K_{O_2} + S_{O_2}} \frac{K_{NO_3}}{K_{NO_3} + S_{NO_3}} \frac{S_F}{K_F + S_F} \frac{S_{ALK}}{K_{ALK} + S_{ALK}} \cdot X_H$
9	Lysis	$b_H \cdot X_H$
Phosphorus accumulating organisms (PAO): X_{PAO}		
10	Storage of X_{PHA}	$q_{PHA} \frac{S_A}{K_A + S_A} \frac{S_{ALK}}{K_{ALK} + S_{ALK}} \frac{X_{PP}/X_{PAO}}{K_{PP} + X_{PP}/X_{PAO}} \frac{X_{Gly}/X_{PAO}}{K_{Gly} + X_{Gly}/X_{PAO}} \cdot X_{PAO}$
11	Aerobic storage of X_{PP}	$q_{PP} \frac{S_{O_2}}{K_{O_2} + S_{O_2}} \frac{S_{PO_4}}{K_{PS} + S_{PO_4}} \frac{S_{ALK}}{K_{ALK} + S_{ALK}} \frac{X_{PHA}/X_{PAO}}{K_{PHA} + X_{PHA}/X_{PAO}} \frac{K_{MAX} - X_{PP}/X_{PAO}}{K_{IPP} + K_{MAX} - X_{PP}/X_{PAO}} \frac{S_{Mg}}{K_{Mg} + S_{Mg}} \cdot X_{PAO}$
12	Anoxic storage of X_{PP}	$\rho_{12} = \rho_{11} \cdot \eta_{NO_3P} \frac{K_{O_2}}{S_{O_2}} \frac{S_{NO_3}}{K_{NO_3} + S_{NO_3}}$
13	Aerobic growth on X_{PHA}	$\mu_{PAO} \frac{S_{O_2}}{K_{O_2} + S_{O_2}} \frac{S_{NH_4}}{K_{NH_4} + S_{NH_4}} \frac{S_{PO_4}}{K_P + S_{PO_4}} \frac{S_{ALK}}{K_{ALK} + S_{ALK}} \frac{X_{PHA}/X_{PAO}}{K_{PHA} + X_{PHA}/X_{PAO}} \cdot X_{PAO}$
14	Anoxic growth on X_{PHA}	$\rho_{14} = \rho_{13} \cdot \eta_{NO_3P} \frac{K_{O_2}}{S_{O_2}} \frac{S_{NO_3}}{K_{NO_3} + S_{NO_3}}$
15	Lysis of X_{PAO}	$b_{PAO} \frac{S_{ALK}}{K_{ALK} + S_{ALK}} \cdot X_{PAO}$
16	Lysis of X_{PP}	$b_{PP} \frac{S_{ALK}}{K_{ALK} + S_{ALK}} \cdot X_{PP}$
17	Lysis of X_{PHA}	$b_{PHA} \frac{S_{ALK}}{K_{ALK} + S_{ALK}} \cdot X_{PHA}$
22	Glycogen storage	$q_{Gly} \frac{S_{O_2}}{K_{O_2} + S_{O_2}} \frac{X_{PHA}/X_{PAO}}{K_{PHAGly} + X_{PHA}/X_{PAO}} \cdot X_{PAO}$
23	Lysis X_{Gly}	$b_{Gly} \frac{S_{ALK}}{K_{ALK} + S_{ALK}} \cdot X_{Gly}$
Nitrifying organisms (autotrophic organisms) : X_{AUT}		
18	Aerobic growth of X_{AUT}	$\mu_{AUT} \frac{S_{O_2}}{K_{O_2AUT} + S_{O_2}} \frac{S_{NH_4}}{K_{NH_4AUT} + S_{NH_4}} \frac{S_{PO_4}}{K_P + S_{PO_4}} \frac{S_{ALK}}{K_{ALKAUT} + S_{ALK}} \cdot X_{AUT}$
19	Lysis of X_{AUT}	$b_{AUT} \cdot X_{AUT}$
Simultaneous precipitation of phosphorus with ferric hydroxide Fe(OH)₃		
20	Precipitation	$k_{PRE} \cdot S_{PO_4} \cdot X_{MeOH}$
21	Redissolution	$k_{RED} \cdot X_{MeP} \frac{S_{ALK}}{K_{ALKRED} + S_{ALK}}$

Table 7.7 Stoichiometry of hydrolysis processes

	Process	S _F	S _{NH4}	S _{PO4}	S _I	S _{ALK}	X _S	X _{TSS}
1	Aerobic hydrolysis	1-f _{SI}	0.01	0.0	f _{SI}	0.001	-1	-0.75
2	Anoxic hydrolysis	1-f _{SI}	0.01	0.0	f _{SI}	0.001	-1	-0.75
3	Anaerobic hydrolysis	1-f _{SI}	0.01	0.0	f _{SI}	0.001	-1	-0.75

Table 7.8 Stoichiometry of the facultative heterotrophic organisms X_H

	Process	S _{O2}	S _F	S _A	S _{NH3}	S _{N2}	X _I	X _S	X _H	S _{NH4}	S _{PO4}	S _{ALK}	X _{TSS}
4	Aerobic growth on S _F	$1 - \frac{1}{Y_H}$	$-\frac{1}{Y_H}$						1	-0.022	-0.004	-0.001	0.9
5	Aerobic growth on S _A	$1 - \frac{1}{Y_H}$		$-\frac{1}{Y_H}$					1	-0.07	-0.02	0.021	0.9
6	Anoxic growth on S _F		$-\frac{1}{Y_H}$		$-\frac{1 - Y_H}{2.86 \cdot Y_H}$	$\frac{1 - Y_H}{2.86 \cdot Y_H}$			1	-0.022	-0.004	0.013	0.9
7	Anoxic growth on S _A			$-\frac{1}{Y_H}$	$-\frac{1 - Y_H}{2.86 \cdot Y_H}$	$\frac{1 - Y_H}{2.86 \cdot Y_H}$			1	-0.07	-0.02	0.035	0.9
8	Fermentation		-1	1						0.03	0.01	-0.014	
9	Lysis						f _{XI}	1-f _{XI}	-1	0.032	0.01	0.002	-0.15

Table 7.9 Stoichiometry of the phosphorus accumulating organisms, PAO

	Process	S _F	S _{O2}	S _A	S _{N2}	S _{NO3}	S _{PO4}	X _I	X _S	X _{PAO}	X _{PP}	X _{PHA}	X _{GLY}	S _{Mg}	S _{ALK}	X _{TSS}	S _{NH4}
10	Storage of X _{PHA}			-Y _{SA}			Y _{PO4}				-Y _{PO4}	1	-(1-Y _{SA})	Y _{MgPHA}	0.011	-0.735	
11	Aerobic storage of X _{PP}		-Y _{PHA}				-1				1	-Y _{PHA}		-Y _{MgXPP}	0.003	3.11	
12	Anoxic storage of X _{PP}				$\frac{Y_{PHA}}{2.86}$	$-\frac{Y_{PHA}}{2.86}$	-1				1	-Y _{PHA}		-Y _{MgXPP}	0.008	3.11	
13	Aerobic growth of X _{PAO}		$1 - \frac{1}{Y_{PAO}}$				-i _{PBM}			1		$-\frac{1}{Y_{PAO}}$			-0.004	-0.052	-0.07
14	Anoxic growth of X _{PAO}				$\frac{(1-Y_{PAO})}{2.86Y_{PAO}}$	$-\frac{(1-Y_{PAO})}{2.86Y_{PAO}}$	-i _{PBM}			1		$-\frac{1}{Y_{PAO}}$			0.011	-0.052	-0.07
15	Lysis of X _{PAO}						0.01	f _{XI}	1-f _{XI}	-1					0.002	-0.15	0.032
16	Lysis of X _{PP}						1				-1			Y _{MgXPP}	-0.003	-3.23	
17	Lysis of X _{PHA}			1								-1			-0.016	-0.6	
22	Storage of X _{GLY}											-1	1			0.24	
23	Lysis of X _{GLY}	1											-1			-0.84	

Table 7.10 Stoichiometry of the growth and decay processes of nitrifying organisms X_{AUT}

	Process	S _{O2}	S _{NH4}	S _{NO3}	S _{PO4}	X _I	X _S	X _{AUT}	S _{ALK}	X _{TSS}
18	Aerobic growth of X _{AUT}	$\frac{4.57-Y_{AUT}}{Y_{AUT}}$	-5.07	$\frac{1}{Y_{AUT}}$	-i _{PBM}			1	-0.718	0.9
19	Lysis		0.032		0.01	f _{XI}	1-f _{XI}	-1	0.002	-0.15

Table 7.11 Stoichiometry of the processes describing simultaneous precipitation of phosphorus

	Process	S _{PO4}	S _{ALK}	X _{MeOH}	X _{MeP}	X _{TSS}
20	Precipitation	-1	0.048	-3.45	4.87	1.42
21	Redissolution	1	-0.048	3.45	-4.87	-1.42

7.3.3 Calibration of the modified ASM 2

The kinetic and stoichiometric coefficients for carbon and nitrogen removal were the same as those used in the ASM 1 model. For modelling the P removal the kinetic parameters were best fitted to the experimental results of the SBR cycle described in Section 6.3.1.1 during calibration using the modified ASM 2 model. The stoichiometric parameters for the modelling of P removal were obtained from the acetate batch study (Trial II) described in Section 6.3.1.3.

Stoichiometric and kinetic parameters : Table 7.12 shows the definition and values of the stoichiometric and kinetic parameters used in the model for this study, compared to the default values in the ASM 2d model (Henze *et al.*, 1999). The numbers given in bold type are those that are different from the default parameters in ASM 2d. The stoichiometric coefficients of components S_A , X_{PHA} , and S_{PO_4} used in the model were determined from the acetate batch study (Trial II, Section 6.3.1.3) as discussed in Chapter VI. The PHA requirement for poly-P storage was taken as the default value in the ASM 2d model. Parameters related to the component X_{GLY} were taken from Mino *et al.* (1995). The value for K_{Mg} was determined as 4.7 mg L^{-1} as discussed in Chapter VI. The yield of Mg^{2+} during PHA and poly-P storage was calculated from the Mg^{2+} to $PO_4 - P$ molar ratio of 0.21 found during the anaerobic period (Section 6.4 in Chapter VI). The autotrophic yield coefficient, the anoxic hydrolysis reduction factor, and the rate coefficient for lysis of heterotrophs and autotrophs were all the same as those obtained from the ASM 1 model calibration. The heterotrophic saturation coefficient for substrates S_F and S_A was taken as the same as the K_S value found in this study (Table 7.12).

The rate constant value for poly-P storage, the rate constant value for PHA storage, the saturation coefficient for fermentation, the anaerobic hydrolysis reduction factor, and the saturation coefficients for oxygen to heterotrophic biomass were obtained by fitting to the experimental results of the SBR cycle described in Section 6.3.1.1. However they are within the values given in the literature (Brenner, 2000; Cinar *et al.*, 1998; Henze *et al.*, 1987a; Wentzel *et al.*, 1992). To simulate the $NO_3 - N$ during the settling period, anoxic hydrolysis was assumed to be negligible during the settling period. However, it is difficult to model this phenomenon, due to the complex nature of the hindered and/or compression settling of sludge (Kazmi *et al.*, 2001).

Table 7.12 Parameters definition and values used in the modified ASM 2 model for meat processing wastewater

Symbol	Parameter	Default valueASM 2d	Model value
Stoichiometric parameters			
Hydrolysis			
f_{SI}	Production of S_I in hydrolysis	0	0
Heterotrophic biomass: X_H			
Y_H	Yield coefficient, g COD (g COD) ⁻¹	0.625	0.63
F_{XI}	Fraction of inert COD generated in biomass lysis	0.10	0.10
Phosphorus accumulating organisms: X_{PAO}			
Y_{PAO}	Yield coefficient (biomass/PHA), g COD (g COD) ⁻¹	0.625	0.63
Y_{PO4}	PO4 release per PHA stored, g P (g COD) ⁻¹	0.40	0.33
Y_{PHA}	PHA requirement for PP storage, g COD (g P) ⁻¹	0.20	0.2
f_{XI}	Fraction of inert COD generated in biomass lysis	0.10	0.10
Y_{SA}	S_A requirement for PHA storage, g COD (g COD) ⁻¹		0.68
Y_{MgPHA}	Yield of magnesium during PHA storage g Mg (g COD) ⁻¹		0.065
Y_{MgPXP}	Yield of magnesium during PP storage g Mg (g P) ⁻¹		0.163
Nitrifying organisms: X_{AUT}			
Y_A	Yield of autotrophic biomass per NO ₃ -N, g COD (g N) ⁻¹	0.24	0.20
f_{XI}	Fraction of inert COD generated in biomass lysis	0.10	0.10
Kinetic parameters			
Hydrolysis of particulate substrate: X_S			
K_h	Hydrolysis rate constant, d ⁻¹	3.00	3.00
η_{NO3}	Anoxic hydrolysis reduction factor	0.60	0.40
η_{fe}	Anaerobic hydrolysis reduction factor	0.40	0.02
K_{O2}	Saturation/inhibition coefficient for oxygen, g O ₂ m ⁻³	0.20	0.50
K_{NO3}	Saturation/ inhibition coefficient for nitrate, g N m ⁻³	0.50	0.50
K_X	Saturation coefficient for particulate COD, g X _S (g X _H) ⁻¹	0.10	0.10
Heterotrophic organisms: X_H			
μ_H	Maximum growth rate on substrate, g X _S (g X _H d) ⁻¹	6.00	2.0
q_{fe}	Maximum rate for fermentation, g S _F (g X _H d) ⁻¹	3.00	3.00

Table 7.12 Parameters definition and values used in the modified ASM 2 model for meat processing wastewater (continued)

Symbol	Parameter	Default valueASM 2d	Model value
Kinetic parameters			
Heterotrophic organisms: X_H			
η_{NO3}	Reduction factor for denitrification	0.80	0.80
b_H	Rate constant for lysis and decay, d^{-1}	0.40	0.24
K_{O2}	Saturation/inhibition coefficient for oxygen, $g O_2 m^{-3}$	0.20	0.50
K_F	Saturation coefficient for growth on S_F , $g COD m^{-3}$	4.00	8.00
K_{fp}	Saturation coefficient for fermentation, $g COD m^{-3}$	4.00	8.00
K_A	Saturation coefficient for growth on acetate, S_A , $g COD m^{-3}$	4.00	8.00
K_{NO3}	Saturation/ inhibition coefficient for nitrate, $g N m^{-3}$	0.50	0.50
K_{NH4}	Saturation coefficient for ammonium, $g N m^{-3}$	0.05	0.05
K_P	Saturation coefficient for phosphate (nutrient), $g P m^{-3}$	0.01	0.01
K_{ALK}	Saturation coefficient for alkalinity (HCO_3), $mol HCO_3 m^{-3}$	0.10	0.10
Phosphorus accumulating organisms: X_{PAO}			
q_{PHA}	Rate constant for storage of X_{PHA} (base X_{PP}), $g X_{PHA} (g X_{PAO} d)^{-1}$	3.00	6.00
q_{PP}	Rate constant for storage of X_{PP} , $g X_{PP} (g X_{PAO} d)^{-1}$	1.50	2.00
μ_{PAO}	Maximum growth rate of PAO, d^{-1}	1.00	1.00
η_{NO3}	Reduction factor for anoxic activity	0.60	0.60
b_{PAO}	Rate for lysis of X_{PAO} , d^{-1}	0.20	0.20
b_{PP}	Rate for lysis of X_{PP} , d^{-1}	0.20	0.20
b_{PHA}	Rate for lysis of X_{PHA} , d^{-1}	0.20	0.20
K_{O2}	Saturation/inhibition coefficient for oxygen, $g O_2 m^{-3}$	0.20	0.20
K_{NO3}	Saturation/inhibition coefficient for nitrate, $g N m^{-3}$	0.50	0.50
K_A	Saturation coefficient for acetate, S_A , $g COD m^{-3}$	4.00	8.00
K_{NH4}	Saturation coefficient for ammonium, $g N m^{-3}$	0.05	0.05
K_{PS}	Saturation coefficient for phosphorus in storage of PP, $g P m^{-3}$	0.20	0.20
K_P	Saturation coefficient for phosphate, $g P m^{-3}$	0.01	0.01
K_{ALK}	Saturation coefficient for alkalinity (HCO_3), $mol HCO_3 m^{-3}$	0.10	0.10
K_{PP}	Saturation coefficient for polyphosphate, $g X_{PP} (g X_{PAO})^{-1}$	0.01	0.01

Table 7.12 Parameters definition and values used in the modified ASM 2 model for meat processing wastewater (continued)

Symbol	Parameter	Default valueASM 2d	Model value
Kinetic parameters			
Phosphorus accumulating organisms: X_{PAO}			
K_{MAX}	Maximum ratio of X_{PP}/X_{PAO} , g X_{PP} (g X_{PAO}) ⁻¹	0.34	0.34
K_{IPP}	Inhibition coefficient for polyphosphate storage, g X_{PP} (g X_{PAO}) ⁻¹	0.02	0.02
K_{PHA}	Saturation coefficient for PHA, g X_{PHA} (g X_{PAO}) ⁻¹	0.01	0.01
q_{GLY}	Rate constant for glycogen storage, g X_{GLY} COD (g X_{PAO} COD d) ⁻¹		3.00
K_{GLY}	Saturation coefficient for X_{GLY} , g X_{GLY} COD (g X_{PAO} COD) ⁻¹		0.01
K_{PHAGLY}	Saturation coefficient for X_{PHA} for X_{GLY} storage, g COD (g X_{PAO} COD) ⁻¹		0.10
b_{GLY}	Rate of lysis of X_{GLY} , d ⁻¹		0.20
K_{Mg}	Mg saturation constant, g Mg m ⁻³		4.7
Nitrifying organisms : X_{AUT}			
μ_{AUT}	Maximum growth rate of X_{AUT} , d ⁻¹	1.00	0.75
b_{AUT}	Decay rate of X_{AUT} , d ⁻¹	0.15	0.10
K_{O_2}	Saturation coefficient for oxygen, g O ₂ m ⁻³	0.50	0.50
K_{NH_4}	Saturation coefficient for ammonium (substrate), g N m ⁻³	1.00	1.00
K_{ALK}	Saturation coefficient for alkalinity (HCO ₃), mol HCO ₃ m ⁻³	0.50	0.50
K_P	Saturation coefficient for phosphorus, g P m ⁻³	0.01	0.01

Active Bio-P was assumed to be 12.5 % of the total VSS in the model simulation corresponding to the sludge P content of 4 – 5 % of VSS (Orhon & Artan, 1994). In the ASM 2 the RBCOD is subdivided into fermented COD and rapidly fermentable COD. As discussed in Chapter IV, the RBCOD in meat processing wastewater employed in this study contained mostly SCFA COD and was assumed to be equivalent to SCFA COD in the model simulation. The biomass fractions in the wastewater were assumed to be negligible compared to the reactor biomass concentrations. TSS was assumed to be the amount measured using GF/C filter papers as discussed in Chapter IV. This amount of TSS might be lower than the actual TSS defined in the ASM 2 (Henze *et al.*, 1995).

The code for the ASM 2 model was written in Matlab 5.3 (The Math Works, Natick, MA, USA). The equations were solved using the Matlab function “ode45” for ordinary differential equations systems. Codes for the script and function files in Matlab 5.3 are given in Appendix D.

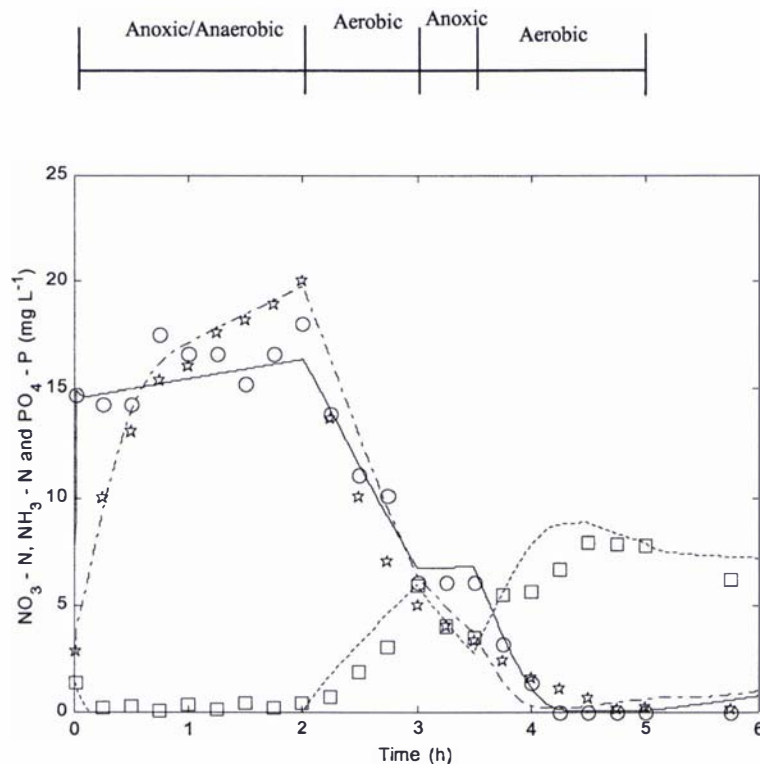


Figure 7.9 Simulated and experimental NH₃-N (—, ○), NO₃-N (----, □) and PO₄-P (- - -, ☆) during the SBR cycle described in Section 6.3.1.1

The wastewater characteristics used for calibrating the SBR cycle are described in Section 6.3.1.1 and Appendix D. A good calibration was possible for the $\text{NH}_3 - \text{N}$, $\text{NO}_3 - \text{N}$ and $\text{PO}_4 - \text{P}$ profiles (Figure 7.9). The experimental results show a faster and slower uptake of P during the first and second aerobic periods respectively than predicted by the calibrated model. This indicates that for P uptake the Bio-P has more affinity to DO at low DO levels than at high DO levels.

For the SBR cycle used for calibration and described in Section 6.3.1.1, the PHA, glycogen, Mg^{2+} and SCFA COD were simulated using the modified ASM 2 model after calibration. The results are discussed below.

PHA and glycogen

In Figure 7.10 the predicted polyhydroxyalkanoate (PHA) and glycogen COD profiles are compared to the experimental results. The overall shape of the simulated PHA COD profile of the SBR cycle is in agreement with the observed PHA COD profile. The PHA COD concentration during the anaerobic period, however, was somewhat over-predicted. Glycogen and PHA, other than PHB and PHV that were not measured in the experiment, may account for this (Henze *et al.*, 1995; Satoh *et al.*, 1992). Also, at the end of aerobic periods, the consumption of PHA COD was over-predicted as there was no PHA left in the simulation, while in the experiment PHA COD was 14.1 mg L^{-1} remained (5.1 mg L^{-1} of PHA COD per g VSS). This is probably due to the Bio-P bacteria, which utilise glycogen instead of PHA during the aerobic period for poly-P storage (Nakamura *et al.*, 1991; Mino *et al.*, 1998). This explanation is supported by the observation that the experimental glycogen COD was lower than the simulated glycogen COD during this aerobic period (Figure 7.10). This PHA COD may not be available for P uptake or growth of Bio-P. Brdjanovic *et al.* (1998b) and Temmink *et al.* (1996) also reported minimum PHA COD concentrations of 2.11 and $2.5 \text{ mg COD per g VSS}$, during a long period of aeration at the starvation condition. These values are lower than the amount determined in this study (5.1 mg L^{-1} of PHA COD per g VSS).

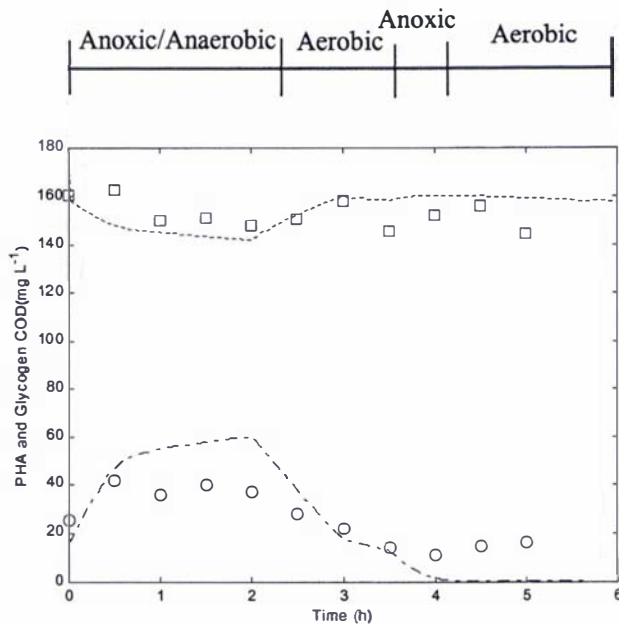


Figure 7.10 Simulated and experimental PHA COD (--- , ○) and glycogen COD (----, □) during the SBR cycle described in Section 6.3.1.1

The results shown in Figure 7.10 show good agreement between the experimental and simulated glycogen COD during the anoxic/anaerobic period and the first aerobic period. The experimental results after 0.5 h show an increase of glycogen but the simulated results do not reflect this. During the anoxic and the final aerobic periods, the model over-predicted the stored glycogen COD compared to the experimental glycogen COD. A possible explanation is that the glycogen was utilised for providing reducing power during the anoxic period (less than 5 mg L⁻¹ of NO₃ – N being present at the time). A second, and more likely, explanation is that the glycogen was utilised for P uptake (Nakamura *et al.*, 1991; Mino *et al.*, 1998). A third possible reason could be that the glycogen was utilised for cell maintenance (Brdjanovic *et al.*, 1998b).

Magnesium and SCFA COD

Figure 7.11 shows the simulated and the experimental results of PO₄ – P, SCFA COD and the Mg²⁺ profiles during the cycle. The model simulated these reasonably well. The higher Mg²⁺ concentration in the first two samples in the experiment could be due to solubilisation of magnesium calcium carbonate from the mixed liquor or errors in Mg²⁺ concentration determination. The simulated SCFA COD concentration is lower than the experimental results from 1 to 2 h. This could be because the ASM 2 model does not account for the acetic acid COD (HAc COD) not utilised by Bio-P bacteria (Satoh *et al.*, 2000). Another simple reason for the deviation between the experimental

and simulated results could be the wider calibration range of $0 - 500 \text{ mg L}^{-1}$ HAc used during the HAc analysis.

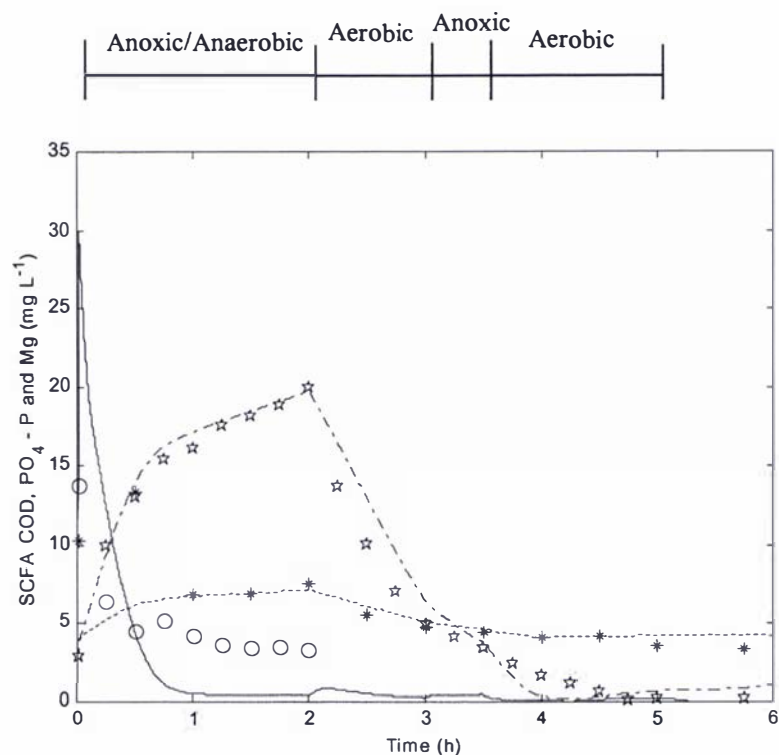


Figure 7.11 Simulated and experimental $\text{PO}_4\text{-P}$ (---, ☆), Mg^{2+} (-----, *) and SCFA COD (—, ○) during the SBR cycle described in Section 6.3.1.1

7.3.4 Simulation of the batch test with wastewater

The results of the batch test carried out using the wastewater (Section 6.3.1.2) were simulated using the modified ASM 2 model after its calibration. The characteristics of the wastewater and the initial conditions for the model simulation are described in Section 6.3.1.2 and Appendix D.

Figure 7.12 shows the simulated and the experimental results for $\text{PO}_4\text{-P}$, $\text{NO}_3\text{-N}$ and $\text{NH}_3\text{-N}$. The simulations mirror closely the results obtained experimentally.

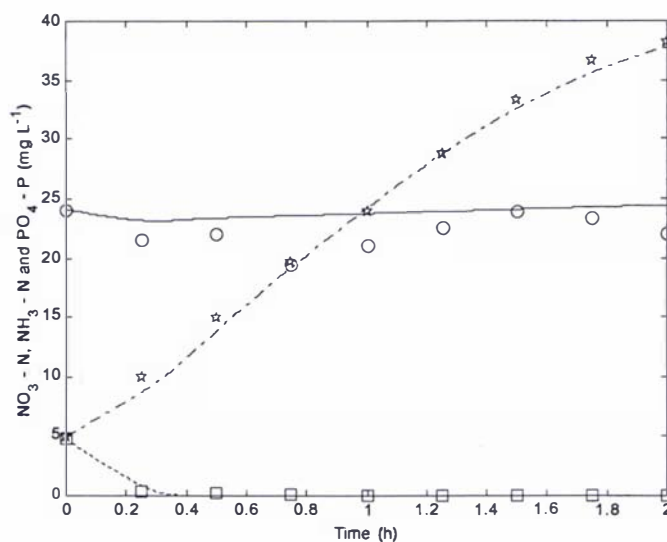


Figure 7.12 Simulated and experimental $\text{NH}_3\text{-N}$ (—, ○), $\text{NO}_3\text{-N}$ (----, □) and $\text{PO}_4\text{-P}$ (- - -, ☆) of batch test with wastewater

Figure 7.13 shows the simulated and experimental SCFA COD, $\text{PO}_4\text{-P}$ and Mg^{2+} data for the same batch test. The experimental soluble Mg^{2+} concentration profile was well predicted by the model. The simulated SCFA COD profile shows a continuous decrease in concentration throughout the two-hour period. In contrast, the experimental results show a rapid decrease during the first hour, with a stable concentration in the second hour (Monod saturation kinetics). The difference between the two could be due to some of the SCFA not being utilised by Bio-P bacteria. The ASM 2 model does not account for the unutilised SCFA COD by Bio-P bacteria. It could also be partly due to the poly-P limitation in the Bio-P bacteria.

In Figure 7.14 the simulated PHA COD is compared to the experimental PHA COD. The experimental PHA COD concentration shows an increase during the first hour. It then reached a plateau, while the simulated results show a continuous increase and a higher PHA COD concentration at the end of the anaerobic period. This difference could be due to the over-predicted consumption of SCFA COD, as shown in Figure 7.13. Other possible reasons for discrepancies between predicted and experimental SCFA COD results were discussed in Section 7.3.3.

The experimental glycogen COD was higher than the simulated glycogen COD, which could be due to uptake of carbohydrate from the wastewater by Bio-P bacteria, as discussed in Section 7.3.3.

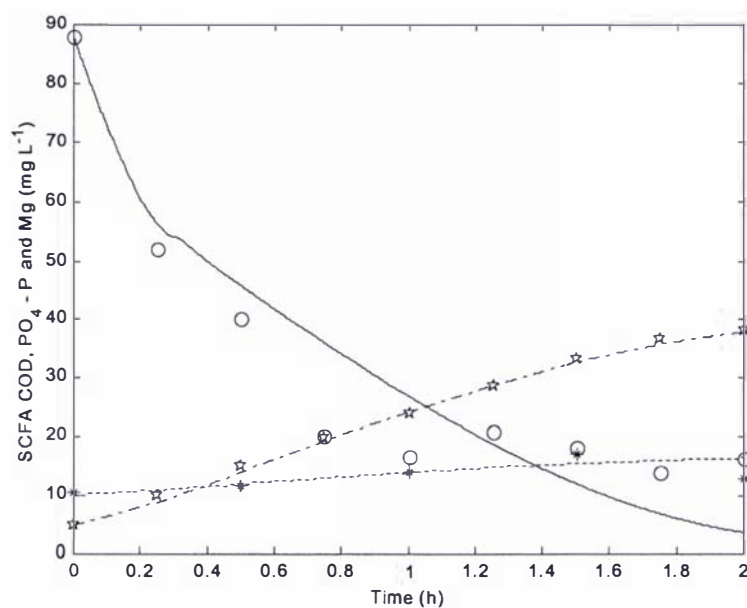


Figure 7.13 Simulated and experimental PO₄-P (---, ☆), Mg²⁺ (-----, *) and SCFA COD (—, ○) of batch test with wastewater

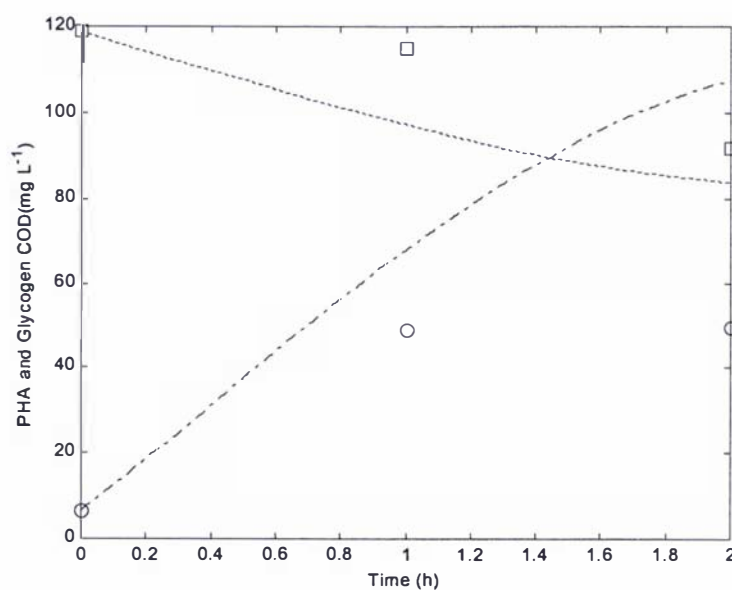


Figure 7.14 Simulated and experimental PHA COD (---, ○) and glycogen COD (-----, □) of batch test with wastewater

7.3.5 Simulation of the batch test results with acetate (Trial II)

The initial conditions for the simulation of the batch test are described in Section 6.3.1.3 and Appendix D.

Figure 7.15 shows the simulated and experimental HAc COD and P profiles. The simulated HAc COD profile follows the observed experimental HAc COD profile, although the experimental HAc COD concentration was slightly lower than the simulated results. The predicted $\text{PO}_4\text{-P}$ concentration shows steady release, whereas the experimental $\text{PO}_4\text{-P}$ concentration shows fast release at the beginning and flattens off at the end. This could be due poly-P and acetate limitation during the end of the anaerobic period. The simulated P uptake profile closely matches the experimental results.

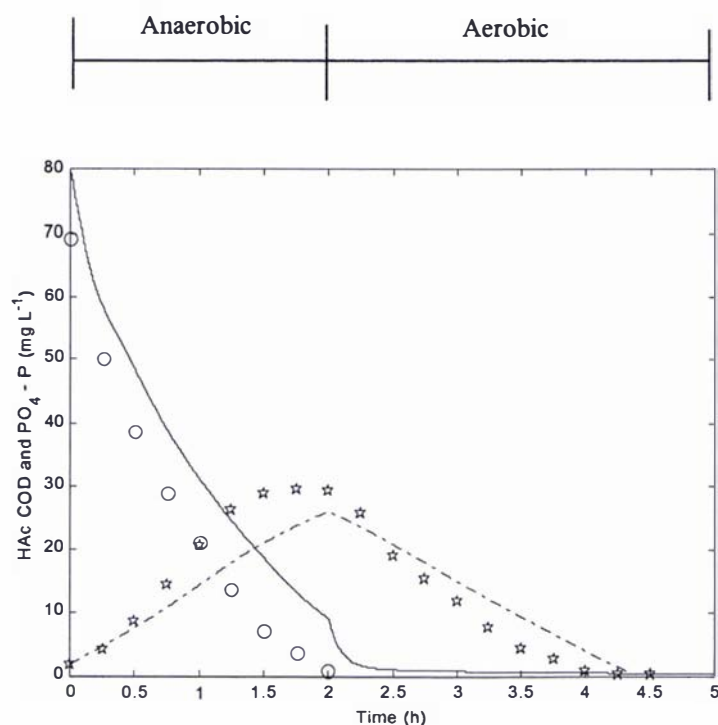


Figure 7.15 Simulated and experimental $\text{PO}_4\text{-P}$ (---, ☆) and HAc COD (—, ○) of acetate batch test (Trial II)

In Figure 7.16 the simulated PHA and glycogen COD are compared to the experimental results. The simulated PHA and glycogen COD profiles match the experimental results except towards the end of the aerobic period, where the model over-predicts the replenishment of glycogen. Utilisation of glycogen for P uptake is a likely reason for the lower values measured in the experiment.

over- predicts the replenishment of glycogen. Utilisation of glycogen for P uptake is a likely reason for the lower values measured in the experiment.

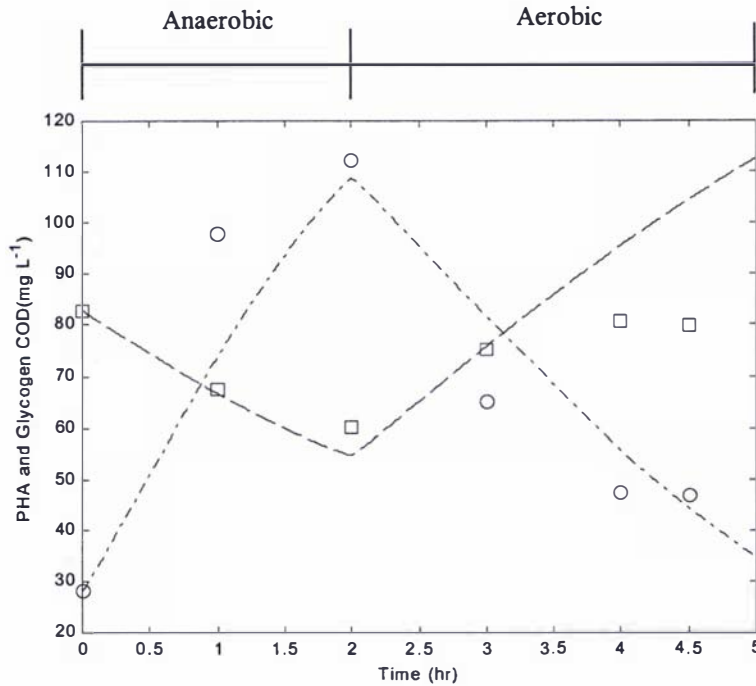


Figure 7.16 Simulated and experimental PHA COD (---, ○) and glycogen COD (—, □) of acetate batch test (Trial II)

7.3.6 Simulation of the batch test results with acetate (Trial I)

The results of the batch test carried out using acetate, described in Section 6.3.1.3 (Trial 1) was simulated using the modified ASM 2 model. Results for the aerobic period were not simulated, as excess HAc COD was carried over into the aerobic period from the anaerobic period. The initial conditions for the simulation of the batch test are described in Section 6.3.1.3 and Appendix D.

Figure 7.17 shows the simulated and experimental HAc COD and $\text{PO}_4\text{-P}$ profiles. The simulated profiles closely follow the experimental results. The decreased rate of HAc COD removal was probably due to the poly-P limitation as discussed in Section 6.3.1.3.

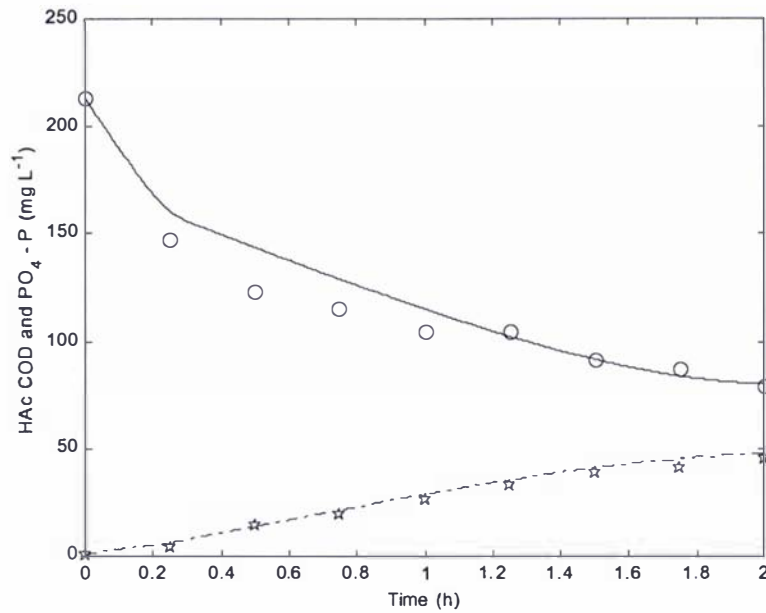


Figure 7.17 Simulated and experimental PO₄-P (---, ☆) and HAc COD (—, ○) of acetate batch test (Trial I)

In Figure 7.18 the simulated PHA and glycogen COD are compared to the experimental results. The model somewhat over-predicted the PHA COD at the end of the anaerobic period. The lower experimental PHA COD at the end of the anaerobic period was probably due to limited acetate uptake by poly-P limitation in the sludge, as discussed in Section 6.3.3. The simulated glycogen profile is in good agreement with the experimental glycogen data.

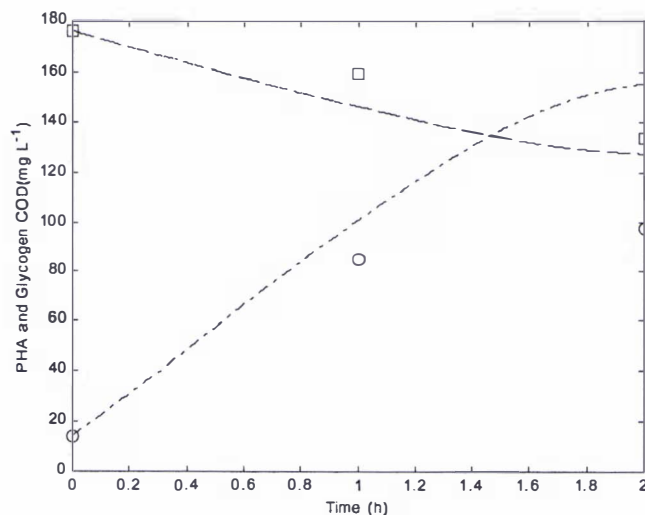


Figure 7.18 Simulated and experimental PHA COD (---, ○) and glycogen COD (----, □) of acetate batch test (Trial I)

7.3.7 Simulation of SBR cycle described in Section 5.5 using ASM 2

The results of the SBR cycle study described in Section 5.5 were modelled using the modified ASM 2 model. The characteristics for the wastewater during this study are described in Section 5.5. The initial conditions for PHA, glycogen and magnesium concentrations were the same as used for the cycle study described in Section 6.3.1.1 in Chapter VI.

Figure 7.19 shows the simulated and experimental $\text{NH}_3 - \text{N}$, $\text{NO}_3 - \text{N}$ and $\text{PO}_4 - \text{P}$ profiles for the SBR cycle described in Section 5.5. The predictions of the model were in good agreement with the experimental results. The slight discrepancy between the predicted and experimental $\text{NO}_3 - \text{N}$ was probably due to more nitrogen removal by SND process in this cycle than in the calibrated cycle during the first aerobic period. The simulated $\text{NH}_3 - \text{N}$ generally agreed with the experimental results, except during the second aerobic period.

The experimental phosphorus profile was predicted well by the model except for the P release during the anaerobic period. The experimental results show a faster release at the beginning and a slower release at the end of the anaerobic period than the simulated results. This suggests that more SCFA COD might have been present in the wastewater than the assumed SCFA COD in the model simulation.

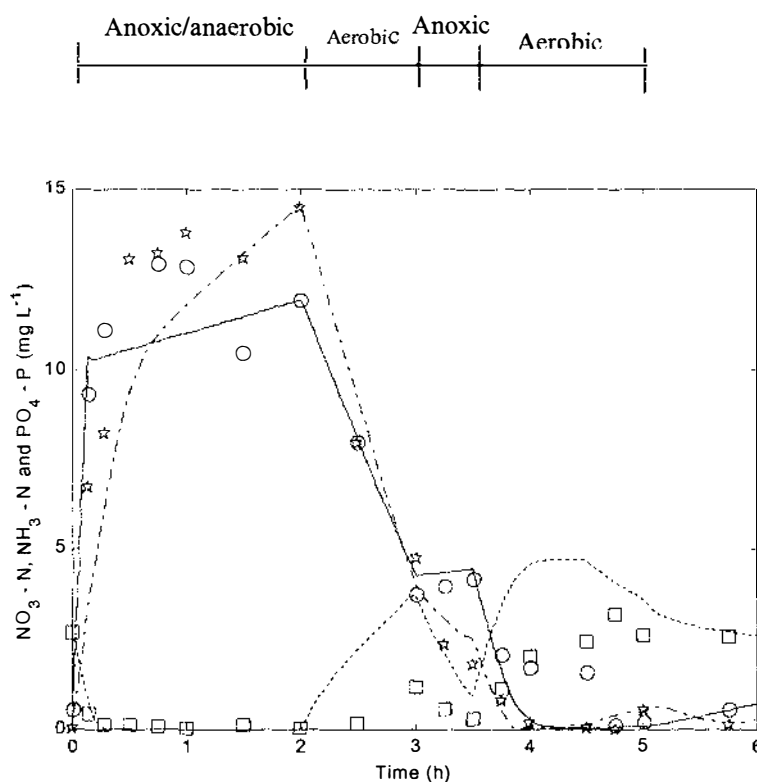


Figure 7.19 Simulated and experimental $\text{NH}_3\text{-N}$ (—, \bigcirc), $\text{NO}_3\text{-N}$ (----, \square) and $\text{PO}_4\text{-P}$ (---, \star) during the SBR cycle described in Section 5.5

7.3.8 Sensitivity of parameters in the modified ASM 2 model

A sensitivity analysis was done for the parameters involved in the ASM 2. The procedure was same as that followed for the ASM 1 (Section 7.2.4). Table 7.13 shows the most sensitive parameters for the effluent $\text{NH}_3\text{-N}$, $\text{NO}_3\text{-N}$ and $\text{PO}_4\text{-P}$.

For all the parameters shown in Table 7.13 the effluent $\text{PO}_4\text{-P}$ concentration is more sensitive than the effluent $\text{NH}_3\text{-N}$ and $\text{NO}_3\text{-N}$. Values for sensitive parameters such as Y_H , Y_{PO_4} , Y_{SA} , heterotrophic and autotrophic growth rates were found in this study. Values for other sensitive parameters were obtained from the calibration. However they are within the range of values given in the literature (Cinar *et al.*, 1998; Henze *et al.*, 1987a; Henze *et al.*, 1999).

Table 7.13 Sensitive parameters in the modified ASM 2 model

Symbol	Default value ASM 2d	Model value	Ammonia nitrogen		Oxidised nitrogen		Phosphate phosphorus	
			-20% model value	+20% model value	-20% model value	+20% model value	-20% model value	20% model value
Heterotrophic biomass								
Y_H	0.625	0.63	0.8	-0.8	0.8	1.9	338.9	-4.0
Y_{PAO}	0.625	0.63	0.0	0.0	-0.8	0.9	84.0	-2.5
Y_{PO4}	0.40	0.33	0.2	-0.1	1.0	-0.1	-2.8	222.4
Y_A	0.24	0.20	-0.1	0.1	-1.4	1.9	-2.9	40.3
Y_{SA}		0.68	-0.3	0.1	-1.4	1.2	-1.3	37.9
K_h	3.00	3.00	-0.1	0.1	1.6	-0.5	25.0	-2.0
Heterotrophic organisms								
μ_H	6.00	2.0	-0.1	0.1	-0.1	0.1	-3.1	26.2
Phosphorus accumulating organisms								
q_{PP}	1.50	2.00	-0.2	0.2	-0.1	0.9	448.4	-3.0
μ_{PAO}	1.00	1.00	0.2	-0.2	0.8	-0.5	-3.2	108.8
K_{MAX}	0.34	0.34	-0.2	0.1	0.0	0.1	1234.5	-2.1
Nitrifying organisms								
μ_{AUT}	1.00	0.75	0.2	-0.1	2.5	-1.3	77.4	-2.7

7.4 Application of the modified ASM 2 model

The modified ASM 2 model with the calibrated model parameters reliably simulated the performance (concentration profiles of $\text{NO}_3 - \text{N}$, $\text{NH}_3 - \text{N}$ and $\text{PO}_4 - \text{P}$) of an SBR cycle carried out over a three month period, and of batch tests. It is therefore appropriate to use the modified ASM 2 model for the determination of treatment strategies for the operation of SBR.

For the study described here, variables such as DO concentration during the third aerobic period, filling time during the feed cycle, and shock loading changes, were examined using the modified ASM 2 model, to estimate the removal of $\text{NO}_3 - \text{N}$, $\text{NH}_3 - \text{N}$ and $\text{PO}_4 - \text{P}$ from the wastewater. It was assumed that the wastewater characteristics, initial conditions, HRT and SRT were similar to those in the SBR cycle study described in Section 5.5.

Figure 7.20 shows the simulated results for $\text{NH}_3 - \text{N}$, $\text{NO}_3 - \text{N}$ and $\text{PO}_4 - \text{P}$ for varied filling times (0.02, 0.5, 1, 2 h). Although the filling duration affected the concentrations during the anoxic/anaerobic period, the effluent concentrations were not significantly affected. Therefore it can be concluded that the shorter duration of fill cycle is suitable for the treatment of meat processing wastewater.

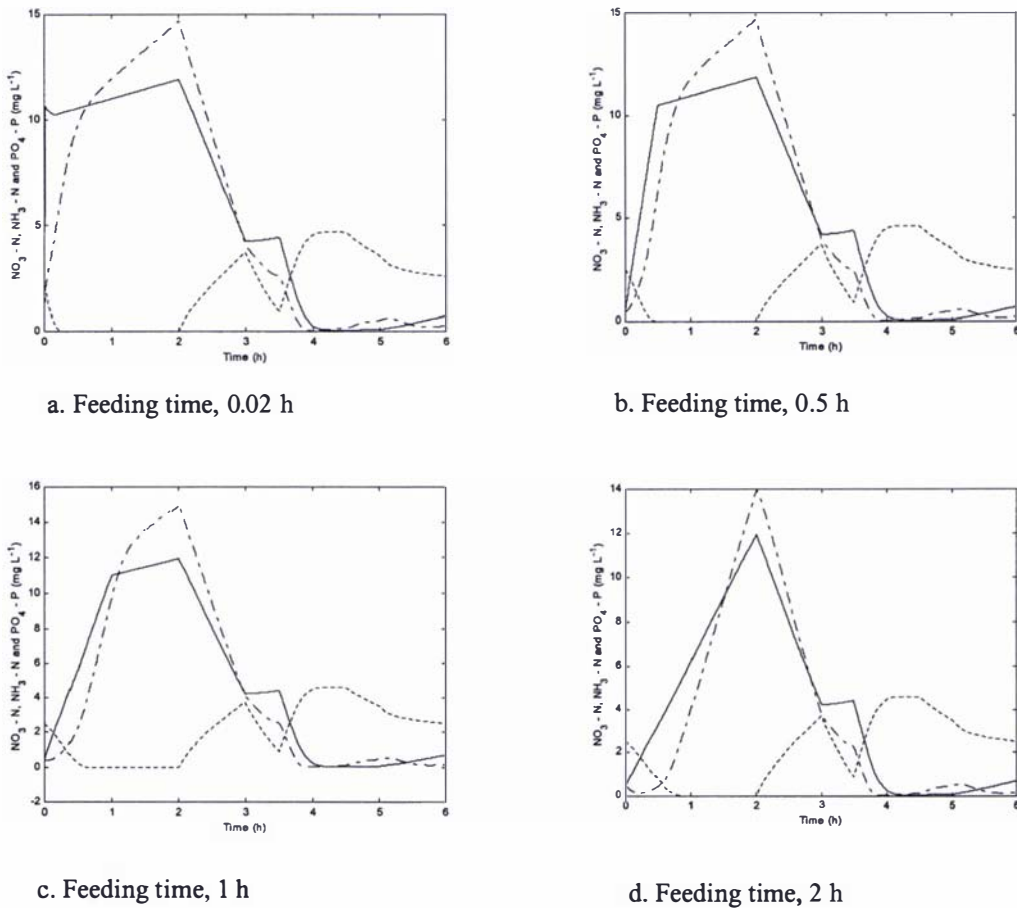


Figure 7.20 Simulated $\text{NH}_3 - \text{N}$ (—), $\text{NO}_3 - \text{N}$ (----), and $\text{PO}_4 - \text{P}$ (-.-.-) with varying filling times

In the calibration SBR cycle the DO concentration was kept at 0.5, 3.75 and 0.5 mg L^{-1} during the first, second and third aerobic periods respectively. It was found that DO was carried over into the subsequent fill cycle when high DO concentration at 2 mg L^{-1} was used in the centrifuged wastewater treatment. To investigate the effect of a higher DO concentration on the behaviour of the system the DO concentration during the third aerobic period was changed to 3.75 mg L^{-1} and the effluent $\text{NH}_3 - \text{N}$, $\text{NO}_3 - \text{N}$ and $\text{PO}_4 - \text{P}$ concentrations again simulated. Figure 7.21 shows the simulated $\text{NH}_3 - \text{N}$, $\text{NO}_3 - \text{N}$ and $\text{PO}_4 - \text{P}$ profiles with the third aeration at 3.75 mg L^{-1} instead of 0.5 mg L^{-1} DO

concentration. The effluent $\text{NO}_3 - \text{N}$ and $\text{PO}_4 - \text{P}$ concentrations were predicted to be 25 and 110 % respectively, higher than for the SBR cycle experiment results shown in Figure 7.19. Therefore a DO concentration of 0.5 mg L^{-1} appears to be more effective in achieving low effluent $\text{NO}_3 - \text{N}$ and $\text{PO}_4 - \text{P}$ concentrations.

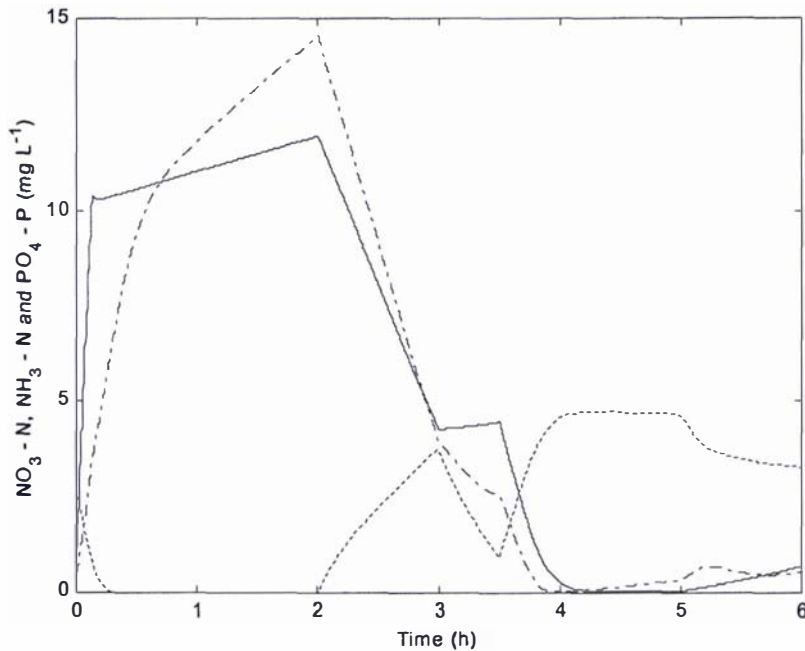


Figure 7.21 Simulated $\text{NH}_3 - \text{N}$ (—), $\text{NO}_3 - \text{N}$ (---) and $\text{PO}_4 - \text{P}$ (-·-·-) with third aeration at 3.75 mg L^{-1} of DO concentration

The next loading condition was changed from the 1735 mg L^{-1} of TCOD, used in the simulation SBR cycle experiment to 2050 (maximum) and then 490 (minimum) mg L^{-1} . Figure 7.22 shows results on $\text{NH}_3 - \text{N}$, $\text{NO}_3 - \text{N}$ and $\text{PO}_4 - \text{P}$ concentrations. The $\text{NH}_3 - \text{N}$, $\text{NO}_3 - \text{N}$ and $\text{PO}_4 - \text{P}$ profiles during the high loading followed the experimental results. The low loading shows more secondary release than uptake of $\text{PO}_4 - \text{P}$ during the third aerobic period. During such low loading periods (which may occur during the rainy season), the third aerobic period may need to be eliminated. The model prediction suggests that higher loading conditions are suitable for achieving greater SBR performance.

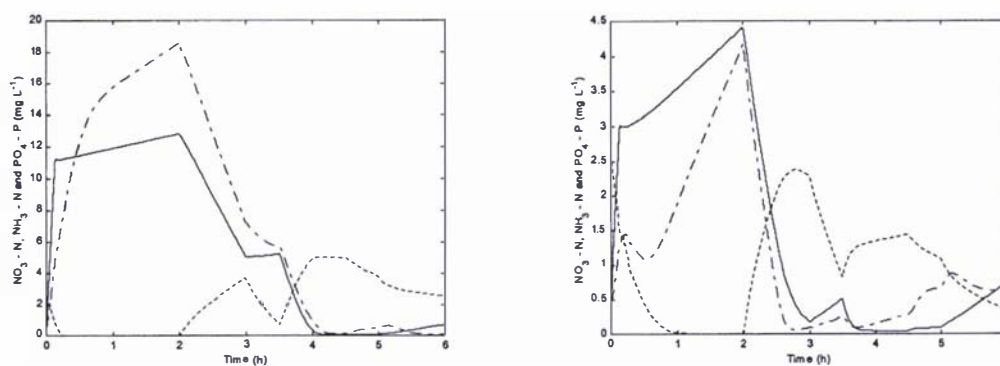


Figure 7.22 Simulated $\text{NH}_3\text{-N}$ (—), $\text{NO}_3\text{-N}$ (-----) and $\text{PO}_4\text{-P}$ (— · — ·) at TCOD concentrations of (a) 2050 and (b) 490 mg L^{-1}

7.5 Summary

In the studies described in this chapter, the SBR performance was simulated using both the modified ASM 1 and ASM 2 models. In general the ASM 1 model successfully simulated the removal of $\text{NH}_3\text{-N}$ and $\text{NO}_3\text{-N}$. The ASM 2 model successfully simulated the removal of $\text{NH}_3\text{-N}$, $\text{NO}_3\text{-N}$ and $\text{PO}_4\text{-P}$. It was necessary, however, to add more processes to the models and to calibrate them with the experimental results.

The ammonification of soluble organic nitrogen rate was modified in the ASM 1 model to account for the $\text{NO}_3\text{-N}$ carry over from the previous cycle. Similarly it was necessary to add anoxic phosphorus uptake and anoxic growth on PHA of Bio-P bacteria in ASM 2 model to successfully simulate the SBR treatment of meat processing wastewater. It was also necessary to add glycogen storage and glycogen lysis processes in order to understand its involvement in phosphorus removal. Also, a modification was performed in the storage process of poly-P in the ASM 2 model to account for a potential magnesium limitation in meat processing wastewater treatment for P removal. During the settling period anoxic hydrolysis was assumed negligible in the modified ASM 2 model simulation.

The key stoichiometric and kinetic model parameters were determined from the batch experimental results using meat processing wastewater and acetate with seed sludge obtained from the SBR. Other parameters necessary for the model simulation were obtained by adjusting the default values of the ASM 1 or ASM 2 model to best fit the SBR results described in Section 6.3.1.1. In order to do this, the model calibration was initialised with the default values proposed in the ASM 1 model (Henze *et al.*,

1987a). Then the parameters were adjusted to improve the fit with the data for calibration of the models.

Parameters such as heterotrophic yield, maximum specific growth rate, substrate half saturation constant and autotrophic maximum specific growth rates were determined from the experimental results. Anaerobic stoichiometric coefficients for the PHA, HAc and P were determined in the acetate batch study. The half saturation constant for Mg^{2+} in the Mg^{2+} limitation function incorporated in the polyphosphate storage process was determined using batch tests. The autotrophic yield coefficient, heterotrophic decay coefficient, oxygen half saturation constant for autotrophs and ammonification rate were obtained from the calibration of the modified ASM 1. Similarly the anaerobic hydrolysis reduction factor, oxygen saturation coefficient for heterotrophs, saturation coefficient for fermentation, rate constant for storage of PHA and rate constant for storage of poly-P were obtained from the modified ASM 2 model calibration. The parameters obtained from calibration were within the range of values given in the literature.

With the calibrated parameters, both the modified ASM 1 and ASM2 models successfully simulated the effluent $NH_3 - N$, $NO_3 - N$ and $PO_4 - P$ of an SBR cycle carried out over a three-month period, and also the results of batch tests.

The sensitivity analysis for parameters in the ASM 1 indicated that the $NO_3 - N$ was sensitive to the maximum specific autotrophic growth rate and oxygen half saturation constants, and the $NH_3 - N$ was sensitive to the heterotrophic decay coefficient. Both $NO_3 - N$ and $NH_3 - N$ were sensitive to the heterotrophic yield coefficient. In the ASM 2 model, most of the kinetic and stoichiometric parameters had more effect on effluent phosphorus concentration than on effluent $NH_3 - N$ and $NO_3 - N$.

As the calibrated modified ASM 2 model was able to predict the performance of the SBR operational data from a distinctly different period (3 months gap) of reactor operation, it was used to identify strategies for improving SBR performance. Filling duration in the 2 h anaerobic period did not affect the effluent $NO_3 - N$, $NH_3 - N$ and $PO_4 - P$ concentrations significantly. But an increase in DO concentration from 0.5 mg L^{-1} to 3.75 mg L^{-1} during the third aerobic period is predicted to substantially increase the effluent $NO_3 - N$ and $PO_4 - P$ concentrations. This demonstrates the significance of

keeping the low DO concentration during the third aerobic period. A sudden increase of influent COD from 1735 mg L^{-1} to 2050 mg L^{-1} decreased the effluent $\text{PO}_4 - \text{P}$ concentration. The effluent $\text{PO}_4 - \text{P}$ concentration increased when there was a sudden decrease in influent COD from 1735 mg L^{-1} to 490 mg L^{-1} .

CHAPTER VIII

SUMMARY AND CONCLUSIONS

Key findings

The removal of organic carbon, and of the nutrients nitrogen and phosphorus, from meat processing wastewaters is an important issue, particularly where the wastewater discharge enters a nutrient sensitive aquatic ecosystem, as is often the case in New Zealand. The simultaneous achievement of very high levels of carbon, nitrogen and phosphorus removal is particularly difficult, given the high incoming concentrations in meat processing effluent. In this study, simultaneous removal of carbon, nitrogen and phosphorus from a primary treated wastewater produced from a medium scale meat processing industry (Manawatu Meat Packers, Feilding) was tested using Sequencing Batch Reactor Technology (SBR). Appropriate reactor operating conditions were determined for maximising the removal. In addition, ASM 1 and ASM 2 models were modified to suit the processes involved in SBR treatment of meat processing wastewater, so that they can realistically predict the removal of carbon, nitrogen and phosphorus.

The characterisation of primary treated wastewater showed that it contains high levels of nutrients and COD and needs treatment before being discharged into free waterways. The high ratios of COD to TKN and TP in the wastewater (100:10.4:2.5) indicate that complete nitrogen and phosphorus removal cannot be achieved by biomass growth coupling alone. It requires advanced treatment technology like SBR. The presence of 4 % inert soluble COD and 4 % inert particulate COD in the wastewater indicates that only 92 % of the wastewater COD can be removed by biological processes.

Biological carbon, nitrogen and phosphorus removal is made effective by having anaerobic, anoxic and aerobic conditions in a cycle during the SBR treatment, and by maintaining the DO concentration in a step pattern during the different aerobic periods. A high quality effluent with more than 99 % removal of soluble biodegradable COD, $\text{NH}_3 - \text{N}$ and $\text{PO}_4 - \text{P}$ was achieved. Simultaneous nitrification and denitrification (SND) removal of 40 % of the influent nitrogen was possible as well. A TSS removal of greater than 90 % was also achieved. Therefore the ratios of COD to TKN and TP in the

wastewater are more than adequate to operate efficient simultaneous biological carbon, nitrogen and phosphorous removal.

Operating conditions in the effective cycle consisted of seven phases. The first two hours of anaerobic period was followed by the aerobic and anoxic periods. The first aerobic period was maintained at a DO concentration of $0.5 \pm 0.25 \text{ mg L}^{-1}$ for 1 h, the second aerobic period for 1 h at a DO concentration of $3.75 \pm 0.25 \text{ mg L}^{-1}$ and the third aerobic period for half an hour at $0.5 \pm 0.25 \text{ mg L}^{-1}$ DO concentration. A half an hour anoxic period followed the first aerobic period. A settling period of 0.75 h followed the third aerobic period. The last quarter of an hour was for decanting and idling. The solids retention time (SRT) was 15 d while the HRT was 2.5 d.

A DO concentration of 0.5 mg L^{-1} during the first aerobic period enhanced the SND and reduced the carryover of DO into the subsequent anoxic period. The third aerobic period ensured a complete removal of ammonia and an increase in the denitrification capability. Also a DO concentration of 0.5 mg L^{-1} during the third aerobic period reduced the carryover of DO into the anaerobic period of the subsequent cycle. A higher DO concentration of 3.75 mg L^{-1} during the second aerobic period increased the rate of degradation of slowly biodegradable COD.

This stepped aeration operating condition also facilitated enhanced biological phosphorous removal. Phosphorus uptake was achieved during the aerobic periods as well as the anoxic period. The anoxic phosphorus uptake and SND reduced the carbon source required for denitrification, therefore the removal of both nitrogen and phosphorous was achieved without adding an external carbon source. The anoxic phosphorus uptake also reduced the energy required for phosphorus uptake. During the biological phosphorus removal process, the pH and alkalinity of the wastewater had an inverse relationship during the anaerobic period and the initial aerobic period, due to CO_2 concentration increase and decrease in the mixed liquor. This finding is new in biological phosphorus removal process.

Preliminary treatment by centrifugation of the wastewater did not help in simultaneous organic carbon and nutrients removal. In the centrifuged wastewater treatment, there was a net loss of alkalinity during nitrification and denitrification. It appears that the alkalinity consumed during nitrification was only partially recovered

during denitrification. The overall performance in terms of organic carbon, nitrogen and phosphorus removal was also poor.

The ammonification process rate in the ASM 1 model was modified. Similarly anoxic phosphorus uptake process and the influence of Mg^{2+} during phosphorus uptake were added in the ASM 2 model to correctly model the nitrogen and phosphorus components. The modified and calibrated ASM 1 and ASM 2 models predicted the performance of the SBR cycle studies conducted in a distinctly different period of reactor operations (3 months gap). The modified and calibrated ASM 1 model in general simulated well the $NH_3 - N$ and $NO_3 - N$ profiles in an SBR cycle, and the modified and calibrated ASM 2 model well simulated the $NH_3 - N$, $NO_3 - N$ and $PO_4 - P$ profiles. The predictions of the modified ASM 2 model at different operating conditions confirmed that the stepped aerating operating conditions identified by the experiment for the maximised simultaneous carbon, nitrogen and phosphorous removal was the best.

The sensitivity analyses of the models indicated that only a few kinetic and stoichiometric parameters have a significant effect in predicting the $NH_3 - N$, $NO_3 - N$ and $PO_4 - P$ profiles, and so on the reactor performance. These parameters have to be determined independently, or be obtained by model calibration for the wastewater. These key parameters are the heterotrophs' maximum specific growth rate, the heterotrophs' yield coefficient, the maximum specific growth rate of autotrophs, the autotrophic yield coefficient, the heterotrophic decay coefficient, the oxygen half saturation constant for autotrophs, and the stoichiometric coefficients for acetate, PHA and phosphate phosphorus.

Significance of the study

Recently there has been an increase in concern over pollution from meat processing wastewater. There has been some investigation of SBR treatment of partially pre-treated meat processing wastewater using anaerobic ponds. But little research has been done on treating raw meat processing wastewater from medium scale meat industries using SBR. The results from this study show that maximised removal of carbon, nitrogen and phosphorus can be achieved using SBR technology without further pre treatment, and that the modified ASM 1 and ASM 2 models are useful in simulating the SBR performance. Specifically, there are four findings of practical significance.

The first finding is the characterisation of the actual effluent from the meat processing plant. It provided details of the carbon, nitrogen and phosphorous components, and also information about the biodegradability of the wastewater. This information was required to develop a carbon, nitrogen and phosphorous removal sequence in SBR. In addition, pre treatment by centrifugation was shown not to be effective for removing carbon, nitrogen and phosphorus. As more meat processing industries begin treating their wastewater this information may be helpful in deciding whether, pre-treatment should be used or not. It also provides a set of characterisation data for comparison purposes. However meat processing wastewater characteristics vary from meat industry to industry, and depend on the number and type of animals and the waste management practices.

Secondly the stepped aerating operating conditions identified in this study could be used for meat processing wastewater with similar characteristics for maximising simultaneous removal of carbon, nitrogen and phosphorous.

The third main finding of practical significance is that the modified ASM 1 and ASM 2 models can be used as tools for designing SBR meat processing wastewater treatment systems. The modifications added to the ASM 2 model provided an understanding of the magnesium ion requirement for phosphorus uptake by running the model with different wastewater magnesium ion concentration. The kinetic and stoichiometric parameter values determined in this study provide data not previously reported in the literature.

Lastly the sensitivity analysis highlights the key parameters that need to be experimentally determined for the simulation of meat processing wastewater treatment. This has the potential to save future researchers time and effort when performing parameter estimations for this type of system.

Some recommendations coming out of the work

- This study demonstrated the large variability that occurs in meat processing wastewater, even from a single meat processing industry. Before the initiation of any treatment process design, the wastewater to be treated at a particular site should be characterised in detail for the concentrations and forms of nitrogen, phosphorus, and carbon present.

- Magnesium ion is required by bacteria during biological phosphorus uptake, and for the production of phospho-lipoproteins and biologically active phosphate esters. Therefore it is recommended that checking be made to ascertain whether the magnesium ion concentration in the wastewater is high enough for continuous operation of the wastewater treatment plant. It should be at least 8.5 mg L^{-1} for a maximum phosphorous uptake rate.
- This study was conducted using just one laboratory scale SBR reactor, and using the wastewater from just one meat processing plant. It would be desirable to confirm the generality of the results with other reactor studies using wastewater from a range of medium scale meat processing plants.

REFERENCES

1. Abeling, U. and Seyfried, C. F. (1992) Anaerobic-aerobic treatment of high strength ammonium wastewater – nitrogen removal via nitrite. *Water Science and Technology*, **26(5-6)**, 1007-1015.
2. Abu-ghararah, Z. H. and Randall, C. W. (1991) The effect of organic compounds in biological phosphorus removal. *Water Science and Technology*, **23**, 585-594.
3. Almeida, J. S., Julio, S. M., Reis, M. A. M. and Carrondo, M. J. T. (1995a) Nitrite inhibition of denitrification by *Pseudomonas fluorescens*. *Biotechnology and Bioengineering*, **46**, 194-201.
4. Almeida, J. S., Reis, M. A. M. and Carrondo, M. J. T. (1995b) Competition between nitrate and nitrite reduction in denitrification by *Pseudomonas fluorescens*. *Biotechnology and Bioengineering*, **46**, 476-484.
5. Annachatre, A. P. and Bhamidimarri, S. M. R. (1993) Aerobic treatment of meat industry wastewater: COD removal and nitrification. In *Proceedings of APCCHE/CHEMECA '93*, **21**, 118-124.
6. Anthonisen, A. C., Loehr, R. C., Prakasam, T. B. S. and Srinath, E. G. (1976) Inhibition of nitrification by ammonia and nitrous acid. *Journal Water Pollution Control Federation*, **48(5)**, 835-852.
7. Antoniou, P., Hamilton, J., Koopman, B., Jain, R. and Holloway, B. (1990) Effect of temperature and pH on the effective maximum specific growth rate of nitrifying bacteria. *Water Research*, **24(1)**, 97-101.
8. APHA, AWWA, WPCF (1995) *Standard Methods for the Examination of Water and Wastewater*. (19th edition), American public health association, Washington DC.
9. Argaman, Y. and Brenner, A. (1986) Single sludge nitrogen removal: modelling and experimental results. *Journal Water Pollution Control Federation*, **58(8)**, 853-860.
10. Artan, N. and Tasli, R. (1999) Effect of aeration and filling patterns on nutrient removal performance in sequencing batch reactor. *Environmental Technology*, **20**, 507-513.
11. Artan, N., Wilderer, P., Orhon, D., Morgenroth, E. and Ozgur, N. (2001) The mechanism and design of sequencing batch reactor systems for nutrient removal-the state of the art. *Water Science and Technology*, **43(3)**, 53-60.
12. Arun, V., Mino, T. and Matsuo, T. (1988) Biological mechanism of acetate uptake mediated by carbohydrate consumption in excess phosphorus removal systems. *Water Research*, **22(5)**, 565-570.
13. Arvin, E. (1983) Observations supporting phosphate removal by biologically mediated chemical precipitation – A review. *Water Science and Technology*, **15**, 43-63.
14. Arvin, E. and Holm Kristensen, G. (1985) Exchange of organics, phosphate and cations between sludge and water in biological phosphorus and nitrogen removal processes and neural nets. *Water Science and Technology*, **17**, 147-162.
15. Azimi, A. A. and Horan, N. J. (1991) The influence of reactor mixing characteristics on the rate of nitrification in the activated sludge process. *Water Research*, **25(4)**, 419-423.

16. Barker, D. J. and Stuckey, D. C. (1999) A review of soluble microbial products (SMP) in wastewater treatment systems. *Water Research*, **33**(14), 3063-3082.
17. Barker, P. S. and Dold, P. L. (1996) Denitrification behaviour in biological excess phosphorus removal activated sludge systems. *Water Research*, **30**(4), 769-780.
18. Barker, P. S. and Dold, P. L. (1997) General model for biological nutrient removal activated sludge systems: model presentation. *Water Environment Research*, **69**, 969-984.
19. Barnard, J. L. (1975) Biological nutrient removal without the addition of chemicals. *Water Research*, **9**, 485-490.
20. Barnes, D. and Bliss, P. J. (1983) *Biological Control of Nitrogen in Wastewater Treatment*. (1st edition), E. and F. N. Spon Ltd. publishers, London EC4P 4EE.
21. Beccari, M., Marani, D. and Ramadori, R. (1979) A critical analysis of nitrification alternatives. *Water Research*, **13**, 185-192.
22. Beun, J. J., Verhoef, E. V., Van Loosdrecht, M. C. M. and Heijnen, J. J. (2000) Stoichiometry and kinetics of poly- β -hydroxybutyrate metabolism under denitrifying conditions in activated sludge cultures. *Biotechnology and Bioengineering*, **68**(5), 496-507.
23. Bhamidimarri, S. M. R. (1991) Appropriate industrial waste management technologies: The New Zealand meat industry. *Water Science and Technology*, **24**(1), 89-95.
24. Bickers, P. O. (1996a) Effects of temperature on nitrification during biological treatment of meat processing effluent. *Technical Report 972*, Meat Industry Research Institute of New Zealand, Hamilton.
25. Bickers, P. O. (1996b) Temperature effects on denitrification. *Technical Report 973*, Meat Industry Research Institute of New Zealand, Hamilton.
26. Bickers, P. O. and Van Oostrom, A. J. (2000) Availability for denitrification of organic carbon in meat-processing wastestreams. *Bioresource Technology*, **73**, 53-58.
27. Bickers, P. O., Bhamidimarri, S. M. R., Thayalakumaran, N. and Hu, Z. B. (2001) Developments in enhanced biological phosphorus removal (EBPR). *New Zealand Water and Wastewater Association 43rd Annual Conference*, Wellington, New Zealand.
28. Bock, E. I., Stueven, R. and Zart, D. (1995) Nitrogen loss caused by denitrifying *Nitrosomanas* cells using ammonium or hydrogen as electron donors and nitrite as electron acceptor. *Archives of Microbiology*, **163**, 16-20.
29. Brdjanovic, D., Slamet, A., Van Loosdrecht, M. C. M., Hooijmans, C. M., Alaerts, G. J. and Heijnen, J. J. (1998b) Impact of excessive aeration on biological phosphorus removal from wastewater. *Water Research*, **32**(1), 200-208.
30. Brdjanovic, D., Slamet, A., Van Loosdrecht, M. C. M., Hooijmans, C. M., Mino, T., Alaerts, G. J. and Heijnen, J. J. (1998c) Effect of polyphosphate limitation on the anaerobic metabolism of phosphorus accumulating microorganisms. *Microbiology Biotechnology*, **50**, 273-276.
31. Brdjanovic, D., Van Loosdrecht, M. C. M., Hooijmans, C. M., Mino, T., Alaerts, G. J. and Heijnen, J. J. (1998a) Bioassay for glycogen determination in biological phosphorus removal systems. *Water Science and Technology*, **37**(4-5), 541-547.
32. Bremmell, K. E., Jameson, G. J. and Farrugia, T. R. (1994) Agglomeration of fats and proteins. *Chemical Engineering*, **19**, 23-26.

33. Brenner, A. (2000) Modelling of N and P transformations in an SBR treating municipal wastewater. *Water Science and Technology*, **42(1-2)**, 55-63.
34. Brodisch, K. E. U. (1985) Interaction of different groups of microorganisms in biological phosphate removal. *Water Science and Technology*, **17(11/12)**, 139-146.
35. Buchan, L. (1983) Possible biological mechanism of phosphorus removal. *Water Science and Technology*, **15**, 87-103.
36. Carlsson, H., Aspegren, H., Lee, N. and Hilmer, A. (1997) Calcium phosphate precipitation in biological phosphorus removal systems. *Water Research*, **31(5)**, 1047-1055.
37. Cech, J. S., Chudoba, J. and Grau, P. (1984) Determination of kinetic constants of activated sludge microorganisms. *Water Science and Technology*, **17**, 259-272.
38. Chang, S. S. (1999) *Characterisation of Aerobic Biotreatment of Meat Plant Effluent*. Master of Philosophy Thesis, Massey University, Palmerston North, New Zealand.
39. Chiesa, S. C. and Irvine, R. L. (1985) Growth and control of filamentous microbes in activated sludge: an integrated hypothesis. *Water Research*, **19 (4)**, 471-479.
40. Chuang, S., Ouyang, C. and Wang, Y. (1996) Kinetic competition between phosphorus release and denitrification on sludge under anoxic condition. *Water Research*, **30(12)**, 2961-2968.
41. Chudoba, P., Capdeville, B. and Chudoba, J. (1992) Explanation of biological meaning of the S0/X0 ratio in batch cultivation. *Water Science and Technology*, **26(3-4)**, 743-751.
42. Cinar, O., Daigger, G. T. and Graef, S. P. (1998) Evaluation of IAWQ Activated Sludge Model No. 2 using steady-state data from four full-scale wastewater treatment plants. *Water Environment Research*, **70(6)**, 1216-1224.
43. Clift, R. C. and Andrews, J. F. (1981) Predicting the dynamics of oxygen utilisation in the activated sludge process. *Journal of Water Pollution Control Federation*, **53(7)**, 1219-1232.
44. Cokgor, E. U., Sozen, S., Orhon, D. and Henze, M. (1998) Respirometric analysis of activated sludge behaviour-I. Assessment of the readily biodegradable substrate. *Water Research*, **32(2)**, 461-475.
45. Comeau, Y., Hall, K. J. and Oldham, W. K. (1988) Determination of poly- β -hydroxybutyrate and poly- β -hydroxyvalerate in activated sludge by gas-liquid chromatography. *Applied and Environmental Microbiology*, **54**, 2325-2327.
46. Comeau, Y., Hall, K. J., Hancock, R. E. W. and Oldham, W. K. (1986) Biochemical model for enhanced biological phosphorus removal. *Water Research*, **20(12)**, 1511-1521.
47. Comeau, Y., Rabionwitz, B., Hall, K. J. and Oldham, W. K. (1987) Phosphate release and uptake in enhanced biological phosphorus removal from wastewater. *Journal Water Pollution Control Federation*, **59(7)**, 707-715.
48. Cooper, R. N. and Russell, J. M. (1988) Effluent treatment in the New Zealand export meat industry. *Technical Report 854*. Meat Industry Research Institute of New Zealand, Hamilton.
49. Cooper, R. N. and Russell, J. M. (1991) Meat industry producing wastes: Characteristics and treatment. *Encyclopaedia of Food Science and Technology*, **3**, 1683-1691.

50. Dague, R. R., Urell, R. F. and Krieger, E. R. (1990) Treatment of pork processing wastewater in covered anaerobic lagoon with gas recovery. In *Proceedings of the 44th Purdue Industrial Waste Conference*. pp. 815-823. Lewis Publishers, Inc., Chelsea, Michigan 48118.
51. Daiger, G. T. and Littleton, H. X. (2000) Characterisation of simultaneous nutrient removal in staged, closed-loop bioreactors. *Water Environment Research*, **72(3)**, 330-339.
52. Daiger, G. T. and Parker, D. S. (2000) Enhancing nitrification in North American activated sludge plants. *Water Science and Technology*, **41(9)**, 97-105.
53. Dold, P. L. and Marais, G. V. R. (1986) Evaluation of the general activated sludge model proposed by the IAWPRC task group. *Water Science and Technology*, **18**, 63-89.
54. Dold, P. L. and Marais, G. V. R. (1987) Benefits of including unaerated zones in nitrifying activated sludge plants. *Water Science and Technology*, **19**, 195-207.
55. Dold, P. L., Ekama, G. A. and Marais, G. V. R. (1980) A general model for the activated sludge process. *Progress in Water Technology*, **12**, 47.
56. Eckenfelder, W. W. (1980) *Principles of Water Quality Management*. CBI Publishing Company, Inc., Boston, Massachusetts 02210, USA.
57. Eckenfelder, W. W. and Musterman, J. L. (1995) *Activated Sludge Treatment of Industrial Wastewater*. Technomic publishing company, Inc., Lancaster, Pennsylvania 17604, USA.
58. Ekama, G. A., Dold, P. L. and Marais, G. V. R. (1986) Procedures for determining influent COD fractions and the maximum specific growth rate of heterotrophs in activated sludge systems. *Water Science and Technology*, **18**, 91-114.
59. Ekama, G. A., Wentzel, M. C., Casey, T. G. and Marais, G. V. R. (1996) Filamentous organism bulking in nutrient removal activated sludge systems. Paper 6 : Review, evaluation and consolidation of results. *Water Science and Technology*, **18**, 91-114.
60. Environmental Protection Agency (1973) *Nitrification and Denitrification Facilities, Wastewater Treatment*. Report No. EPA/625/4-73/004a, E. P. A Cincinnati, Ohio.
61. Environmental Protection Agency (1985) *Ambient Water Quality Criteria for Ammonia-1984*. EPA-44015-85-001, Criteria and Standards Division, U.S. E.P.A.
62. Environmental Protection Agency (1993) *Manual Nitrogen Control*. EPA/625/R-93/010.
63. Farrimond, M. and Upton, J. (1993) A strategy to meet the nutrient Standard of the Urban Wastewater Directive. *Water Science and Technology*, **27(5-6)**, 297-306.
64. Filipe, C. D. M. and Daigger, G. T. (1999) Evaluation of the capacity of phosphorus accumulating organisms to use nitrate and oxygen as final electron acceptors: a theoretical study on population dynamics. *Water Environment Research*, **71(6)**, 1140-1150.
65. Fleit, E. (1995) Intracellular pH regulation in biological excess phosphorus removal systems. *Water Research*, **29(7)**, 1787-1792.
66. Focht, D. D. and Chang, A. C. (1975) Nitrification and denitrification processes related to wastewater treatment. *Advances in Applied Microbiology*. Perlman, D. (ed.), Volume 19, pp. 153-186. Academic press, Inc., New York, USA.

67. Froese, G. and Kayser, R. (1985) Effective treatment of wastewater from rendering plants. In *Proceedings of the 40th Purdue Industrial Waste Conference*. pp. 69-77. Butterworth publishers, Stoneham, MA 02180.
68. Fuhs, G. W. and Chen, M. (1975) Microbiological basis of phosphate removal in the activated sludge process for the treatment of wastewater. *Microbial Ecology*, **2(2)**, 119-138.
69. Gerber, A., Mostert, E. S., Winter, C. T. and De villiers, R. H. (1987) Interactions between phosphate, nitrate and organic substrate in biological nutrient removal processes. *Water Science and Technology*, **19**, 183-194.
70. Germirli, F., Orhon, D. and Artan N. (1991) Assessment of the initial inert soluble COD in industrial wastewater. *Water Science and Technology*, **23**, 1077-1086.
71. Ginsburg, V. and Robbins, P. W. (1984) *Biology of Carbohydrates*. Volume 2, pp. 101-102. A Wiley-Inter science publication, John Wiley and Sons, Inc., New York, USA.
72. Gorgun, E., Cokgor, E. U., Orhon, D., Germirli, F. and Artan, N. (1995) Modelling biological treatability for meat processing effluent. *Water Science and Technology*, **32(12)**, 43-52.
73. Gottschalk, G. (1979) *Bacterial metabolism*. 2nd edition. Springer series in microbiology. Springer-Verlag, New York, USA.
74. Grady, C. P. L. (1989) Dynamic modelling of suspended growth biological wastewater treatment processes. In *Dynamic Modelling and Expert Systems in Wastewater Engineering*. Patry, G. G. and Chapman (ed.), pp. 1-38. D. Lewis Publishers, Inc., Chelsea, Michigan 48118.
75. Green, T., Shell, G. and Witmayer, G. (1981) Case history of nitrification of a rendering meat packing wastewater. In *Proceedings of the 35th Purdue Industrial Waste Conference*. pp. 653-664. Ann Arbor Science publishers, Ann Arbor, Michigan 48106.
76. Greenfield, P. and Johns, M. (1995) High rate anaerobic treatment of abattoir effluents. In *Abattoir Wastewater and Odour Management*. Mc Donald, B. (ed.), pp. 69-93. CSIRO Meat Research Laboratory, Cannon Hill Q 4170, Australia.
77. Gujer, W., Henze, M., Mino, T. and Van Loosdrecht, M. C. M. (1999) Activated Sludge Model No. 3. *Water Science and Technology*, **39(1)**, 183-193.
78. Hanaki, K., Wantawin, C. and Ohgaki, S. (1990) Nitrification at low levels of dissolved oxygen with and without organic loading in a suspended growth reactor. *Water Research*, **24(3)**, 297-302.
79. Harper, H. A. (1969) *A Review of Physiological Chemistry*. (12th edition), Lange medical publications, Los Altos, California, USA.
80. Harremoes P. and Sinkjaer, O. (1995) Kinetic interpretation of nitrogen removal in pilot scale experiments. *Water Research*, **29(3)**, 899-905.
81. Hascoet, M. C. and Florentz, M. (1985) Influence of nitrate on biological phosphorus removal from wastewater. *Water SA* **11(1)**, 1-8.
82. Heddle, J. H. (1979) Activated sludge treatment of slaughterhouse wastes with protein recovery. *Water Research*, **13**, 581-584.
83. Hellinga, C., Schellen, A. A. J. C., Mulder, J. W., Van Loosdrecht, M. C. M. and Heijnen, J. J. (1997) The SHARON process; an innovative method for nitrogen removal from ammonium rich wastewater. *Water Science and Technology*, **37(9)**, 135-142.

84. Henze, M. (1986) Nitrate versus oxygen utilisation rates in wastewater and activated sludge systems. *Water Science and Technology*, **18**, 115-122.
85. Henze, M. (1991) Capabilities of biological nitrogen removal processes from wastewater. *Water Science and Technology*, **23**, 669-679.
86. Henze, M. (1992) Characterisation of wastewater for modelling of activated sludge processes. *Water Science and Technology*, **25(6)**, 1-15.
87. Henze, M. (2002) Basic biological processes. In *Wastewater Treatment, Biological and Chemical Processes*. (3rd edition), Henze, M., Harremoës, P., Jansen, J. L. C. and Arvin, E. (ed.), Springer-Verlag Berlin, Germany.
88. Henze, M., Grady Jr, C. P. L., Gujer, W., Marais, G. V. R. and Matsuo, T. (1987b) A general model for single-sludge wastewater treatment systems. *Water Research*, **21(5)**, 505-515.
89. Henze, M., Grady, C. P. L., Gujer, W., Marais, G. V. R. and Matsuo, T. (1987a) Activated Sludge Model No.1, *IAWPRC Scientific and Technical Report No.1*, IAWPRC, London.
90. Henze, M., Gujer, W., Mino, T., Matsuo, T., Wentzel, M. C., Marais, G. V. R. and Van Loosdrecht, M. C. M. (1999) Activated Sludge Model No. 2d, ASM 2d. *Water Science and Technology*, **39(1)**, 165-182.
91. Henze, M., Gujer, W., Mino, T., Matsuo, T., Wentzel, M. C., Marais, G. V. R. (1995) Activated Sludge Model No.2, *IAWQ Scientific and Technical Report No.3*, IAWQ, London.
92. Hesselmann, R. P. X., Rummell, R. V., Resnick, S. L., Hany, R. and Zehnder, A. J. B. (2000) Anaerobic metabolism of bacteria performing enhanced biological phosphate removal. *Water Research*, **34(14)**, 3487-3494.
93. Hood, C. R. and Randall, A. A. (2001) A biochemical hypothesis explaining the response of enhanced biological phosphorus removal biomass to organic substrates. *Water Research*, **35(11)**, 2758-2766.
94. Hopwood, D. (1977) Effluent treatment in meat and poultry processing industries. *Process Biochemistry*, **12(8)**, 5-8, 44, 46.
95. Huisman, J. L. and Mino, T. (2002) Predation, turnover rate and community dynamics as crucial aspects of nutrient removing activated sludge. *IWA World Water Congress*, Melbourne (CD ROM), e21348a.
96. Husband, P. (1995a) Primary effluent treatment. In *Abattoir Wastewater and Odour Management*. Mc Donald, B. (ed.), pp. 27-38. CSIRO Meat Research Laboratory, Cannon Hill Q 4170, Australia.
97. Husband, P. (1995b) Physical chemical treatment. In *Abattoir Wastewater and Odour Management*. Mc Donald, B. (ed.), pp. 97-104. CSIRO Meat Research Laboratory, Cannon Hill Q 4170, Australia.
98. Imai, H., Endoh, K., and Kozuka, T. (1988) Magnesium requirement for biological removal of phosphate by activated sludge. *Journal of Fermentation Technology*, **66(6)**, 657-666.
99. Imura, M., Suzuki, K., Kitao, T. and Iway, S. (1993) Advanced treatment of domestic wastewater using sequencing batch reactor activated sludge process. *Water Science and Technology*, **28(10)**, 267-274.
100. Irvine, R. L. and Ketchum Jr, L. H. (1989) Sequencing batch reactors for biological wastewater treatment. *CRC Critical Reviews in Environmental Control*, **18(4)**, 255-294.

101. Irvine, R. L., Wilderer, P. A. and Flemming, H. C. (1997) Controlled unsteady state processes and technologies-an overview. *Water Science and Technology*, **35**(1), 1-10.
102. Isaacs, S., Hansen, J. A., Schmidt, K. and Henze, M. (1995) Examination of the Activated Sludge Model No. 2 with an alternating process. *Water Science and Technology*, **31**(2), 55-66.
103. Jenkins, D., Richard, M. G. and Daigger, G. T. (1993) *Manual on the Causes and Control of Activated Sludge Bulking and Foaming*. (2nd edition), Lewis publishers, Chelsea, Michigan 48118, USA.
104. Johns, M. R. (1995) Developments in wastewater treatment in the meat processing industry: A review. *Bioresource Technology*, **54**, 203-216.
105. Kappeler, J. and Gujer, W. (1992) Estimation of kinetic parameters of the heterotrophic biomass under aerobic conditions and characterisation of wastewater for activated sludge modelling. *Water Science and Technology*, **25**(6), 125-139.
106. Kaszas, R., Harries, R. C. and Shannon, E. E. (1992) Lime treatment and ammonia volatilization for industrial wastewater. In *Proceedings of the 46th Purdue Industrial Waste Conference*. pp. 511-519. Lewis Publishers, Inc., Chelsea, Michigan 48118.
107. Kazmi, A. A., Fujita, M. and Furumai, H. (2001) Modelling effect of remaining nitrate on phosphorus removal in SBR. *Water Science and Technology*, **42**(3), 175-182.
108. Keller, J., Subramaniam, K., Gosswein, J. and Greenfield, P. F. (1997) Nutrient removal from industrial wastewater using single tank sequencing batch reactors. *Water Science and Technology*, **35**(6), 137-144.
109. Kern-Jespersen, J. P. and Henze, M. (1993) Biological phosphorus uptake under anoxic and aerobic conditions. *Water Research*, **27**, 617-624.
110. Koch, G., Kühni, M., Gujer, W. and Siegrist, H. (2000) Calibration and validation of Activated Sludge Model No. 3 for Swiss municipal wastewater. *Water Research*, **34**(14), 3580-3590.
111. Kristensen, G. H., Jorgensen, P. E. and Henze, M. (1992) Characterisation of functional microorganism groups and substrate in activated sludge wastewater by AUR, NUR, and OUR. *Water Science and Technology*, **25**(6), 43-57.
112. Kuba, T., Murnleitner, E., Van Loosdrecht, M. C. M. and Heijnen, J. J. (1996) A metabolic model for the biological phosphorus removal by denitrifying organisms. *Biotechnology and Bioengineering*, **52**, 685-695.
113. Kuba, T., Smolders, G., Van Loosdrecht, M. C. M. and Heijnen, J. J. (1993) Biological phosphorus removal from wastewater by anaerobic-anoxic sequencing batch reactor. *Water Science and Technology*, **27**(5-6), 241-252.
114. Ky, R. C., Comeau, Y., Perrier, M. and Takacs, I. (2001) Modelling biological phosphorus removal from a cheese factory effluent by an SBR. *Water Science and Technology*, **43**(3), 257-264.
115. Laanbroek, H. J. and Gerards, S. (1993) Competition for limiting amounts of oxygen between *Nitrosomonas europaea* and *Nitrobacter winogradsky* grown in mixed continuous cultures. *Archives of Microbiology*, **159**, 453-459.
116. Lakay, M. T., Hulsman, A., Ketley, D., Warburton, C., De Villiers, M., Casey, T. G., Wentzel, M. C. and Ekama, G. A. (1999) Filamentous organism bulking in

- nutrient removal activated sludge systems Paper 7: Exploratory experimental investigations. *Water SA*, **25(4)**, 383-396.
117. Lee, D. S., Jeon, C. O. and Park, J. M. (2001) Biological nitrogen removal with enhanced phosphate uptake in a sequencing batch reactor using single sludge system. *Water Research*, **35(16)**, 3968-3976.
 118. Leonard, A. M. (1996) *Activated Sludge Treatment of Dairy Processing Wastewaters: The Role of Selectors for the Control of Sludge Bulking*. PhD Thesis, Massey University, Palmerston North, New Zealand.
 119. Levin, G. V. and Shapiro, J. (1965) Metabolic uptake of phosphorus by wastewater organisms. *Journal of Water Pollution Control Federation*, **87**, 800-821.
 120. Lovett, D. A., Travers, S. M. and Davey, K. R. (1984) Activated sludge treatment of slaughterhouse wastewater-I. Influence of sludge age and feeding pattern. *Water Research*, **18**, 429-434.
 121. Macfarlane, D. (1995) Waste minimisation and management. In *Abattoir Wastewater and Odour Management*. Mc Donald, B. (ed.), pp. 13-26. CSIRO Meat Research Laboratory, Cannon Hill Q 4170, Australia.
 122. Manderson, G. J. (2000) Personnel communication, Massey University, Palmerston North, New Zealand.
 123. Manjunath, N. T., Mehrotra, I. and Mathur, R. P. (2000) Treatment of wastewater from slaughterhouse by DAF-UASB system. *Water Research*, **34(6)**, 1930-1936.
 124. Marais, G. V. R., Loewenthal, R. E. and Siebritz, I. P. (1983) Observations supporting phosphate removal by biological excess uptake- a review. *Water Science and Technology*, **15**, 15-41.
 125. McClintock, S. A., Randall, C. W. and Pattarkine, V. M. (1993) Effects of temperature and mean cell residence time on biological nutrient removal processes. *Water Environment Research*, **65(2)**, 110-118.
 126. McClintock, S. A., Sherrard, J. H., Novak, J. T. and Randall, C. W. (1988) Nitrate versus oxygen respiration in the activated sludge process. *Journal Water Pollution Control Federation*, **60(3)**, 342-350.
 127. Meat New Zealand statistical information, 2000-2001. Meat New Zealand home page. <http://www.meatnz.co.nz> (accessed, 2002).
 128. Meijer, S. C. F., Van Loosdrecht, M. C. M. and Heijnen (2001) Metabolic modelling of full scale biological nitrogen and phosphorus removing WWTP'S. *Water Research*, **35(11)**, 2711-2723.
 129. Metcalf and Eddy, Inc. (1991) *Wastewater Engineering, Treatment, Disposal and Reuse*. (3rd edition), McGraw-Hill, Inc., Singapore.
 130. Metzner, G. and Temper, U. (1990) Operation and optimisation of a full scale fixed bed reactor for anaerobic digestion of animal rendering wastewater. *Water Science and Technology*, **22(1/2)**, 373-384.
 131. Mikkelsen, K. A. and Lowery, K. W. (1992) Designing a sequencing batch reactor system for the treatment of high strength meat processing wastewater. In *Proceedings of the 47th Purdue Industrial Waste Conference*. pp. 765-774. Lewis Publishers, Inc., Chelsea, Michigan 48118.
 132. Mino, T., Liu, W, Kurisu, F. and Matsuo, T. (1995) Modelling glycogen storage and denitrification capability of microorganisms in enhanced biological phosphate removal processes. *Water Science and Technology*, **31(2)**, 25-34.

133. Mino, T., Van Loosdrecht, M.C.M. and Heijnen, J. (1998) Microbiology and biochemistry of the enhanced biological phosphate removal process. *Water Research*, **32**(11), 3193-3207.
134. Munch, E. V., Lant, P. and Keller, J. (1996) Simultaneous nitrification and denitrification in bench-scale sequencing batch reactors. *Water Research*, **30**(2), 277-284.
135. Murnleitner, E., Kuba, T., Van Loosdrecht, M. C. M. and Heijnen, J. J. (1997). An integrated metabolic model for the aerobic and denitrifying biological phosphorus removal. *Biotechnology and Bioengineering*, **54**(5), 434-450.
136. Nakamura, K., Masuda, K. and Mikami, E. (1991) Isolation of a new type of polyphosphate accumulating bacteria and its phosphate removal characteristics. *Journal of fermentation and bioengineering*, **71**, 258-263.
137. Nowak, O. and Svardal, K. (1993) Observations on the kinetics of nitrification under inhibiting conditions caused by industrial wastewater compounds. *Water Science and Technology*, **28**(2), 115-123.
138. Okada, M., Murakami, A., Lin, C. K., Ueno, Y. and Okubo, T. (1991) Population dynamics of bacteria for phosphorus removal in sequencing batch reactor (SBR) activated sludge processes. *Water Science and Technology*, **23**, 755-763.
139. Oles, J. and Wilderer, P. A. (1991) Computer aided design of sequencing batch reactors based on the IAWPRC activated sludge model. *Water Science and Technology*, **23**, 1087-1095.
140. Orhon, D. and Artan, N. (1994) *Modelling of Activated Sludge Systems*. Technomic publishing company, Pennsylvania, USA.
141. Orhon, D., Cimsit, Y. and Tunay, O. (1986) Substrate removal mechanism for sequencing batch reactors. *Water Science and Technology*, **18**, 21-33.
142. Orhon, D., Karahan, O. and Sözen, S. (1999a) The effect of residual microbial products on the experimental assessment of the particulate inert COD in wastewaters. *Water Research*, **33**(14), 3191-3203.
143. Orhon, D., Sözen, S. and Artan, N. (1996) The effect of heterotrophic yield on the assessment of the correction factor for anoxic growth. *Water Science and Technology*, **38**(1), 265-273.
144. Orhon, D., Tash, R. and Sözen, S. (1999b) Experimental basis of activated sludge treatment for industrial wastewaters-the state of the art. *Water Science and Technology*, **40**(1), 1-11.
145. Otte, S., Grobber, N. G., Robertson, L. A., Jetten, M. S. M. and Kuenen, J. G. (1996) Nitrous oxide production by *Alcaligenes faecalis* under transient and dynamic aerobic and anaerobic conditions. *Applied and Environmental Microbiology*, **62**, 2421-2426.
146. Pereira, H., Lemos, P. C., Reis, M. A., Crespo, J. P. S. G., Carrondo, M. J. T. and Santos, H. (1996) Model for carbon metabolism in biological phosphorus removal processes based on *in vivo* ¹³C-NMR labelling experiments. *Water Research*, **30**(9), 2128-2138.
147. Philips, S. and Verstraete, W. (2001) Effect of repeated addition of nitrite to semi-continuous activated sludge reactors. *Bioresource Technology*, **80**, 73-82.
148. Pitman, A. R. (1991) Design considerations for nutrient removal activated sludge plants, *Water Science and Technology*, **23**(4-6), 781-790.

149. Randall, A. A., Chen, Y., Liu, Y. H. and McCue, T. (2002) Polyhydroxyalkanoate form and polyphosphate regulation: Keys to biological phosphorus and glycogen transformations? *IWA world water congress*, Melbourne (CD ROM), e20127a.
150. Randall, C. W. and Buth, D. (1984) Nitrite build-up in activated sludge resulting from temperature effects. *Journal of Water Pollution Control Federation*, **56**, 1039-1044.
151. Rickard, L. F. and McClintock, S. A. (1992) Potassium and magnesium requirements for enhanced biological phosphorus removal from wastewater. *Water Science and Technology*, **26(9-11)**, 2203-2206.
152. Russell J. M. (1980) Components of chemical oxygen demand in slaughterhouse and fellmongery effluents. *Technical Report No. 759*, Meat Industry Research Institute of New Zealand, Hamilton.
153. Russell, J. and Cooper, R. (1992) Nitrogen transformations and removal in three lagoon systems treating meat processing wastes. Publication No. **898**, Meat Industry Research Institute of New Zealand, Hamilton.
154. Russell, J. M., Cooper, R. N., and Lindsey, S. B. (1993) Soil denitrification rates at wastewater irrigation sites receiving primary treated and anaerobically treated meat processing effluent. *Bioresource Technology*, **43**, 41-46.
155. Safley, L. M. and Westerman, P. W. (1992) Performance of a low temperature lagoon digester. *Bioresource Technology*, **41**, 167-175.
156. Sanin, D. and Vesilind, P. A. (2000) Bioflocculation of activated sludge: The role of calcium ions and extracellular polymers. *Environmental Technology*, **21**, 1405-1412.
157. Satoh, H., Mino, T. and Matsuo, T. (1992) Uptake of organic substrates and accumulation of polyhydroxyalkanoates linked with glycolysis of intracellular carbohydrates under anaerobic conditions in the biological excess phosphate removal processes. *Water Science and Technology*, **26(5-6)**, 933-942.
158. Satoh, H., Okuda, E., Mino, T. and Matsuo, T. (2000) Calibration of kinetic parameters in the IAWQ Activated Sludge Model: a pilot scale experience. *Water Science and Technology*, **42(3-4)**, 29-34.
159. Satoh, H., Ramey, W. D., Koch, F. A., Oldham, W. K., Mino, T. and Matsuo, T. (1996) Anaerobic substrate uptake by the enhanced biological phosphorus removal activated sludge treating real sewage. *Water Science and Technology*, **34(1-2)**, 9-16.
160. Sayed, S., van Campen, L. and Lettinga, L. (1987) Anaerobic treatment of slaughterhouse waste using a granular sludge UASB reactor. *Biological wastes*, **21**, 11-28.
161. Schmidt, I. and Bock, E. (1997) Anaerobic ammonia oxidation with nitrogen dioxide by *Nitrosomonas eutropha*. *Archives of Microbiology*, **167**, 106-111.
162. Schönborn., Bauer, H. and Roske, I. (2001) Stability of enhanced biological phosphorus removal and composition of polyphosphate granules. *Water Research*, **35(13)**, 3190-3196.
163. Sharma, B. and Ahlert, R. C. (1977) Nitrification and nitrogen removal. *Water Research*, **11**, 897-925.
164. Siegrist, H. and Gujer, W. (1994) Nitrogen removal in activated sludge systems including denitrification in secondary clarifiers. *Water Science and Technology*, **30(6)**, 101-111.

165. Slaney, A. and Van Oostrom, A. (1997) Meat processing wastewater treatment in a sequencing batch reactor. In *Proceedings of the 43rd International Congress of Meat Science and Technology*. pp. 526-527. Auckland, New Zealand.
166. Smolders, G. J. F., Van der Meij, J., Van Loosdrecht, M. C. M. and Heijnen, J. J. (1994a) Model of the anaerobic metabolism of the biological phosphorus removal process: Stoichiometry and pH influence. *Biotechnology and Bioengineering*, **43**, 461-470.
167. Smolders, G. J. F., Van der Meij, J., Van Loosdrecht, M. C. M. and Heijnen, J. J. (1995a) A structured metabolic model for anaerobic and aerobic stoichiometry and kinetics of the biological phosphorus removal process. *Biotechnology and Bioengineering*, **47**, 277-287.
168. Smolders, G. J. F., Van Loosdrecht, M. C. M. and Heijnen, J. J. (1994b) pH : key factor in the biological phosphorus removal process. *Water Science and Technology*, **29(7)**, 71-74.
169. Smolders, G. J. F., Van Loosdrecht, M. C. M. and Heijnen, J. J. (1995b) A metabolic model for the biological phosphorus removal process. *Water Science and Technology*, **31(2)**, 79-93.
170. Snoeyink, V. L. and Jenkins, D. (1980) *Water Chemistry*. John Wiley and Sons, Inc., New York, USA.
171. Sollfrank, U. and Gujer, W. (1991) Characterisation of domestic wastewater for mathematical modelling of the activated sludge process. *Water Science and Technology*, **23**, 1057-1066.
172. Somiya, I., Tsuno, H. and Matsumoto, M. (1988) Phosphorus release-storage reaction and organic substrate behaviour in biological phosphorus removal. *Water Research*, **22(1)**, 49-58.
173. Sorm R., Bortone, G., Saltarelli, R., Jenicek, P., Wanner, J. and Tilche, A. (1996) Phosphate uptake under anoxic conditions and fixed film nitrification in nutrient removal activated sludge system. *Water Research*, **30(7)**, 1573-1584.
174. Sözen, S., Cokgor, E. U., Orhon, D. and Henze, M. (1998) Respirometric analysis of activated sludge behaviour-II. Heterotrophic growth under aerobic and anoxic conditions. *Water Research*, **32(2)**, 476-488.
175. Sözen, S., Orhon, D. and San, H. A. (1996) A new approach for the evaluation of the maximum specific growth rate in nitrification. *Water Research*, **30(7)**, 1661-1669.
176. Stebor, T. W., Berndt, C. L., Marman, S. and Gabriel, R. (1990) Operating experience: Anaerobic treatment at Packerland Packing. In *Proceedings of the 44th Purdue Industrial Waste Conference*. pp. 825-834. Lewis Publishers, Inc., Chelsea, Michigan 48118.
177. Steiner, N. and Gec, R. (1992) Plant experience using hydrogen peroxide for enhanced fat floatation and BOD removal. *Environmental Progress*, **11**, 261-264.
178. Stenstrom, M. K. and Song, S. S. (1991) Effects of oxygen transport limitation on nitrification in the activated sludge process. *Research Journal Water Pollution Control Federation*, **63(3)**, 208-219.
179. Subramaniam, K., Greenfield, P. F., Ho, K. M., Johns, M. R. and Keller, J. (1994) Efficient biological nutrient removal in high strength wastewater using combined anaerobic-sequencing batch reactor treatment. *Water Science and Technology*, **30(6)**, 315-321.

180. Suwa, Y., Suzuki, T., Toyohara, H., Yamagishi, T and Urushigawa, Y. (1992) Single stage, single-sludge nitrogen removal by an activated sludge process with cross-flow filtration. *Water Research*, **26(9)**, 1149-1157.
181. Temmink, H., Petersen, B., Isaacs, S. and Henze, M. (1996) Recovery of biological phosphorus removal after periods of low organic loading. *Water Science and Technology*, **34(1-2)**, 1-8.
182. Travers, S. M. and Lovett, D. A. (1984) Activated sludge treatment of slaughterhouse wastewater-II. Influence of dissolved oxygen concentration. *Water Research*, **18**, 435-439.
183. Travers, S. M. and Lovett, D. A. (1985) Pressure flotation of slaughterhouse wastewaters using carbon dioxide. *Water Research*, **19**, 1479-1482.
184. Turk, O. and Mavinic, D. S. (1989) Maintaining nitrite build up in a system acclimated to free ammonia. *Water Research*, **23**, 1383-1388.
185. Van Bentum, W. A. J., Garrido, J., Mathijse, C., Sunde, J., Van Loosdrecht, M. C. M. and Heijnen, J. J. (1998) Nitrogen removal in intermittent aerated biofilm airlift suspension reactor. *Journal of Environmental Engineering*, **124**, 239-248.
186. Van Loosdrecht, M. C. M. and Henze, M. (1999) Maintenance, endogenous respiration, lysis, decay and predation. *Water Science and Technology*, **39(1)**, 107-117.
187. Van Loosdrecht, M. C. M. and Jetten, M. S. M. (1998) Microbiological conversions in nitrogen removal. *Water Science and Technology*, **38(1)**, 1-7.
188. Van Loosdrecht, M. C. M., Pot, M. A. and Heijnen, J. J. (1997) Importance of bacterial storage polymers in bioprocesses. *Water Science and Technology*, **35(1)**, 41-47.
189. Van Starckenburg, W., Rensink, J. H. and Rijs, G. B. (1993) Biological phosphorus removal: State of the art in Netherlands. *Water Science and Technology*, **27(5-6)**, 317-328.
190. Van Veldhuizen, H. M., Van Loosdrecht, M. C. M. and Heijnen, J. J. (1999) Modelling biological phosphorus and nitrogen removal in a full scale activated sludge process. *Water Research*, **33(16)**, 3459-3468.
191. Wachtmeister, A. Kuba, T. Van Loosdrecht, M. C. M. and Heijnen, J. J. (1997) A sludge characterisation assay for aerobic and denitrifying phosphorus removing sludge. *Water Research*, **31(3)**, 471-478.
192. Wang, N., Peng, J. and Hill, G. (2002) Biochemical model of glucose induced enhanced biological phosphorus removal under anaerobic condition. *Water Research*, **36**, 49-58.
193. Wanner J., Chudoba, J., Kucman, K. and Proske, L. (1987) Control of activated sludge filamentous bulking – VII. Effect of anoxic conditions. *Water Research*, **21(12)**, 1447-1451.
194. Wanner, J. (1992) Comparison of biocenoses from continuous and sequencing batch reactors, *Water Science and Technology*, **25(6)**: 239-249.
195. Wentzel, M. C., Dold, P. L., Ekama, G. A. and Marais, G. V. R. (1985) Kinetics of biological phosphorus release. *Water Science and Technology*, **17(11-12)**, 57-71.
196. Wentzel, M. C., Ekama, G. A. and Marais, G. V. R. (1992) Processes and modelling of nitrification denitrification biological excess phosphorus removal systems - a review. *Water Science and Technology*, **25(6)**, 59-82.

197. Wentzel, M. C., Ekama, G. A., Loewenthal, R. E., Dold, P. L. and Marais, G. V. R. (1989) Enhanced polyphosphate organism cultures in activated sludge – Part III: Kinetic model. *Water SA*, **15**(2), 89-102.
198. Wentzel, M. C., Lotter, L. H., Ekama, G. A., Loewenthal, R. E. and Marais, G. V. R. (1991) Evaluation of biochemical models for biological excess phosphorus removal. *Water Science and Technology*, **23**, 567-576.
199. Wentzel, M. C., Lotter, L. H., Loewenthal, R. E. and Marais, G. V. R. (1986) Metabolic behaviour of *Acinetobacter spp.* in enhanced biological phosphate removal - a biochemical model. *Water SA*, **12**(4), 209-244.
200. Wilderer, P. A., Irvine, R. L. and Goronszy, C. (2001) *Sequencing Batch Reactor Technology*. IWA publishing, London SW1H 0QS, UK.
201. Wilderer, P. A., Jones, W. L. and Dau, U. (1987) Competition in denitrification systems affecting reduction rate and accumulation of nitrite. *Water Research*, **21**(2), 239-245.
202. Willers, H. C., ten Have, P. J. W., Derikx, P. J. L. and Alen M. W. (1993) Temperature dependency of nitrification and required anoxic volume for denitrification in the biological treatment of veal calf manure. *Bioresource Technology*, **43**, 47-52.
203. Williamson, K. J. and McCarty, P. L. (1975) Rapid measurement of Monod half-velocity coefficients for bacterial kinetics. *Biotechnology and Bioengineering*, **14**, 915-924.
204. Witmayer, G., Froula, D. and Shell, G. (1985) Effective salinity on a rendering meat packing hide curing wastewater activated sludge process. In *Proceedings of the 40th Purdue Industrial Waste Conference*. pp. 79-87. Butterworth publishers, Stoneham, MA 02180.
205. Wong-Chong, G. M. and Loehr, R. G. (1975) The kinetics of microbial nitrification. *Water Research*, **9**, 1099-1106.
206. Yeoman, S., Stephenson, T., Lester, J. N. and Perry, R. (1988) The removal of phosphorus during wastewater treatment: A review. *Environmental pollution*, **49**, 183-233.

APPENDIX A

Assessment of Initial Soluble and Particulate Inert COD

The batch test results of the assessment of initial soluble and particulate inert COD are tabulated in Table A1.

Table A1 Meat processing wastewater and glucose reactor COD (mg L^{-1}) with time

Date	Days	Glucose (soluble)	Filtered meat wastewater		Raw sample	
			Soluble	Total	Soluble	Total
10/02/00	0	656	656	656	656	1072
12/02/00	2	423	162	495	189	621
14/02/00	4	61	157	340	192	419
16/02/00	6	44	185	336	185	428
18/02/00	8	32.5	181	289	190	389
22/02/00	12	38.9	141	251	163	364
24/02/00	14	48.8	77.4	186	158	330
28/02/00	18	29.5	69.2	164.5	151	325
1/03/00	20	26	64	140.2	161	330
5/03/00	24	24.8	62.1	130.3	186	341

Calculation

The soluble and particulate inert COD were obtained as described by Orhon *et al.* (1999).

Nomenclature

C_{S1} –Initial total biodegradable COD of wastewater (mg COD L^{-1})

C_{T1} –Initial total COD of wastewater (mg COD L^{-1})

$(C_T)_1, (C_T)_2$ –Final total COD in the raw wastewater and filtered wastewater reactors (mg COD L^{-1})

f_{ES}, f_{EX} –Fraction of soluble and particulate inert COD generated in biomass decay

S_{G1} –Initial COD in the glucose reactor (mg COD L^{-1})

$(S_G)_1$ –Final soluble COD of glucose reactor (mg COD L^{-1})

S_{I1} –Initial soluble inert COD of wastewater (mg COD L^{-1})

$(S_P)_G$ –residual soluble microbial products generated in glucose reactor

	(mg COD L ⁻¹)
(S _P) ₂	–residual soluble microbial products generated in filtered wastewater reactor (mg COD L ⁻¹)
S _{S1}	–Initial soluble biodegradable COD of wastewater (mg COD L ⁻¹)
S _{T1}	–Initial soluble COD of wastewater (mg COD L ⁻¹)
(S _T) ₁ , (S _T) ₂	–Final soluble COD in the raw wastewater and filtered wastewater reactors (mg COD L ⁻¹)
X _{I1}	–Initial particulate inert COD of wastewater (mg COD L ⁻¹)
X _P	–Residual particulate microbial products generated (mg COD L ⁻¹)
(X _P) ₁	–Residual particulate microbial products generated in raw wastewater reactor (mg COD L ⁻¹)
(X _P) ₂	–Residual particulate microbial products generated in filtered wastewater reactor (mg COD L ⁻¹)
(X _T) ₁	–Final particulate COD of raw wastewater reactor (mg COD L ⁻¹)
Y _H	–Heterotrophic yield coefficient (mg cell COD (mg COD) ⁻¹)
Y _{SP}	–fraction of biodegradable COD converted into soluble inert metabolic products (mg cell COD (mg COD) ⁻¹)
Y _{SP}	–fraction of biodegradable COD converted into soluble inert metabolic products (mg cell COD (mg COD) ⁻¹)

Assessment of f_{ES} from the glucose reactor

$$Y_{SP} = f_{ES} \cdot Y_H = \frac{(S_P)_G}{S_{G1}} = \frac{24.8}{656} = 0.0378$$

$$\text{Therefore, } f_{ES} = \frac{0.0378}{0.63} = 0.06$$

Assessment of S_{I1} from the soluble wastewater reactor

$$(S_P)_2 = (S_T)_2 - S_{I1} = f_{ES} \cdot Y_H (S_{T1} - S_{I1})$$

$$S_{I1} = \frac{(S_T)_2 - f_{ES} \cdot Y_H \cdot S_{T1}}{(1 - f_{ES} \cdot Y_H)}$$

$$S_{I1} = \frac{62.1 - 0.06 * 0.63 * 656}{(1 - 0.06 * 0.63)}$$

$$S_{I1} = 38.77 \text{ mg } L^{-1}$$

$$S_{T1} = 656 \text{ mg } L^{-1} \quad (C_T)_2 = 130.3 \text{ mg } L^{-1} \quad (S_T)_2 = 62.1 \text{ mg } L^{-1}$$

$$X_{P2} = (C_T)_2 - (S_T)_2 = 130.3 - 62.1 = 68.2 \text{ mg } L^{-1}$$

$$S_{S1} = S_{T1} - S_{I1} = 656 - 38.8 = 617.2 \text{ mg } L^{-1}$$

$$Y_{XP} = f_{EX} Y_H = \frac{(X_P)_2}{S_{S1}} = \frac{68.2}{617.2} = 0.110$$

$$f_{EX} = \frac{1}{Y_H} \cdot \frac{[(C_T)_2 - (S_T)_2]}{(S_{T1} - S_{I1})} = \frac{1}{0.63} * 0.110 = 0.174$$

$$(X_T)_1 = (C_T)_1 - (S_T)_1 = X_{I1} + (X_P)_1 = 341 - 186 = 155$$

$$C_{S1} = C_{T1} - X_{I1} - S_{I1}$$

$$(X_P)_1 = f_{EX} \cdot Y_H (C_{T1} - X_{I1} - S_{I1})$$

$$X_{I1} = \frac{(X_T)_1 - f_{EX} Y_H (C_{T1} - S_{I1})}{(1 - f_{EX} Y_H)}$$

$$X_{I1} = \frac{155 - 0.174 * 0.63 * (1072 - 38.8)}{(1 - 0.174 * 0.63)} = 46.9 \text{ mg } L^{-1} \text{ COD}$$

$$C_{T1} = 1072 \text{ mg } L^{-1} \quad S_{T1} = 656 \text{ mg } L^{-1} \quad S_{I1} = 38.8 \text{ mg } L^{-1}$$

$$X_{I1} = 46.9 \text{ mg } L^{-1} \quad S_{S1} = 617.2 \text{ mg } L^{-1}$$

$$\frac{S_{S1}}{C_{T1}} = \frac{617.2}{1072} = 0.58$$

$$\frac{C_{T1} - X_{I1} - S_{I1}}{C_{T1}} = \frac{1072 - 46.9 - 38.8}{1072} = 0.92$$

APPENDIX B

%script file for determination of maximum specific growth rate of nitrifiers (example)

global Data

Data = [0 1.0894

0.8035 4.1719

1.0521 5.3757

1.7653 9.9655

2.1347 13.2957

2.7708 21.7264

3.016 25.351

];

xdata = Data(:,1);

ydata = Data(:,2);

x0 = [0.5,0.5,0.5]; % Starting guess

[x,resnorm] = lsqcurvefit('funnit',x0,xdata,ydata)

yi = 1.1727+1/0.2198*(exp(0.6127*xdata)-1);

plot(xdata,yi,'k-',xdata,ydata,'ko')

%function file for maximum specific growth rate of nitrifiers

function F = funnit(x,xdata)

F = x(3)+1/x(2)*(exp(x(1)*xdata)-1);

%x(1) = mumaxA-bA

%x(2) = k = Ya(mumaxA-bA)/(mumaxA*XA0)

%x(3) = initial nox nitrogen

Table B1 Conversion table (Smolders *et al.*, 1995 b)

Component	Chemical formulae	Unit	M (g)	COD (g)
Acetate	CH ₃ COO ⁻	1 C-mol	30	32
PHB	(C ₄ H ₆ O ₂) _n	1 C-mol	21.5	36
PHV	(C ₅ H ₈ O ₂) _n	1 C-mol	20	38.4
Biomass	C ₆₇ H ₁₃₉ O ₃₆ N ₁₃ P	1 C-mol	26	36
Glycogen	C ₆ H ₁₀ O ₅	1 C-mol	27	32
Phosphate	PO ₄ ³⁻	1 P-mol	31	0
Propionic acid	C ₃ H ₆ O ₂	1 C-mol	24.67	37.3
Butyric acid	C ₄ H ₈ O ₂	1 C-mol	22	40
Valeric acid	C ₅ H ₁₀ O ₂	1 C-mol	20.4	41.5
Caproic acid	C ₆ H ₁₂ O ₂	1 C-mol	19.3	42.6

APPENDIX C

```

clear all
% script file for modified ASM 1 model
% N.Thayalakumaran

global qset; % feed rate , l/h
global yh; % yield for heterotrophic biomass, g cell COD formed /
g COD oxidized
global ixb; % mass nitrogen per mass of COD in biomass
global ya; % yield for autotrophic biomass, g cell COD formed / g N
oxidized
global fp; % fraction of biomass leading to particulate products,
dimensionless
global ixp; % mass nitrogen per mass of COD in products from
biomass,
global mumaxh; % maximum specific growth rate for heterotrophic
biomass, h-1
global ks; % half saturation constant for heterotrophic biomass,
g COD m-3
global koh; % oxygen half saturation coefficient for heterotrophic
biomass, g O2 m-3
global kno; % nitrate half saturation coefficient for denitrifying
heterotrophic biomass, g NO3 - N m-3
global etag; % correction factor for heterotrophic growth in anoxic
condition
global mumaxa; % maximum specific growth rate for autotrophic biomass,
d-1
global knh; % ammonia half saturation coefficient for autotrophic
biomass, g NH3 - N m-3
global koa; % oxygen half saturation coefficient for autotrophic
biomass, g O2 m-3
global bh; % decay coefficient for heterotrophic biomass, h-1
global ba; % decay coefficient for autotrophic biomass, h-1
global ka; % ammonification rate, m3 (g COD h)-1
global kh; % maximum specific hydrolysis rate, g slowly
biodegradable COD (g cell COD h)-1
global kx; % half saturation coefficient for hydrolysis of slowly
biodegradable substrate, g slowly biodegradable COD (g
cell COD)-1
global etah; % correction factor for hydrolysis under anoxic
condition, dimensionless
global si0; % soluble inert COD in wastewater, mg COD/L
global ss0; % concentration of readily biodegradable COD in
wastewater, mg COD/L
global xi0; % inert suspended organic matter concentration in
wastewater, mg COD/L
global xs0; % slowly biodegradable organic matter concentration in
wastewater, mg COD/L
global so0; % oxygen concentration (negative COD), mg O2/L
global sno0; % soluble nitrate nitrogen concentration in wastewater,
mg N/L
global snh0; % soluble ammonia nitrogen concentration in wastewater,
mg N/L
global snd0; % soluble biodegradable organic nitrogen concentration
in wastewater, mg N/L
global xnd0; % slowly biodegradable organic nitrogen concentration
in wastewater, mg N/L
global salk0; % Alkalinity, bicarbonate molar unit

```

```

%get input data
Simtime = 6.0;
qset = 6.0;
yh = 0.63;
ixb = 0.086;
ya = 0.20;
fp = 0.08;
ixp = 0.06;
mumaxh = 2.0/24.0;
ks = 8.0;
koh = 0.20;
kno = 0.50;
etag = 0.80;
mumaxa = 0.75/24.0;
knh = 1.0;
koa = 1.2;
bh = 0.24/24.0;
ba = 0.10/24.0;
ka = 0.40/24.0;
kh = 3.0/24.0;
kx = 0.03;
etah = 0.40;

si0 = 70.0;
ss0 = 295.0;
xi0 = 70.0;
xs0 = 1300.0;
so0 = eps;
sno0 = 0.5;
snh0 = 101.8;
snd0 = 19.0;
xnd0 = 24.0;
salk0 = 7.50;

%SBR batch test
%so0= eps;
%si0= 68.70;
%ss0= 329.6;
%xi0= 68.70;
%xs0= 1251.0;
%snh0= 121.0;
%sno0= 2.493;
%salk0= 7.5;
%snd0 = 19.0;
%xnd0 = 24.0;

%set initial values
yi=[13.5,70.0,eps,1394/0.9,eps,2535.0/0.9,120.0/0.9,517.0/0.9,eps,2.50
,0.53,eps,eps,3.5];
%yi=[13.5,70.0,eps,1394/0.9,eps,2535.0/0.9,120.0/0.9,517.0/0.9,eps,1.3
7,3.53,eps,eps,3.5];

% ODE solver options
options=odeset('MaxStep', 0.01);
Tspan = [0, Simtime];
% Solve ODE's
[t,y]= ode45('cod', Tspan, yi,options);
%output graphs
plot(t,y(:,10), 'k:',t,y(:,11), 'k-');
hold on;

```

```

t1=[0.0,8.0/60.0,17.0/60.0,45.0/60.0,60.0/60.0,90.0/60.0,120.0/60.0,15
0.0/60.0,180.0/60.0,195.0/60.0,210.0/60.0,225.0/60.0,240.0/60.0,270.0/
60.0,285.0/60.0,300.0/60.0,345.0/60.0];
y1=[.53,9.32,11.14,12.95,12.84,10.45,11.93,7.95,3.75,3.98,4.2,2.05,1.7
,1.59,.11,.23,.57];
xlabel('Time (hr)');
ylabel('NO_3 - N and NH_3 - N (mg L^{-1})');
%legend('NO_3 - N','NH_3 - N');
t4=[0.0,8.0/60.0,17.0/60.0,30.0/60.0,45.0/60.0,60.0/60.0,90.0/60.0,120
.0/60.0,150.0/60.0,180.0/60.0,195.0/60.0,210.0/60.0,225.0/60.0,240.0/6
0.0,270.0/60.0,285.0/60.0,300.0/60.0,345.0/60.0];
y4=[2.5,0.45,0.14,0.12,0.09,0.05,0.11,0.05,0.196,1.19,0.564,0.328,1.12
9,2.006,2.418,3.182,2.578,2.541];
plot(t1,y1,'ko',t4,y4,'ks');
hold off;

```

```

%batch sbr
%plot(t,y(:,10),'k:',t,y(:,11),'k-');
%hold on;
%t1=[1.0/60.0,15.0/60.0,30.0/60.0,45.0/60.0,60.0/60.0,75.0/60.0,90.0/6
0.0,105.0/60.0,120.0/60.0,135.0/60.0,150.0/60.0,165.0/60.0,180.0/60.0,
195.0/60.0,210.0/60.0,225.0/60.0,240.0/60.0,255.0/60.0,270.0/60.0,285.
0/60.0,300.0/60.0,345.0/60.0];
%y2=[14.77,14.31,14.31,17.54,16.62,16.62,15.23,16.62,18.0,13.85,11.08,
10.15,6.08,6.11,6.11,3.23,1.38,0.0,0.0,0.0,0.0,0.0];
%y1=[1.369,0.229,0.309,0.107,0.391,0.136,0.178,0.19,0.426,0.712,1.891,
3.081,5.971,4.064,3.527,5.515,5.614,6.663,7.915,7.843,7.758,6.173];
%plot(t1,y1,'ks',t1,y2,'ko');
%xlabel('Time (hr)');
%ylabel('NO_3 - N and NH_3 - N (mg L^{-1})');
%legend('NO_3 - N','NH_3 - N');
%hold off;

```

```

function dy=cod(t,y)
% function file for modified ASM 1 model
% N.Thayalakumaran

```

```

%define global variables
global qset;
global yh;
global ixb;
global ya;
global fp;
global ixp;
global mumaxh;
global ks;
global koh;
global kno;
global etag;
global mumaxa;
global knh;
global koa;
global bh;
global ba;
global ka;
global kh;
global kx;
global etah;
global si0;
global ss0;

```

```

global xi0;
global xs0;
global so0;
global sno0;
global snh0;
global snd0;
global xnd0;
global salk0;

%calculate new values for dependent variables
vr=y(1);
si=y(2);
ss=y(3);
xi=y(4);
xs=y(5);
xbh=y(6);
xba=y(7);
xp=y(8);
so=y(9);
sno=y(10);
snh=y(11);
snd=y(12);
xnd=y(13);
salk=y(14);

if t<=8.0/60.0
    q=1.5/(8.0/60.0);
else
    q=eps;
end
if t<=2.0
    so=eps;
elseif t<=3.0
    so=0.50;
elseif t<=3.5
    so=eps;
elseif t<=4.5
    so=3.75;
elseif t<=5.0
    so=0.50;
else
    so=eps;
end

%process rate vectors
rho=[mumaxh*(ss/(ks+ss))*(so/(koh+so))*xbh;
      mumaxh*(ss/(ks+ss))*(koh/(koh+so))*(sno/(kno+sno))*etah*xbh;
      mumaxa*(snh/(knh+snh))*(so/(koa+so))*xba;
      bh*xbh;
      ba*xba;
      ka*snd*xbh*(so/(koh+so)+sno/(kno+sno)*etah*koh/(koh+so)];

kh*(xs/xbh)/(kx+xs/xbh)*(so/(koh+so)+etah*(koh/(koh+so))*(sno/(kno+sno)
)))*xbh;

kh*(xs/xbh)/(kx+xs/xbh)*(so/(koh+so)+etah*(koh/(koh+so))*(sno/(kno+sno)
)))*xbh*(xnd/xs)];
%differential equations
dvr=q;
dsi=q*(si0-si)/vr;
dss=q*(ss0-ss)/vr-1/yh*rho(1)-1/yh*rho(2)+rho(7);

```

```

dxi=q*(xi0-xi)/vr;
dxs=q*(xs0-xs)/vr+(1-fp)*rho(4)+(1-fp)*rho(5)-rho(7);
dxbh=-q*xbh/vr+rho(1)+rho(2)-rho(4);
dxba=-q*xba/vr+rho(3)-rho(5);
dxp=-q*xp/vr+fp*rho(4)+fp*rho(5);
dso=q*(so0-so)/vr-(1-yh)/yh*rho(1)-(4.57-ya)/ya*rho(3);
dsno=q*(sno0-sno)/vr-(1-yh)/(2.86*yh)*rho(2)+1/ya*rho(3);
dsnh=q*(snh0-snh)/vr-ixb*rho(1)-ixb*rho(2)+(-ixb-1/ya)*rho(3)+rho(6);
dsnd=q*(snd0-snd)/vr-rho(6)+rho(8);
dxnd=q*(xnd0-xnd)/vr+(ixb-fp*ixp)*rho(4)+(ixb-fp*ixp)*rho(5)-rho(8);
dsalk=q*(salk0-salk)/vr-ixb/14*rho(1)+((1-yh)/(14*2.86*yh)-
ixb/14)*rho(2)+(-ixb/14-1/(7*ya))*rho(3)+1/14*rho(6);

%produce output vector
dy=[dvr;dsi;dss;dxi;dxs;dxbh;dxba;dxp;dso;dsno;dsnh;dsnd;dxnd;dsalk];

```

APPENDIX D

```

clear all
% script file for modified ASM 2 model
% N.Thayalakumaran

global qset; % feed rate , l/h
% conversion factors for conservation equation
global insf;
global insi;
global inxi;
global inxs;
global inbm;
global ipsf;
global ipsi;
global ipxi;
global ipxs;
global ipbm;
global itssxi;
global itssxs;
global itssbm;
%stoichiometric parameters
global fsi;
global yh;
global fxi;
global ypao;
global ypo4;
global ypha;
global fxi;
global yaut;
global ymgpha;
global ymgxpp;
%kinetic parameters
%hydrolysis of particulate substrate
global kh;
global etano3h;
global etafe;
global ko2h;
global kno3;
global kx;
%heterotrophic organism
global muh;
global qfe;
global etano3;
global ko2;
global bh;
global kf;
global kfe;
global ka;
global knh4;
global kp;
global kalk;
%phosphorus accumulating organisms
global qpha;
global qpp;
global mupao;
global bpao;
global bpp;
global bpha;
global ko2p;

```

```
global kno3p;
global kps;
global kpp;
global kmax;
global kipp;
global kpha;
global etano3p;
global ysa;
global qgly;
global kgly;
global kphagly;
global bgly;
global kmg;
%nitrifying organism
global muaut;
global baut;
global ko2aut;
global knh4aut;
global kalkaut;
%precipitation
global kpre;
global kred;
global kalkred;
%initial condition
global so20;
global sf0;
global sa0;
global snh40;
global sno30;
global spo40;
global si0;
global salk0;
global sn20;
global xi0;
global xs0;
global xtss0;
global xh0;
global xmeoh0;
global xmep0;
global smg0;
%stoichiometric parameters have to be found by with the continuity
equation
global nu1nh4;
global nu2nh4;
global nu3nh4;
global nu1po4;
global nu2po4;
global nu3po4;
global nu1alk;
global nu2alk;
global nu3alk;
global nu1tss;
global nu2tss;
global nu3tss;
global nu12no3;
global nu13o2;
global nu14no3;
global nu15po4;
global nu18nh4;
global nu19nh4;
global nu19po4;
```

```

global nu20alk;
global nu21alk;
global nu4nh4;
global nu5nh4;
global nu6nh4;
global nu7nh4;
global nu8nh4;
global nu9nh4;
global nu13nh4;
global nu14nh4;
global nu15nh4;
global nu4po4;
global nu5po4;
global nu6po4;
global nu7po4;
global nu8po4;
global nu9po4;
global nu4alk;
global nu5alk;
global nu6alk;
global nu7alk;
global nu8alk;
global nu9alk;
global nu10alk;
global nu11alk;
global nu12alk;
global nu13alk;
global nu14alk;
global nu15alk;
global nu16alk;
global nu17alk;
global nu18alk;
global nu19alk;
global nu4tss;
global nu5tss;
global nu6tss;
global nu7tss;
global nu9tss;
global nu10tss;
global nu11tss;
global nu12tss;
global nu13tss;
global nu14tss;
global nu15tss;
global nu16tss;
global nu17tss;
global nu18tss;
global nu19tss;
global nu22tss;
global nu23tss;
%get input data

Simtime = 6.0; hours
qset = 9.0;
%Typical conversion factors for conservation equation
%nitrogen
insf=0.03; % N content of soluble substrate SF, gN(g COD)-1
insi=0.01; % N content of inert soluble COD SI, gN(g COD)-1
inxi=0.02; % N content of inert particulate COD XI, gN(g COD)-1
inxS=0.04; % N content of particulate substrate XS, gN(g COD)-1
inbm=0.07; % N content of biomass XH, XPAO, XAUT, gN(g COD)-1

```

```

%phosphorus
ipsf=0.01; % P content of soluble substrate SF, gP(g COD)-1
ipsi=0.0; % P content of inert soluble COD SI, gP(g COD)-1
ipxi=0.01; % P content of inert particulate COD XI, gP(g COD)-1
ipxs=0.01; % P content of particulate substrate XS, gP(g COD)-1
ipbm=0.02; % P content of biomass XH, XPAO, XAUT, gP(g COD)-1
%total suspended solids
itssxi=0.75; % TSS to XI ratio, gTSS(g COD)-1
itssxs=0.75; % TSS to XS ratio, gTSS(g COD)-1
itssbm=0.90; % TSS to biomass ratio for XH, XPAO, XAUT, gTSS(g COD)-1
%Typical stoichiometric parameters
fsi=0.0; % Fraction of inert COD in particulate substrate, gCOD(g COD)-1
yh=0.63; % Yield coefficient of heterotrophic organisms, gCOD(g COD)-1
fxi=0.1; % Fraction of inert COD generated in biomass lysis, gCOD(g
COD)-1
ypao=0.63; % Yield coefficient (biomass/PHA), gCOD(g COD)-1
ypo4=0.33; % PP requirement (SPO4 release) for PHA storage, gP(g COD)-1
ypha=0.2; % PHA requirement for PP storage, gCOD(g P)-1
yaut=0.20; % Yield coefficient (biomass/nitrate), gCOD(g N)-1
ysa=0.68; % SA requirement for PP storage gCOD(g COD)-1
ymgpha=0.065; % yield of Mg during PHA storage g Mg(g COD)-1
ymgpp=0.163; % yield of Mg during PP storage g Mg(g P)-1
% typical values for kinetic parameters
%hydrolysis of particulate substrate
kh=3.0/24.0; % Hydrolysis rate constant h-1
etano3h=0.4; % anoxic hydrolysis reduction factor
etafe=0.02; % anaerobic hydrolysis reduction factor
ko2h=0.50; % saturation/inhibition coefficient for oxygen g O2 m-3
kno3=0.50; % saturation/inhibition coefficient for nitrate g N m-3
kx=0.10; % saturation coefficient for particulate COD g COD (gCOD)-1
%heterotrophic organism
muh=2.0/24.0; % maximum growth rate on substrate h-1
qfe=3.0/24.0; % maximum rate for fermentation, g COD (gCOD)-1h-1
etano3=0.80; % reduction factor for denitrification
ko2=0.50;% saturation/inhibition coefficient for oxygen g O2 m-3
bh=0.24/24.0; % rate constant for lysis h-1
kf=8.0; % saturation coefficient for growth on SF g COD m-3
kfe=8.0; % saturation coefficient for fermentation of SF g COD m-3
ka=8.0; % saturation coefficient for SA (acetate) g COD m-3
knh4=0.05; % saturation coefficient for ammonium (nutrient) g N m-3
kp=0.01; % saturation coefficient for phosphorus (nutrient) g P m-3
kalk=0.10; % saturation coefficient for alkalinity mol HCO3-m-3
%phosphorus accumulating organisms
qpha=6.0/24.0; % rate constant for storage of PHA (base: XPP) g XPHA(g
XPAO)-1h-1
qpp=2.0/24.0; % rate constant for storage of PP g XPP(g XPAO)-1h-1
mupao=1.0/24.0; % maximum growth rate h-1
etano3p=0.60; % reduction factor for anoxic activity
bpao=0.20/24.0; % rate constant for lysis of XPAO h-1
bpp=0.20/24.0; % rate constant for lysis of XPP h-1
bpha=0.20/24.0; % rate constant for lysis of XPHA h-1
ko2p=0.20; % saturation/inhibition coefficient for oxygen g O2 m-3
kno3p=0.50; % saturation coefficient for nitrate g N m-3
kps=0.20; % saturation coefficient for phosphorus in PP storage g P m-3
kpp=0.01; % saturation coefficient for poly-phosphate g PP (g PAO)-1
kmax=0.34; % maximum ratio of XPP/XPAO g PP (g PAO)-1
kipp=0.02; % inhibition coefficient for XPP storage g PP (g PAO)-1
kpha=0.01; % saturation coefficient for PHA g PHA (g PAO)-1
qgly=3.0/24.0; % rate constant for glycogen storage
kgly=0.01; % saturation coefficient for XGly, gXgly COD (g XPAO COD)-1

```

```

kphagly=0.10; % saturation coefficient for XPHA for XGly storage, gCOD
(g XPAO COD)-1
bgly=0.2/24.0; % decay rate constant of glycogen (h)-1
kmg=4.7; % Mg saturation constant (mg L-1)
%nitrifying organisms
muaut=0.75/24.0; % maximum growth rate h-1
baut=0.10/24.0; % decay rate h-1
ko2aut=0.50; % saturation coefficient for oxygen g O2 m-3
knh4aut=1.0; % saturation coefficient for ammonium g N m-3
kalkaut=0.50; % saturation coefficient for alkalinity mol HCO3-m-3
%precipitation
kpre=1.0; % Rate constant for P precipitation m3 (g Fe(OH)3-1h-1)
kred=0.60; % Rate constant for redissolution h-1
kalkred=0.50; % saturation coefficient for alkalinity mol HCO3-m-3
%influent data
%so20=eps;
%sf0=eps;
%sa0=295.0;
%snh40=101.8;
%sno30=0.5;
%spo40=13.3;
%si0=70.0;
%salk0=7.5;
%sn20=15.0;
%xi0=70.0;
%xs0=1300.0;
%xtss0=505.0;
%xh0=eps;
%xmep0=eps;
%xmeoh0=eps;
%smg0=9.30;
%acetate influent data
so20=eps;
sf0=eps;
sa0=eps;
snh40=eps;
sno30=eps;
spo40=eps;
si0=eps;
salk0=eps;
sn20=eps;
xi0=eps;
xs0=eps;
xtss0=eps;
xh0=eps;
xmep0=eps;
xmeoh0=eps;
smg0=eps;
%SBR batch test
%so20=eps;
%sf0=eps;
%sa0=329.60;
%snh40=121.0;
%sno30=2.10;
%spo40=19.3;
%si0=68.70;
%salk0=7.5;
%sn20=15.0;
%xi0=68.70;
%xs0=1251.0;
%xtss0=450.0;

```

```

% xh0=eps;
% xmep0=eps;
% xmeoh0=eps;
% smg0=9.3;

% stoichiometric parameters have to be found by with the continuity
equation
% initial values
nu1nh4=0.01;
nu2nh4=0.01;
nu3nh4=0.01;
nu1po4=0.0;
nu2po4=0.0;
nu3po4=0.0;
nu1alk=0.001;
nu2alk=0.001;
nu3alk=0.001;
nu1tss=-0.75;
nu2tss=-0.75;
nu3tss=-0.75;
nu12no3=-0.07;
nu13o2=-0.6;
nu14no3=0.21;
nu15po4=0.01;
nu18nh4=-5.07;
nu19nh4=0.032;
nu19po4=0.01;
nu20alk=0.048;
nu21alk=-0.048;
nu4nh4=-0.022;
nu5nh4=-0.07;
nu6nh4=-0.022;
nu7nh4=-0.07;
nu8nh4=0.03;
nu9nh4=0.032;
nu13nh4=-0.07;
nu14nh4=-0.07;
nu15nh4=0.032;
nu4po4=-0.004;
nu5po4=-0.02;
nu6po4=-0.004;
nu7po4=-0.02;
nu8po4=0.01;
nu9po4=0.01;
nu4alk=-0.001;
nu5alk=0.021;
nu6alk=0.013;
nu7alk=0.035;
nu8alk=-0.014;
nu9alk=0.002;
nu10alk=0.012;
nu11alk=-0.003;
nu12alk=-0.008;
nu13alk=-0.004;
nu14alk=0.011;
nu15alk=0.002;
nu16alk=0.003;
nu17alk=-0.016;
nu18alk=-0.718;
nu19alk=0.002;
nu4tss=0.90;

```



```

0.0,0.0,0.0,nu19nh4,0.0,nu19po4,0.0,nu19alk,0.0,fxi,(1-
fxi),0.0,0.0,0.0,0.0,-1.0,nu19tss,0.0,0.0,0.0,0.0;
0.0,0.0,0.0,0.0,0.0,-
1.0,0.0,nu20alk,0.0,0.0,0.0,0.0,0.0,0.0,0.0,0.0,1.42,-
3.45,4.87,0.0,0.0;
0.0,0.0,0.0,0.0,0.0,1.0,0.0,nu21alk,0.0,0.0,0.0,0.0,0.0,0.0,0.0,0.0,-
1.42,3.45,-4.87,0.0,0.0;
0.0,0.0,0.0,0.0,0.0,0.0,0.0,0.0,0.0,0.0,0.0,0.0,0.0,-
1.0,0.0,nu22tss,0.0,0.0,1.0,0.0;

0.0,1.0,0.0,0.0,0.0,0.0,0.0,0.0,0.0,0.0,0.0,0.0,0.0,0.0,0.0,nu23ts
s,0.0,0.0,-1.0,0.0];

ici=[-1.0,0.0,0.0,0.0,0.0;
1.0,insf,ipsf,0.0,0.0;
1.0,0.0,0.0,-1.0/64.0,0.0;
0.0,1.0,0.0,1.0/14.0,0.0;
-64.0/14.0,1.0,0.0,-1.0/14.0,0.0;
0.0,0.0,1.0,-1.5/31.0,0.0;
1.0,insi,ipsi,0.0,0.0;
0.0,0.0,0.0,-1.0,0.0;
-24.0/14.0,1.0,0.0,0.0,0.0;
1.0,inxi,ipxi,0.0,itssxi;
1.0,inxs,ipxs,0.0,itssxs;
1.0,inbm,ipbm,0.0,itssbm;
1.0,inbm,ipbm,0.0,itssbm;
0.0,0.0,1.0,-1.0/31.0,3.23;
1.0,0.0,0.0,0.0,0.6;
1.0,inbm,ipbm,0.0,itssbm;
0.0,0.0,0.0,0.0,-1.0;
0.0,0.0,0.0,0.0,1.0;
0.0,0.0,0.205,0.0,1.0;
1.0,0.0,0.0,0.0,0.84;
0.0,0.0,0.0,2.0/24.0,0.0];
nulnh4=-
1*(vji(1,2)*ici(2,2)+vji(1,7)*ici(7,2)+vji(1,11)*ici(11,2))/ici(4,2);
nu2nh4=-
1*(vji(2,2)*ici(2,2)+vji(2,7)*ici(7,2)+vji(2,11)*ici(11,2))/ici(4,2);
nu3nh4=-
1*(vji(3,2)*ici(2,2)+vji(3,7)*ici(7,2)+vji(3,11)*ici(11,2))/ici(4,2);
nulpo4=-
1*(vji(1,2)*ici(2,3)+vji(1,7)*ici(7,3)+vji(1,11)*ici(11,3))/ici(6,3);
nu2po4=-
1*(vji(2,2)*ici(2,3)+vji(2,7)*ici(7,3)+vji(2,11)*ici(11,3))/ici(6,3);
nu3po4=-
1*(vji(3,2)*ici(2,3)+vji(3,7)*ici(7,3)+vji(3,11)*ici(11,3))/ici(6,3);
nulalk=-1*(vji(1,4)*ici(4,4)+vji(1,6)*ici(6,4))/ici(8,4);
nu2alk=-1*(vji(2,4)*ici(4,4)+vji(2,6)*ici(6,4))/ici(8,4);
nu3alk=-1*(vji(3,4)*ici(4,4)+vji(3,6)*ici(6,4))/ici(8,4);
nultss=-1*(vji(1,11)*ici(11,5))/ici(17,5);
nu2tss=-1*(vji(2,11)*ici(11,5))/ici(17,5);
nu3tss=-1*(vji(3,11)*ici(11,5))/ici(17,5);
nul3o2=-1*(vji(13,13)*ici(13,1)+vji(13,15)*ici(15,1))/ici(1,1);
nul5po4=-
1*(vji(15,10)*ici(10,3)+vji(15,11)*ici(11,3)+vji(15,13)*ici(13,3))/ici
(6,3);
nul8nh4=-1*(vji(18,5)*ici(5,2)+vji(18,16)*ici(16,2))/ici(4,2);
nul9nh4=-
1*(vji(19,10)*ici(10,2)+vji(19,11)*ici(11,2)+vji(19,16)*ici(16,2))/ici
(4,2);

```

```

nu19po4=-
1*(vji(19,10)*ici(10,3)+vji(19,11)*ici(11,3)+vji(19,16)*ici(16,3))/ici
(6,3);
nu20alk=-1*(vji(20,6)*ici(6,4))/ici(8,4);
nu21alk=-1*(vji(21,6)*ici(6,4))/ici(8,4);
nu4nh4=-1*(vji(4,2)*ici(2,2)+vji(4,12)*ici(12,2))/ici(4,2);
nu5nh4=-1*(vji(5,3)*ici(3,2)+vji(5,12)*ici(12,2))/ici(4,2);
nu6nh4=-
1*(vji(6,2)*ici(2,2)+vji(6,5)*ici(5,2)+vji(6,9)*ici(9,2)+vji(6,12)*ici
(12,2))/ici(4,2);
nu7nh4=-
1*(vji(7,5)*ici(5,2)+vji(7,9)*ici(9,2)+vji(7,12)*ici(12,2))/ici(4,2);
nu8nh4=-1*(vji(8,2)*ici(2,2)+vji(8,3)*ici(3,2))/ici(4,2);
nu9nh4=-
1*(vji(9,10)*ici(10,2)+vji(9,11)*ici(11,2)+vji(9,12)*ici(12,2))/ici(4,
2);
nu13nh4=-1*(vji(13,13)*ici(13,2))/ici(4,2);
nu14nh4=-
1*(vji(14,9)*ici(9,2)+vji(14,5)*ici(5,2)+vji(14,13)*ici(13,2))/ici(4,2
);
nu15nh4=-
1*(vji(15,10)*ici(10,2)+vji(15,11)*ici(11,2)+vji(15,13)*ici(13,2))/ici
(4,2);
nu4po4=-1*(vji(4,2)*ici(2,3)+vji(4,12)*ici(12,3))/ici(6,3);
nu5po4=-1*(vji(5,3)*ici(3,3)+vji(5,12)*ici(12,3))/ici(6,3);
nu6po4=-1*(vji(6,2)*ici(2,3)+vji(6,12)*ici(12,3))/ici(6,3);
nu7po4=-1*(vji(7,12)*ici(12,3))/ici(6,3);
nu8po4=-1*(vji(8,2)*ici(2,3)+vji(8,3)*ici(3,3))/ici(6,3);
nu9po4=-
1*(vji(9,10)*ici(10,3)+vji(9,11)*ici(11,3)+vji(9,12)*ici(12,3))/ici(6,
3);
nu4alk=-1*(vji(4,4)*ici(4,4)+vji(4,6)*ici(6,4))/ici(8,4);
nu5alk=-
1*(vji(5,3)*ici(3,4)+vji(5,4)*ici(4,4)+vji(5,6)*ici(6,4))/ici(8,4);
nu6alk=-
1*(vji(6,5)*ici(5,4)+vji(6,4)*ici(4,4)+vji(6,6)*ici(6,4))/ici(8,4);
nu7alk=-
1*(vji(7,3)*ici(3,4)+vji(7,5)*ici(5,4)+vji(7,4)*ici(4,4)+vji(7,6)*ici(
6,4))/ici(8,4);
nu8alk=-
1*(vji(8,3)*ici(3,4)+vji(8,4)*ici(4,4)+vji(8,6)*ici(6,4))/ici(8,4);
nu9alk=-1*(vji(9,4)*ici(4,4)+vji(9,6)*ici(6,4))/ici(8,4);
nu10alk=-
1*(vji(10,3)*ici(3,4)+vji(10,6)*ici(6,4)+vji(10,14)*ici(14,4)+vji(10,2
1)*ici(21,4))/ici(8,4);
nu11alk=-
1*(vji(11,6)*ici(6,4)+vji(11,14)*ici(14,4)+vji(11,21)*ici(21,4))/ici(8
,4);
nu12alk=-
1*(vji(12,5)*ici(5,4)+vji(12,6)*ici(6,4)+vji(12,14)*ici(14,4)+vji(12,2
1)*ici(21,4))/ici(8,4);
nu13alk=-1*(vji(13,6)*ici(6,4)+vji(13,4)*ici(4,4))/ici(8,4);
nu14alk=-
1*(vji(14,5)*ici(5,4)+vji(14,6)*ici(6,4)+vji(14,4)*ici(4,4))/ici(8,4);
nu15alk=-1*(vji(15,6)*ici(6,4)+vji(15,4)*ici(4,4))/ici(8,4);
nu16alk=-
1*(vji(16,6)*ici(6,4)+vji(16,14)*ici(14,4)+vji(16,21)*ici(21,4))/ici(8
,4);
nu17alk=-1*(vji(17,3)*ici(3,4))/ici(8,4);
nu18alk=-
1*(vji(18,4)*ici(4,4)+vji(18,5)*ici(5,4)+vji(18,6)*ici(6,4))/ici(8,4);

```

```

nu19alk=-1*(vji(19,4)*ici(4,4)+vji(19,6)*ici(6,4))/ici(8,4);
nu4tss=-1*(vji(4,12)*ici(12,5))/ici(17,5);
nu5tss=-1*(vji(5,12)*ici(12,5))/ici(17,5);
nu6tss=-1*(vji(6,12)*ici(12,5))/ici(17,5);
nu7tss=-1*(vji(7,12)*ici(12,5))/ici(17,5);
nu9tss=-
1*(vji(9,10)*ici(10,5)+vji(9,11)*ici(11,5)+vji(9,12)*ici(12,5))/ici(17,5);
nu10tss=-
1*(vji(10,14)*ici(14,5)+vji(10,15)*ici(15,5)+vji(10,20)*ici(20,5))/ici(17,5);
nulltss=-1*(vji(11,14)*ici(14,5)+vji(11,15)*ici(15,5))/ici(17,5);
nul2tss=-1*(vji(12,14)*ici(14,5)+vji(12,15)*ici(15,5))/ici(17,5);
nul3tss=-1*(vji(13,13)*ici(13,5)+vji(13,15)*ici(15,5))/ici(17,5);
nul4tss=-1*(vji(14,13)*ici(13,5)+vji(14,15)*ici(15,5))/ici(17,5);
nul5tss=-
1*(vji(15,10)*ici(10,5)+vji(15,11)*ici(11,5)+vji(15,13)*ici(13,5))/ici(17,5);
nul6tss=-1*(vji(16,14)*ici(14,5))/ici(17,5);
nul7tss=-1*(vji(17,15)*ici(15,5))/ici(17,5);
nul8tss=-1*(vji(18,16)*ici(16,5))/ici(17,5);
nul9tss=-
1*(vji(19,10)*ici(10,5)+vji(19,11)*ici(11,5)+vji(19,16)*ici(16,5))/ici(17,5);
nu22tss=-1*(vji(22,15)*ici(15,5)+vji(22,20)*ici(20,5))/ici(17,5);
nu23tss=-1*(vji(23,20)*ici(20,5))/ici(17,5);
%set initial values
%yi=[13.5,eps,eps,eps,0.53,2.50,0.5,70.0,3.5,15.0,1394.0/0.9,eps,2040.0/0.9,495.0/0.9,86.7/0.9,16.0/0.9,120.0/0.9,3435.0/0.9,eps,eps,158.6/0.9,3.50];
%yi=[15.0,eps,eps,80.0,0.53,2.839,1.927,70.0,3.5,15.0,730.0,eps,1085.6,259.0,31.8,28.13,63.4,1815.0,eps,eps,82.88,10.00]; %hac -75
yi=[15.0,eps,eps,87.905,24.11,4.798,4.931,70.0,3.5,15.0,605.0,350.9,1489.1,355.0,44.3,6.705,87.27,2455.0,eps,eps,118.8,10.0]; %ww
%yi=[15.0,eps,eps,213.2,24.1,5.536,0.811,70.0,3.5,15.0,1236.0,eps,1917.5,457.0,47.52,14.467,111.9,3165.0,eps,eps,176.43,4.0]; %hac-200
%yi=[13.5,eps,eps,eps,3.53,1.37,2.0,70.0,3.5,15.0,1394.0/0.9,eps,2040.0/0.9,495.0/0.9,74.5/0.9,16.0/0.9,120.0/0.9,3435.0/0.9,eps,eps,158.6/0.9,3.5];

% ODE solver options
options=odeset('MaxStep', 0.01);
Tspan = [0, Simtime];

% Solve ODE's
[t,y]= ode45('asm2e', Tspan, yi,options);

%plot(t,y(:,5), 'k-',t,y(:,6), 'k:',t,y(:,7), 'k-.');
%colordef black;
%hold on;
%t1=[0.0,8.0/60.0,17.0/60.0,45.0/60.0,60.0/60.0,90.0/60.0,120.0/60.0,150.0/60.0,180.0/60.0,195.0/60.0,210.0/60.0,225.0/60.0,240.0/60.0,270.0/60.0,285.0/60.0,300.0/60.0,345.0/60.0];
%t2=[0.0,8.0/60.0,17.0/60.0,30.0/60.0,45.0/60.0,60.0/60.0,90.0/60.0,120.0/60.0,150.0/60.0,180.0/60.0,195.0/60.0,210.0/60.0,225.0/60.0,240.0/60.0,270.0/60.0,285.0/60.0,300.0/60.0,345.0/60.0];
%t3=[0.0,8.0/60.0,17.0/60.0,30.0/60.0,45.0/60.0,60.0/60.0,90.0/60.0,120.0/60.0,150.0/60.0,180.0/60.0,195.0/60.0,210.0/60.0,225.0/60.0,240.0/60.0,270.0/60.0,285.0/60.0,300.0/60.0,345.0/60.0];
%y1=[.57,9.32,11.14,12.95,12.84,10.45,11.93,7.95,3.75,3.98,4.2,2.05,1.7,1.59,.11,.23,.57];

```

```

%y2=[2.67,0.45,0.14,0.12,0.09,0.05,0.11,0.05,0.196,1.19,0.564,0.328,1.
129,2.006,2.418,3.182,2.578,2.541];
%y3=[0.06,6.75,8.20,13.04,13.20,13.78,13.08,14.49,7.91,4.74,2.31,1.8,0
.77,0.16,0.06,0.00,0.53,0.11];
%plot(t1,y1,'ko',t2,y2,'ks',t3,y3,'kp');
%xlabel('Time (hr)');
%ylabel('NO_3 - N, NH_3 - N and PO_4 - P (mg L^{-1})');
%legend('Ammonia nitrogen','NO_X - nitrogen','Soluble phosphorus');
%hold off;

% 75 mg L-1 Acetate batch test

%plot(t,y(:,7),'k-.',t,y(:,4),'k-');
%hold on;
%t1=[0,15/60,30/60,45/60,60/60,75/60,90/60,105/60,120/60,135/60,150/60
,165/60,180/60,195/60,210/60,225/60,240/60,255/60,270/60];
%y1=[1.927,4.131,8.705,14.500,20.432,26.344,28.796,29.555,29.253,25.71
6,18.903,15.426,11.89,7.841,4.409,2.777,1.019,0.473,0.382];
%t2=[0,15/60,30/60,45/60,60/60,75/60,90/60,105/60,120/60];
%y2=[69.12,49.92,38.36,28.84,20.97,13.63,6.97,3.55,1.02];
%plot(t1,y1,'kp',t2,y2,'ko');
%xlabel('Time (hr)');
%ylabel('HAC COD and PO_4 - P (mg L^{-1})');
%legend('Soluble phosphorus','HAC-COD');
%hold off;
%plot(t,y(:,16),'k-.',t,y(:,21),'k--');
%hold on;
%t1=[0,60/60,120/60,180/60,240/60,270/60];
%y1=[28.13,98.01,112.4,65.17,47.68,47.08];
%t2=[0,60/60,120/60,180/60,240/60,270/60];
%y2=[82.88,67.61,60.17,75.04,80.56,79.92];
%plot(t1,y1,'ko',t2,y2,'ks');
%xlabel('Time (hr)');
%ylabel('PHA and Glycogen COD(mg L^{-1})');
%legend('PHA COD','Glycogen COD');
%hold off;

%batch sbr
%plot(t,y(:,5),'k-',t,y(:,6),'k:',t,y(:,7),'k-.');
%hold on;
%t1=[1.0/60.0,15.0/60.0,30.0/60.0,45.0/60.0,60.0/60.0,75.0/60.0,90.0/6
0.0,105.0/60.0,120.0/60.0,135.0/60.0,150.0/60.0,165.0/60.0,180.0/60.0,
195.0/60.0,210.0/60.0,225.0/60.0,240.0/60.0,255.0/60.0,270.0/60.0,285.
0/60.0,300.0/60.0,345.0/60.0];
%y1=[14.77,14.31,14.31,17.54,16.62,16.62,15.23,16.62,18.0,13.85,11.08,
10.15,6.08,6.11,6.11,3.23,1.38,0.0,0.0,0.0,0.0,0.0];
%y2=[1.369,0.229,0.309,0.107,0.391,0.136,0.456,0.19,0.426,0.712,1.891,
3.081,5.971,4.064,3.527,5.515,5.614,6.663,7.915,7.843,7.758,6.173];
%y3=[2.835,9.972,13.031,15.374,16.091,17.568,18.151,18.905,20.038,13.6
45,10.061,7.025,4.961,4.068,3.377,2.405,1.596,1.115,0.645,0.133,0.185,
0.155];
%plot(t1,y1,'ko',t1,y2,'ks',t1,y3,'kp');
%xlabel('Time (hr)');
%ylabel('NO_3 - N, NH_3 - N and PO_4 - P (mg L^{-1})');
%legend('Ammonia nitrogen','NO_3 - nitrogen','orthophosphorus');
%hold off;

%plot(t,y(:,4),'k-',t,y(:,7),'k-.',t,y(:,22),'k:');
%hold on;
%t1=[1.0/60.0,15.0/60.0,30.0/60.0,45.0/60.0,60.0/60.0,75.0/60.0,90.0/6
0.0,105.0/60.0,120.0/60.0];

```

```

%y1=[13.706,6.41,4.534,5.098,4.253,3.547,3.393,3.48,3.273];
%t2=[1.0/60.0,15.0/60.0,30.0/60.0,45.0/60.0,60.0/60.0,75.0/60.0,90.0/60.0,105.0/60.0,120.0/60.0,135.0/60.0,150.0/60.0,165.0/60.0,180.0/60.0,195.0/60.0,210.0/60.0,225.0/60.0,240.0/60.0,255.0/60.0,270.0/60.0,285.0/60.0,300.0/60.0,345.0/60.0];
%y2=[2.835,9.972,13.031,15.374,16.091,17.568,18.151,18.905,20.038,13.645,10.061,7.025,4.961,4.068,3.377,2.405,1.596,1.115,0.645,0.133,0.185,0.155];
%t3=[1.0/60.0,30.0/60.0,60.0/60.0,90.0/60.0,120.0/60.0,150.0/60.0,180.0/60.0,210.0/60.0,240.0/60.0,270.0/60.0,300.0/60.0,345.0/60.0];
%y3=[10.29,13.36,6.82,6.89,7.46,5.56,4.71,4.41,4.12,4.12,3.54,3.31];
%plot(t1,y1,'ko',t2,y2,'kp',t3,y3,'k*');
%xlabel('Time (hr)');
%ylabel('SCFA COD, PO_4 - P and Mg (mg L^{-1})');
%hold off;

%plot(t,y(:,16),'k-.',t,y(:,21),'k:');
%hold on;
%t1=[0,30.0/60.0,60.0/60.0,90.0/60.0,120.0/60.0,150.0/60.0,180.0/60.0,210.0/60.0,240.0/60.0,270.0/60.0,300.0/60.0];
%y1=[25.90,41.46,36.09,39.88,37.03,28.2,21.96,14.24,11.21,14.97,15.94];
%t2=[0,30.0/60.0,60.0/60.0,90.0/60.0,120.0/60.0,150.0/60.0,180.0/60.0,210.0/60.0,240.0/60.0,270.0/60.0,300.0/60.0];
%y2=[160.4,162.8,149.9,150.81,147.62,150.48,157.8,145.5,152.02,155.54,144.22];
%plot(t1,y1,'ko',t2,y2,'ks');
%xlabel('Time (hr)');
%ylabel('PHA and Glycogen COD(mg L^{-1})');
%legend('PHA COD','Glycogen COD');
%hold off;

%batch test with wastewater
%plot(t,y(:,5),'k-',t,y(:,6),'k:',t,y(:,7),'k-.');
%hold on;
%t1=[0.0,15.0/60.0,30.0/60.0,45.0/60.0,60.0/60.0,75.0/60.0,90.0/60.0,105.0/60.0,120.0/60.0];
%y1=[24.1,21.6,22.0,19.5,21.1,22.5,23.9,23.4,22.0];
%y2=[4.798,0.339,0.177,0.094,0.057,0.037,0.000,0.058,0.041];
%y3=[4.931,9.979,14.944,19.676,23.944,28.795,33.309,36.69,38.211];
%plot(t1,y1,'ko',t1,y2,'ks',t1,y3,'kp');
%xlabel('Time (hr)');
%ylabel('NO_3 - N, NH_3 - N and PO_4 - P (mg L^{-1})');
%legend('Ammonia nitrogen','NO_X - nitrogen','orthophosphorus');
%hold off;

plot(t,y(:,4),'k-',t,y(:,7),'k-.',t,y(:,22),'k:');
hold on;
t2=[0.0,15.0/60.0,30.0/60.0,45.0/60.0,60.0/60.0,75.0/60.0,90.0/60.0,105.0/60.0,120.0/60.0];
y2=[4.931,9.979,14.944,19.676,23.944,28.795,33.309,36.69,38.211];
t1=[0.0,15.0/60.0,30.0/60.0,45.0/60.0,60.0/60.0,75.0/60.0,90.0/60.0,105.0/60.0,120.0/60.0];
y1=[87.905,51.969,40.172,20.133,16.547,20.778,18.180,13.860,16.297];
t3=[0.0/60.0,30.0/60.0,60.0/60.0,90.0/60.0,120.0/60.0];
y3=[10.64,11.61,13.91,17.23,12.81];
plot(t1,y1,'ko',t2,y2,'kp',t3,y3,'k*');
xlabel('Time (hr)');
ylabel('SCFA COD, PO_4 - P and Mg (mg L^{-1})');
hold off;

```

```

%plot(t,y(:,16),'k-.',t,y(:,21),'k:');
%hold on;
%t1=[0,60.0/60.0,120.0/60.0];
%y1=[6.705,48.9,49.7];
%t2=[0,60.0/60.0,120.0/60.0];
%y2=[118.8,115.2,91.9];
%plot(t1,y1,'ko',t2,y2,'ks');
%xlabel('Time (hr)');
%ylabel('PHA and Glycogen COD(mg L^{-1})');
%legend('PHA COD','Glycogen COD');
%hold off;

%HAC batch test = 200mg/L
%plot(t,y(:,7),'k-.',t,y(:,4),'k--');
%hold on;
%t1=[0,15/60,30/60,45/60,60/60,75/60,90/60,105/60,120/60];
%y1=[0.811,4.391,14.852,19.49,26.444,33.087,38.554,41.256,45.281];
%t2=[0,15/60,30/60,45/60,60/60,75/60,90/60,105/60,120/60];
%y2=[213.2,147.48,123.459,114.844,104.673,105.044,91.769,87.026,79.093
];
%plot(t1,y1,'kp',t2,y2,'ks');
%xlabel('Time (hr)');
%ylabel('HAC COD and PO_4 - P (mg L^{-1})');
%legend('Soluble phosphorus','HAC-COD');
%hold off;
%plot(t,y(:,16),'k-.',t,y(:,21),'k--');
%hold on;
%t1=[0,60/60,120/60];
%y1=[14.467,85.221,97.874];
%t2=[0,60/60,120/60];
%y2=[176.43,159.62,133.59];
%plot(t1,y1,'ko',t2,y2,'ks');
%xlabel('Time (hr)');
%ylabel('PHA and Glycogen COD(mg L^{-1})');
%legend('PHA COD','Glycogen COD');
%hold off;

function dy=pos(t,y)
% function file for modified ASM 2 model
% N.Thayalakumaran

%define global variables

global qset;
% conversion factors for conservation equation
global insf;
global insi;
global inxi;
global inxs;
global inbm;
global ipsf;
global ipsi;
global ipxi;
global ipxs;
global ipbm;
global itssxi;
global itssxs;
global itssbm;
%stoichiometric parameters
global fsi;

```

```
global yh;
global fxi;
global ypao;
global ypo4;
global ypha;
global fxi;
global yaut;
global ymgpha;
global ymgxpp;
%kinetic parameters
%hydrolysis of particulate substrate
global kh;
global etano3h;
global etafe;
global ko2h;
global kno3;
global kx;
%heterotrophic organism
global muh;
global qfe;
global etano3;
global ko2;
global bh;
global kf;
global kfe;
global ka;
global knh4;
global kp;
global kalk;
%phosphorus accumulating organisms
global qpha;
global qpp;
global mupao;
global bpao;
global bpp;
global bpha;
global ko2p;
global kno3p;
global kps;
global kpp;
global kmax;
global kipp;
global kpha;
global etano3p;
global ysa;
global qgly;
global kgly;
global kphagly;
global bgly;
global kmg;
%nitrifying organism
global muaut;
global baut;
global ko2aut;
global knh4aut;
global kalkaut;
%precipitation
global kpre;
global kred;
global kalkred;
%initial condition
```

```
global so20;
global sf0;
global sa0;
global snh40;
global sno30;
global spo40;
global si0;
global salk0;
global sn20;
global xi0;
global xs0;
global xtss0;
global xh0;
global xmeoh0;
global xmep0;
global smg0;
%stoichiometric parameters have to be found by with the continuity
equation
global nu1nh4;
global nu2nh4;
global nu3nh4;
global nu1po4;
global nu2po4;
global nu3po4;
global nu1alk;
global nu2alk;
global nu3alk;
global nu1tss;
global nu2tss;
global nu3tss;
global nu12no3;
global nu13o2;
global nu14no3;
global nu15po4;
global nu18nh4;
global nu19nh4;
global nu19po4;
global nu20alk;
global nu21alk;
global nu4nh4;
global nu5nh4;
global nu6nh4;
global nu7nh4;
global nu8nh4;
global nu9nh4;
global nu13nh4;
global nu14nh4;
global nu15nh4;
global nu4po4;
global nu5po4;
global nu6po4;
global nu7po4;
global nu8po4;
global nu9po4;
global nu4alk;
global nu5alk;
global nu6alk;
global nu7alk;
global nu8alk;
global nu9alk;
global nu10alk;
```

```

global nu1alk;
global nu12alk;
global nu13alk;
global nu14alk;
global nu15alk;
global nu16alk;
global nu17alk;
global nu18alk;
global nu19alk;
global nu4tss;
global nu5tss;
global nu6tss;
global nu7tss;
global nu9tss;
global nu10tss;
global nu11tss;
global nu12tss;
global nu13tss;
global nu14tss;
global nu15tss;
global nu16tss;
global nu17tss;
global nu18tss;
global nu19tss;
global nu22tss;
global nu23tss;
%global xo; %initial biomass concentration, mg/L
%calculate new values for dependent variables
vr=y(1);
so2=y(2);
sf=y(3);
sa=y(4);
snh4=y(5);
sno3=y(6);
spo4=y(7);
si=y(8);
salk=y(9);
sn2=y(10);
xi=y(11);
xs=y(12);
xh=y(13);
xpao=y(14);
xpp=y(15);
xpha=y(16);
xaut=y(17);
xtss=y(18);
xmeoh=y(19);
xmep=y(20);
xgly=y(21);
smg=y(22);

%if vr<=15.0
% q=qset;
%if t<=8.0/60.0
%q=1.5/(8.0/60.0);
%else
%q=eps;
%end;
%if t<=2.0
%so2=eps;
%elseif t<=3.0

```

```

%so2=0.5;
%elseif t<=3.5
%so2=eps;
%elseif t<=4.5
%so2=3.75;
%elseif t<=5.0
%so2=0.5;
%else
%so2=eps;
%end
%etano3h=eps;
%etafe=eps;
%end

q=eps;
if t<=2.0
so2=eps;
else
so2=3.75;
end

%process rate vectors
rho=[kh*(so2/(ko2h+so2))*(xs/xh)/(kx+(xs/xh))*xh;

      kh*etano3h*(ko2h/(ko2h+so2))*(sno3/(kno3+sno3))*(xs/xh)/(kx+(xs/xh)
      )]*xh;

kh*etafe*(ko2h/(ko2h+so2))*(kno3/(kno3+sno3))*(xs/xh)/(kx+(xs/xh))*x
h;

muh*(so2/(ko2+so2))*(sf/(kf+sf))*(sf/(sf+sa))*(snh4/(knh4+snh4))*(spo4
/(kp+spo4))*(salk/(kalk+salk))*xh;

muh*(so2/(ko2+so2))*(sa/(ka+sa))*(sa/(sf+sa))*(snh4/(knh4+snh4))*(spo4
/(kp+spo4))*(salk/(kalk+salk))*xh;

muh*etano3*(ko2/(ko2+so2))*(sf/(kf+sf))*(sf/(sf+sa))*(snh4/(knh4+snh4)
)*(sno3/(kno3+sno3))*(salk/(kalk+salk))*(spo4/(kp+spo4))*xh;

muh*etano3*(ko2/(ko2+so2))*(sa/(ka+sa))*(sa/(sf+sa))*(snh4/(knh4+snh4)
)*(sno3/(kno3+sno3))*(salk/(kalk+salk))*(spo4/(kp+spo4))*xh;

qfe*(ko2/(ko2+so2))*(kno3/(kno3+sno3))*(sf/(kfe+sf))*(salk/(kalk+salk)
)*xh;
      bh*xh;

qpha*(sa/(ka+sa))*(salk/(kalk+salk))*((xpp/xpao)/(kpp+(xpp/xpao)))*((x
gly/xpao)/(kgly+(xgly/xpao)))*xpao;

qpp*(so2/(ko2p+so2))*(spo4/(kps+spo4))*(salk/(kalk+salk))*((xpha/xpao)
/(kpha+(xpha/xpao)))*(kmax-(xpp/xpao))/((kipp+kmax-
(xpp/xpao))*xpao*smg/(kmg+smg));

(qpp*(ko2p/(ko2p+so2))*(spo4/(kp+spo4))*(salk/(kalk+salk))*((xpha/xpao)
)/(kpha+(xpha/xpao)))*(kmax-(xpp/xpao))/((kipp+kmax-
(xpp/xpao))*xpao)*etano3p*(sno3/(kno3p+sno3))*smg/(kmg+smg);

mupao*(so2/(ko2p+so2))*(snh4/(knh4+snh4))*(spo4/(kp+spo4))*(salk/(kalk
+salk))*((xpha/xpao)/(kpha+(xpha/xpao)))*xpao;

```

```

(mupao*(ko2p/(ko2p+so2))* (snh4/(knh4+snh4))* (spo4/(kp+spo4))* (salk/(kalk+salk))* ((xpha/xpao)/(kpha+(xpha/xpao)))*xpao)*etano3p*(sno3/(kno3p+sno3));
    bpao*xpao*(salk/(kalk+salk));
    bpp*xpp*(salk/(kalk+salk));
    bpha*xpha*(salk/(kalk+salk));

muaut*(so2/(ko2aut+so2))* (snh4/(knh4aut+snh4))* (spo4/(kp+spo4))* (salk/(kalkaut+salk))*xaut;
    baut*xaut;
    kpre*spo4*xmeoh;
    kred*xmep*(salk/(kalkred+salk));
    qgly*(so2/(ko2p+so2))* ((xpha/xpao)/(kphagly+(xpha/xpao)))*xpao;
    bgly*xgly*(salk/(kalk+salk));

    %differential equations
dvr=q;
dso2=q*(so20-so2)/vr+(1-1/yh)*rho(4)+(1-1/yh)*rho(5)-ypha*rho(11)+(1-1/ypao)*rho(13)-(4.57-yaut)/yaut*rho(18);
dsf=q*(sf0-sf)/vr+(1-fsi)*rho(1)+(1-fsi)*rho(2)+(1-fsi)*rho(3)-1/yh*rho(4)-1/yh*rho(6)-rho(8)+rho(23);
dsa=q*(sa0-sa)/vr-1/yh*rho(5)-1/yh*rho(7)+rho(8)-ysa*rho(10)+rho(17);
dsnh4=q*(snh40-snh4)/vr+nu1nh4*rho(1)+nu2nh4*rho(2)+nu3nh4*rho(3)+nu18nh4*rho(18)+nu19nh4*rho(19)+nu4nh4*rho(4)+nu5nh4*rho(5)+nu6nh4*rho(6)+nu7nh4*rho(7)+nu8nh4*rho(8)+nu9nh4*rho(9)+nu13nh4*rho(13)+nu14nh4*rho(14)+nu15nh4*rho(15);
dsno3=q*(sno30-sno3)/vr-((1-yh)/(2.86*yh))*rho(6)-((1-yh)/(2.86*yh))*rho(7)-ypha/2.86*rho(12)-(1-ypao)/(2.86*ypao)*rho(14)+1/yaut*rho(18);
dspo4=q*(spo40-spo4)/vr+nu1po4*rho(1)+nu2po4*rho(2)+nu3po4*rho(3)+ypo4*rho(10)-rho(11)-rho(12)-ipbm*rho(13)-ipbm*rho(14)+nu15po4*rho(15)+rho(16)-ipbm*rho(18)+nu19po4*rho(19)-rho(20)+rho(21)+nu4po4*rho(4)+nu5po4*rho(5)+nu6po4*rho(6)+nu7po4*rho(7)+nu8po4*rho(8)+nu9po4*rho(9);
dsi=q*(si0-si)/vr+fsi*rho(1)+fsi*rho(2)+fsi*rho(3);
dsalk=q*(salk0-salk)/vr+nu1alk*rho(1)+nu2alk*rho(2)+nu3alk*rho(3)+nu20alk*rho(20)+nu21alk*rho(21)+nu4alk*rho(4)+nu5alk*rho(5)+nu6alk*rho(6)+nu7alk*rho(7)+nu8alk*rho(8)+nu9alk*rho(9)+nu10alk*rho(10)+nu11alk*rho(11)+nu12alk*rho(12)+nu13alk*rho(13)+nu14alk*rho(14)+nu15alk*rho(15)+nu16alk*rho(16)+nu17alk*rho(17)+nu18alk*rho(18)+nu19alk*rho(19);
dsn2=q*(sn20-sn2)/vr+((1-yh)/(2.86*yh))*rho(6)+((1-yh)/(2.86*yh))*rho(7)+nu12no3*rho(12)+nu14no3*rho(14);
dxi=q*(xi0-xi)/vr+fxi*rho(9)+fxi*rho(15)+fxi*rho(19);
dxs=q*(xs0-xs)/vr-rho(1)-rho(2)-rho(3)+(1-fxi)*rho(9)+(1-fxi)*rho(15)+(1-fxi)*rho(19);
dxh=q*(xh0-xh)/vr+rho(4)+rho(5)+rho(6)+rho(7)-rho(9);
dypao=-q*xpao/vr+rho(13)+rho(14)-rho(15);
dyppp=-q*xpp/vr-ypp4*rho(10)+rho(11)+rho(12)-rho(16);
dyppha=-q*xpha/vr+rho(10)-ypha*rho(11)-ypha*rho(12)-1/ypao*rho(13)-1/yh*rho(14)-rho(17)-rho(22);
dxaut=-q*xaut/vr+rho(18)-rho(19);
dxtss=q*(xtss0-xtss)/vr+nu1tss*rho(1)+nu2tss*rho(2)+nu3tss*rho(3)+1.42*rho(20)-1.42*rho(21)+nu4tss*rho(4)+nu5tss*rho(5)+nu6tss*rho(6)+nu7tss*rho(7)+nu9tss*rho(9)+nu10tss*rho(10)+nu11tss*rho(11)+nu12tss*rho(12)+nu13tss*rho(13)+nu14tss*rho(14)+nu15tss*rho(15)+nu16tss*rho(16)+nu17tss*rho(17)+nu22tss*rho(22)+nu23tss*rho(23)+nu18tss*rho(18)+nu19tss*rho(19);

```

```

dxmeoh=q*(xmeoh0-xmeoh)/vr-3.45*rho(20)+3.45*rho(21);
dxmep=q*(xmep0-xmep)/vr+4.87*rho(20)-4.87*rho(21);
dxgly=-q*xgly/vr-(1-ysa)*rho(10)+rho(22)-rho(23);
dsmg=q*(smg0-smg)/vr+ymgpha*rho(10)-ymgxpp*rho(11)-
ymgxpp*rho(12)+ymgxpp*rho(16);
%produce output vector
dy=[dvr;dso2;dsf;dsa;dsnh4;dsno3;dspo4;dsi;dsalk;dsn2;dxl;dxs;dxh;dxpa
o;dxpp;dxpha;dxaut;dxtss;dxmeoh;dxmep;dxgly;dsmg];

```